

DETECTION OF BIPARTITE QUANTUM CORRELATIONS BY LOCAL GENERALIZED MEASUREMENTS



TECHNISCHE
UNIVERSITÄT
DARMSTADT

Vom Fachbereich Physik
der Technischen Universität Darmstadt

zur Erlangung des Grades
eines Doktors der Naturwissenschaften (Dr. rer. nat.)

genehmigte Dissertation von
MAXIMILIAN SCHUMACHER

ERSTGUTACHTER: Prof. Dr. Gernot Alber
ZWEITGUTACHTER: Prof. Dr. Enno Giese

Darmstadt 2024

Maximilian Schumacher:

Detection of bipartite quantum correlations by local generalized measurements

ERSTGUTACHER: Prof. Dr. Gernot Alber

ZWEITGUTACHTER: Prof. Dr. Enno Giese

DARMSTADT, Technische Universität Darmstadt

TAG DER EINREICHUNG: 11.12.2023

TAG DER PRÜFUNG: 29.01.2024

Darmstadt, Technische Universität Darmstadt

Jahr der Veröffentlichung der Dissertation auf TUpriints: 2024

URN: urn:nbn:de:tuda-tuprints-269136

URI: <https://tuprints.ulb.tu-darmstadt.de/id/eprint/26913>

Veröffentlicht unter CC BY-SA 4.0 International

Namensnennung – Weitergabe unter gleichen Bedingungen

<https://creativecommons.org/licenses/>



"Quantum phenomena do not occur in a Hilbert space, they occur in a laboratory."

– Asher Peres, [1, p. 112]

ABSTRACT

Driven by the need for efficient local entanglement detection for quantum information processing applications, this dissertation investigates sufficient conditions for arbitrary-dimensional local bipartite entanglement detection based on correlation matrices and joint probability distributions. Furthermore, the detection of quantum correlations can also be used to verify Einstein-Podolsky-Rosen (EPR) steerable quantum states from Alice to Bob. In particular, different classes of local informationally complete measurements are explored to determine the detection efficiency of entanglement and EPR steering. These local measurements are specialized to the recently introduced one-parameter class of (N, M) -positive operator valued measures ((N, M) -POVMs).

The first part of this thesis discusses necessary or sufficient conditions for the existence of (N, M) -POVMs in arbitrary dimensional quantum systems. A sufficient condition for the existence of (N, M) -POVMs is derived, which guarantees that all POVM elements are positive semidefinite for the continuous parameters below an upper bound. Furthermore, the existence of isospectral traceless Hermitian operator bases (IHOBs) is necessary for the existence of optimal (N, M) -POVMs. When the number of measurement results M of a POVM is less than or equal to the dimension of the quantum system, a commutator relation of the basis elements constructed from a single POVM can be used to extend the necessary condition to a sufficient one. In these cases, optimal (N, M) -POVMs are necessarily projection operators of equal rank.

The second part of this dissertation utilizes local informationally complete (N, M) -POVMs to detect bipartite entanglement. It is demonstrated that the symmetries of (N, M) -POVMs imply a characteristic scaling relation connecting equivalent sufficient entanglement conditions. Based on the scaling relation, the efficiency of different measurement settings can be investigated quantitatively. Furthermore, the Euclidean volume ratios between entangled and all quantum states are computed numerically using a hit-and-run Monte Carlo algorithm. The numerical results show that the physically feasible local (N, M) -POVMs are sufficient for entanglement detection. In particular, optimal (N, M) -POVMs are not needed for entanglement detection.

The final part of this dissertation discusses the verification of EPR steerability by local informationally complete (N, M) -POVMs. Another application of the scaling relation is to identify the efficiency of the correlation matrix-based sufficient condition for EPR steerability of local informationally complete (N, M) -POVMs. The Euclidean volume ratios of the EPR steerable states quantify the efficiency of the correlation matrix-based sufficient condition. Except for the two-qubit case, the numerical results demonstrate that the Euclidean volume ratios significantly underestimate the EPR steerable quantum states. Moreover, these results are compared to a recently proposed sufficient condition that determines the steerability from Alice to Bob by detecting the entanglement of a transformed quantum state. The numerical results demonstrate that this method is significantly more efficient. However, it is only valid if Alice's quantum system is a qubit.

ZUSAMMENFASSUNG

Die Detektion von Verschränkung durch lokale Messungen zweier möglicher räumlich getrennter Beobachter ist für Anwendungen in der Quanteninformationsverarbeitung von großer Bedeutung. Aus diesem Grund wird in dieser Dissertation die Verschränkungsdetektion durch Spurnormen von Korrelationsmatrizen und gemeinsame Wahrscheinlichkeitsverteilungen von lokalen verallgemeinerten Quantenmessungen diskutiert. Darüber hinaus eignen sich die Korrelationsmatrizen auch für die Detektion von Einstein-Poldolsky-Rosen (EPR) Steering. Es wird insbesondere der Einfluss lokaler Messungen auf die detektierten Quantenkorrelationen untersucht. Die lokalen Messungen sind auf die kürzlich eingeführten (N, M) -Positive Operator Value Measures ((N, M) -POVMs) spezialisiert.

Der erste Teil dieser Dissertation befasst sich mit der Existenz von (N, M) -POVMs in beliebig dimensionalen Quantensystemen. Zunächst wird eine hinreichende Bedingung hergeleitet, für welche kontinuierliche Parameter (N, M) -POVMs immer existieren und somit garantiert ist, dass alle POVM-Elemente positiv semidefinit sind. Weiterhin werden notwendige Bedingungen für die Existenz optimaler (N, M) -POVMs hergeleitet. Diese zeigen den Zusammenhang zwischen isospektralen, hermiteschen, spurlosen, orthonormalen Operatorbasen (IHOBs) und optimalen (N, M) -POVMs. Optimale (N, M) -POVMs können nur existieren, wenn eine solche Basis existiert. Wenn die Anzahl der Messergebnisse eines POVMs M kleiner als die Dimension des Quantensystems d ist, wird diese notwendige Bedingung zu einer hinreichenden Bedingung, indem eine Kommutatorrelation zwischen Basiselementen eines POVMs berücksichtigt wird. In diesem Fall handelt es sich bei den Elementen der POVMs um Projektionen gleichen Ranges.

Im zweiten Teil der Arbeit werden lokale (N, M) -POVMs zur Verschränkungsdetektion verwendet. Weiterhin wird gezeigt, dass aus den Symmetrien der (N, M) -POVMs eine Skalierungseigenschaft für die Verschränkungsdetektion abgeleitet werden kann, die verschiedene äquivalente hinreichende Bedingungen miteinander verknüpft. Mithilfe dieser Skalierungseigenschaft kann die Effizienz der Verschränkungsdetektion bestimmt werden, ohne die zugehörigen (N, M) -POVMs konstruieren zu müssen. Ein Hit-and-Run Monte-Carlo-Algorithmus wird verwendet, um die Effizienz der hinreichenden Bedingungen durch euklidische Volumenverhältnisse der verschränkten Zustände zu allen Zuständen zu bestimmen. Diese Volumenverhältnisse besagen, dass konstruierbare lokale (N, M) -POVMs für die Verschränkungsdetektion ausreichend sind. Im Gegensatz dazu sind optimale (N, M) -POVMs für die Verschränkungsdetektion nicht erforderlich.

Im dritten Teil der Arbeit werden Korrelationsmatrizen lokaler (N, M) -POVMs verwendet, um EPR steuerbare Quantenzustände zu detektieren. Mit dem Hit-and-Run Monte-Carlo-Algorithmus können auch die euklidischen Volumenverhältnisse der von Alice nach Bob steuerbaren Quantenzustände bestimmt werden. Mit Ausnahme des Zwei-Qubit-Systems werden die euklidischen Volumenverhältnisse durch die hinreichende Bedingung fast vollständig unterschätzt. Daher wird die hinreichende Bedingung für EPR Steering von Alice nach Bob durch Verschränkungsdetektion verwendet, um die steuerbaren Zustände zu detektieren. Numerische Ergebnisse zeigen, dass diese Methode wesentlich effizienter ist als die auf Korrelationsmatrizen basierende Methode. Allerdings kann diese Methode nur angewendet werden, wenn Alice ein Qubit als lokales Quantensystem besitzt.

CONTENTS

1	Introduction	1
1.1	Detection of entanglement and EPR steering by local generalized measurements	2
1.2	Outline	2
I Theoretical foundations		
2	Fundamental concepts and methods	7
2.1	Density matrices	7
2.1.1	Hilbert-Schmidt representation of Hermitian operators	8
2.1.2	Distance measure between quantum states	11
2.2	Bipartite systems and entanglement	14
2.2.1	The negative partial transpose	15
2.2.2	Entanglement witnesses	16
2.2.3	Entanglement detection by local measurements	17
2.3	Measurements in quantum mechanics	20
2.3.1	Projective measurements	20
2.3.2	Positive operator valued measures (POVM)	21
2.4	Randomly generated density matrices	24
2.5	Local realism and bipartite Einstein-Podolsky-Rosen steerability	27
2.5.1	Nonlocality of quantum mechanics	27
2.5.2	Definition of EPR steerability	30
2.5.3	Joint measurability and EPR steerability	32
II (N, M)-POVMs		
3	Properties of (N, M) -POVMs	35
3.1	Definition of (N, M) -POVMs	35
3.2	Construction of (N, M) -POVMs	39
3.2.1	Construction of (N, M) -POVMs by Siudzińska	39
3.2.2	Recursive construction of (N, M) -POVMs	41
3.3	Representation of (N, M) -POVMs in arbitrary Hermitian operator bases	43
4	Existence of (N, M) -POVMs	49
4.1	Positive semidefiniteness of POVM elements	49
4.1.1	Positive semidefiniteness of MUM elements for qutrits	50
4.1.2	Positive semidefiniteness of POVM elements for $M = 4$	55
4.2	Necessary conditions for constructing (N, M) -POVMs	62
4.2.1	Optimal (N, M) -POVMs for $M \geq d$	65
4.2.2	Optimal (N, M) -POVMs for $2 < M < d$	67
4.2.3	Optimal $(N, 2)$ -POVMs	69
4.2.4	Conclusion	70
4.3	Overview SIC-POVMs	71
4.4	Overview Mutually unbiased basis	72
III Entanglement detection		
5	Entanglement detection by local measurements	77

5.1	Correlation matrices of local measurements	78
5.1.1	Correlation matrices of local orthonormal Hermitian operators	80
5.1.2	Correlation matrices of (N, M) -POVMs	82
5.2	Joint probability distributions	84
5.3	Comparison with literature	87
5.4	Simulation results	88
IV Einstein-Podolsky-Rosen steering		
6	Detection of EPR steering	97
6.1	EPR steerability for qubit-qubit systems	97
6.2	EPR steering detection through correlation matrices	102
6.2.1	EPR Steering detection with local Hermitian operator bases (LOOs) .	107
6.2.2	EPR Steering detection with (N, M) -POVMs	109
6.3	EPR steering detection through entanglement detection	110
6.4	Simulation results	112
7	Conclusion	115
V Appendix		
A	Important (N, M) -POVMs	119
A.1	Mutually unbiased bases	119
A.2	SIC-POVMs	120
B	Hermitian operators bases	123
B.1	Isospectral operators basis	126
C	Standard deviations of the Monte Carlo algorithm	129
	Bibliography	130
	List of publications	141
	Curriculum vitae	142

INTRODUCTION

The development of quantum mechanics started in the early 20th century when Max Planck published his description of black body radiation in 1900 [2, 3], followed by Albert Einstein's explanation of the photoelectric effect in 1905 [4]. These gave rise to the fast-expanding field of quantum mechanics. Further, the quantum mechanical theories were able to describe the physics of hydrogen atoms [5], the alpha decay of heavy elements like uranium through the tunneling effect [6, 7], diatomic molecules [8, 9] and the wave-particle dualism [10].

After the first mathematical formulation of quantum mechanics by Werner Heisenberg [11], this process cumulated in a closed mathematical description by John von Neumann and Paul Dirac [12, 13]. The uncertainty relation between two observables has been derived from the wave structure of quantum mechanics. Despite the success of quantum mechanics, Albert Einstein, Boris Podolsky and Nathan Rosen raised concerns about its completeness in 1935, pointing out that a bipartite quantum system could violate the locality condition [14]. However, Niels Bohr argued in favor of quantum mechanics [15]. In response to the Einstein-Podolsky-Rosen (EPR) paradox, Erwin Schrödinger introduced entangled quantum states of bipartite quantum systems [16, 17]. Furthermore, the EPR steering was introduced as the influence on a local quantum state from local measurements on the other party of a bipartite quantum system. These phenomena exhibit correlations that surpass the classical correlations between local observables. For several decades entanglement, nonlocality and EPR steering did not receive much attention due to the lack of experimental implementations and verifications. However, the pioneering contributions of lasers, which enable the precise trapping and control of single atoms and ions [18–21], changed this. Since then, these new technologies have been used for the experimental realizations of quantum optics and quantum information processing [1].

In the 1960s, John Bell picked up the EPR paradox and reformulated it for spin observables [22]. The result was the Bell inequality, which is experimentally accessible and enables to prove the nonlocality of quantum mechanics. The equivalence between locality and hidden variable theory made an experimental implementation of the EPR paradox possible [23]. Bell nonlocality has been demonstrated experimentally with increasing contentment [24–26]. Loophole-free Bell inequalities have been violated in various quantum systems, like superconducting circuits [27], spins in nitrogen-vacancy centers [28], optical photons [29–31] and neutral atoms [32].

The introduction of local hidden state (LHS) models allowed a rigorous definition of EPR steering by Wisemann *et al.* [33]. Unlike to Bell locality the existence of a LHS model is asymmetric for the observers. By demonstrating these quantum correlations, entanglement has been experimentally verified in different quantum systems like polarization of photons, superconducting qubits, and trapped atoms. Moreover, the entanglement of two photons has been demonstrated between two observers who were 248 km apart [34]. Despite the fundamental interest in these non-intuitive correlations, they gave rise to applications like quantum infor-

mation, computation, metrology, cryptography and simulation of quantum systems [35, 36]. It is advantageous to classify different types of entanglement through local operations and classical communication [37, 38]. The quantum mechanical phenomena of entanglement, nonlocality and EPR steering are valuable resources for applications in quantum information processing, such as quantum cryptography [39, 40], quantum communication [41–43], computing [44–46], simulation [47], sensing [48–51] and teleportation [52, 53]. For quantum networks [54] or spatially separated observers [28, 34, 55] it is important to verify the entanglement of quantum states by local measurements. Therefore, the focus of this thesis is set to the detection of bipartite entanglement by local measurements.

1.1 DETECTION OF ENTANGLEMENT AND EPR STEERING BY LOCAL GENERALIZED MEASUREMENTS

For the development of quantum information processing applications, it is crucial to identify the quantum states that are most suitable for the task. Positive maps that act on subsystems are used to characterize bipartite entanglement entirely [56]. As a result, the sufficient Peres-Horodecki condition, which serves as a criterion for qubit-qubit and qubit-qutrit systems, can be derived to detect entanglement [57, 58]. This dissertation investigates entanglement detection using correlation matrices and joint probability distributions of local measurements, to enable separated observers to identify entangled quantum states. The focus is on informationally complete measurements that permit the complete quantum state reconstruction. The local measurements used are the class of single-parameter (N, M) -POVMs [59], which includes the commonly used symmetric informationally complete POVMs (SIC-POVMs) [60, 61], their generalization the general SIC-POVMs (GSICs) [62], maximally mutually unbiased bases (MUBs) [63] and their generalization the mutually unbiased measurements (MUMs) [64]. The existence of these measurements remains an ongoing research inquiry, even for the special classes of SIC-POVMs and MUBs [65, 66]. Hence, this dissertation focuses on the existence of (N, M) -POVMs by establishing necessary conditions and sufficient conditions. These local informationally complete POVMs are used for detecting entanglement by local measurements.

In cases where only one party trusts their measurement apparatus, the EPR steerable quantum states are valuable resources in quantum information processing. For instance, EPR steerable quantum states are necessary for one-sided device-independent quantum key distribution [67–69]. Additionally, the EPR steerability is closely linked to the joint measurable observables [70]. However, for the simple case of two-qubits numerically feasible necessary and sufficient conditions for EPR steering are only known for projective measurements [71]. Therefore, the focus is on more straightforward and less demanding sufficient conditions using local informationally complete measurements for finite-dimensional quantum systems.

1.2 OUTLINE

This thesis is divided into four parts.

Part I explains the fundamentals of bipartite quantum systems. The concept of a single quantum system density matrix is discussed in Section 2.1, including the Hilbert-Schmidt representation and the trace distance as a measure for distinguishing quantum states. Section 2.2 introduces bipartite quantum systems of finite dimension and defines entangled quantum states. The following subsections outline various techniques for detecting entanglement. They cover the Peres-Horodecki condition, entanglement witnesses, and trace norm-based entan-

glement detections. Quantum measurements are discussed in Section 2.3. The projective measurements are generalized to POVMs. A hit-and-run Monte Carlo algorithm generating random bipartite qudit density matrices over the complete state space is discussed in Section 2.4. This algorithm is used to test the efficiency of the sufficient entanglement conditions. Section 2.5 introduces the nonlocality of quantum mechanics and defines EPR steering.

Part II provides an in-depth analysis of (N, M) -POVMs. Chapter 3 focuses on the definition, construction and important properties of (N, M) -POVMs in Sections 3.1 and 3.2. Section 3.3 presents the derivation of the representation of arbitrary (N, M) -POVMs in a Hermitian operator basis, forming the basis for the scaling relation of the entanglement and EPR steering detection in Parts III and IV. Chapter 4 discusses the existence of optimal (N, M) -POVMs. The positive semidefiniteness of Hermitian operators with a fixed trace is examined to illustrate the challenge of constructing optimal (N, M) -POVMs in Section 4.1. Additionally, Section 4.2 derives a sufficient condition for which parameters (N, M) -POVMs can be constructed from an arbitrary traceless Hermitian orthonormal operator basis. Furthermore, the relationship between optimal (N, M) -POVMs and IHOBs is introduced. The existence of an IHOB is necessary for the existence of optimal (N, M) -POVMs. Moreover, the state of the art of constructing optimal (N, M) -POVMs of the special classes of SIC-POVMs and MUBs is summarized in Sections 4.3 and 4.4.

The bipartite entanglement detection using local informationally complete (N, M) -POVMs is discussed in Part III. The entanglement detection based on the trace norm of correlation matrices of arbitrary local measurements is introduced. Additionally, the general sufficient condition is applied to local Hermitian orthonormal operator bases (LOOs) and local informationally complete (N, M) -POVMs. The scaling relation shows that all local informationally complete (N, M) -POVMs and LOOs result in the same sufficient condition. In Section 5.2, the joint probability-based sufficient condition and its associated scaling relation, which unifies various (N, M) -POVMs into a single class, is derived. An overview of the existing literature on detecting entanglement with local informationally complete (N, M) -POVMs is presented in Section 5.3. To evaluate the effectiveness of these introduced sufficient conditions, the hit-and-run Monte Carlo algorithm from Section 2.4 is used to determine the Euclidean volume ratios of detected entangled states. The lower bounds on the volume ratios of the identified entangled quantum states are then compared to those of corresponding negative partial transpose (NPT) quantum states.

The discussion on the detection of EPR steering is presented in detail in part IV. Section 6.1 provides an overview of the EPR steerability for qubit-qubit systems and presents a simple criterion for the special class of T -states. Section 6.2 introduces the sufficient EPR steering condition based on correlation matrices for arbitrary local quantum measurements. This general sufficient condition is applied to LOOs and local informationally complete (N, M) -POVMs. Moreover, the scaling relation shows the equivalence of such measurements. The verification of EPR steerability by detecting entanglement on a transformed quantum state is shown in Section 6.3. Additionally, sufficient conditions are used to determine the Euclidean volume ratios of the steerable quantum states from Alice to Bob in Section 6.4. The Euclidean volume ratios have been computed using the hit-and-run Monte Carlo algorithm of Section 2.4.

The central results of this thesis are or will be published in the following journals:

- M. Schumacher, G. Alber
Typical bipartite steerability and generalized local quantum measurements
Phys. Scr. **98**, 115234 (2023)
Based on Chapters 3 and 6

- M. Schumacher, G. Alber
Detection of typical bipartite entanglement by local generalized measurements
Phys. Rev. A **108**, 042424 (2023)
Based on Chapters [3](#) and [5](#)
- M. Schumacher, G. Alber
Conditions for the existence of positive operator valued measures
Canadian Journal of Physics (submitted)
Based on Chapter [4](#)

Part I

THEORETICAL FOUNDATIONS

FUNDAMENTAL CONCEPTS AND METHODS

This chapter discusses the physical foundations of bipartite quantum systems of finite dimensions. Section 2.1 introduces the concept of the density matrix, the Hilbert-Schmidt representation and the trace distance of quantum states. The concept of entanglement and its detection is presented in Section 2.2. The von Neumann measurement and its generalization are discussed in Section 2.3. Additionally, Section 2.4 presents an effective method for generating random bipartite qudit states. Finally, the nonlocality of quantum systems and the asymmetric effect of EPR steering are discussed. These provide the foundation for the discussed problems of the existence of (N, M) -POVMs and their application in verifying entanglement or EPR steerability.

2.1 DENSITY MATRICES

In this section, properties of density matrices that depict the state ensembles of a quantum system are introduced and discussed. For the discussed problems it is sufficient to assume a quantum system of finite dimension d . The state vector $|\phi\rangle \in \mathcal{H}_d$ has been introduced to describe the statistics of experimental measurement results. There, the Hilbert space \mathcal{H}_d is a complex vector space of dimension d . The vector $|\phi\rangle$ contains information about the quantum state of the system and is used to compute the average value of an observable O

$$\langle O \rangle = \langle \phi | O | \phi \rangle. \quad (2.1)$$

The quantum state $|\phi\rangle$ can determine the measurement statistics but cannot predict a measurement result, only its probability. We assume an ensemble of n quantum states $|\phi_i\rangle \in \mathcal{H}$ where the quantum systems is in the state $|\phi_i\rangle$ with a probability $p_i \geq 0$ and it holds $\sum_{i=1}^n p_i = 1$. The average value for the observable O for a state ensemble is given by

$$\langle O \rangle_{\text{ens}} = \sum_{i=1}^n p_i \langle \phi_i | O | \phi_i \rangle = \text{tr}\{O\rho\} \quad (2.2)$$

Here,

$$\rho = \sum_{i=1}^n p_i |\phi_i\rangle\langle\phi_i| \quad (2.3)$$

is the density matrix. The properties of the density matrix are [1, 72]:

- 1) The normalization $\text{tr}\{\rho\} = 1$ follows from

$$\text{tr}\{\rho\} = \text{tr}\left\{\sum_{i=1}^n p_i |\phi_i\rangle\langle\phi_i|\right\} = \sum_{i=1}^n p_i = 1. \quad (2.4)$$

2) A density matrix is Hermitian $\rho = \rho^\dagger$.

3) The purity is given by

$$\text{tr}\{\rho^2\} \leq 1. \quad (2.5)$$

4) The positive semidefiniteness $\rho \geq 0$ follows from

$$\langle \phi | \rho | \phi \rangle = \sum_{i=1}^n p_i |\langle \phi | \phi_i \rangle|^2 \geq 0, \quad \forall |\phi\rangle \in \mathcal{H}_d. \quad (2.6)$$

It is noted that the positive semidefiniteness of the density matrix is equivalent to the case that all eigenvalues λ_i of the density matrix are non-negative [73]. Additionally, the normalization of the density matrix restricts the eigenvalues to values smaller or equal to one. This implies that the eigenvalues of a density matrix must satisfy $0 \leq \lambda_i \leq 1$. So far, it has not been shown under which conditions a density matrix represents a pure state. Starting from a pure state $|\phi\rangle \in \mathcal{H}_d$, the density matrix is given by $\rho = |\phi\rangle\langle\phi|$ and it follows $\rho = \rho^2$. This implies that $\text{tr}\{\rho^2\} = 1$. Assuming a density matrix ρ that satisfies $\text{tr}\{\rho^2\} = 1$. Such a density matrix fulfills

$$\text{tr}\{\rho\} = \sum_{i=1}^d \lambda_i = 1, \quad (2.7)$$

$$\text{tr}\{\rho^2\} = \sum_{i=1}^d \lambda_i^2 = 1, \quad (2.8)$$

where it has been used that a Hermitian matrix can be diagonalized. By subtracting both equations

$$\text{tr}\{\rho - \rho^2\} = \sum_{i=1}^d \lambda_i(1 - \lambda_i) = 0 \quad (2.9)$$

and using that the eigenvalues fulfill $0 \leq \lambda_i \leq 1$, one obtains a sum over positive terms, which has to vanish. This condition can only be fulfilled if the eigenvalues are either zero or one. Furthermore, due to normalization, one eigenvalue must be equal to one while the others are equal to zero. This implies that the density operator has rank one and belongs to a pure state. In summary, a density matrix ρ belongs to a pure quantum state if and only if $\text{tr}\{\rho^2\} = 1$ or $\rho^2 = \rho$ is fulfilled.

2.1.1 Hilbert-Schmidt representation of Hermitian operators

A basis representation of Hermitian operators is introduced to visualize the state space of quantum states or POVMs geometrically. Starting from a representation of Hermitian operators, the normalization and positive semidefiniteness restrictions are imposed. A Hermitian matrix A acts on vectors of the Hilbert space of dimension d and satisfies $A = A^\dagger$. It is shown that such matrices form a vector space over the field of real numbers: let $A, B \in \mathcal{H}_{d \times d}$ with $a, b \in \mathbb{R}$ then

$$(aA + bB)^\dagger = aA^\dagger + bB^\dagger = aA + bB \quad (2.10)$$

is a Hermitian matrix. The aim is to represent the Hermitian operators in a basis of such a vector space in order to visualize the positive semidefinite matrices or generate random quantum states. First, the Hilbert-Schmidt scalar product of complex matrices is introduced by $\langle A|B \rangle = \text{tr}\{A^\dagger B\}$. The definition fulfills the defining properties of a scalar product [74]:

1) The symmetry $\langle A|B\rangle = \overline{\langle B|A\rangle}$ is shown by

$$\langle A|B\rangle = \text{tr}\{A^\dagger B\} = \text{tr}\{BA^\dagger\} = \overline{\langle B|A\rangle}.$$

2) The sesquilinearity follows from the linearity of the trace

$$\begin{aligned}\langle r_1 A_1 + r_2 A_2 | B \rangle &= \bar{r}_1 \langle A_1 | B \rangle + \bar{r}_2 \langle A_2 | B \rangle, \\ \langle A | r_1 B_1 + r_2 B_2 \rangle &= r_1 \langle A | B_1 \rangle + r_2 \langle A | B_2 \rangle.\end{aligned}$$

3) The non-negativity is shown by

$$\begin{aligned}0 &\leq \langle A|A\rangle = \text{tr}\{A^\dagger A\}, \\ 0 = \langle A|A\rangle &= \sum_{i=1}^d \lambda_i^2 \Leftrightarrow \forall \lambda_i = 0 \Leftrightarrow A = 0.\end{aligned}$$

Thus, a Hermitian operator can be expanded in a basis of linearly independent Hermitian operators

$$G = \{G_0, \dots, G_{d^2-1}\}, \quad (2.11)$$

acting on \mathcal{H}_d . The properties of such Hermitian operator bases are discussed in more detail in Appendix B. These operators can always be chosen as orthonormal Hermitian operators with respect to the Hilbert-Schmidt scalar product

$$\langle G_i | G_j \rangle = \text{tr}\{G_i G_j\} = \delta_{ij}. \quad (2.12)$$

These operators form an Hermitian orthonormal basis of the Euclidean vector space \mathcal{H}_{d^2} of linear Hermitian operators. Therefore, a Hermitian operator H can be expanded in this basis by

$$H = \sum_{i=0}^{d^2-1} h_i G_i \quad (2.13)$$

and the coefficients are given by

$$\text{tr}\{H G_j\} = \sum_{i=0}^{d^2-1} h_i \text{tr}\{G_j G_i\} = h_j. \quad (2.14)$$

When dealing with density matrices and (N, M) -POVMs, it is only necessary to consider Hermitian operators that have a fixed trace of $\text{tr}\{H\} = p$. For this purpose, it is helpful to choose a Hermitian orthonormal operator basis with

$$\tilde{G} = \left\{ \tilde{G}_0 = \frac{\mathbb{1}_d}{\sqrt{d}}, \tilde{G}_1, \dots, \tilde{G}_{d^2-1} \right\}. \quad (2.15)$$

From this definition, it follows that the operators are traceless $\text{tr}\{\tilde{G}_i\} = 0$ for $i = \{1, \dots, d^2-1\}$. Operators with a fixed trace can be represented by

$$H = \frac{p}{d} \mathbb{1}_d + \sum_{i=1}^{d^2-1} h_i \tilde{G}_i = \frac{p}{d} \mathbb{1}_d + \mathbf{h} \cdot \tilde{\mathbf{G}}. \quad (2.16)$$

Here the $d^2 - 1$ vectors $\mathbf{h} = (h_1, \dots, h_{d^2-1})^T$ and $\tilde{\mathbf{G}} = (\tilde{G}_1, \dots, \tilde{G}_{d^2-1})^T$ have been introduced, where the vector \mathbf{h} is called the Bloch vector for quantum states ($p = 1$). Representation (2.16) implies that the Hermitian operators with fixed trace are elements of a $d^2 - 1$ Euclidean vector space over the field of real numbers. Furthermore, we focus on density matrices, which have the representation of [75]

$$\rho = \frac{1}{d} \mathbb{1}_d + \sum_{i=1}^{d^2-1} h_i \tilde{G}_i = \frac{1}{d} \mathbb{1}_d + \mathbf{h} \cdot \tilde{\mathbf{G}}. \quad (2.17)$$

The normalization and hermiticity of a density matrix are encoded in the density matrix representation. However, the positive semidefiniteness and purity still have to be introduced. From Eq. (2.5) follows [74]

$$1 \geq \text{tr}\{\rho^2\} = \frac{1}{d} + |\mathbf{h}|^2 \Rightarrow |\mathbf{h}|^2 \leq \frac{d-1}{d}. \quad (2.18)$$

Here, the inequality states that the norm of the Bloch vector \mathbf{h} is bounded by $\sqrt{(d-1)/d}$. This restriction confirms the space of Hermitian operators with a trace equal to one to a ball with radius $\sqrt{(d-1)/d}$. In addition, the positive semidefinite operators on the boundary of the ball are the pure states. However, the positive semidefiniteness of the Hermitian operators is not encoded in the Bloch vector. First, it is shown that the density matrices form a convex set. Let $r_i \in [0, 1]$ with $\sum_{i=1}^n r_i = 1$, ρ_i density matrices and p_{ij} parameters of a convex combination of pure states of ρ_i with $\sum_{j=1}^{n_i} p_{ij} = 1$ for all i . Then holds

$$\sum_{i=1}^n r_i \sum_{j=1}^{n_i} p_{ij} = \sum_{i=1}^n r_i \quad (2.19)$$

and the operators have the convex combination into pure states $|\phi_{ij}\rangle$

$$\sum_{i=1}^n r_i \rho_i = \sum_{i=1}^n \sum_{j=1}^{n_i} r_i p_{ij} |\phi_{ij}\rangle \langle \phi_{ij}|. \quad (2.20)$$

This implies that density matrices form a convex set. It can be shown that all Hermitian operator with a trace equal to one and [74]

$$|\mathbf{h}|^2 \leq \frac{1}{(d-1)d} \quad (2.21)$$

are positive semidefinite. This minimal radius will be derived in Section 4.2 and is a sufficient condition for positive semidefiniteness. The convex set's interior consists of density matrices with strictly positive eigenvalues, while the boundary consists of density matrices with at least one eigenvalue equal to zero. The density matrices representing pure states are extremal points of the convex set with only one non-zero eigenvalue. For any Hermitian operator with a norm of the Bloch vector between the inner and outer radii, positive semidefiniteness must be checked. A detailed discussion of the convex set is shown in Section 4.2 for (N, M) -POVMs, which also holds for density matrices. For a qubit $d = 2$, the inner and outer radius are identical, $r_{\text{in}} = r_{\text{out}} = 1/2$. This leads to the Bloch ball, where all vectors inside the 3-dimensional ball represent density matrices [74]. A traceless Hermitian orthonormal basis used for qubits is

$$\tilde{G}_1 = \frac{\sigma_x}{\sqrt{2}}, \quad \tilde{G}_2 = \frac{\sigma_y}{\sqrt{2}}, \quad \text{and} \quad \tilde{G}_3 = \frac{\sigma_z}{\sqrt{2}} \quad (2.22)$$

with σ_i the Pauli matrices Eq. (B.8). The set of density matrices for a qubit is given by

$$\rho = \frac{1}{2}\mathbb{1}_2 + \frac{1}{\sqrt{2}}\mathbf{h} \cdot \boldsymbol{\sigma} = \frac{1}{2}\mathbb{1}_2 + \frac{1}{\sqrt{2}}(h_1\sigma_x + h_2\sigma_y + h_3\sigma_z), \quad (2.23)$$

where $|\mathbf{h}|^2 \leq 1/2$. It is stated that the definition of the prefactor $1/\sqrt{2}$ is a convention. In the case of qubit density matrices, the pure states define the boundary of the state space. In $d = 2$, all density matrices with an eigenvalue equal to zero must be pure. For a general qudit with $d \geq 2$, the density matrices are given by

$$\rho(\mathbf{h}) = \frac{1}{d}\mathbb{1}_d + \mathbf{h} \cdot \tilde{\mathbf{G}}. \quad (2.24)$$

Such a basis can be the generalized Gell-Mann basis, Eq. (B.10), which is a generalization of the Pauli matrices for $d \geq 3$ and can be constructed in arbitrary dimensions. Here, only the vectors with $\rho(\mathbf{h}) \geq 0$ belong to density matrices. The density matrices with at least one eigenvalue equal to zero form the boundary of the state space in $(d^2 - 1)$ -dimensional Euclidean vector space. The convex set for qudits is more complicated than for qubits because the pure states are only a part of this boundary. Applications for the basis representation are the simple calculation of average values and the generation of arbitrary quantum states.

2.1.2 Distance measure between quantum states

In this section, a distance measure between two quantum states is introduced, which allows to check if two quantum states are identical or similar. Starting from a measure for comparing classical probability distributions, a generalization to density matrices is discussed. Consider two probability distributions $\{p_x\}$ and $\{q_x\}$ over the same index set x . What does it mean if the two sets of probability distributions are similar to one another? There is no unique answer to such a question. A suitable measure that can be introduced is the trace distance [1]

$$D(p_x, q_x) \equiv \frac{1}{2} \sum_x |p_x - q_x|. \quad (2.25)$$

Its name anticipates its quantum mechanical generalization. However, it is also known more generally as L_1 or Kolmogorov distance. It turns out that Eq. (2.25) is a metric that fulfills the following conditions [76]:

- The distance of a point to itself is zero: $D(p_x, p_x) = 0$
- Positivity: $D(p_x, q_x) > 0$ for $p_x \neq q_x$
- Symmetry: $D(p_x, q_x) = D(q_x, p_x)$
- Triangle inequality: $D(p_x, r_x) \leq D(p_x, q_x) + D(q_x, r_x)$

for all probability distributions $\{p_x\}$, $\{q_x\}$ and $\{r_x\}$ over the same index set x . To motivate this definition physically, it can be shown that the trace distance is given by

$$D(p_x, q_x) = \max_S |p(S) - q(S)| = \max_S \left| \sum_{x \in S} p_x - \sum_{x \in S} q_x \right|, \quad (2.26)$$

where the maximization is performed over all subsets S of the index set x . The maximum is taken for the event S_{\max} , which is ideal to distinguish the probability distributions $\{p_x\}$

and $\{s_x\}$. The value of the trace distance governs how well it is possible to distinguish between two probability distributions.

In quantum information the object equivalent to the probability distribution is the density matrix. The trace distance of two density matrices ρ and σ is given by

$$D(\rho, \sigma) \equiv \frac{1}{2} \text{tr}\{|\rho - \sigma|\} = \frac{1}{2} \|\rho - \sigma\|_{\text{tr}}, \quad (2.27)$$

where the absolute value of an operator is defined as $|A| = \sqrt{A^\dagger A}$. By definition, the trace norm is equivalent to the sum over the singular values of $\rho - \sigma$. The trace distance of two commuting density matrices Eq. (2.27), is a generalization of the classical result Eq. (2.25). For two commuting density matrices, exists a common eigenbasis

$$\rho = \sum_{i=1}^d r_i |i\rangle \langle i|, \quad \sigma = \sum_{i=1}^d s_i |i\rangle \langle i|. \quad (2.28)$$

with the eigenvectors $\{|1\rangle, \dots, |d\rangle\}$ and the eigenvalues r_i of ρ and s_i of σ . From the definition, it follows that the trace distance of two simultaneously diagonalizable density matrices is the classical trace distance of the eigenvalues

$$D(\rho, \sigma) = \frac{1}{2} \left| \sum_{i=1}^d (r_i - s_i) |i\rangle \langle i| \right| = D(r_i, s_i). \quad (2.29)$$

The invariance of the trace distance under unitary transformations is inherited from the trace norm [73]

$$D(U\rho U^\dagger, U\sigma U^\dagger) = D(\rho, \sigma) \quad (2.30)$$

for all unitary transformations U . To relate the classical definition of the trace distance to that of quantum states, the difference $\rho - \sigma$ can be represented by two positive semidefinite operators Q and S with orthogonal support

$$\rho - \sigma = Q - S. \quad (2.31)$$

Therefore, the absolute value fulfills $|\rho - \sigma| = S + Q$ and

$$0 = \text{tr}\{\rho - \sigma\} = \text{tr}\{Q - S\} = \text{tr}\{Q\} - \text{tr}\{S\} \Rightarrow \text{tr}\{Q\} = \text{tr}\{S\}, \quad (2.32)$$

$$D(\rho, \sigma) = \frac{1}{2} \|\rho - \sigma\| = \frac{1}{2} (\text{tr}\{Q\} + \text{tr}\{S\}) = \text{tr}\{Q\}. \quad (2.33)$$

Measurements to distinguish density matrices can be found by the trace distance. Consider a POVM $\{\Pi_1, \dots, \Pi_n\}$ with $\sum_{i=1}^n \Pi_i = \mathbb{1}_d$ and $\Pi_i \geq 0$ for all $i \in \{1, \dots, n\}$. POVMs are dis-

cussed in detail in Section 2.3.2. The probability distributions of the measurement results are $p_i = \text{tr}\{\rho\Pi_i\}$ and $q_i = \text{tr}\{\sigma\Pi_i\}$. For the classical trace distance holds [c.f. Eq. (2.25)]

$$\begin{aligned}
D(p_n, q_n) &= \frac{1}{2} \sum_{i=1}^n |\text{tr}\{\Pi_i(\rho - \sigma)\}| \\
&= \frac{1}{2} \sum_{i=1}^n |\text{tr}\{\Pi_i(Q - S)\}| \\
&\leq \frac{1}{2} \sum_{i=1}^n \text{tr}\{\Pi_i(Q + S)\} \\
&= \frac{1}{2} \sum_{i=1}^n \text{tr}\{\Pi_i|\rho - \sigma|\} \\
&\leq \frac{1}{2} \text{tr}\{|\rho - \sigma|\} \\
&= D(\rho, \sigma).
\end{aligned} \tag{2.34}$$

Here, it has been used that the difference between two density matrices can be separated into two positive semidefinite operators S and Q and that the POVM elements sum to the identity. The trace distance for density matrices is given by

$$D(\rho, \sigma) = \max_{\Pi_i} \frac{1}{2} \sum_{i=1}^n |\text{tr}\{\Pi_i(\rho - \sigma)\}|, \tag{2.35}$$

where the maximization is performed over all POVMs. Therefore, a POVM that takes the maximum is optimal to measure the distance of two density matrices. Furthermore, such a POVM can be used to measure a classical distribution, with the same trace distance as the two quantum states. Thus, the trace distance can be interpreted as an upper bound of the difference between probability distributions of measurement results of the same POVM resulting from the quantum states ρ and σ . It can be easily seen that the trace distance of two quantum states fulfills the four defining properties of a metric

- The distance of a point to itself is zero: $D(\rho, \rho) = 0$
- Positivity: $D(\rho, \sigma) > 0$ for $\rho \neq \sigma$
- Symmetry: $D(\rho, \sigma) = D(\sigma, \rho)$
- Triangle inequality: $D(\rho, \tau) \leq D(\rho, \sigma) + D(\sigma, \tau)$

for all density matrices ρ , σ and τ . It has been shown that the trace distance defined over the trace norm of the difference between two quantum states is a natural tool to measure the distance between two quantum states [1]. Therefore, it is suitable to measure the distance between separable and entangled quantum states. The invariance under unitary transformations simplifies the calculation of the distance between these objects. It is noted that the difference between two quantum states can also be quantified by other measures, for example, the fidelity $F(\rho, \sigma) = \sqrt{\rho^{1/2}\sigma\rho^{1/2}}$. However, the subsequent sections will focus on trace norms to detect entanglement.

2.2 BIPARTITE SYSTEMS AND ENTANGLEMENT

Up to this point, only single-particle systems have been discussed, which will now be extended to distinguishable bipartite quantum systems. The state space of the bipartite system is given by the tensor product of the Hilbert spaces $\mathcal{H}_{AB} = \mathcal{H}_A \otimes \mathcal{H}_B$ with dimensions d_A and d_B . If the first subsystem is in a state $|\phi\rangle_A \in \mathcal{H}_A$ and the second subsystem in $|\psi\rangle_B \in \mathcal{H}_B$, then the composed system is in the product state [1]

$$|\phi\rangle = |\phi_A\rangle \otimes |\psi_B\rangle. \quad (2.36)$$

It is assumed that each subsystem has a local observer, Alice and Bob. Alice's observables or states are denoted by subscript A and Bob's by B.

Let $\{|k\rangle_A : k = 0, \dots, d_A - 1\}$ and $\{|l\rangle_B : l = 0, \dots, d_B - 1\}$ be orthonormal bases of the subsystems, then an orthonormal basis of the composed vector space is given by

$$|kl\rangle = |k\rangle \otimes |l\rangle : k = 0, \dots, d_A - 1, l = 0, \dots, d_B - 1\}. \quad (2.37)$$

The average value of a product state and an observable $O_A = O \otimes \mathbb{1}_{d_B}$ on the first subsystem is given by

$$\langle \phi | O_A | \phi \rangle = \langle \phi_A | O | \phi_A \rangle \langle \psi_B | \psi_B \rangle = \langle \phi_A | O | \phi_A \rangle. \quad (2.38)$$

For a general state $|\Psi\rangle \in \mathcal{H}_A \otimes \mathcal{H}_B$ and an observable on the first subsystem holds

$$\begin{aligned} \langle O_A \rangle &= \langle \Psi | O \otimes \mathbb{1}_{d_B} | \Psi \rangle \\ &= \sum_{k=0}^{d_A-1} \sum_{l=0}^{d_B-1} \langle \Psi | O \otimes \mathbb{1}_{d_B} | kl \rangle \langle kl | \Psi \rangle \end{aligned} \quad (2.39)$$

$$= \sum_{k=0}^{d_A-1} \sum_{l=0}^{d_B-1} \langle k | (\langle l | \Psi \rangle \langle \Psi | l \rangle) O | k \rangle. \quad (2.40)$$

This allows the definition of Alice's reduced density matrix

$$\rho_A = \text{tr}_B \{ |\Psi\rangle \langle \Psi| \} = \sum_{l=0}^{d_B-1} \langle l | \Psi \rangle \langle \Psi | l \rangle, \quad (2.41)$$

and analog for the second subsystem

$$\rho_B = \text{tr}_A \{ |\Psi\rangle \langle \Psi| \} = \sum_{k=0}^{d_A-1} \langle k | \Psi \rangle \langle \Psi | k \rangle. \quad (2.42)$$

The reduced density matrix of a subsystem contains all the information necessary to calculate the average values of a local observable of that subsystem. The Schmidt decomposition allows to write each state $|\Psi\rangle \in \mathcal{H}_A \otimes \mathcal{H}_B$ as a finite sum of orthogonal product states

$$|\Psi\rangle = \sum_{i=1}^n a_i |\phi_i\rangle \otimes |\psi_i\rangle \quad (2.43)$$

with the positive parameters $a_i > 0$ and orthogonal vectors $|\phi_i\rangle$ and $|\psi_i\rangle$. The Schmidt rank n refers to the number of product states required to represent the state vector. If a state has a

Schmidt rank $n = 1$, it is called separable, while, otherwise, it is called entangled. Therefore, a pure state is entangled if and only if the reduced density matrices are not pure.

Up to now, entanglement for mixed states has yet to be discussed. A separable mixed state is defined by a convex combination of product density matrices [74]

$$\rho = \sum_{i=1}^n p_i \rho_{A,i} \otimes \rho_{B,i}, \quad (2.44)$$

where $0 \leq p_i \leq 1$ and $\sum_{i=1}^n p_i = 1$. If ρ is not separable, it is entangled. To verify that a quantum state is entangled, it has to be shown that the representation Eq. (2.44) does not exist for this state. Even for the simple case of two qubits, it is difficult to determine if such a representation exists. Therefore, sufficient conditions for entanglement detection are needed to circumvent the search for such a representation. For two-qubits, the Bell states are an example of entangled states

$$\begin{aligned} |\Psi_{\pm}\rangle &= \frac{1}{\sqrt{2}} (|0\rangle \otimes |1\rangle \pm |1\rangle \otimes |0\rangle), \\ |\Phi_{\pm}\rangle &= \frac{1}{\sqrt{2}} (|0\rangle \otimes |0\rangle \pm |1\rangle \otimes |1\rangle) \end{aligned} \quad (2.45)$$

with two basis elements of the qubit subsystem $|0\rangle$ and $|1\rangle$. The four Bell states also form a basis for all pure two-qubit quantum states. Another way to think of entanglement is in terms of state preparation. A separable state can be prepared separately in both systems without communicating between the subsystems. However, preparing an entangled quantum state requires global operations on the quantum system.

2.2.1 The negative partial transpose

In the previous section, bipartite entanglement has been defined, but no simple condition has been given if a quantum state is entangled. The entanglement of bipartite quantum systems can be equivalently characterized by positive but not completely positive maps. A quantum state is separable if and only if

$$(\mathbb{1}_{d_A} \otimes \Phi_B)\rho \geq 0 \quad (2.46)$$

for all positive but not completely positive maps Φ_B [56, 58]. Restricting the positive maps to the matrix transpose leads to the negative partial transpose (NPT) condition. To formulate the sufficient NPT condition a closer look at the representation of a density matrix is required. A bipartite density matrix in the Hilbert space $\mathcal{H}_A \otimes \mathcal{H}_B$ can be represented in a product basis by [57, 58]

$$\rho = \sum_{i,j=0}^{d_A-1} \sum_{k,l=0}^{d_B-1} \rho_{ij,kl} |i\rangle\langle j| \otimes |k\rangle\langle l|. \quad (2.47)$$

In this basis, the partial transposition of the subsystems is defined by

$$\rho^{T_A} = (T \otimes \mathbb{1}_{d_B})\rho = \sum_{i,j=0}^{d_A-1} \sum_{k,l=0}^{d_B-1} \rho_{ji,kl} |i\rangle\langle j| \otimes |k\rangle\langle l|, \quad (2.48)$$

$$\rho^{T_B} = (\mathbb{1}_{d_A} \otimes T)\rho = \sum_{i,j=0}^{d_A-1} \sum_{k,l=0}^{d_B-1} \rho_{ij,lk} |i\rangle\langle j| \otimes |k\rangle\langle l|, \quad (2.49)$$

where T is the local transposition operator. For the partial transpose on the first subsystem, the indices i and j have been exchanged; for the second system, the indices k and l . A state is called positive partial transpose (PPT) if [57, 58]

$$\rho^{\text{T}_A} \geq 0 \Leftrightarrow \rho^{\text{T}_B} \geq 0. \quad (2.50)$$

If the matrix is not PPT, or the partial transposed matrix has at least one negative eigenvalue, such a matrix is called NPT. For a separable bipartite density matrix holds [57, 58]

$$\rho^{\text{T}_A} = \sum_{i=1}^n p_i \rho_{A,i}^{\text{T}} \otimes \rho_{B,i} = \sum_{i=1}^n p_i \tilde{\rho}_{A,i} \otimes \rho_{B,i} \geq 0. \quad (2.51)$$

If a density matrix is NPT, it is entangled. The NPT quantum states are independent of the basis representation of the density matrix. It has been demonstrated by the Horodeckis that the PPT quantum states are separable for two-qubit and qubit-qutrit systems [58]. In these particular dimensions, the sufficient condition is also necessary. It is often also called the Peres-Horodecki criterion. A disadvantage of the sufficient NPT condition is the difficulty in implementing the partial transpose for arbitrary quantum states. Thus, the emphasis is on detecting entanglement through local measurements that observers can conduct even at far distances.

2.2.2 Entanglement witnesses

In this section, the concept of the entanglement witness is discussed. The separable states are defined in Eq. (2.44) as a convex combination of product density matrices and such states also form a convex set within the convex set of all quantum states. The set of separable states can be characterized geometrically by average values of entanglement witnesses. An entanglement witness is an operator that has to have at least one negative eigenvalue and the average value for pure product states is non-negative

$$\langle \psi_A | \langle \psi_B | W | \psi_A \rangle | \psi_B \rangle \geq 0 \quad (2.52)$$

for all $|\psi_A\rangle \in \mathcal{H}_A$ and $|\psi_B\rangle \in \mathcal{H}_B$. The separable states have to fulfill

$$\text{tr}\{W \rho_{\text{sep}}\} \geq 0 \quad (2.53)$$

for all entanglement witnesses W [58, 77]. The proof utilizes the Hahn-Banach theorem [78]. However, it is important to note that the description of the entanglement witnesses does not require finite dimensional subsystems. A geometric representation of the entanglement witness is shown in Fig. 2.1. The green area denotes the convex set of separable quantum states, while the blue area represents entangled quantum states. The lines outline the hyperareas defined by the entanglement witness W and W_{opt} . An entanglement witness W' is called finer than W if it can certify all the entangled states detected by W [79]. In Fig. 2.1 the entanglement witness W_{opt} is both finer and optimal compared to W . An entanglement witness is called optimal if no finer witness exists. The optimal witness's solid line in Fig. 2.1 intersects with the set of separable quantum states. An example of an entanglement witness for bipartite systems with local dimensions d is given by [56, 80]

$$V = \sum_{i,j=0}^{d-1} |i\rangle \langle j| \otimes |j\rangle \langle i|. \quad (2.54)$$

It satisfies $\langle \psi_A | \langle \psi_B | V | \psi_A \rangle | \psi_B \rangle = |\langle \phi_A | \phi_B \rangle|^2 \geq 0$ and has the eigenvalue minus one. Entanglement witnesses are practical in identifying the entanglement of a specific quantum state. Furthermore, they can be implemented as an average value of a Hermitian operator W . However, a single entanglement witness cannot verify all entangled states. At least one entanglement witness can detect each entangled state. Therefore, to overcome this problem, sufficient entanglement conditions, including more than a single average value of a Hermitian operator, have to be considered.

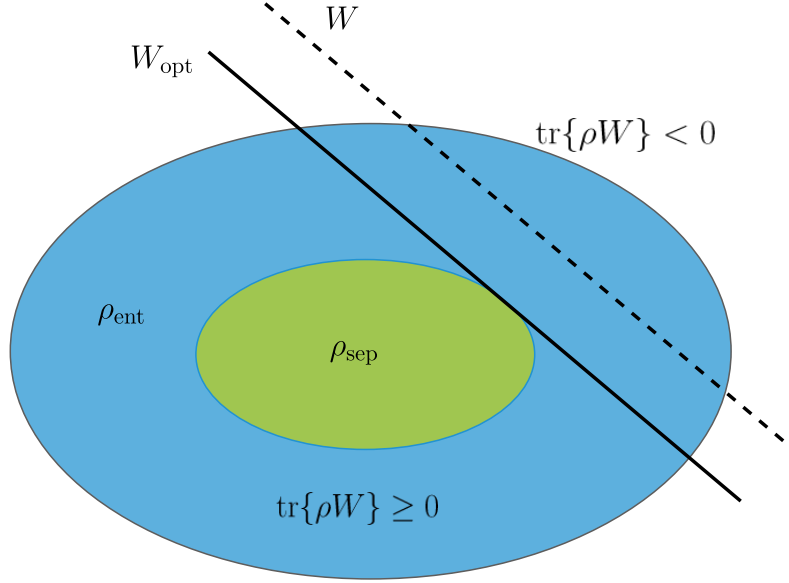


Figure 2.1: The geometric representation of a convex set of quantum states [56]: The green area marks the convex set of separable states surrounded by the entangled states (blue area). The hyperareas belonging to the entanglement witnesses are illustrated by lines. The quantum states on the left of the lines or the hyperplane itself, including the separable states fulfilling $\text{tr}\{W\rho\} \geq 0$. The quantum states on the right of the lines are witnessed as entangled by $\text{tr}\{\rho_{\text{ent}}W\} < 0$. The solid line denotes an optimal entanglement witness W_{opt} .

2.2.3 Entanglement detection by local measurements

In this section, a first method is shown how to detect entanglement of a bipartite quantum state by local measurements. It is assumed that Alice and Bob measure a Hermitian orthonormal basis G_A and G_B in their subsystems. This set of local measurements is called local orthonormal Hermitian operators basis (LOO). Here, the sets G_A and G_B are defined by Eq. (2.11). An arbitrary density matrix can be represented in the Hilbert-Schmidt vector space by

$$\rho = \sum_{k=0}^{d_A^2-1} \sum_{l=0}^{d_B^2-1} \rho_{kl} G_k^A \otimes G_l^B \quad (2.55)$$

with $\rho_{kl} = \langle G_k^A \otimes G_l^B | \rho | G_k^A \otimes G_l^B \rangle = \text{tr}\{\rho G_k^A \otimes G_l^B\}$. For further discussions, it is assumed that $d_A \leq d_B$. By using the Schmidt theorem, it can be shown that a basis \tilde{G}_A on Alice's subsystem exists, as

well as an orthonormal system \bar{G}_B on Bob's subsystem exists, such that any bipartite density matrix can be written as

$$\rho = \sum_{k=0}^{d_A^2-1} \lambda_k \bar{G}_k^A \otimes \bar{G}_k^B, \quad \lambda_k = \langle \bar{G}_k^A \otimes \bar{G}_k^B \rangle = \text{tr}\{\rho \bar{G}_k^A \otimes \bar{G}_k^B\} \quad (2.56)$$

where $\lambda_k \geq 0$. By using that separable density matrices are convex combinations of product density matrices [Eq. (2.44)], follows that all separable states have to fulfill [81]

$$\sum_{k=0}^{d_A^2-1} \lambda_k \leq 1. \quad (2.57)$$

This is the so-called computable cross norm realignment (CCNR) condition and a violation of this inequality is a sufficient condition for entanglement detection [82, 83]. An optimal representation of the form of Eq. (2.56) is required to determine whether a quantum state is entangled. This method of entanglement detection is closely related to the entanglement witness [84]

$$W = \mathbb{1}_{d_A} \otimes \mathbb{1}_{d_B} - \sum_{k=0}^{d_A^2-1} \bar{G}_k^A \otimes \bar{G}_k^B. \quad (2.58)$$

A quantum state ρ is entangled if the average value of the entanglement witness is negative $\langle W \rangle = \text{tr}\{W\rho\} < 0$. The entanglement witness is a measurement operator and can easily test if a quantum state is entangled. However, the detected entanglement depends on the chosen LOO. The next step is to unify this family of entanglement witnesses derived from different LOOs into a single inequality. The trace norm has previously been employed in Section 2.1.2 to quantify the dissimilarity between quantum states. Therefore, the trace norm can be used to detect entanglement. For this purpose, the joint probability matrix P is defined by

$$[P]_{kl} = \langle G_k^A \otimes G_l^B \rangle = \text{tr}\{G_k^A \otimes G_l^B \rho\} = p_{kl}. \quad (2.59)$$

The components of such a matrix for a separable quantum state Eq. (2.44) can be represented by

$$\begin{aligned} p_{kl} &= \sum_{i=1}^n p_i \langle \rho_i^A \otimes \rho_i^B G_k^A \otimes G_l^B \rangle \\ &= \sum_{i=1}^n p_i \langle \rho_i^A G_k^A \rangle \langle \rho_i^B G_l^B \rangle \\ &= \sum_{i=1}^n p_i a_{i,k} b_{i,l}. \end{aligned} \quad (2.60)$$

By introducing the vectors $\mathbf{a}_i = (a_{i,0} \dots a_{i,d_A^2-1})^T$ and $\mathbf{b}_i = (b_{i,0} \dots b_{i,d_B^2-1})^T$, the joint probability matrix can be written as sum of dyadic products

$$P = \sum_{i=1}^n p_i \mathbf{a}_i \mathbf{b}_i^T. \quad (2.61)$$

The trace or 1-norm defined by the sum of the singular values of such a matrix can be used to derive an inequality to detect entanglement. Moreover, the trace norm of the joint probability distribution is bounded by [85]

$$\begin{aligned}
\|P\|_{\text{tr}} &= \left\| \sum_{i=1}^n p_i \mathbf{a}_i \mathbf{b}_i^T \right\|_{\text{tr}} \\
&\leq \sum_{i=1}^n p_i \|\mathbf{a}_i \mathbf{b}_i^T\|_{\text{tr}} \\
&= \sum_{i=1}^n p_i \|\mathbf{a}_i\| \|\mathbf{b}_i\| \\
&= \sum_{i=1}^n p_i \sqrt{\sum_{k=0}^{d_A^2-1} a_{i,k}^2 \sum_{l=0}^{d_B^2-1} b_{i,l}^2} \\
&= \sum_{i=1}^n p_i \sqrt{\text{tr}\{\rho_i^{A^2}\} \text{tr}\{\rho_i^{B^2}\}} \\
&\leq \sum_{i=1}^n p_i = 1
\end{aligned} \tag{2.62}$$

On the first lesser equal sign, the triangle inequality has been used, followed by the cross norm property of the trace norm for dyadics. At the last line, the purity condition of density matrices has been used. This implies that all separable states have to fulfill

$$\|P\|_{\text{tr}} \leq 1. \tag{2.63}$$

Violating this inequality detects a quantum state as entangled. An important property of the trace norm is the invariance under local orthogonal transformations O_A and O_B [73]

$$\|O_A P O_B\|_{\text{tr}} = \|P\|_{\text{tr}} \tag{2.64}$$

with $O_A^T O_A = \mathbb{1}_{d_A}$ and $O_B^T O_B = \mathbb{1}_{d_B}$. This means that two LOOs, which can be transformed into each other by orthogonal transformations (B.4)

$$(G_0^A, \dots, G_{d_A^2-1}^A)^T = O_A (\tilde{G}_0^A, \dots, \tilde{G}_{d_A^2-1}^A)^T \tag{2.65}$$

$$(G_0^B, \dots, G_{d_B^2-1}^B)^T = O_B (\tilde{G}_0^B, \dots, \tilde{G}_{d_B^2-1}^B)^T \tag{2.66}$$

have joint probability matrices with identical trace norms. Therefore, the trace norm-based inequality Eq. (2.63) is basis independent. By using the basis of Eq. (2.56), the trace norm is given by

$$\|P\|_{\text{tr}} = \sum_{k=0}^{d_A^2-1} \lambda_k \leq 1. \tag{2.67}$$

This example illustrates the applicability of trace norms in entanglement detection. These equivalent sufficient conditions based on LOOs [Eqs. (2.57), (2.58) and (2.63)], have been discussed in this section. However, it is important to note that the first two conditions depend on the selected LOOs for a given density matrix. The entanglement witness offers an advantage as it can be measured directly. However, the LOO has to be optimized to detect the most

entangled quantum states. The basis-independent trace norm-based sufficient condition does not require an optimized measurement, making it well-suited for detecting entanglement of arbitrary density matrices without the need to select an optimal LOO. Therefore, the focus on entanglement detection in Chapter 5 is on trace norms of correlation or joint probability matrices.

2.3 MEASUREMENTS IN QUANTUM MECHANICS

The state of a quantum system can only be figured out by performing measurements. To do this, the observer must couple their external system to the quantum system of interest [72]. As a consequence, the quantum system is not necessarily closed anymore and can experience a non-unitary evolution. Thus, the postulates for quantum measurements are presented. In the first subsection, projective measurements are described. These definitions are extended to generalized measurements in the second subsection.

2.3.1 Projective measurements

In quantum mechanics, a projective or von Neumann measurement in a d -dimensional quantum system is described by a Hermitian operator X [1]. A Hermitian operator has the spectral decomposition of

$$X = \sum_{j=1}^n P_j \lambda_j \quad (2.68)$$

with the real-valued eigenvalues λ_j , the spectral projections P_j and the number of different eigenvalues n . If the spectrum of the measurement operators is non-degenerate, it can be written with rank one spectral projectors

$$X = \sum_{j=1}^d \lambda_j |j\rangle\langle j|. \quad (2.69)$$

The following six points summarize how the measurement affects the state and distribution of the outcomes [72]:

1. The projectors are complete $\sum_{j=1}^n P_j = \mathbb{1}_d$.
2. The spectral projections of a measurement operator fulfill $P_i P_j = P_i \delta_{ij}$. Therefore, their eigenvalues are zero and one.
3. The measurement results of X are the eigenvalues λ_i .
4. The quantum state after performing the measurement after an initial preparation $|\phi\rangle$ or ρ and recording the result λ_j is

$$|\phi_j\rangle = \frac{P_j |\phi\rangle}{\sqrt{\langle \phi | P_j | \phi \rangle}},$$

$$\rho_j = \frac{P_j \rho P_j}{\text{tr}\{P_j \rho\}}.$$

5. The probability to measure λ_j is given by

$$p_j = \langle \phi | P_j P_j | \phi \rangle = \langle \phi | P_j | \phi \rangle,$$

$$p_j = \text{tr}\{P_j \rho\}.$$

6. If the measurement is performed but the state is not recorded, the post-measurement quantum state is

$$\tilde{\rho} = \sum_{j=1}^n p_j |\phi_j\rangle\langle\phi_j|,$$

$$\tilde{\rho} = \sum_{j=1}^n p_j \rho_j.$$

For postulates 4.-6., pure and mixed states have been discussed. Summarizing the postulates 1.-3., for a given von Neumann measurement and a quantum state, the average value and the probability of a particular outcome are known. However, the occurrence of a specific measurement outcome is unpredictable. The statistical behavior of repeating measurements on copies of an initial quantum state is described by the quantum state $|\phi\rangle$ or density matrix ρ . The measurement result can only be predicted for outcomes with a probability of one. Moreover, the eigenvalues λ_j and the probabilities p_j can be used to determine the average values of an observable

$$\langle X \rangle = \sum_{j=1}^n \lambda_j p_j = \sum_{j=1}^n \lambda_j \text{tr}\{P_j \rho\} = \text{tr}\{X \rho\}. \quad (2.70)$$

Furthermore, higher moments can be calculated for $k \geq 2$ by

$$\langle X^k \rangle = \sum_{j=1}^n \lambda_j^k p_j = \sum_{j=1}^n \lambda_j^k \text{tr}\{P_j \rho\} = \text{tr}\{X^k \rho\} \quad (2.71)$$

and most importantly, from such moments is the second moment $k = 2$, which is related to the variance by

$$V(X, \rho)^2 = \langle (X - \langle X \rangle)^2 \rangle = \langle X^2 \rangle - \langle X \rangle^2. \quad (2.72)$$

The variance or standard deviation is a measure that describes the deviation of measurement results from their average value. If a measurement for a given state is repeated multiple times, the standard deviation is given by $\sqrt{V(X, \rho)}$. The number of possible different eigenvalues limits the outcomes of a von Neumann measurement. In the case of a Hermitian operator with a non-degenerate spectrum, the maximum number of different measurement results is the dimension d . In the subsequent section, von Neumann measurements are generalized to support any number of possible outcomes.

2.3.2 Positive operator valued measures (POVM)

In the previous section, the von Neumann measurement has been introduced. The number of distinct measurement outcomes λ_j is limited by the dimension of the Hilbert Space d , since the maximum number of orthogonal projections satisfying $P_i P_j = \delta_{ij} P_i$ is restricted to d . It

is desirable to perform measurements with more results. To achieve this the postulates of projective measurements are applied to compute the probability distribution of $0 \leq p_j \leq 1$ with $\sum_{j=1}^M p_j = 1$. In postulate 5, it is observed that the positive semidefiniteness is only required for P_j^2 and can be relaxed for P_j . Therefore, a new probability distribution is proposed with positive semidefinite operators $\Pi_j \geq 0$ by

$$p_j = \text{tr}\{\Pi_j \rho\}. \quad (2.73)$$

From the definition of probability distributions follows

$$1 = \sum_{j=1}^M p_j = \sum_{j=1}^M \text{tr}\{\Pi_j \rho\} = \text{tr}\left\{\sum_{j=1}^M \Pi_j \rho\right\}, \quad (2.74)$$

$$\Rightarrow \sum_{j=1}^M \Pi_j = \mathbb{1}_d. \quad (2.75)$$

Here, M denotes the number of measurement results. Therefore, the operators Π_j have to sum up to the identity so that the parameters p_j form a probability distribution for any quantum state ρ . A generalized measurement is defined by a decomposition of the identity operator into M positive semidefinite operators. These operators are called a positive operator valued measure (POVM). For projective measurements, the P_j describing the post-measurement states (postulate 4) are generalized for POVMs. Assuming arbitrary operators A_j , which describe the post-measurement state by

$$|\phi_j\rangle = \frac{A_j |\phi\rangle}{\sqrt{\langle \phi | A_j^\dagger A_j | \phi \rangle}}. \quad (2.76)$$

The operators are related to positive semidefinite operators by $\Pi_j = A_j^\dagger A_j$. Additionally, it is seen that the form $A_j = U_j \Pi_j^{1/2}$ maintains the positive semidefinite operator invariant, where U_j is an arbitrary unitary matrix. From the positive semidefiniteness of Π_j , it follows that the square root of such operators exists. The same POVM may generate various measurement operators A_j . Thus, the POVM elements are not described by unique measurement operators A_j . For POVMs, the measurement operators have been generalized from P_j to A_j and the probability defining operators from P_j^2 to Π_j . The following postulates summarize the definition of a POVM [72]:

- (i) The POVM elements $\Pi_j \geq 0$ are complete, i.e. $\sum_j \Pi_j = \mathbb{1}_d$.
- (ii) The POVM elements can be generated by operators A_j with $\Pi_j = A_j^\dagger A_j$, which have a polar decomposition $A_j = U_j \Pi_j^{1/2}$. The unitary operators U_j keep the POVM elements Π_j invariant.
- (iii) The measurement yields alternatives belonging to one of its elements.
- (iv) The quantum state belonging to the measurement output Π_j is given by

$$|\phi_j\rangle = \frac{A_j |\phi\rangle}{\sqrt{\langle \phi | A_j^\dagger A_j | \phi \rangle}},$$

$$\rho_j = \frac{A_j \rho A_j^\dagger}{\text{tr}\{A_j \rho A_j^\dagger\}}.$$

(v) The probability to measure Π_j is given by

$$p_j = \langle \phi | \Pi_j | \phi \rangle = \langle \phi_j | A_j^\dagger A_j | \phi_j \rangle,$$

$$p_j = \text{tr}\{\Pi_j \rho\}.$$

(vi) If a measurement is performed but the result is not recorded, the post-measurement quantum state is

$$\tilde{\rho} = \sum_{j=1}^M p_j \rho_j = \sum_{j=1}^M A_j \rho A_j^\dagger.$$

Often, it is enough to know only the probability distribution of the outcomes, in which case only postulates (i), (iii) and (v) are needed. Moreover, the operators A_j are not uniquely defined by the POVM, as various measurement operators A_j can create POVMs with identical probability distributions for arbitrary quantum states. For instance, operators A_j and $U_j A_j$, where U_j represents an arbitrary unitary operators, produce identical POVM elements Π_j . The operator A_j represents a physical implementation of the POVM Π_j . The POVM elements do not need to be orthogonal to fulfill the postulates. This implies that the dimension of the quantum system d does not limit the number of measurement results M . By coupling the quantum system to an ancilla system $\mathcal{H}_A \otimes \mathcal{H}_B$, the equivalence between a POVM $\{\Pi_j\}$ and von Neumann measurement on the composite system can be shown by Neumark's theorem [72].

An advantage of POVMs over projective measurements is demonstrated by an example. Suppose there are two linearly independent non-orthogonal quantum states $|\langle \phi_1 | \phi_2 \rangle| > 0$. In an experiment, one of the two states is randomly prepared. An observer wants to measure which of these two states has been prepared. In order to unambiguously discriminate between the two pure states, the observer cannot make an error. It is forbidden to announce that $|\phi_1\rangle$ has been measured if in reality $|\phi_2\rangle$ has been prepared or vice versa. Firstly, it is demonstrated that this task cannot be accomplished with absolute certainty. Assuming a POVM with two measurement results Π_1 and Π_2 , which fulfills

$$\Pi_1 + \Pi_2 = \mathbb{1}_d \quad (2.77)$$

$$\Pi_1 |\phi_2\rangle = 0, \quad (2.78)$$

$$\Pi_2 |\phi_1\rangle = 0. \quad (2.79)$$

From the completeness relation of the POVMs follows that

$$p_1 = \langle \phi_1 | \Pi_1 | \phi_1 \rangle = 1, \quad (2.80)$$

$$p_2 = \langle \phi_2 | \Pi_2 | \phi_2 \rangle = 1. \quad (2.81)$$

Both probabilities are equal to one, which means that this represents perfect state discrimination, but multiplying Eq. (2.77) by $\langle \phi_1 |$ and $|\phi_2\rangle$ leads to

$$0 = \langle \phi_1 | \Pi_1 | \phi_2 \rangle + \langle \phi_1 | \Pi_2 | \phi_2 \rangle = \langle \phi_1 | \phi_2 \rangle. \quad (2.82)$$

This can only be fulfilled if the states are orthogonal, which is inconsistent with the assumption of non-orthogonal quantum states. It is impossible to obtain a perfect state discrimination for two non-orthogonal quantum states. For error-free identification of the two quantum states,

an additional measurement result is necessary, so that the observer is uncertain about which state has been prepared. Thus, the modified POVM is given by

$$\mathbb{1}_d = \Pi_1 + \Pi_2 + \Pi_0 \quad (2.83)$$

so that the Eqs. (2.78) and (2.79) are still fulfilled. The probability distributions for the two quantum states are given by

$$p_1 = \langle \phi_1 | \Pi_1 | \phi_1 \rangle, \quad (2.84)$$

$$q_1 = \langle \phi_1 | \Pi_0 | \phi_1 \rangle, \quad (2.85)$$

$$p_2 = \langle \phi_2 | \Pi_2 | \phi_2 \rangle, \quad (2.86)$$

$$q_2 = \langle \phi_2 | \Pi_0 | \phi_2 \rangle. \quad (2.87)$$

The state $|\phi_1\rangle$ can be identified with a success probability of p_1 , while the observer remains uncertain which state has been prepared with a probability of q_1 . Analog for q_2 and p_2 if state $|\phi_2\rangle$ was prepared. By defining an inconclusive detection outcome, a POVM can identify the prepared state without an error. Thus far, unambiguous discrimination has solely been explored for POVMs and has not been analyzed on projective measurements. Let's consider the projection $P_1 = |\phi_1\rangle\langle\phi_1|$ of the subspace spanned by $|\phi_1\rangle$ and $\bar{P}_1 = \mathbb{1} - |\phi_1\rangle\langle\phi_1|$ the projection on the subspace orthogonal to $|\phi_1\rangle$. The projection operators have to fulfill

$$\mathbb{1} = P_1 + \bar{P}_1. \quad (2.88)$$

If the observer detects the measurement result for \bar{P}_1 , then the state $|\phi_2\rangle$ must be prepared. It is important to note that the measurement result for P_1 can belong to both states. However, these measurement settings cannot certify that $|\phi_1\rangle$ has been prepared. Nonetheless, $|\phi_1\rangle$ can be certified with an analogous result achieved from projections $P_2 = |\phi_2\rangle\langle\phi_2|$ and $\bar{P}_2 = \mathbb{1} - |\phi_2\rangle\langle\phi_2|$. Identifying both quantum states through a single projective measurement without an error is impossible. However, POVMs have an advantage in identifying both states with non-zero probability.

2.4 RANDOMLY GENERATED DENSITY MATRICES

The efficiency and statistical features of the discussed sufficient conditions will be analyzed by calculating the Euclidean volume ratios of detected entangled quantum states. To efficiently generate bipartite qudit density matrices, a Monte Carlo algorithm is utilized through a hit-and-run approach [86, 87]. It is important to note that a bipartite density matrix can be by Eq. (2.17)

$$\rho = \frac{1}{\sqrt{d_A d_B}} \tilde{G}_0^A \otimes \tilde{G}_0^B + \sum_{i=1}^{d_A^2-1} a_i \tilde{G}_i^A \otimes \tilde{G}_0^B + \sum_{j=1}^{d_B^2-1} b_j \tilde{G}_0^A \otimes \tilde{G}_j^B + \sum_{i=1}^{d_A^2-1} \sum_{j=1}^{d_B^2-1} t_{ij} \tilde{G}_i^A \otimes \tilde{G}_j^B \quad (2.89)$$

$$= \frac{1}{d_A d_B} \mathbb{1}_{d_A d_B} + \sum_{i=1}^{d_A^2-1} \frac{a_i}{\sqrt{d_B}} \tilde{G}_i^A \otimes \mathbb{1}_{d_B} + \sum_{j=1}^{d_B^2-1} \frac{b_j}{\sqrt{d_A}} \mathbb{1}_{d_A} \otimes \tilde{G}_j^B + \sum_{i=1}^{d_A^2-1} \sum_{j=1}^{d_B^2-1} t_{ij} \tilde{G}_i^A \otimes \tilde{G}_j^B. \quad (2.90)$$

The correlation matrix is defined by $[T]_{ij} = t_{ij}$ and the vectors \mathbf{a} and \mathbf{b} describe the reduced density matrices of Alice's and Bob's subsystems

$$\rho_A = \frac{1}{d_A} \mathbb{1}_{d_A} + \sum_{i=1}^{d_A^2-1} a_i \tilde{G}_i^A = \frac{1}{d_A} \mathbb{1}_{d_A} + \mathbf{a} \cdot \tilde{\mathbf{G}}^A, \quad (2.91)$$

$$\rho_B = \frac{1}{d_B} \mathbb{1}_{d_B} + \sum_{j=1}^{d_B^2-1} b_j \tilde{G}_j^B = \frac{1}{d_B} \mathbb{1}_{d_B} + \mathbf{b} \cdot \tilde{\mathbf{G}}^B. \quad (2.92)$$

Thus, the bipartite density matrices belong to a convex subset of a real vector space of dimension $d_A^2 d_B^2 - 1 = \bar{d}^2 - 1$. However, a vector can represent a density matrix only if it represents a positive semidefinite matrix. The positive semidefiniteness of a matrix ρ is equivalently defined by [73]:

1. A matrix $\rho \geq 0$ is positive semidefinite.
2. The eigenvalues $\lambda_i \geq 0$ of ρ are non-negative.
3. The average value $\langle \phi | \rho | \phi \rangle \geq 0$ is non-negative for all $|\phi\rangle \in \mathcal{H}_{\bar{d}}$.
4. The matrix ρ can be decomposed by $\rho = A^\dagger A$.
5. The matrix ρ can be decomposed by $\rho = B B$.

Calculating the eigenvalues is the easiest way to check if a matrix is positive semidefinite because it does not require checking the average values $\langle \phi | \rho | \phi \rangle$ for an infinite number of vectors or constructing the matrices A or B . The characteristic polynomial $p_\rho(\lambda)$ is given by

$$p_\rho(\lambda) = \det(\xi \mathbb{1}_{\bar{d}} - \rho) = \sum_{k=0}^{\bar{d}} (-1)^k c_k^{(\bar{d})} \lambda^{\bar{d}-k} \quad (2.93)$$

with

$$\begin{aligned} c_0^{(\bar{d})} &= 1, \\ &\vdots \\ c_1^{(\bar{d})} &= \sum_{i=1}^{\bar{d}} \lambda_i, \\ c_{\bar{d}}^{(\bar{d})} &= \lambda_1 \lambda_2 \dots \lambda_{\bar{d}}. \end{aligned} \quad (2.94)$$

The coefficients can be calculated with the Cayley-Hamilton theorem, which first was introduced by [88]. The positive semidefiniteness of the matrix ρ is equivalently characterized by Descartes' rule of signs [86]

$$\rho \geq 0 \Leftrightarrow c_k^{(\bar{d})} \geq 0, \forall k \in \{0, 1, \dots, \bar{d}\}. \quad (2.95)$$

Therefore, the coefficients $c_k^{(\bar{d})}$ can be related to the trace of the powers of the matrix $\theta_k = \text{tr}\{\rho^k\}$ by the Newton identities [89]

$$\begin{aligned}\theta_1 &= c_1^{(\bar{d})} \\ \theta_k &= \sum_{i=1}^{k-1} (-1)^{i+1} c_i^{(\bar{d})} \theta_{k-1} + (-1)^{k+1} c_k^{(\bar{d})}, \quad 1 < k \leq \bar{d} \\ \theta_{\bar{d}} &= \sum_{i=1}^{k-1} (-1)^{i+1} c_i^{(\bar{d})} \theta_{k-1}, \quad k > \bar{d}.\end{aligned}\tag{2.96}$$

Moreover, for a Hermitian matrix with $\text{tr}\{\rho\} = 1$, all the coefficients $c_k^{(\bar{d})}$ can be obtained from the Newton identities. The first four Newton coefficients are

$$\begin{aligned}c_1^{(\bar{d})} &= 1, \\ c_2^{(\bar{d})} &= \frac{1}{2} - \frac{1}{2}\theta_2, \\ c_3^{(\bar{d})} &= \frac{1}{6} - \frac{1}{2}\theta_2 + \frac{1}{3}\theta_3, \\ c_4^{(\bar{d})} &= \frac{1}{24} - \frac{1}{4}\theta_2 + \frac{1}{3}\theta_3 + \frac{1}{8}\theta_2^2 - \frac{1}{4}\theta_4.\end{aligned}\tag{2.97}$$

The non-negativity of the coefficients $c_i \geq 0$ completely characterizes the positive semidefiniteness of the matrix ρ [86]. This effective method is used to verify whether a generated matrix is positive semidefinite. Furthermore, a generated positive semidefinite matrix is a density matrix. The bipartite quantum state is completely described by the vector $\mathbf{r} = (\mathbf{a}, \mathbf{b}, \text{vec}(T))^T \in \mathcal{H}_{\bar{d}^2-1}$ within the convex set of quantum states. This provides a comprehensive description of bipartite quantum states. A hit-and-run Monte Carlo algorithm can produce quantum states that are uniformly distributed [86, 87]. Additionally, this algorithm is applicable to general convex sets [90]. The formalism can be outlined in 5 steps:

- (1) Initialize the start point \mathbf{r}^j , for $j = 1$.
- (2) Generate a random direction $\hat{e}^{(j)}$ in dimension $\bar{d}^2 - 1$.
- (3) Define the maximum distance to the boundary $r_b = 2\sqrt{\bar{d}-1}/\sqrt{\bar{d}}$ Eq. (2.18) and set the interval $I = [-r, r]$.
- (4) Generate a uniformly random variable l in the interval I .
- (5) Check if $\mathbf{r}^j + l\hat{e}^{(j)}$ represents a density matrix, then $\mathbf{r}^{j+1} = \mathbf{r}^j + l\hat{e}^{(j)}$ and go back to step (2). Otherwise, set the interval to $I = [-r, l]$ or $I = [l, r]$, so that zero is included inside the interval and go back to (4).

A simulation begins with the maximally mixed density matrix, represented by the zero vector $\mathbf{0}$. This algorithm reaches convergence in polynomial time [91]. Consider l_b as the closest distance from the starting point to the boundary of the convex set, the algorithm converges in $O(\bar{d}^4 \ln^3(\bar{d}/l_b))$ steps [92]. When the convex set is in a near-isotropic position [93], the time of convergence is $O(\bar{d}^3)$ [92]. It is assumed that a uniform distribution occurs after a sample size between $O(\bar{d}^3)$ and $O(\bar{d}^4 \ln^3(\bar{d}))$. The hit-and-run Monte Carlo algorithm enables the efficient generation of low-dimensional bipartite density matrices for testing the effectiveness of sufficient conditions for entanglement and EPR steering detection.

2.5 LOCAL REALISM AND BIPARTITE EINSTEIN-PODOLSKY-ROSEN STEERABILITY

The concept of entanglement has been defined in Section 2.2, along with the first set of inequalities that can detect entanglement. However, the influence of entanglement on the results of local measurements on a bipartite quantum system still has to be discussed. Einstein had already pointed out the occurrence of "spooky action at a distance" during the collapse of the entire wave function during a local measurement. Therefore, Einstein, Podolsky and Rosen questioned the reality and locality of quantum mechanics [14]. Modifying this gedankenexperiment to spin-1/2 particles enabled an experimental verification of the locality of quantum mechanics [94]. Thus, in the first part of this section, the nonlocality of quantum mechanics and potential verifications are discussed. Another nonlocal quantum effect is the EPR steerability of quantum systems, in which case local measurements can affect the results of local measurements on a composite system. This asymmetric effect is introduced in the second section, including possible verifications, followed by the relation between EPR steerability and joint measurability of POVMs.

2.5.1 Nonlocality of quantum mechanics

The theory of special relativity distinguishes between space-like and time-like events, which are governed by local realism. This led Einstein, Podolsky and Rosen to question the completeness of quantum mechanics. They defined physical reality as follows: "*If without in any way disturbing a system, we can predict with certainty (i.e. with probability equal to unity) the value of a physical quantity, there exists an element of physical reality corresponding to this physical quantity*" [14]. The principle of locality states that two objects must be in proximity to interact with each other. Even in the interaction between a transmitter and receiver by long-range forces like electromagnetic waves, the signals can maximally travel with the speed of light. A far-distant separated system cannot be instantaneously disturbed by local measurement. In order to describe this physical phenomenon, two spatially distant observers, Alice and Bob, are considered. A source emits bipartite particles, with one particle traveling to Alice and the other to Bob, as shown in Fig. 2.2. Both parties can perform measurements on their local systems. Furthermore, Alice can choose a measurement setting $\alpha \in \mathcal{O}_A$ and Bob can choose $\beta \in \mathcal{O}_B$ with the results $a \in \mathcal{M}_A$ for Alice's measurements and $b \in \mathcal{M}_B$ for Bob's. The labels of the measurements are of a macroscopic nature to distinguish the different measurement outputs. Only the measurement statistics are important. In general, the joint probability distribution of choosing a measurement and receiving the outputs does not necessarily fulfill

$$P(a, b|\alpha, \beta) = P(a|\alpha)P(b|\beta), \quad (2.98)$$

implying that the statistics of both parties are not independent. For example, this can be physically realized by performing local measurements on two spin 1/2-particles. This statistical behavior can be explained by particles that have interacted in the past and are observed by distant observers. If the two particles have been emitted from a common source, the correlation can be established at the source. A local theory implies that during the interaction in the past, a correlation between the two particles has been established. The emission process's state can be described by the variable λ , which influences the outcomes of Alice's and Bob's local measurements. The parameter λ describes uncontrollable physical parameters of the system that can vary between experiment repetitions. If the hidden parameter λ would be

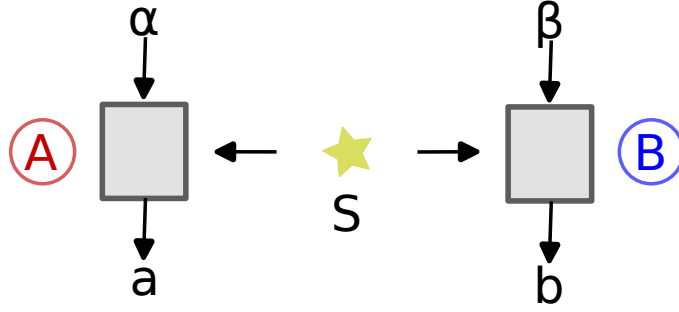


Figure 2.2: Schematic representation of Alice's and Bob's bipartite quantum system: Alice and Bob can perform measurements on their local quantum system with settings α and β , and their associated results a and b . A common source S emits a bipartite quantum state.

known, the results of Alice's and Bob's measurements could be predicted with certainty. For a local hidden variable, the outcomes of the systems decouple

$$P(a, b|\alpha, \beta, \lambda) = P(a|\alpha, \lambda)P(b|\beta, \lambda). \quad (2.99)$$

The different values of λ are characterized by a probability distribution $p(\lambda)$. The separability of the joint probability distribution for a given λ allows writing the joint probability distribution as

$$P(a, b|\alpha, \beta) = \sum_{\lambda \in \Lambda} p(\lambda)P(a|\alpha, \lambda)P(b|\beta, \lambda), \quad (2.100)$$

while the normalization gives

$$1 = \sum_{\lambda \in \Lambda} p(\lambda) \quad (2.101)$$

with the hidden parameters λ belonging to the index set Λ . This explanation of joint probabilities is called a local hidden variable model (LHV). Correlations that a LHV model cannot explain are said to be nonlocal.

The statistical behavior of quantum systems can differ from that of classical systems. Thus, the joint probability distributions of local POVMs are examined and compared to those of LHV models. Consider Alice and Bob sharing a Hilbert space $\mathcal{H}_A \otimes \mathcal{H}_B$ with local dimensions d_A and d_B . Furthermore, they can perform local POVMs their respective subsystems $\{\Pi_{\alpha,a} \geq 0\}$ and $\{\Pi_{\beta,b} \geq 0\}$ with

$$\sum_a \Pi_{\alpha,a} = \mathbb{1}_{d_A}, \quad \sum_b \Pi_{\beta,b} = \mathbb{1}_{d_B}. \quad (2.102)$$

For more details about POVMs, see Section 2.3.2. For a given quantum state ρ , the joint probability distribution is given by

$$P(a, b|\alpha, \beta) = \text{tr}\{\Pi_{\alpha,a} \otimes \Pi_{\beta,b} \rho\}. \quad (2.103)$$

The joint probability distribution of a separable quantum state can be calculated by inserting Eq. (2.44) into Eq. (2.103)

$$P(a, b|\alpha, \beta) = \sum_{i=1}^n p_i \text{tr}\{\Pi_{\alpha,a} \rho_{A,i}\} \text{tr}\{\Pi_{\beta,b} \rho_{B,i}\}. \quad (2.104)$$

It is immediately evident that a LHV model can explain the correlations of a separable quantum state. Therefore, separable quantum states are local. In order to verify if the correlations of entangled quantum states can be explained by a LHV model from Eq. (2.100), the Bell inequalities can be derived [22, 95]. Consider that each observer performs two local quantum measurements on their subsystem with settings α_0 and α_1 for Alice and β_0 and β_1 for Bob. The possible outcomes are limited to two values $a, b \in \{-1, 1\}$. The average value of a joint measurement of Alice and Bob is given by

$$\langle \alpha_i \beta_j \rangle = \sum_{a,b} ab p(a, b | \alpha, \beta) = \sum_{a,b} \sum_{\lambda \in \Lambda} ab p(\lambda) P(a | \alpha, \lambda) P(b | \beta, \lambda). \quad (2.105)$$

These average values allow the definition of

$$\begin{aligned} S &= \langle \alpha_0 \beta_0 \rangle + \langle \alpha_0 \beta_1 \rangle + \langle \alpha_1 \beta_0 \rangle - \langle \alpha_1 \beta_1 \rangle \\ &= \sum_{\lambda \in \Lambda} p(\lambda) S_\lambda, \end{aligned} \quad (2.106)$$

$$S_\lambda = \langle \alpha_0 \rangle_\lambda \langle \beta_0 \rangle_\lambda + \langle \alpha_0 \rangle_\lambda \langle \beta_1 \rangle_\lambda + \langle \alpha_1 \rangle_\lambda \langle \beta_0 \rangle_\lambda - \langle \alpha_1 \rangle_\lambda \langle \beta_1 \rangle_\lambda. \quad (2.107)$$

It has been used that for a LHV model, the joint probability distribution for a given λ factorizes and the local average values are given by

$$\langle \alpha_i \rangle_\lambda = \sum_a a P(a | \alpha_i, \lambda), \quad (2.108)$$

$$\langle \beta_j \rangle_\lambda = \sum_b b P(b | \beta_j, \lambda). \quad (2.109)$$

The allowed values of S can be calculated by

$$\begin{aligned} |S_\lambda| &\leq |\langle \alpha_0 \rangle_\lambda| |\langle \beta_0 \rangle_\lambda + \langle \beta_1 \rangle_\lambda| + |\langle \alpha_1 \rangle_\lambda| |\langle \beta_0 \rangle_\lambda - \langle \beta_1 \rangle_\lambda| \\ &\leq |\langle \beta_0 \rangle_\lambda + \langle \beta_1 \rangle_\lambda| + |\langle \beta_0 \rangle_\lambda - \langle \beta_1 \rangle_\lambda| = 2. \end{aligned} \quad (2.110)$$

It has been used that $|\langle \alpha_i \rangle_\lambda| \leq 1$ holds. Therefore, the value of S is bounded by

$$-2 \leq S = \sum_{\lambda \in \Lambda} p(\lambda) S_\lambda \leq 2. \quad (2.111)$$

This inequality is called the Clauser-Horne-Shimony-Holt (CHSH) inequality [96]. The values inside the bounds are the allowed values under consideration of a LHV model.

In the quantum mechanical case, Alice and Bob have a qubit as a local quantum system and the measurements are denoted by 3-dimensional unit vectors α_i and β_j , which describe the quantum measurements $\alpha_i = \alpha_i \cdot \sigma$ and $\beta_j = \beta_j \cdot \sigma$ with the Pauli matrices $\sigma = (\sigma_1, \sigma_2, \sigma_3)^T$ Eq. (B.8). The CHSH operator is given by

$$S = \alpha_0 \otimes \beta_0 + \alpha_0 \otimes \beta_1 + \alpha_1 \otimes \beta_0 - \alpha_1 \otimes \beta_1 \quad (2.112)$$

and the average value is

$$\langle S \rangle = \text{tr}\{\rho S\} = 2\langle \alpha_0, T_\rho(\beta_0 + \beta_1) \rangle + 2\langle \alpha_1, T_\rho(\beta_0 - \beta_1) \rangle. \quad (2.113)$$

The representation of a quantum state in a LOO has been used, as introduced in Eq. (2.90). By utilizing the orthogonality of the vectors $\beta_0 + \beta_1$ and $\beta_0 - \beta_1$, it has been shown that the CHSH inequality is violated if and only if the following condition is fulfilled [86]

$$\mu_1 + \mu_2 > 1/4 \quad (2.114)$$

where μ_1 and μ_2 are the two largest eigenvalues of $T_\rho^T T_\rho$, defined in Eq. (2.90). This implies that a set of measurement operators defined by the four vectors $\alpha_0, \alpha_1, \beta_0$ and β_1 exists so that the CHSH inequality is violated. For example, the Bell diagonal quantum state

$$|\Phi\rangle = \frac{1}{\sqrt{2}}(|01\rangle - |10\rangle) \quad (2.115)$$

with the measurements $\alpha_0 = \hat{e}_1, \alpha_1 = \hat{e}_2, \beta_0 = -(\hat{e}_1 + \hat{e}_2)/\sqrt{2}$ and $\beta_1 = (-\hat{e}_1 + \hat{e}_2)/\sqrt{2}$ results in

$$S = 2\sqrt{2} > 2. \quad (2.116)$$

This inequality demonstrates the nonlocality of bipartite quantum systems. In Eq. (2.104), it has been established that only entangled quantum states display nonlocal behavior. The violation of Bell inequalities was shown for the first time in 1972 by Freedman and Clauser [24]. Over the years, many impressive experiments with increasing degrees of sophistication have been performed [25, 26]. These experiments demonstrate that quantum mechanical correlations can exceed those allowed by classical mechanics, and that the LHV model is unable to account for such strong correlations. Therefore, it is concluded that a quantum system cannot satisfy either locality or reality.

2.5.2 Definition of EPR steerability

Inspired by the work of Einstein, Podolsky and Rosen [14], questioning the completeness of quantum mechanics and discussing the well-known EPR paradox, another quantum concept was originally introduced by Schrödinger [16, 17], the so-called Einstein-Podolsky-Rosen steering. It can be viewed as a generalization of the experimental scenario of the EPR paradox. The scenario assumes a bipartite quantum system with two observers, Alice and Bob, as shown in Fig. 2.3. The Hilbert space of the combined systems is given by $\mathcal{H}_{AB} = \mathcal{H}_A \otimes \mathcal{H}_B$ with local dimensions d_A and d_B . Similar to the nonlocal scenario, Alice and Bob can perform local measurements on their respective systems, using settings α and β to obtain results a and b . In EPR steering, Alice attempts to convince Bob that they share a bipartite entangled quantum state, but Bob does not trust Alice. Two sets of local POVMs $\{\Pi_{\alpha,a} \geq 0\}$ and $\{\Pi_{\beta,b} \geq 0\}$ are defined as in Section 2.3.2. After preparing a bipartite quantum state, Bob tries to explain the quantum mechanical joint probability distribution

$$P(a, b|\alpha, \beta) = \text{tr}\{\Pi_{\alpha,a} \otimes \Pi_{\beta,b} \rho\} \quad (2.117)$$

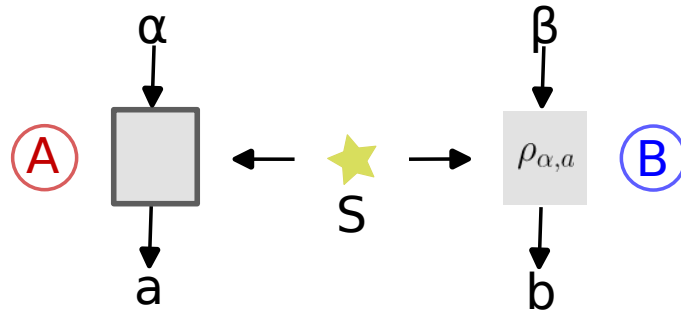


Figure 2.3: Schematic representation of Alice's and Bob's bipartite quantum system: Alice and Bob can perform measurements on their local quantum system with settings α and β , and their associated results a and b . A common source S emits a bipartite quantum state. The measurements on Alice's side are not further specified, while Bob performs quantum measurements on the conditional state $\rho_{\alpha,a}$ depending on Alice's measurement settings and results.

by a local hidden state model (LHS) [33, 97]. For Alice's measurements α with the result a , Bob remains with an unnormalized conditional quantum state

$$\rho_{\alpha,a}^B = \text{tr}_A\{\Pi_{\alpha,a} \otimes \mathbb{1}\rho\} \quad (2.118)$$

and from the completeness relation of the POVM follows (Eq. (2.102))

$$\rho_B = \text{tr}_A\{\rho\} = \sum_a \text{tr}_A\{\Pi_{\alpha,a} \otimes \mathbb{1}\rho\}. \quad (2.119)$$

Bob tries to explain his conditional state by some initially prepared hidden state σ_λ with a probability $p(\lambda)$. It can be seen that Alice's measurements give him additional information about the hidden state. So, the conditional state is given by [33, 97]

$$\rho_{\alpha,a}^B = \sum_{\lambda \in \Lambda} p(\lambda) p(a|\alpha, \lambda) \sigma_\lambda. \quad (2.120)$$

This representation can be interpreted as Alice simulating the drawing of the conditional states $\rho_{\alpha,a}^B$ by choosing a hidden state σ_λ with probability $p(\lambda)$ while simultaneously announcing her measurement setting and result. Therefore, the initial bipartite quantum does not need to be entangled. If all conditional states can be explained by LHS models, then the state is called unsteerable from Alice to Bob. Otherwise, the state is called EPR steerable from Alice to Bob. The joint probability distribution of an unsteerable state is given by

$$\begin{aligned} P(a, b|\alpha, \beta) &= \sum_{\lambda \in \Lambda} p(\lambda) P(a|\alpha, \lambda) P(b|\beta, \lambda), \\ P(b|\beta, \lambda) &= \text{tr}\{\Pi_{\beta,b} \sigma_\lambda\}. \end{aligned} \quad (2.121)$$

From this definition, it is apparent that an unsteerable quantum state is also local [c.f. Eq. (2.100)] and that a separable quantum state is unsteerable [c.f. Eq. (2.104)]. This implies that a LHV model can also explain joint probability distributions, which a LHS model can explain. However, the opposite is not necessarily true. Using the completeness relation of POVMs Eq. (2.102) and Eq. (2.119) we obtain

$$\sum_a P(a, b|\alpha, \beta) = \text{tr}_B\{\Pi_{\beta,b} \rho_B\} = \text{tr}_B\left\{\Pi_{\beta,b} \sum_{\lambda \in \Lambda} p(\lambda) \sigma_\lambda\right\}, \quad (2.122)$$

$$\sum_b P(a, b|\alpha, \beta) = \text{tr}_A\{\Pi_{\alpha,a} \rho_A\} = \sum_{\lambda \in \Lambda} p(\lambda) P(a|\alpha, \lambda). \quad (2.123)$$

This means that Bob's POVMs $\{\Pi_{\beta,b}\}$ cannot distinguish the reduced quantum state ρ_B from a LHS model $\sum_{\lambda \in \Lambda} p(\lambda) \sigma_\lambda$.

By interchanging the observers, EPR steering from Bob to Alice can be defined analogously

$$\begin{aligned} P(a, b|\alpha, \beta) &= \sum_{\lambda \in \Lambda} p(\lambda) \text{tr}\{\Pi_{\alpha,a} \sigma_\lambda\} P(b|\beta, \lambda) \\ \rho_A &= \text{tr}_B\{\rho\} = \sum_b \text{tr}_B\{\mathbb{1} \otimes \Pi_{\beta,b} \rho\}, \\ \rho_{\beta,b}^A &= \sum_{\lambda \in \Lambda} p(\lambda) p(b|\beta, \lambda) \sigma_\lambda. \end{aligned} \quad (2.124)$$

Einstein-Podolsky-Rosen steering is an asymmetric property. Quantum states can be EPR steerable from Alice to Bob but not from Bob to Alice, and vice versa. Similar to nonlocality and

entanglement, EPR steerability can be detected by inequalities. Also, like nonlocality, whether a quantum state is EPR steerable from Alice to Bob or not it depends on the available local measurements on Alice's and Bob's subsystems. For example, consider that Alice performs N local measurements A_k with results $\{a_k = \pm 1\}$ and Bob performs local measurements on arbitrary observables B_k . As a result, a straightforward inequality can be derived in which all unsteerable quantum states fulfill [98]

$$\sum_{k=1}^N |\text{tr}\{A_k \otimes B_k \rho\}| \leq \max_{\{a_k\}} \left[\lambda_{\max} \left(\sum_{k=1}^N a_k B_k \right) \right], \quad (2.125)$$

where λ_{\max} is the maximum eigenvalue of the operator $\sum_{k=1}^N a_k B_k$. In this section, the definition of EPR steering has been discussed and a first inequality to verify quantum states which can be used for EPR steering from Alice to Bob has been shown. Even in the simplest bipartite quantum system of two-qubits, finding the EPR steerable quantum states is challenging. The two-qubit case is discussed in detail in Section 6.1. Einstein-Podolsky-Rosen steering has been verified in several experiments [98–100]. Furthermore, the existence of one-way steerable quantum states has been shown experimentally as well [101–105].

2.5.3 Joint measurability and EPR steerability

In this subsection, the link between joint measurability and EPR steering is presented. A set of POVMs $\{\Pi_{\alpha,a} \geq 0\}$ is jointly measurable if there exists another POVM $\{\bar{\Pi}_\lambda\}_{\lambda \in \Lambda}$ with classical conditional probabilities $\{P(a|\alpha, \lambda)\}$ such that [70, 106]

$$\Pi_{\alpha,a} = \sum_{\lambda \in \Lambda} p(a|\alpha, \lambda) \bar{\Pi}_\lambda. \quad (2.126)$$

The POVM $\{\bar{\Pi}_\lambda \geq 0\}$ is called the joint observable for the POVMs $\{\Pi_{\alpha,a}\}$. This definition reveals similarities between EPR steerability from Alice to Bob and joint measurability. It has been shown that a set of measurements $\{\Pi_{\alpha,a}\}$ on Alice's side is not jointly measurable if and only if these measurements can be used to demonstrate EPR steering from Alice to Bob [107, 108]. For example, a joint measurable POVM $\{\Pi_{\alpha,a}\}$ can construct a LHS model for a given quantum state by

$$\rho_{\alpha,a}^B = \text{tr}_A\{\Pi_{\alpha,a} \otimes \mathbb{1}_{d_B} \rho\} = \sum_{\lambda \in \Lambda} p(a|\alpha, \lambda) \text{tr}_A\{\bar{\Pi}_\lambda \otimes \mathbb{1}_{d_B} \rho\} = \sum_{\lambda \in \Lambda} p(a|\alpha, \lambda) \sigma_\lambda \quad (2.127)$$

with the local hidden states $\sigma_\lambda = \text{tr}_A\{\bar{\Pi}_\lambda \otimes \mathbb{1}_{d_B} \rho\}$. A similar statement has been shown for POVMs on Bob's side. Namely, that a state ensemble $\{\rho_{\alpha,a}\}$ is steerable if and only if the POVMs $\{\tilde{\Pi}_{\alpha,a} = \rho_B^{-1/2} \rho_{\alpha,a}^B \rho_B^{-1/2}\}$ are not jointly measurable [109]. If the matrix ρ_B cannot be inverted, its pseudoinverse replaces $\rho_B^{-1/2}$. These conditions imply an interesting relationship between the criterion for joint measurability and EPR steering. Thus, a joint measurability criterion can be utilized to verify whether quantum states can be used for EPR steering or a steering criterion can be used to find joint measurable POVMs.

Part II

(N, M) -POVMS

PROPERTIES OF (N, M) -POVMS

In this part, the recently introduced special class of (N, M) -POVMS is discussed, which includes several classes of POVMS, such as MUMs, MUBs, GSICs and SIC-POVMS [59]. Due to the symmetry and the informational completeness of (N, M) -POVMS, these POVMS can be used to detect the entanglement of bipartite quantum states by local measurements and verify EPR steerable quantum states from Alice to Bob.

Section 3.1 provides the definition, properties, and primary proofs for the allowed parameter regions and informational completeness. The construction of (N, M) -POVMS from a given Hermitian orthonormal operator basis is discussed in Section 3.2. The foundation for determining the efficiencies of the sufficient conditions for entanglement and EPR steering from Alice to Bob is derived as a main result in Section 3.3. This scaling relation is necessarily fulfilled by (N, M) -POVMS regardless of the positive semidefiniteness of the POVM elements.

3.1 DEFINITION OF (N, M) -POVMS

This section introduces the (N, M) -POVMS and the condition for informational completeness. The basic proofs are presented to clarify the definitions and conditions of (N, M) -POVMS.

A set of N POVMS is considered, with each POVM containing M measurement results, and the POVM elements acting on a d -dimensional Hilbert space. The POVMS can be represented by a tuple of positive semidefinite operators $\Pi = (\Pi_1, \dots, \Pi_{NM})$. The tuple's elements can be identified by the bijective map $i : (\alpha, a) | \alpha \in \{1, \dots, N\}, a \in \{1, \dots, M\} \rightarrow \{1, \dots, NM\}$ with $i(\alpha, a) = (\alpha - 1)M + a$. The POVM is described by α and the associated measurement result by a . Each POVM fulfills the characteristic completeness relation

$$\sum_{a=1}^M \Pi_{i(\alpha, a)} = \mathbb{1}_d \quad (3.1)$$

for all α . Details of the definition and properties of POVMS are discussed in Section 2.3.2. For (N, M) -POVMS the additional restrictions are imposed [59]

$$\text{tr}\{\Pi_{i(\alpha, a)}\} = w \quad (3.2)$$

$$\text{tr}\{\Pi_{i(\alpha, a)} \Pi_{i(\alpha, a)}\} = x \quad (3.3)$$

$$\text{tr}\{\Pi_{i(\alpha, a)} \Pi_{i(\alpha, a')}\} = y \quad (3.4)$$

$$\text{tr}\{\Pi_{i(\alpha, a)} \Pi_{i(\beta, b)}\} = z \quad (3.5)$$

for $a, a', b \in \{1, \dots, M\}$, $\alpha, \beta \in \{1, \dots, N\}$, $a \neq a'$ and $\alpha \neq \beta$. It will be demonstrated that the real-valued coefficients x, y, z and w can only take specific values, which are restricted by the positive semidefiniteness of the POVM elements and the completeness relation (3.1). In

the case of $N = 1$, only the relations (3.2)–(3.4) are defined. The completeness relation (3.1) calculates the parameters w , y and z of Eqs. (3.3)–(3.5)

$$d = \text{tr}\{\mathbb{1}_d\} = \sum_{a=1}^M \text{tr}\{\Pi_{i(\alpha,a)}\} = wM, \quad (3.6)$$

$$w = \text{tr}\{\Pi_{i(\alpha,a)}\} = \sum_{b=1}^M \text{tr}\{\Pi_{i(\alpha,a)}\Pi_{i(\alpha,b)}\} = x + (M-1)y, \quad (3.7)$$

$$w = \text{tr}\{\Pi_{i(\alpha,a)}\} = \sum_{b=1}^M \text{tr}\{\Pi_{i(\alpha,a)}\Pi_{i(\beta,b)}\} = Mz. \quad (3.8)$$

These equations limit the parameters to

$$w = \frac{d}{M}, \quad y = \frac{d - Mx}{M(M-1)}, \quad z = \frac{d}{M^2}. \quad (3.9)$$

The next step is to calculate the boundaries of the parameter x . For a given parameter x the POVM elements can range from operators that are proportional to the identity operator to rank one matrices

$$\Pi_{i(\alpha,a)} = \frac{d}{M} |\alpha, a\rangle \langle \alpha, a| \quad (3.10)$$

for a given unit vector $|\alpha, a\rangle$. For rank one operators holds

$$x = \text{tr}\{\Pi_{i(\alpha,a)}^2\} = \frac{d^2}{M^2} \text{tr}\{|\alpha, a\rangle \langle \alpha, a|\} = \frac{d^2}{M^2} \quad (3.11)$$

and the lower bound follows from the Cauchy-Schwarz inequality

$$\begin{aligned} \frac{d}{M} &= \text{tr}\{\Pi_{i(\alpha,a)}\} = \text{tr}\{\Pi_{i(\alpha,a)}\mathbb{1}_d\} < \sqrt{\text{tr}\{\Pi_{i(\alpha,a)}^2\} \text{tr}\{\mathbb{1}_d\}} = \sqrt{dx} \\ &\Rightarrow \frac{d}{M^2} < x. \end{aligned} \quad (3.12)$$

The non-negativity of the trace of the product of two positive semidefinite matrices implies

$$\begin{aligned} 0 &\leq \text{tr}\{\sqrt{\Pi_{i(\alpha,a)}}\Pi_{i(\alpha,b)}\sqrt{\Pi_{i(\alpha,a)}}\} = \text{tr}\{\Pi_{i(\alpha,a)}\Pi_{i(\alpha,b)}\} = \frac{d - Mx}{M(M-1)}, \\ &\Rightarrow x \leq \frac{d}{M} \end{aligned} \quad (3.13)$$

for $a \neq b$. By combining Eqs. (3.11)–(3.13) the (N, M) -POVM's parameter x , is limited to

$$\frac{d}{M^2} < x \leq \min\left\{\frac{d^2}{M^2}, \frac{d}{M}\right\}. \quad (3.14)$$

This is necessary for the existence of (N, M) -POVMS. Furthermore, it has to be shown that for an x -value inside the interval a (N, M) -POVM can be constructed. By using Eq. (3.9), the definition for a (N, M) -POVMS reads

$$\text{tr}\{\Pi_{i(\alpha,a)}\} = \frac{d}{M}, \quad (3.15)$$

$$\text{tr}\{\Pi_{i(\alpha,a)}\Pi_{i(\alpha,b)}\} = x\delta_{a,b} + (1 - \delta_{a,b})\frac{d - Mx}{M(M-1)}, \quad (3.16)$$

$$\text{tr}\{\Pi_{i(\alpha,a)}\Pi_{i(\beta,b)}\} = \frac{d}{M^2} \quad (3.17)$$

for $a, b \in \{1, \dots, M\}$, $\alpha, \beta \in \{1, \dots, N\}$ and $\alpha \neq \beta$. The value of parameter x is constrained by Eq. (3.14). In the case of $N = 1$, only Eqs. (3.15) and (3.16) are defined. If x reaches the upper boundary of the allowed values, the (N, M) -POVM is called optimal.

Informationally complete measurements are of special interest because they allow the complete reconstruction of a density matrix. Therefore, the values of (N, M) for a fixed dimension are determined such that the (N, M) -POVMs are informationally complete. A (N, M) -POVM is informationally complete if its elements span the set of all Hermitian linear operators. This definition is equivalent to the (N, M) -POVMs containing d^2 linearly independent operators. A (N, M) -POVM is informationally complete if

$$N(M-1)+1 = d^2 \quad (3.18)$$

is fulfilled. The proof of this condition is given in the following lines. For simplicity, the traceless (N, M) -operators $\pi_{i(\alpha,a)} = \Pi_{i(\alpha,a)} - \mathbb{1}_d/M$ are introduced. The defining relations of the traceless (N, M) -operators are derived from Eqs. (3.15)-(3.17)

$$\text{tr}\{\pi_{i(\alpha,a)}\} = 0, \quad (3.19)$$

$$\text{tr}\{\pi_{i(\alpha,a)} \pi_{i(\alpha,b)}\} = \left(x - \frac{d}{M^2}\right) \delta_{a,b} + (1 - \delta_{a,b}) \frac{d - M^2 x}{M^2(M-1)}, \quad (3.20)$$

$$\text{tr}\{\pi_{i(\alpha,a)} \pi_{i(\beta,b)}\} = 0 \quad (3.21)$$

for $a, b \in \{1, \dots, M\}$, $\alpha, \beta \in \{1, \dots, N\}$ and $\alpha \neq \beta$. In case of $N = 1$, only Eqs. (3.19) and (3.20) are imposed. From the completeness relation of POVMs (3.1) follows

$$\sum_{a=1}^M \pi_{i(\alpha,a)} = 0. \quad (3.22)$$

To prove the informational completeness it is necessary to demonstrate that the set of (N, M) -POVMs contains d^2 linearly independent operators. It suffices to show that the set of the traceless (N, M) -operators $\{\pi_{i(\alpha,a)} : \alpha \in \{1, \dots, N\}, a \in \{1, \dots, M\}\}$ contains $d^2 - 1$ linearly independent operators. The completeness relation (3.22) reduces the number of linearly independent elements to $N(M-1)$

$$\pi_{i(\alpha,M)} = - \sum_{a=1}^{M-1} \pi_{i(\alpha,a)}. \quad (3.23)$$

To prove the linear independence of the remaining operators, it has to be shown that from

$$\sum_{\alpha=1}^N \sum_{a=1}^{M-1} r_{\alpha,a} \pi_{i(\alpha,a)} = 0 \quad (3.24)$$

follows that all real numbers are zero $r_{\alpha,a} = 0$. Multiplying Eq. (3.24) by $\pi_{i(\beta,M)}$ and using Eq. (3.20) lead to

$$\begin{aligned}
0 &= \text{tr} \left\{ \sum_{\alpha=1}^N \sum_{a=1}^{M-1} r_{\alpha,a} \pi_{i(\alpha,a)} \pi_{i(\beta,M)} \right\} \\
&= \sum_{\alpha=1}^N \sum_{a=1}^{M-1} r_{\alpha,a} \text{tr} \{ \pi_{i(\alpha,a)} \pi_{i(\beta,M)} \} \\
&= \sum_{a=1}^{M-1} r_{\beta,a} \text{tr} \{ \pi_{i(\beta,a)} \pi_{i(\beta,M)} \} \\
&= \frac{d - M^2 x}{M^2(M-1)} \sum_{a=1}^{M-1} r_{\beta,a}.
\end{aligned} \tag{3.25}$$

The prefactor $(d - M^2 x)$ vanishes only for $x = d/M^2$, which is outside the definition space of x . Therefore, the sum has to vanish

$$\sum_{a=1}^{M-1} r_{\beta,a} = 0 \tag{3.26}$$

for all β . Multiplying Eq. (3.24) by $\pi_{i(\beta,b)}$ for $b \in \{1, \dots, M-1\}$ and using the definition of the (N, M) -operators Eqs. (3.20) and (3.21) lead to

$$\begin{aligned}
0 &= \text{tr} \left\{ \sum_{\alpha=1}^N \sum_{a=1}^{M-1} r_{\alpha,a} \pi_{i(\alpha,a)} \pi_{i(\beta,b)} \right\} \\
&= \sum_{\alpha=1}^N \sum_{a=1}^{M-1} r_{\alpha,a} \text{tr} \{ \pi_{i(\alpha,a)} \pi_{i(\beta,b)} \} \\
&= \sum_{a=1}^{M-1} r_{\beta,a} \text{tr} \{ \pi_{i(\beta,a)} \pi_{i(\beta,b)} \} \\
&= r_{\beta,b} x + \frac{d - M^2 x}{M^2(M-1)} \sum_{a=1, a \neq b}^{M-1} r_{\beta,a} \\
&= r_{\beta,b} \left(x - \frac{d - M^2 x}{M^2(M-1)} \right) + \frac{d - M^2 x}{M^2(M-1)} \underbrace{\sum_{a=1}^{M-1} r_{\beta,a}}_{=0} \\
&= r_{\beta,b} \frac{M^3 x - d}{M^2(M-1)}.
\end{aligned} \tag{3.27}$$

Within the limits of x , the prefactor cannot vanish. Therefore, $r_{\beta,b} = 0$ for all β and b . This implies that the remaining $N(M-1)$ operators are linearly independent. Thus, they are informationally complete if $N(M-1) = d^2 - 1$ is fulfilled, which matches Eq. (3.18). Siudzińska has provided a similar proof [59].

For (N, M) -POVMS in dimension $d \geq 3$, there are at least four classes of different informationally complete (N, M) -POVMS.

The possible solutions of Eq. (3.18) are $(N, M) \in \{(1, d^2), (d+1, d), (d^2-1, 2), (d-1, d+2)\}$ [59]. The solution $(N, M) = (1, d^2)$ characterizes the special case of a one-parameter family of GSICs [62], which is parameterized by the parameter x . SIC-POVMS correspond to the special

case of GSICs with $x = 1/d^2$. The solution $(N, M) = (d + 1, d)$ describes MUMs [64], which in the special case of $x = d^2/M^2 = d/M = 1$ further reduce to projective measurements of rank one with maximal sets of $d + 1$ MUBs. In the special case of a qubit, i.e. $d = 2$, the four possible solutions of Eq. (3.18) reduce to two cases, namely GSICs for $(N, M) = (1, 4)$ and MUMs for $(N, M) = (3, 2)$. The first informationally complete (N, M) -POVMS, which do not belong to the four classes of solutions, exist in dimension $d = 5$ with the additional solutions $(N = 8, M = 4)$, $(N = 3, M = 9)$, $(N = 2, M = 13)$ and $(N = 12, M = 3)$.

This section discussed the definition of (N, M) -POVMS and the condition of informational completeness. The existence of (N, M) -POVMS for certain parameters N, M and x has not yet been addressed and will be discussed in detail in Chapter 4. Local informationally complete (N, M) -POVMS will be used to detect entangled quantum states in Chapter 5 and to verify EPR steerable quantum states in Chapter 6. The following section outlines techniques for constructing informationally complete (N, M) -POVMS using a given traceless Hermitian orthonormal operator basis.

3.2 CONSTRUCTION OF (N, M) -POVMS

The previous section introduced (N, M) -POVMS. In this section, the construction of informationally complete (N, M) -POVMS in dimension d from a given traceless Hermitian orthonormal operator basis is discussed. Two different methods are analyzed. The first has been introduced by [59, 62, 64] and the second is motivated by a recursive construction. These procedures allow the construction of informationally complete (N, M) -POVMS for some x -values in arbitrary dimension d .

3.2.1 Construction of (N, M) -POVMS by Siudzińska

The subsequent procedure has been introduced by Siudzińska [59] to construct informationally complete (N, M) -POVMS for all solutions (N, M) of Eq. (3.18), including the special cases of GSICs [62] and MUMs [64]. The starting point of the construction is an orthonormal Hermitian operator basis of the form

$$\tilde{G} = \left\{ \tilde{G}_0 = \frac{\mathbb{1}_d}{\sqrt{d}}, \tilde{G}_i; i = 1, \dots, d^2 - 1 \right\} \quad (3.28)$$

with $\text{tr}\{\tilde{G}_i\} = 0$ for $1 \leq i \leq d^2 - 1$, $\tilde{G}_i^\dagger = \tilde{G}_i$ and $\text{tr}\{\tilde{G}_i \tilde{G}_j\} = \delta_{ij}$. The indices of the traceless elements of the basis must be linked to the (α, a) indices identifying the elements of (N, M) -POVMS for $\alpha \in \{1, \dots, N\}$ and $a \in \{1, \dots, M - 1\}$. A possible map connecting these indices is $i(\alpha, a) = (\alpha - 1)M + a$. It is important to note that this map is not unique and can influence the constructed (N, M) -POVMS. The basis used for the construction is enumerated by

$$\tilde{G} = \{ \tilde{G}_0, \tilde{G}_{i(\alpha, a)} \}. \quad (3.29)$$

The operator

$$\tilde{G}_\alpha = \sum_{a=1}^{M-1} \tilde{G}_{i(\alpha, a)} \quad (3.30)$$

is defined and used for the construction of the traceless (N, M) -operators

$$\pi_{i(\alpha, a)} = t \begin{cases} \tilde{G}_\alpha - \sqrt{M}(\sqrt{M} + 1)\tilde{G}_{i(\alpha, a)} & , a = 1, \dots, M - 1 \\ (\sqrt{M} + 1)\tilde{G}_\alpha & , a = M. \end{cases} \quad (3.31)$$

The possible (N, M) -POVM elements are given by

$$\begin{aligned}\Pi_{i(\alpha,a)} &= \frac{\mathbb{1}_d}{M} + \pi_{i(\alpha,a)} \\ &= \frac{\mathbb{1}_d}{M} + t \begin{cases} \tilde{G}_\alpha - \sqrt{M}(\sqrt{M}+1)\tilde{G}_{i(\alpha,a)} & , a = 1, \dots, M-1 \\ (\sqrt{M}+1)\tilde{G}_\alpha & , a = M. \end{cases}\end{aligned}\quad (3.32)$$

The admissible range of the parameter t , for which the positive semidefiniteness of all POVM elements is guaranteed, is given by

$$-\frac{1}{M} \frac{1}{\lambda_{\max}} \leq t \leq \frac{1}{M} \frac{1}{|\lambda_{\min}|}, \quad (3.33)$$

where λ_{\max} and λ_{\min} are the maximal and minimal eigenvalues of all normalized traceless (N, M) -operators $\pi_{i(\alpha,a)}/t$. The relation between x and t is given by

$$x = \frac{d}{M^2} + t^2(M-1)(\sqrt{M}+1)^2. \quad (3.34)$$

By construction, the matrices $\pi_{i(\alpha,a)}$ fulfill Eqs. (3.19) and (3.21). It has to be shown that this construction also satisfies Eq. (3.20). It holds

$$\begin{aligned}\text{tr}\{\pi_{i(\alpha,M)}\pi_{i(\alpha,M)}\} &= t^2(\sqrt{M}+1)^2 \text{tr}\{\tilde{G}_\alpha, \tilde{G}_\alpha\} \\ &= t^2(\sqrt{M}+1)^2 \sum_{a,b=1}^{M-1} \text{tr}\{\tilde{G}_{i(\alpha,a)}, \tilde{G}_{a,b}\} \\ &= t^2(\sqrt{M}+1)^2(M-1) \\ &= x - \frac{d}{M^2}\end{aligned}\quad (3.35)$$

and for $1 \leq a < M$

$$\begin{aligned}\text{tr}\{\pi_{i(\alpha,a)}\pi_{i(\alpha,a)}\} &= t^2(\text{tr}\{(\tilde{G}_\alpha, \tilde{G}_\alpha) - 2\sqrt{M}(\sqrt{M}+1)\tilde{G}_{i(\alpha,a)}\tilde{G}_\alpha + M(\sqrt{M}+1)^2\tilde{G}_{i(\alpha,a)}\tilde{G}_{i(\alpha,a)}\}) \\ &= t^2(M-1-2\sqrt{M}(\sqrt{M}+1) + M(\sqrt{M}+1)^2) \\ &= t^2(\sqrt{M}+1)^2(M-1) \\ &= x - \frac{d}{M^2}.\end{aligned}\quad (3.36)$$

For $1 \leq a, b < M$ and $a \neq b$ follows

$$\begin{aligned}\text{tr}\{\pi_{i(\alpha,a)}\pi_{i(\alpha,b)}\} &= t^2(M-1-2\sqrt{M}(\sqrt{M}+1)) \\ &= \frac{x - \frac{d}{M^2}}{(M-1)(\sqrt{M}+1)^2}(M-1-2\sqrt{M}(\sqrt{M}+1)) \\ &= \frac{d - M^2x}{M^2(M-1)} \frac{(\sqrt{M}+1)^2}{1 - M + 2\sqrt{M}(\sqrt{M}+1)} \\ &= \frac{d - M^2x}{M^2(M-1)} \frac{(\sqrt{M}+1)^2}{1 + 2\sqrt{M} + M} \\ &= \frac{d - M^2x}{M^2(M-1)}\end{aligned}\quad (3.37)$$

and

$$\begin{aligned}
\text{tr}\{\pi_{i(\alpha,a)}\pi_{i(\alpha,M)}\} &= t^2((M-1)(\sqrt{M}+1)-\sqrt{M}(\sqrt{M}+1)^2) \\
&= \frac{x-\frac{d}{M^2}}{(M-1)(\sqrt{M}+1)^2}((M-1)(\sqrt{M}+1)-\sqrt{M}(\sqrt{M}+1)^2) \\
&= \frac{d-M^2x}{M^2(M-1)} \frac{(1-M)(\sqrt{M}+1)+\sqrt{M}(\sqrt{M}+1)^2}{(\sqrt{M}+1)^2} \\
&= \frac{d-M^2x}{M^2(M-1)}. \tag{3.38}
\end{aligned}$$

The calculation shows that Eq. (3.16) is also fulfilled and the constructed set of $\Pi_{i(\alpha,a)}$ is a (N, M) -POVM. The $(1, d^2)$ -POVMs only need to satisfy conditions (3.19) and (3.20). If x belongs to a constructed (N, M) -POVM, then for all $x' \in (d/M^2, x)$, the constructed operators are also (N, M) -POVMs. This ansatz allows the construction of informationally complete (N, M) -POVMs for any dimension d and all solutions of Eq. (3.18) for some values of x . The selected traceless Hermitian orthonormal operator basis restricts the parameter x of the constructed (N, M) -POVM.

3.2.2 Recursive construction of (N, M) -POVMs

This section shows a recursive construction of informationally complete (N, M) -POVMs. This ansatz provides a better geometric understanding of (N, M) -POVMs as $N \times M$ points within the convex set of positive semidefinite operators with a trace equal to d/M . The discussed formalism allows the construction of normalized traceless Hermitian (N, M) -operators

$$\hat{\pi}_{i(\alpha,a)} = \frac{\Pi_{i(\alpha,a)} - \mathbb{1}_{d/M}}{\sqrt{\text{tr}\{(\Pi_{i(\alpha,a)} - \mathbb{1}_{d/M})^2\}}} = \frac{\pi_{i(\alpha,a)}}{\sqrt{\text{tr}\{\pi_{i(\alpha,a)}^2\}}} = \frac{\pi_{i(\alpha,a)}}{\sqrt{x-d/M^2}} \tag{3.39}$$

and the definition of the traceless (N, M) -operators, as in Eqs. (3.19)–(3.21), are reformulated to

$$\text{tr}\{\hat{\pi}_{i(\alpha,a)}\} = 0, \tag{3.40}$$

$$\text{tr}\{\hat{\pi}_{i(\alpha,a)}\hat{\pi}_{i(\alpha,b)}\} = \delta_{a,b} + (1-\delta_{a,b})\frac{1}{1-M}, \tag{3.41}$$

$$\text{tr}\{\hat{\pi}_{i(\alpha,a)}\hat{\pi}_{i(\beta,b)}\} = 0. \tag{3.42}$$

A recursive construction of the normalized traceless (N, M) -operators is performed with an orthonormal basis \tilde{G} defined in Eq. (3.29)

$$\begin{aligned}
\hat{\pi}_{i(\alpha,1)}^{(M)} &= \tilde{G}_{i(\alpha,M-1)} \\
\hat{\pi}_{i(\alpha,a)}^{(M)} &= \frac{1}{1-M}\tilde{G}_{i(\alpha,M-1)} + \sqrt{1-\frac{1}{(1-M)^2}}\hat{\pi}_{i(\alpha,a-1)}^{(M-1)} \tag{3.43}
\end{aligned}$$

for $2 \leq a \leq M$ and the operator $\hat{\pi}_{i(\alpha,1)}^{(1)} = 0$ is set to zero. The construction has to be performed for $2 \leq \tilde{M} \leq M$ to construct the (N, M) -POVMs. By definition, this approach fulfills Eqs. (3.40) and (3.42). By complete induction, it is proven that the operators of Eq. (3.43) fulfill Eq. (3.41). For $M = 2$, the operators are given by

$$\hat{\pi}_{i(\alpha,1)}^{(2)} = \tilde{G}_{i(\alpha,1)} \quad \text{and} \quad \hat{\pi}_{i(\alpha,2)}^{(2)} = -\tilde{G}_{i(\alpha,1)} \tag{3.44}$$

and fulfill Eq. (3.41). The statement is true for $M = 2$, and in the following calculation, it has been assumed that the statement holds for a single value of M . For $M' = M + 1$, the construction of Eq. (3.43) reads

$$\begin{aligned}\hat{\pi}_{i(\alpha,1)}^{(M+1)} &= \tilde{G}_{i(\alpha,M)} \\ \hat{\pi}_{i(\alpha,a)}^{(M+1)} &= -\frac{1}{M} \tilde{G}_{i(\alpha,M)} + \sqrt{1 - \frac{1}{M^2}} \hat{\pi}_{i(\alpha,a-1)}^{(M)}\end{aligned}\quad (3.45)$$

and for identical operators, it holds

$$\text{tr}\left\{\left(\hat{\pi}_{i(\alpha,1)}^{(M+1)}\right)^2\right\} = \text{tr}\left\{\tilde{G}_{i(\alpha,M)}\tilde{G}_{i(\alpha,M)}\right\} = 1 \quad (3.46)$$

$$\begin{aligned}\text{tr}\left\{\left(\hat{\pi}_{i(\alpha,a)}^{(M+1)}\right)^2\right\} &= \text{tr}\left\{\left(-\frac{1}{M}\tilde{G}_{i(\alpha,M)} + \sqrt{1 - \frac{1}{M^2}}\hat{\pi}_{i(\alpha,a-1)}^{(M)}\right)^2\right\} \\ &= \frac{1}{M^2} + \left(1 - \frac{1}{M^2}\right)\text{tr}\left\{\left(\hat{\pi}_{i(\alpha,a-1)}^{(M)}\right)^2\right\} \\ &= \frac{1}{M^2} + 1 - \frac{1}{M^2} = 1.\end{aligned}\quad (3.47)$$

For different operators with $2 \leq a, b \leq M$ and $a \neq b$, it holds

$$\text{tr}\left\{\hat{\pi}_{i(\alpha,1)}^{(M+1)}\hat{\pi}_{i(\alpha,a)}^{(M+1)}\right\} = -\frac{1}{M}\text{tr}\left\{\tilde{G}_{i(\alpha,M)}\tilde{G}_{i(\alpha,M)}\right\} = \frac{1}{1-M'} \quad (3.48)$$

$$\begin{aligned}\text{tr}\left\{\hat{\pi}_{i(\alpha,a)}^{(M+1)}\hat{\pi}_{i(\alpha,b)}^{(M+1)}\right\} &= \text{tr}\left\{\left(-\frac{1}{M}\tilde{G}_{i(\alpha,M)} + \sqrt{1 - \frac{1}{M^2}}\hat{\pi}_{i(\alpha,a-1)}^{(M)}\right)\left(-\frac{1}{M}\tilde{G}_{i(\alpha,M)} + \sqrt{1 - \frac{1}{M^2}}\hat{\pi}_{i(\alpha,b-1)}^{(M)}\right)\right\} \\ &= \frac{1}{M^2} - \left(1 - \frac{1}{M^2}\right)\frac{1}{1-M} \\ &= -\frac{1}{M} = \frac{1}{1-M'}.\end{aligned}\quad (3.49)$$

It has been shown that Eq. (3.43) fulfills the defining equations of the normalized traceless (N, M) -operators, as in Eqs. (3.40-3.42). An informationally complete (N, M) -POVM is constructed by

$$\Pi_{i(\alpha,a)} = \frac{\mathbb{1}_d}{M} + \sqrt{x - \frac{d}{M^2}} \hat{\pi}_{i(\alpha,a)}^{(M)} \quad (3.50)$$

if (N, M) is a solution of Eq. (3.18) and x is chosen so that $\Pi_{i(\alpha,a)}$ is positive semidefinite for all $\alpha \in \{1, \dots, N\}$ and $a \in \{1, \dots, M\}$. For $M = 3$ and $M = 4$, the constructed normalized traceless (N, M) -operators are given by

$$\begin{aligned}\hat{\pi}_{i(\alpha,1)}^{(3)} &= \tilde{G}_{i(\alpha,2)}, \\ \hat{\pi}_{i(\alpha,2)}^{(3)} &= -\frac{1}{2}\tilde{G}_{i(\alpha,2)} + \sqrt{\frac{3}{4}}\hat{\pi}_{i(\alpha,1)}^{(2)} = -\frac{1}{2}\tilde{G}_{i(\alpha,2)} + \sqrt{\frac{3}{4}}\tilde{G}_{i(\alpha,1)}, \\ \hat{\pi}_{i(\alpha,2)}^{(3)} &= -\frac{1}{2}\tilde{G}_{i(\alpha,2)} + \sqrt{\frac{3}{4}}\hat{\pi}_{i(\alpha,2)}^{(2)} = -\frac{1}{2}\tilde{G}_{i(\alpha,2)} - \sqrt{\frac{3}{4}}\tilde{G}_{i(\alpha,1)}\end{aligned}\quad (3.51)$$

and

$$\begin{aligned}
 \hat{\pi}_{i(\alpha,1)}^{(4)} &= \tilde{G}_{i(\alpha,3)}, \\
 \hat{\pi}_{i(\alpha,2)}^{(4)} &= -\frac{1}{3}\tilde{G}_{i(\alpha,3)} + \sqrt{\frac{8}{9}}\hat{\pi}_{i(\alpha,1)}^{(3)} = -\frac{1}{3}\tilde{G}_{i(\alpha,3)} + \sqrt{\frac{8}{9}}\tilde{G}_{i(\alpha,2)}, \\
 \hat{\pi}_{i(\alpha,2)}^{(4)} &= -\frac{1}{3}\tilde{G}_{i(\alpha,3)} + \sqrt{\frac{8}{9}}\hat{\pi}_{i(\alpha,1)}^{(3)} = -\frac{1}{3}\tilde{G}_{i(\alpha,3)} + \sqrt{\frac{8}{9}}\left(-\frac{1}{2}\tilde{G}_{i(\alpha,2)} + \sqrt{\frac{3}{4}}\tilde{G}_{i(\alpha,1)}\right), \\
 \hat{\pi}_{i(\alpha,2)}^{(4)} &= -\frac{1}{3}\tilde{G}_{i(\alpha,3)} + \sqrt{\frac{8}{9}}\hat{\pi}_{i(\alpha,1)}^{(3)} = -\frac{1}{3}\tilde{G}_{i(\alpha,3)} + \sqrt{\frac{8}{9}}\left(-\frac{1}{2}\tilde{G}_{i(\alpha,2)} - \sqrt{\frac{3}{4}}\tilde{G}_{i(\alpha,1)}\right). \tag{3.52}
 \end{aligned}$$

These examples illustrate how to construct (N, M) -POVMS. In the case of $M = 3$, the elements of a single POVM are represented by the vertices of an equilateral triangle with its centroid at the origin of a vector space over the field of real numbers. The centroid of the real vector space represents the matrix $\mathbb{1}_d/M$. The basis vectors are given by $\tilde{G}_{i(\alpha,a)}$ for $a = \{1, 2\}$. The distance of the vertices from the origin defines the parameter x . In the case of $M = 4$, the elements of a single POVM are the vertices of a tetrahedron with its centroid at the origin of the 3-dimensional vector space over the real numbers spanned by $\tilde{G}_{i(\alpha,a)}$ for $a = \{1, 2, 3\}$. In general, the elements of a single POVM are given by the vertices or extreme points of a $(M - 1)$ -simplex. Geometrically, the Hilbert space H_{d^2-1} , which represents the linear Hermitian operators with a trace equal to d/M , has to be divided into $N = (d^2 - 1)/(M - 1)$ subspaces of dimension $M - 1$. In each subspace, a $(M - 1)$ -simplex has to be constructed within the set of positive semidefinite operators with a trace equal to d/M . For an optimal (N, M) -POVM, the distance of the vertices of the $(M - 1)$ -simplex from the origin has to be maximized. The geometry of positive semidefinite operators is visualized in Section 4.1. The constructed traceless (N, M) -operators of a single POVM span identical linear subspaces for a given basis and enumeration, regardless of the construction method. However, the directions of the $(M - 1)$ -simplexes differ, which can affect the positive semidefiniteness of the constructed operators. Rotations within the subspaces can affect the obtained x -values but they do not alter the defining Eqs. (3.40)-(3.42).

This section covers the construction of (N, M) -POVM from a given traceless Hermitian orthonormal operator basis. In the subsequent section, the representation of a given (N, M) -POVM in an arbitrary Hermitian orthonormal bases is discussed.

3.3 REPRESENTATION OF (N, M) -POVMS IN ARBITRARY HERMITIAN OPERATOR BASES

In this section, the linear map between (N, M) -POVMS and arbitrary Hermitian orthonormal operator bases is discussed. This property will be essential to analyze the efficiency of different types of (N, M) -POVMS for entanglement and EPR steering detection. The informationally complete (N, M) -POVMS are linear Hermitian operators acting on the Hilbert space \mathcal{H}_d and can be expanded into an arbitrary basis of Hermitian operators $\{G\}$ defined in Eq. (2.11). In this section, it is assumed that a (N, M) -POVM with parameter x exists. The positive semidefiniteness of the POVM elements is not used to derive the following statements. An arbitrary (N, M) -POVM can be expanded in an arbitrary Hermitian operator basis by

$$\mathbf{\Pi} = \mathbf{G}^T \mathbf{S}, \tag{3.53}$$

where \mathbf{G} is a d^2 -dimensional vector and each component is a basis element of the basis $\{G\}$. The components of the NM -dimensional vector $\mathbf{\Pi}$ are given by the POVM elements $\Pi_{i(\alpha,a)}$. The linear map $S : \mathcal{H}_{d^2} \rightarrow \mathcal{H}_{NM}$ maps basis elements from the Hilbert space \mathcal{H}_{d^2} to the possibly higher dimensional Hilbert space \mathcal{H}_{NM} . The dimension of the Hilbert space is an upper bound for the relation $NM + N - 1 \leq d^2$. The structure of this map is examined under the assumption that a (N, M) -POVM exists. In particular, the influence of the conditions (3.15)-(3.17) is imposed, but positive semidefiniteness of the POVM elements is not required. The linear map can be associated with a $d^2 \times NM$ dimensional matrix. The connection between the constraints (3.16) and (3.17), and the matrix elements is given by

$$\begin{aligned}
\text{tr}\{\Pi_{i(\alpha,a)} \Pi_{i(\alpha,b)}\} &= \text{tr}\{(\mathbf{G}^T S)_{i(\alpha,b)} (\mathbf{G}^T S)_{i(\alpha,a)}\} \\
&= \sum_{k,l=0}^{d^2-1} S_{k,i(\alpha,a)} S_{l,i(\alpha,b)} \text{tr}\{G_k G_l\} \\
&= \sum_{k=0}^{d^2-1} S_{k,i(\alpha,a)} S_{k,i(\alpha,b)} \\
&= (S^T S)_{i(\alpha,a),i(\alpha,b)} \\
&= x \delta_{a,b} + (1 - \delta_{a,b}) \frac{d - Mx}{M(M-1)} \\
&= \Gamma \delta_{a,b} - \frac{\Gamma}{M} + \frac{d}{M^2}, \tag{3.54}
\end{aligned}$$

$$\begin{aligned}
\text{tr}\{\Pi_{i(\alpha,a)} \Pi_{i(\beta,b)}\} &= \text{tr}\{(\mathbf{G}^T S)_{i(\beta,b)} (\mathbf{G}^T S)_{i(\alpha,a)}\} \\
&= \sum_{k,l=0}^{d^2-1} S_{k,i(\alpha,a)} S_{l,i(\beta,b)} \text{tr}\{G_k G_l\} \\
&= \sum_{k=0}^{d^2-1} S_{k,i(\alpha,a)} S_{k,i(\beta,b)} \\
&= (S^T S)_{i(\alpha,a),i(\beta,b)} \\
&= \frac{d}{M^2} \tag{3.55}
\end{aligned}$$

for $N \geq 2$, $\alpha, \beta \in \{1, \dots, N\}$, $a, b \in \{1, \dots, M\}$ and $\alpha \neq \beta$. Compactly, the matrix elements can be written as

$$(S^T S)_{i(\alpha,a),j(\alpha',a')} = \Gamma \delta_{i(\alpha,a),j(\alpha',a')} - \frac{\Gamma}{M} \left(\bigoplus_{\alpha=1}^N J_\alpha \right)_{i(\alpha,a),j(\alpha',a')} + \frac{d}{M^2} J_{i(\alpha,a),j(\alpha',a')} \tag{3.56}$$

with

$$\Gamma = \frac{M^2 x - d}{M(M-1)}. \tag{3.57}$$

The all-ones matrices J of dimension $NM \times NM$ and J_α of dimension $M \times M$ are used to write the result compactly, i.e. $(J_\alpha)_{i(\alpha,a),j(\alpha',a')} = \delta_{\alpha,\alpha'}$. The spectral representation of the matrix S is derived from the symmetric real-valued matrix $S^T S$. The rank of the $NM \times NM$ matrix $S^T S$ is bounded by [73]

$$\text{rank}(S^T S) \leq \min(\text{rank}(S^T), \text{rank}(S)) \leq \min(d^2, NM) \leq d^2. \tag{3.58}$$

Therefore, the maximum number of non-zero eigenvalues is d^2 . The matrix fulfills

$$\begin{aligned} S^T S J &= \left(\mathbb{1}_{NM} \Gamma - \frac{\Gamma}{M} \left(\bigoplus_{\alpha=1}^N J_\alpha \right) + \frac{d}{M^2} J \right) \\ &= \Gamma J - \frac{\Gamma}{M} M \Gamma + \frac{d}{M^2} N M J \\ &= \frac{dN}{M} J, \end{aligned} \quad (3.59)$$

and consequently, the first eigenvalue is $\Lambda_1 = dN/M$ with the corresponding eigenvector $X_{i,1} = 1/\sqrt{NM}$ for all $i \in \{1, \dots, NM\}$. To compute the remaining eigenvalues and corresponding eigenvectors, a tensor product structure is introduced

$$\mathbf{X}_k = x_{N,\alpha(k)} \otimes x_{M,a(k)}, \quad (3.60)$$

$$S^T S = \Gamma \mathbb{1}_N \otimes \mathbb{1}_M - \frac{\Gamma}{M} \mathbb{1}_N \otimes J_M + \frac{d}{M^2} J_N \otimes J_M. \quad (3.61)$$

The sum of the three matrices is simultaneously diagonalizable. Only the all-ones matrices J_N and J_M have to be diagonalized. The eigenvalues and corresponding eigenvectors of J_N are

$$\lambda_1 = N, \quad x_{N,1} = \frac{1}{\sqrt{N}}(1, \dots, 1), \quad (3.62)$$

$$\lambda_\alpha = 0, \quad x_{N,\alpha} \quad \text{with} \quad \sum_{l=1}^N x_{N,\alpha,l} = 0, \quad (3.63)$$

for $\alpha = \{2, \dots, N\}$ and analog for J_M

$$\mu_1 = M, \quad x_{M,1} = \frac{1}{\sqrt{M}}(1, \dots, 1), \quad (3.64)$$

$$\mu_a = 0, \quad x_{M,a} \quad \text{with} \quad \sum_{l=1}^M x_{M,a,l} = 0, \quad (3.65)$$

for $a = \{2, \dots, M\}$. The eigenvectors of $S^T S$ in Eq. (3.60) can be divided into three groups with different eigenvalues. The first eigenvalue $\Lambda_1 = dN/M$ with the eigenvector $\mathbf{x}_{N,1} \otimes \mathbf{x}_{M,1}$ has already been calculated in Eq. (3.59). The second set of eigenvectors is

$$\Lambda_k = \Gamma \quad \mathbf{X}_k = \mathbf{x}_{N,\alpha} \otimes \mathbf{x}_{M,a} \quad (3.66)$$

with $k(\alpha, a) = \alpha - M + aN - 1$ for $\alpha \in \{1, \dots, N\}$ and $a \in \{2, \dots, M\}$. The degeneracy of this eigenvalue is $N(M-1)$. The informational completeness of the (N, M) -POVM $d^2 = N(M-1) + 1$ states that the remaining eigenvalues have to be zero

$$\Lambda_{NM-N+\alpha} = \Gamma - \frac{\Gamma}{M} M = 0, \quad \mathbf{X}_{NM-N+\alpha} = \mathbf{x}_{N,\alpha} \otimes \mathbf{x}_{M,1} \quad (3.67)$$

for $\alpha \in \{2, \dots, N\}$. A complete set of $N(M-1) + 1 + N - 1 = NM$ eigenvectors has been calculated and the spectrum is fully characterized. From the definition of the eigenvectors follows that for $k \geq 2$ the sum over the components vanishes

$$\sum_{v=1}^{NM} X_{k,v} = 0. \quad (3.68)$$

The spectrum for $N \geq 2$ reads

$$\text{Sp}(S^T S) = \left\{ \Gamma^{(N(M-1))}, \frac{dN^{(1)}}{M}, 0^{(N-1)} \right\}. \quad (3.69)$$

The numbers in the round brackets indicate the multiplicity of the eigenvalues. For the case of $N = 1$, the matrix has to be replaced by

$$S^T S = \mathbb{1}_M \Gamma + \left(-\frac{\Gamma}{M} + \frac{d}{M^2} \right) J_M = \mathbb{1}_M \Gamma + \frac{d - Mx}{M(M-1)} J_M. \quad (3.70)$$

The eigenvalues and corresponding eigenvectors of $S^T S$ for $N = 1$ and $a \geq 2$ are given by

$$\Lambda_1 = \frac{d}{M}, \quad \mathbf{X}_a = \mathbf{x}_{M,1} \quad (3.71)$$

$$\Lambda_1 = \Gamma, \quad \mathbf{X}_a = \mathbf{x}_{M,a}. \quad (3.72)$$

The spectrum reads

$$\text{Sp}(S^T S) = \left\{ \Gamma^{(M-1)}, \frac{dN^{(1)}}{M} \right\} \quad (3.73)$$

and the eigenvalue zero no longer appears. The spectral representation of the components of the symmetric operator map is given by

$$(S^T S)_{i,j} = \sum_{\mu=1}^{d^2} X_{i,\mu} \Lambda_{\mu} X_{\mu,j}^T \quad (3.74)$$

$$X_{i,\mu} = \hat{v}_i \cdot (\mathbf{X}_{\mu} \hat{u}_{\mu}^T) \quad (3.75)$$

with the canonical bases $\{\hat{v}_i, i \in \{1, \dots, NM\}\}$ of \mathcal{H}_{NM} and $\{\hat{u}_{\mu}, \mu \in \{1, \dots, d^2\}\}$ of \mathcal{H}_{d^2} . From Eq. (3.68) follows that the sum over the components of $X_{i,\mu}$ has to vanish

$$\sum_{a=1}^M X_{i(a,a),v} = 0. \quad (3.76)$$

The $NM \times d^2$ matrix $X_{i,\mu}$ fulfills the orthogonality condition

$$\sum_{i=1}^{NM} (X^T)_{\mu,i} X_{i,v} = \delta_{\mu v} \quad (3.77)$$

for $\mu, v \in \{1, \dots, d^2\}$. As a consequence of Eq. (3.18), the most general form of the $d^2 \times NM$ matrix $S_{\mu,i}$, which is consistent with the Eqs. (3.16) and (3.17) is given by

$$S_{\mu,i} = \sum_{\mu'=1}^{d^2} O_{\mu,\mu'}^T \sqrt{\Lambda_{\mu'}} X_{\mu',i}^T \quad (3.78)$$

with the arbitrary real-valued orthogonal $d^2 \times d^2$ matrix O , i.e. $OO^T = O^T O = P_{d^2}$. Here, P_{d^2} denotes the projection operator onto the d^2 -dimensional eigenspace of non-zero eigenvalues

of the linear operator $S^T S$ in the Hilbert space \mathcal{H}_{NM} . The additional condition (3.1), which characterizes any POVM, is obtained from

$$\mathbb{1}_d = \sum_{a=1}^M \Pi_{i(\alpha, a)} = \sqrt{d} \sum_{\mu=1}^{d^2} G_\mu O_{\mu,1}^T, \quad (3.79)$$

where the vanishing of the sum over the components of the eigenvectors of $S^T S$ has been used [Eq. (3.76).] This implies that condition (3.1) is fulfilled and ensures that the elements of a single POVM sum to identity. Therefore, the relations (3.15)-(3.17) and the informational completeness relation (3.1) are encoded in the map $S : \mathcal{H}_{d^2} \rightarrow \mathcal{H}_{NM}$. This map can be represented in a basis of traceless Hermitian operators, $\tilde{G} = OG$, where O is defined in Eq. (3.79), by $\Pi = G^T S = \tilde{G}^T \tilde{S}$. The components of the linear map are given by

$$\tilde{S}_{\nu,i} = \sqrt{\Lambda_\nu} X_{\nu,i}^T. \quad (3.80)$$

In this new basis \tilde{G} , it is clear that the map S injectively maps \mathcal{H}_{d^2} onto a d^2 -dimensional subspace of \mathcal{H}_{NM} , while preserving orthogonality. All basis operators \tilde{G}_ν with $\nu \in \{1, \dots, d^2-1\}$ are conformally mapped onto a (d^2-1) -dimensional subspace of \mathcal{H}_{NM} by stretching the norms of all operators by a factor of $\sqrt{\Gamma}$, according to Eq. (3.69) or (3.73). As these basis operators are orthogonal to \tilde{G}_0 , they are characterized by the basis-independent property $\text{tr}\{\tilde{G}_\nu\} = 0$ for $\nu \in \{1, \dots, d^2-1\}$. Only the basis operator \tilde{G}_0 is stretched by a different factor, namely $\sqrt{\Lambda_1} = \sqrt{dN/M}$. Additionally, it is important to note that the matrix $\tilde{S}\tilde{S}^T = \Lambda$ is diagonal for (N, M) -POVMS.

In the derivation it has been assumed that for the parameters (N, M, x) there exist a (N, M) -POVM. These relations hold for all Hermitian operators that fulfill the defining equations of (3.15)-(3.17) and (3.1), regardless of their positive semidefiniteness. For entanglement detection and EPR steering verification from Alice to Bob, this map leads to a scaling relation that allows the calculation of the efficiency of a (N, M) -POVM without the need to construct (N, M) -POVMS. This is the foundation of the results of the Chapters 5 and 6. The connection between (N, M) -POVMS and arbitrary Hermitian operator bases is used to derive the following relations, which are then employed to establish EPR steering and entanglement detection inequalities. The first relation is

$$\begin{aligned} \sum_{a=1}^N \sum_{a=1}^M \Pi_{i(\alpha, a)}^2 &= \text{tr}\{\mathbf{\Pi}\mathbf{\Pi}^T\} = \text{tr}\{\tilde{G}^T \tilde{S}\tilde{S}^T \tilde{G}\} \\ &= \frac{dN}{M} \tilde{G}_0^2 + \Gamma \sum_{k=1}^{d^2-1} \tilde{G}_k^2 \\ &= \left(\frac{dN}{M} - \Gamma \right) \tilde{G}_0^2 + \Gamma \sum_{k=0}^{d^2-1} \tilde{G}_k^2 \\ &= \left(\frac{d^2-1}{M(M-1)} - \frac{\Gamma}{d} + \frac{d^2-1}{d} \Gamma \right) \mathbb{1}_d \\ &= \frac{d^2-1}{(M-1)Md} (d + M^2 x - d) \mathbb{1}_d \\ &= \frac{(d^2-1)Mx}{(M-1)d} \mathbb{1}_d. \end{aligned} \quad (3.81)$$

In the first line, the representation Eq. (3.53) has been used and in the third line, has been used that $\tilde{S}\tilde{S}^T$ is diagonal in the basis of \tilde{G} . Furthermore, the definition of Γ [Eq. (3.57)] and the

invariant Eq. (B.18) has been used. For a given density matrix $\rho = \tilde{\mathbf{G}}^T \mathbf{r}$, the second important relation is the index of coincidence [59]

$$\begin{aligned}
\mathcal{C}(\rho) &= \sum_{\alpha=1}^N \sum_{a=1}^M \text{tr}\{\Pi_{i(\alpha,a)}\rho\}^2 \\
&= \sum_{\alpha=1}^N \sum_{a=1}^M (\mathbf{r}^T \tilde{\mathbf{S}}_{i(\alpha,a)})^2 \\
&= \sum_{\alpha=1}^N \sum_{a=1}^M \mathbf{r}^T (\tilde{\mathbf{S}}_{i(\alpha,a)} \tilde{\mathbf{S}}_{i(\alpha,a)}^T) \mathbf{r} \\
&= \mathbf{r} \tilde{\mathbf{S}} \tilde{\mathbf{S}}^T \mathbf{r} \\
&= r_0^2 \frac{dN}{M} + \Gamma \sum_{i=1}^{d^2-1} r_i^2 \\
&= r_0^2 \left(\frac{dN}{M} - \Gamma \right) + \Gamma \sum_{i=0}^{d^2-1} r_i^2 \\
&= \frac{N}{M} - \frac{\Gamma}{d} + \Gamma \text{tr}\{\rho^2\} \\
&= \frac{d^3 - M^2 x + d(M^2 x - d) \text{tr}\{\rho^2\}}{dM(M-1)} \tag{3.82}
\end{aligned}$$

with $r_0 = 1/\sqrt{d}$. For pure states, \mathcal{C} reaches its maximum

$$\begin{aligned}
\mathcal{C}(\rho) &\leq \frac{d^3 - M^2 x + d(M^2 x - d)}{dM(M-1)} \\
&= \frac{d-1}{d} \frac{d^2 + M^2 x}{M(M-1)}. \tag{3.83}
\end{aligned}$$

The purpose of these relations is to derive the entanglement and EPR steering detection inequalities without imposing the positive semidefiniteness of the POVM elements. This section's main result is the scaling relation, which simplifies the calculation of such inequalities by eliminating the need to construct (N, M) -POVMs. The scaling relation is valid for all parameters x within its definition space, but it does not answer whether a (N, M) -POVM exists for a given parameter x . The reason for this is that the scaling relation has been derived from the positive semidefinite operator $S^T S$, instead of S . It is important to note that the positive semidefinite operator $S^T S$ can also be generated from Hermitian operators, which are not necessarily positive semidefinite. The existence of (N, M) -POVMs remains an open question and is discussed in detail in Chapter 4.

EXISTENCE OF (N, M) -POVMS

In the previous chapter, the properties of (N, M) -POVMS have been discussed in detail. Furthermore, the characteristics of the linear map S connecting (N, M) -POVMS to Hermitian operator bases have been derived. Thereby, this is the foundation to derive sufficient conditions for entanglement or EPR steering detection regardless of the positive definiteness of the POVM elements. Section 3.2 construction methods ensure that the relations Eqs. (3.15)-(3.17) are fulfilled but do not guarantee the positive semidefiniteness of the constructed operators. This limits the possible parameters x of informationally complete (N, M) -POVMS constructed from a given orthonormal basis of traceless Hermitian operators. For example, in order to violate the derived entanglement detection inequalities (5.33), (5.48) and (5.49) in an experiment, it is necessary to know which local informationally complete (N, M) -POVMS can be implemented. Therefore, an investigation is required to identify the parameters x for which informationally complete (N, M) -POVMS exist.

In Section 4.1, the positive semidefinite operators spanned by a given traceless Hermitian orthonormal operator basis and its partitioning are analyzed. The goal is to show the dependence of the positive semidefiniteness from a given basis and its partitioning, in order to identify the constructible (N, M) -POVMS by the chosen approach. The area or volume of the positive semidefinite operators with an equal trace is shown for dimensions $d = \{2, 3, 4\}$ and possible (N, M) -POVMS with parameter $M = 3$ in Section 4.1.1 and $M = 4$ in Section 4.2, respectively. Furthermore, in Section 4.2, a MUB is constructed from the Clifford basis, where the basis elements spanning a single POVM are commutative for all POVMS. Necessary and sufficient conditions for the existence of informationally complete optimal (N, M) -POVMS are given in Section 4.2. First, a sufficient condition is shown for which x -values (N, M) -POVMS can be constructed from arbitrary traceless Hermitian orthonormal operator bases in arbitrary dimensions d . The connection between an isospectral traceless Hermitian orthonormal operator basis (IHOB) and optimal (N, M) -POVMS is introduced in Sections 4.2.1-4.2.4. The existence of such an IHOB is sufficient for the existence of optimal informationally complete (N, M) -POVMS. Furthermore, in Section 4.2.2 for $M < d$, the sufficient condition is generalized to a necessary condition by including two additional relations of the basis elements. In Section 4.2.3, it is shown that the existence of an optimal (N, M) -POVM is both necessary and sufficient for $(N, 2)$ -POVMS. Sections 4.3 and 4.4 discuss the current state of the art regarding the existence and construction of SIC-POVMS and MUBs.

4.1 POSITIVE SEMIDEFINITENESS OF POVM ELEMENTS

In this section, the positive semidefiniteness of POVM elements is discussed. The approach to construct (N, M) -POVM in Section 3.2.2 is sufficient to fulfill the relations (3.15)-(3.17). However, the positive semidefiniteness has to be checked for all POVM elements for a given x -value.

Therefore, the set of positive semidefinite operators with fixed trace spanned by a given orthonormal basis of traceless Hermitian operators and its partitioning is analyzed in detail.

Consider a (N, M) -POVM $\Pi = \{\Pi_{i(\alpha, a)}\}$ where $\alpha \in \{1, \dots, N\}$ denotes the POVM and the measurement results are denoted by $a \in \{1, \dots, M\}$. Such POVM elements can be represented by Eq. (3.78)

$$\Pi_{i(\alpha, a)} = \frac{\mathbb{1}_d}{M} + \sqrt{\Gamma} \sum_{\mu=1}^{d^2-1} X_{i(\alpha, a), \mu} \tilde{G}_\mu \quad (4.1)$$

for each POVM element with $\Gamma = (M^2 x - d)/(M(M-1))$. The set $\{\tilde{G}_\mu\}$ is an arbitrary traceless Hermitian operator basis, where $\mu \in \{1, \dots, d^2-1\}$. The basis elements are only determined up to an orthogonal transformation $O(d^2-1)$. Furthermore, the $d^2 \times NM$ matrices $X_{i(\alpha, a)}$ can be freely chosen as long as they fulfill relation (3.76). It is apparent that restricting these choices of freedom severely reduces the parameter ranges x for which (N, M) -POVMS can be constructed.

The completeness relation (3.18) states that the POVM elements consist of $d^2-1 = N(M-1)$ linearly independent Hermitian operators. To ensure that condition (3.17) is met, the (d^2-1) -dimensional vector space over the field of real numbers is partitioned into N basis tuples B_α of $M-1$ elements, using the traceless Hermitian orthonormal operator basis $\{\tilde{G}_\mu\}$. Each tuple B_α corresponds to a single POVM, denoted by α . This restricts the general definition of Eq. (4.1) to the ansatz

$$\Pi_{i(\alpha, a)} = \frac{\mathbb{1}_d}{M} + \sqrt{\Gamma} \sum_{\mu \in B_\alpha} X_{i(\alpha, a), \mu} \tilde{G}_\mu. \quad (4.2)$$

This method restricts transformations to $O(M-1)$ for each partition of basis elements B_α , while the construction methods outlined in Section 3.2 fix the coefficients entirely for a given partition. Therefore, the attainable (N, M) -POVMS depend on the chosen traceless Hermitian orthonormal operator basis $\{\tilde{G}_\mu\}$ and its partitioning. Examples for $M=3$ and $M=4$ are discussed to illustrate the restrictions of the positive semidefiniteness of the POVM elements imposed by a given basis and its partitioning.

4.1.1 Positive semidefiniteness of MUM elements for qutrits

In the previous sections, it has been discussed that positive semidefiniteness limits the existence of (N, M) -POVMS. In dimension $d=3$ and for $(4, 3)$ -POVMS (MUMs), the positive semidefiniteness of a single POVM and its dependence on the chosen basis is investigated. For this purpose, three traceless Hermitian operator bases are examined: the Gell-Mann basis and two IHOBs constructed from a MUB and a SIC-POVM. For the construction of a MUM, the 8-dimensional real vector space must be decomposed into four 2-dimensional subspaces. The origin of the vector space represents the identity matrix divided by the dimension $\mathbb{1}_d/d$. The basis elements of each subspace are given by $\tilde{G}_{i(\alpha)}$ and $\tilde{G}_{j(\alpha)}$, and the coefficient associated with a single POVM are given by $g_{i(\alpha, a)}$ and $g_{j(\alpha, a)}$. A POVM element has the basis representation

$$\Pi_{i(\alpha, a)} = \frac{\mathbb{1}_3}{3} + g_{i(\alpha, a)} \tilde{G}_{i(\alpha)} + g_{j(\alpha, a)} \tilde{G}_{j(\alpha)} = \frac{\mathbb{1}_3}{3} + \mathbf{g}_{\alpha, a} \cdot \tilde{\mathbf{G}}_\alpha. \quad (4.3)$$

Analogous to the Bloch vector of a qudit, a real vector $\mathbf{g}_{\alpha, a}$ representing the POVM element is defined and called the (N, M) -vector. For a MUM, all (N, M) -vectors have the same length of

$$|\mathbf{g}_{\alpha, a}| = \sqrt{x-1/d} \quad (4.4)$$

and fixed angles to each other. As explained in Section 3.2, the three (N, M) -vectors that represent a single POVM have to be the vertices of an equilateral triangle with its centroid at the origin. A necessary condition for the positive semidefiniteness follows from Eq. (3.16)

$$\begin{aligned} 1 = \text{tr}\{\Pi_{i(\alpha,a)}^2\} &= \frac{1}{3} + g_{i(\alpha,a)}^2 + g_{j(\alpha,a)}^2 \\ \Rightarrow g_{i(\alpha,a)}^2 + g_{j(\alpha,a)}^2 &\leq \frac{2}{3}. \end{aligned} \quad (4.5)$$

The discussed examples show that the set of positive semidefinite operators with a trace equal to one contains a circle of radius

$$|\mathbf{g}_{\alpha,a}| \leq r_{\text{in}} = \frac{1}{\sqrt{6}}. \quad (4.6)$$

The details for deriving this boundary for arbitrary (N, M) -POVMs will be discussed in Section 4.2 and its expression can be found in Eq. (4.29). All the operators $\Pi_{i(\alpha,a)}$ whose (N, M) -vectors fulfill this condition are positive semidefinite for any vector direction. The sufficient condition guarantees that MUMs fulfilling Eq. (4.6) can be constructed by the methods of Section 3.2 for arbitrary traceless Hermitian operator bases. The construction of MUMs in dimension $d = 3$ can be interpreted geometrically as a construction of equilateral triangles in each 2-dimensional subspace. The centroid of each triangle is located at the origin of the real vector space and the edge length is $2\sqrt{3}\sqrt{x-1/d}$. The vertices of the triangle represent the POVM elements. To maximize the x -value of a (N, M) -POVM generated from a given basis, the distance from the vertices to the origin has to be maximized inside the positive semidefinite operators Eq. (4.3) generated from the partitions B_α . To archive this, the triangle can be rotated by $O(2)$ transformations as long as the Hermitian operators remain positive semidefinite. The $O(2)$ transformations do not change the orthogonality condition of Eq. (3.17) for (N, M) -vectors of different POVMs. To be a (N, M) -POVM, the x -values have to be identical for all generated POVMs.

The positive semidefinite matrices are visualized in Figs. 4.1-4.3 to show the restrictions on the positive semidefiniteness from a chosen basis and its partitioning. Visualizing the set of positive semidefinite operators in the 2-dimensional subspaces enhances the construction methods in Sections 3.2.1 and 3.2.2. First, the Gell-Mann basis, enumerated as in Eq. (B.10), is evaluated. The partition of the basis elements is $B_\alpha = \{(1, 8), (3, 4), (2, 5), (6, 7)\}$. The area for which the coefficients lead to positive semidefinite operators is shown in Fig. 4.1. The yellow circle shows the necessary condition defined by the outer circle Eq. (4.5) and the green circle shows the basis-independent sufficient condition for positive semidefiniteness Eq. (4.6). The blue area shows the convex set of positive semidefinite operators spanned from the two basis elements. The first POVM is spanned by the two basis elements of \tilde{G}_1^{GM} and \tilde{G}_8^{GM} in Fig. 4.1a. Regarding this POVM alone, it is possible to fit in a maximal triangle inside the positive semidefinite elements, which intersects with the boundary of the necessary condition (yellow circle) [c.f. Eq. (4.5)]. The vertices of the blue equilateral triangle represent an optimal POVM, these points are also the extreme points of the convex set of the positive semidefinite operators with a trace equal to one. The second POVM is described by the (N, M) -vector with the basis elements \tilde{G}_3^{GM} and \tilde{G}_4^{GM} and shown in Fig. 4.1b. The area of positive semidefinite operators generated by the two basis elements changes compared to the first POVM, which is no longer an equilateral triangle. It only has two intersections with the boundary of the necessary condition. The set of positive semidefinite operators has a curved and a straight boundary. The boundary intersections cannot be used to fit in an equilateral triangle with a centroid at the origin. The last two POVMs have geometrically identical sets of positive

semidefinite operators, a circle of radius $r_p = \sqrt{2}/3$ in Fig. 4.1c. All elements have to be positive semidefinite to form a (N, M) -POVMS. The maximum value of x for the Gell-Mann basis and the chosen partition is denoted by the vertices of the red and purple triangles in Fig. 4.1. The vertices of the red triangle in Fig. 4.1c represent the POVM spanned by the Gell-Mann matrices \tilde{G}_2^{GM} and \tilde{G}_5^{GM} , while the vertices of the purple triangle represent the POVM spanned by \tilde{G}_6^{GM} and \tilde{G}_7^{GM} . It is shown that the red and purple triangles do not have to be aligned like in the construction methods of Section 3.2. The triangles can be rotated freely for the partitions B_3 and B_4 in Fig. 4.1c. For the partition B_1 in Fig. 4.1a, there are some rotations that leave the positive semidefiniteness of the POVM elements invariant. In contrast, the orientation of the triangle of partition B_2 in Fig. 4.1b cannot be altered. The set of realizable MUMs is slightly larger than the sufficient condition for arbitrary bases Eq. (4.6). The red triangle belongs to a MUM with maximal $x_{\text{GM}} = 5/9 \approx 0.556 > 0.5 = x_{\text{in}}$, which can be achieved by the cutting of 8-dimensional vector space induced by the Gell-Mann basis. This is a slight increase of the parameter x over the always achievable MUMs. The orientation of the red triangle is not unique for Gell-Mann matrices. The size of the triangles cannot be increased because it already intersects with the boundary of the circle of positive semidefinite operators in Fig. 4.1. Permutation of the basis elements cannot improve the maximum x -values of the constructed POVMs. The positive semidefinite operators spanned by all combinations of two Gell-Mann basis elements have been calculated [110].

The next orthonormal basis is the MUB basis \tilde{G}^{MUB} constructed from a given MUB (B.22). This traceless Hermitian orthonormal operator basis is isospectral, which means that all basis elements have an identical spectrum Eq. (4.52), and it is given by

$$\text{Sp}(\tilde{G}_i^{\text{MUB}}) = \left\{ \frac{3 - \sqrt{3}}{6}, \frac{-3 - \sqrt{3}}{6}, \frac{1}{\sqrt{3}} \right\}. \quad (4.7)$$

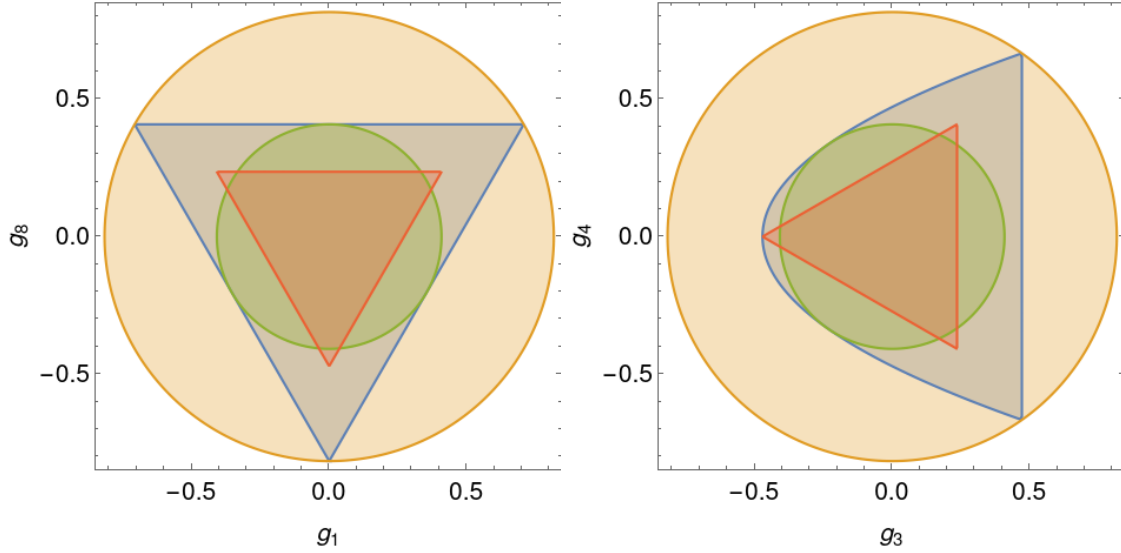
By construction, this basis can construct a MUB (optimal MUM), as seen in Eq. (3.32). The positive semidefiniteness of the operators spanned in the 2-dimensional subspaces is shown in Fig. (4.2a). For all POVMs, the area of positive semidefinite operators (red triangle) is identical and the intersection points with the outer yellow circle describe the MUB elements. The identical positive semidefinite convex set for different partitions is explained by the isospectrality of the basis elements and for the particular case of MUBs, the Hermitian basis elements of a single POVM have to be simultaneously diagonalizable.

The region of positive semidefiniteness changes if two or more basis elements are exchanged between different partitions, such that the basis elements within a partition are not simultaneously diagonalizable (Fig. 4.2b). The red triangle in the figure represents the possible POVMs constructed from the partition $B_\alpha = \{(1, 3), (2, 4), (5, 7), (6, 8)\}$. Positive semidefiniteness limits the MUMs that can be constructed to a maximum parameter, which is close to the always achievable limit. This example shows that the selecting of the traceless Hermitian orthonormal operator basis and its partitioning is essential for constructing optimal MUMs.

A SIC-POVM in dimension $d = 3$ is an optimal (N, M) -POVM for $N = 1$ and $M = 9$, as defined in Section 3.1. Therefore, the SIC basis, derived from the SIC-POVM in Eq. (A.8), is isospectral (B.19) with

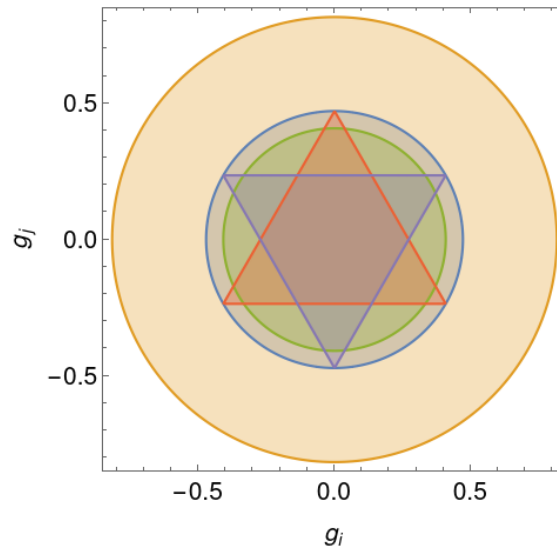
$$\text{Sp}(\tilde{G}_i^{\text{SIC}}) = \left\{ \frac{1}{12}(-\sqrt{3} - 3\sqrt{7}), \frac{1}{12}(-\sqrt{3} + 3\sqrt{7}), \frac{1}{2\sqrt{3}} \right\}. \quad (4.8)$$

and the exact enumeration is given in Eq. (B.20). The positive semidefiniteness of possible MUM elements is examined to check if knowledge of the SIC basis can be used to construct a MUB. Fig. 4.3 displays the positive semidefinite regions of the 2-dimensional subset. The



(a) Shows the region of positive semidefiniteness for $(i, j) = (1, 8)$.

(b) Shows the region of positive semidefiniteness for $(i, j) = (3, 4)$.

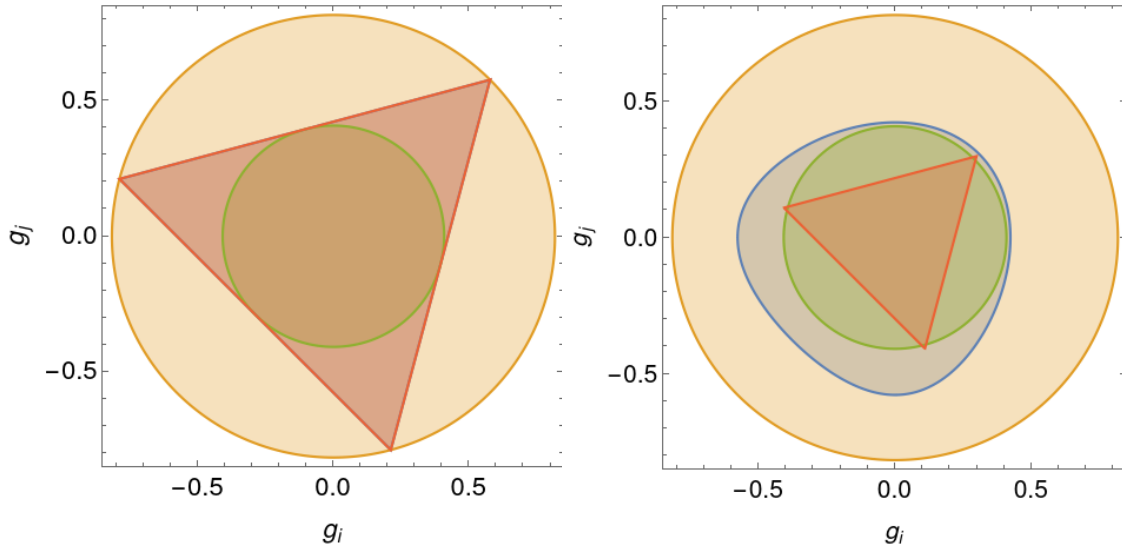


(c) Shows the region of positive semidefiniteness for $(i, j) = \{(2, 5), (6, 7)\}$.

Figure 4.1: Regions of positive semidefinite operators corresponding to the four different partitions B_α , $\alpha \in \{1, \dots, 4\}$ of the four POVMs of an informationally complete MUM: The yellow region represents the necessary condition for positive semidefiniteness Eq. (4.5), while the green area is the sufficient condition Eq. (4.6). The region depicted in blue comprises the positive semidefinite operators generated by the Gell-Mann basis and its partitioning. The vertices of the red and purple triangles are the POVM elements of a maximal achievable MUM of $x = 5/9$.

asymmetric regions of positive semidefiniteness only allow for fitting in equilateral triangles close to the always achievable limit. Therefore, the SIC basis has no important properties for constructing MUMs.

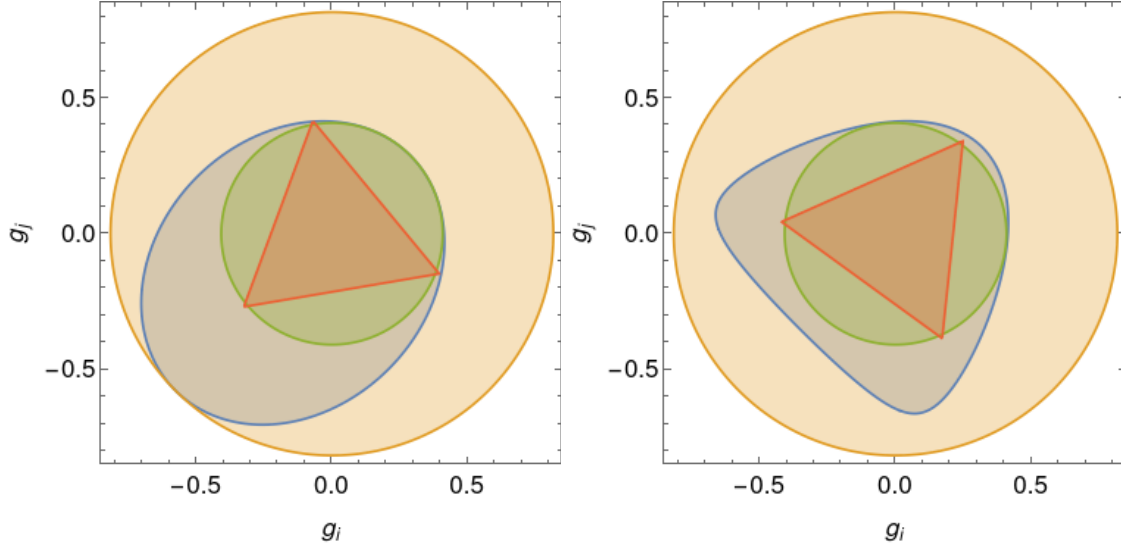
The graphical illustrations of the area of positive semidefiniteness in Figs. 4.1-4.3 show how to construct MUMs with a maximal x -value for a given basis. The area of the positive semidefinite operators can significantly change depending on the traceless Hermitian orthonormal operator basis used and its partition B_α . The construction process begins with a given traceless Hermitian orthonormal operator basis and its partitioning into four tuples of two elements. This divides 8-dimensional vector space into four 2-dimensional subspaces. The cutting of the subspaces affects the area of positive semidefiniteness. Therefore, the approach of selecting a traceless Hermitian orthonormal operator basis and its partitioning influences the achievable (N, M) -POVMS with parameter x . First, the Gell-Mann basis has been discussed, showing that it is possible to construct MUMs with $x \geq x_{\text{in}}$ using this basis. However, a MUB (optimal MUM) has not been achieved. The second basis discussed is the MUB basis, constructed from a given MUB. By definition, this basis can construct an optimal MUM. The partitioning of the basis elements is crucial for constructing optimal MUMs. Only by changing the partitions the generated MUMs can be changed from MUBs to far from optimal MUMs, which are near the always achievable limit. The SIC basis can only construct MUMs that are close to the always achievable limit. Therefore, the SIC basis and its partitioning are not well-suited for constructing optimal MUMs. These three bases demonstrate the importance of selecting the appropriate basis and its partitioning for constructing MUMs. From a geometric point of view, it is essential to cut the vector space of Hermitian operators with a fixed trace into the appro-



(a) Shows the region of positive semidefiniteness of a MUB for $(i, j) \in \{(1, 2), (3, 4), (5, 6), (7, 8)\}$.

(b) Shows the region of positive semidefiniteness of a MUB for $(i, j) = \{(1, 3), (2, 4), (5, 7), (6, 8)\}$.

Figure 4.2: Regions of positive semidefinite operators corresponding to the MUB basis Eq. (B.22): The yellow region represents the necessary condition for positive semidefiniteness Eq. (4.5), while the green area represents the sufficient condition Eq. (4.6). The region depicted in blue comprises the positive semidefinite operators generated by the MUB basis and its partitioning. The vertices of the red triangles represent the POVM elements. The first partition forms an optimal MUM (MUB), while the second only forms a MUM with a parameter close to Eq. (4.5).



(a) Shows the region of positive semidefiniteness for $(i, j) = (1, 2)$

(b) Shows the region of positive semidefiniteness for $(i, j) = \{(3, 4), (5, 6), (7, 8)\}$.

Figure 4.3: Regions of positive semidefinite operators corresponding to the four different partitions B_α , $\alpha \in \{1, \dots, 4\}$ of the four POVMs of an informationally complete MUM: The yellow region denotes the necessary condition for positive semidefiniteness Eq. (4.5), while the green area representing the sufficient condition Eq. (4.6). The blue area encompasses the positive semidefinite operators spanned by the SIC basis and its partitioning. The vertices of the red triangles are the POVM elements of a MUM, which are outside of the green area.

priate subspaces. The positive semidefiniteness of the operators is not a basis-independent property of the vector space, making it difficult to ensure the positive semidefiniteness of the POVM elements. The visualization of the positive semidefiniteness is extended in the subsequent section by considering $(N, 4)$ -POVMs.

4.1.2 Positive semidefiniteness of POVM elements for $M = 4$

In Section 4.1.1, the dependence of the positive semidefiniteness of the constructed operators from the chosen traceless Hermitian orthonormal operator basis and its partitions, has been visualized for the case of $M = 3$ but only in dimension $d = 3$. This section expands on this topic by examining the positive semidefiniteness for $M = 4$ but for different dimensions d . A special case of positive semidefinite operators is those acting on qubits. The change of the positive semidefiniteness is shown for a $(N, 4)$ -POVM by increasing the dimension from $d = 2$ to $d = 4$. Firstly, the $(1, 4)$ -POVM (GSIC in dimension $d = 2$) is discussed and followed by a $(5, 4)$ -POVM (MUM) in dimension $d = 4$. Two different Hermitian orthonormal bases are discussed for the $(5, 4)$ -POVM.

For the case of $d = 2$, the inner and outer radii of the (N, M) -POVMs Eqs. (4.29) and (4.30) are identical

$$r_{\text{in}}^2 = r_{\text{out}}^2 = \frac{2}{M^2}. \quad (4.9)$$

for GSICs and MUMs, the only possible (N, M) -POVMs. This means that the positive semidefinite operators with a trace of $2/M$ can be represented by all points inside the ball with a radius of $\sqrt{2}/M$ around the origin. For MUMs the set of positive semidefinite operators is equivalent

to the Bloch ball, which represents qubit quantum states. However, the $(3, 2)$ -POVMS are described by three orthogonal lines inside the ball with a centroid at the origin. The endpoints of the lines must have the same distance from the origin. The lines' endpoints represent a single POVM, while the lines intersecting with the boundary are optimal MUMs (MUBs). In contrast, a density matrix is only represented by a single point inside the Bloch ball, and the pure states are located on the boundary.

For $M = 4$, the POVM elements form a regular tetrahedron (3-simplex) with its centroid at the origin of real vector space in Fig. 4.4. The edges of the tetrahedron represent the POVM elements. Since sufficient and necessary conditions are identical for $d = 2$, the tetrahedron can be oriented in any direction for any value of the parameter x . The construction of GSICs and MUMs is trivial for $d = 2$ due to the simple condition of positive semidefiniteness.

The change of the necessary and sufficient conditions of the positive semidefiniteness for MUMs ($M = d = 4$) is examined. The vertices of the tetrahedron represent the single POVM elements like GSICs in $d = 2$ and the elements are given by

$$\Pi_{i(\alpha, a)} = \frac{\mathbb{1}_4}{4} + g_{i(\alpha, a)} \tilde{G}_{i(\alpha)} + g_{j(\alpha, a)} \tilde{G}_{j(\alpha)} + g_{k(\alpha, a)} \tilde{G}_{k(\alpha)} = \frac{\mathbb{1}_4}{4} + \mathbf{g}_{\alpha, a} \cdot \tilde{\mathbf{G}}_{\alpha} = \frac{\mathbb{1}_4}{4} + \sum_{i \in B_{\alpha}} g_{i, a} \tilde{G}_i \quad (4.10)$$

The basis elements $G_{i(\alpha)}$, $G_{j(\alpha)}$ and $G_{l(\alpha)}$ are used to construct a single POVM, denoted by α . Here, $\tilde{\mathbf{G}}$ is a traceless Hermitian orthonormal operator basis, which is partitioned into five tuples with three elements (i, j, k) . Geometrically, this means that the 15-dimensional real-valued vector space is cut into five subspaces of dimension three. Each partition B_{α} generates a single POVM. The (N, M) -vector $\mathbf{g}_{\alpha, a}$ describes the POVM elements and the norm of the

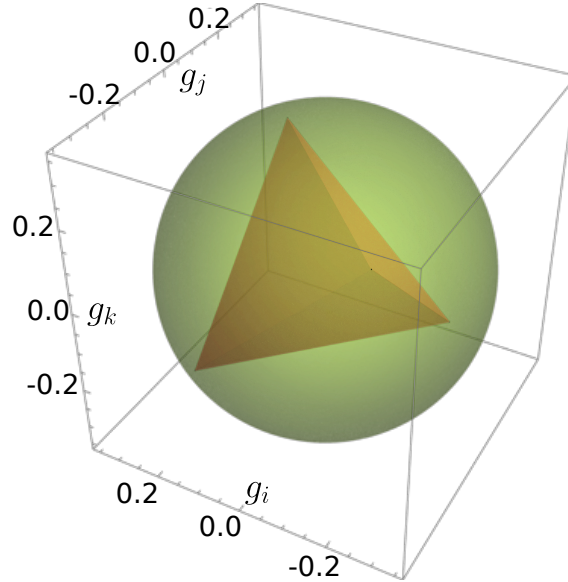


Figure 4.4: Positive semidefiniteness of the Hermitian operators in $d = 2$ with a trace equal to $1/2$: The green ball represents the positive semidefinite operators, while the elements of the SIC-POVM are the vertices of the red tetrahedron. The red tetrahedron can rotate freely inside the volume of positive semidefiniteness.

vectors must be identical for all $\alpha \in \{1, \dots, N\}$ and $a \in \{1, \dots, M\}$. The inner and outer radii are given by Eqs. (4.29) and (4.30)

$$r_{\text{in}} = \sqrt{\frac{1}{6}}, \quad (4.11)$$

$$r_{\text{out}} = \sqrt{\frac{3}{4}}. \quad (4.12)$$

The trivial construction of (5,4)-POVM is only possible for $x \leq x_{\text{in}} = 1/3$ [c.f. Eq. (4.32)] because all vectors of $|\mathbf{g}_{\alpha,a}| \leq r_{\text{in}}$ describe positive semidefinite operators. For larger x -values, it is necessary to examine the volume of positive semidefiniteness spanned from a given basis and its partition. First, the generalized Gell-Mann basis $\{\tilde{G}_i^{\text{GM}}\}$ in Eq. (B.11) with the enumeration of Eq. (B.12) is used. The Gell-Mann basis is used to divide the 15-dimensional vector space into five 3-dimensional subspaces. The POVMs are placed within the subspaces. The positive semidefinite volumes are shown in Fig. 4.5. Analogous to the case of $d = 3$, the volume of positive semidefiniteness spanned by the diagonal Gell-Mann matrices allows the construction of a single optimal POVM Fig. 4.5a. The set of three POVMs is bounded by a sphere of radius

$$r_b^2 = \frac{1}{8} \quad (4.13)$$

which includes the minimal ball Fig. 4.5b. The tetrahedron of the last POVM has to fit into the bicone shown in Fig. 4.5c. Constructing a (5,4)-POVM requires the positive semidefiniteness of all POVM elements. The vertices of the red tetrahedrons in Fig. 4.5 are the (5,4)-POVMs with the maximum value of x that can be constructed from the Gell-Mann basis. The POVM elements correspond to the vertices of the tetrahedrons. In this example, all tetrahedrons are all oriented in the same direction. The orientation of all tetrahedrons does not need to be identical. In any subspace, they can be transformed by the group $O(3)$ as long as they remain within the blue volumes of the positive semidefinite operators. For simplicity, only one tetrahedron is shown in Fig. 4.5b, representing the positive semidefinite volumes for three partitions. These POVMs intersect with the boundary of the positive sphere of radius r_b . The positive semidefiniteness of the partitioning to construct a MUM by the generalized Gell-Mann basis in $d = 4$ shows the similarities to the Gell-Mann basis in $d = M = 3$ Fig. 4.1. This example shows that the partitioning of the generalized Gell-Mann basis is not suitable for constructing MUBs.

To construct MUMs, another operator basis is utilized, which inherits important properties from the 2-dimensional case. The question arises whether these properties are adequate to construct a MUB. In dimension $d = 4$, the Clifford basis can be used, which is a tensor product of Pauli matrices Eq. (B.8)

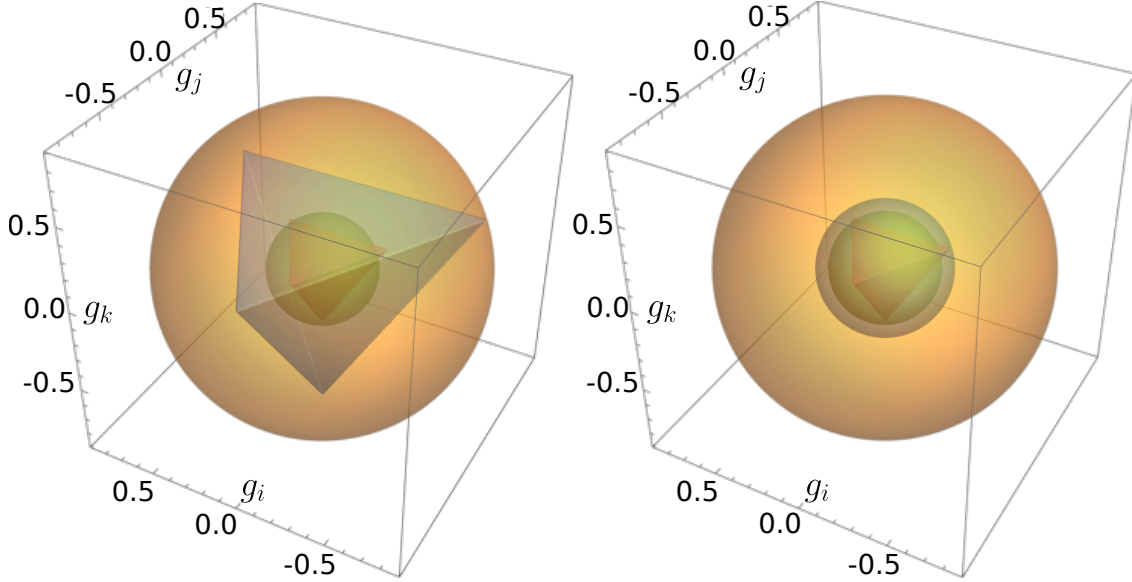
$$G_i = \frac{1}{2} \mathbb{1}_2 \otimes \sigma_i, \quad (4.14)$$

$$G_{3+i} = \frac{1}{2} \sigma_i \otimes \mathbb{1}_2, \quad (4.15)$$

$$G_{3+3j+i} = \frac{1}{2} \sigma_j \otimes \sigma_i \quad (4.16)$$

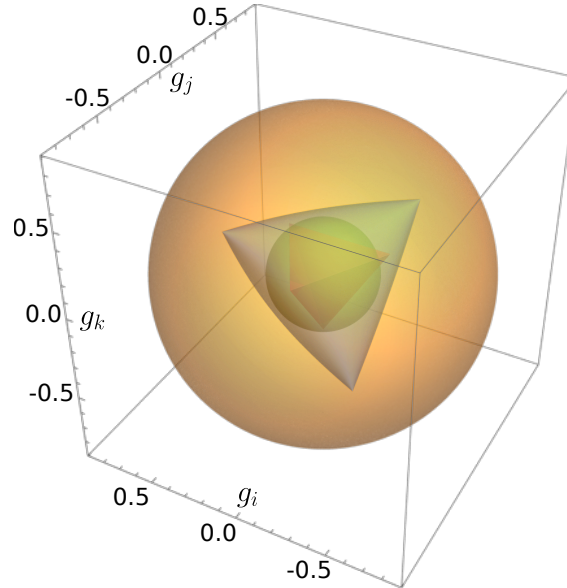
for $i, j = \{1, 2, 3\}$. The subsequent discussion shows which of the essential properties of the positive semidefinite operators generated by the Pauli matrices can be transferred to the Clifford basis. The chosen partition of the Clifford basis is

$$B_1 = (1, 2, 3), \quad B_2 = (4, 5, 6), \quad B_3 = (8, 9, 10), \quad B_4 = (14, 13, 12), \quad \text{and} \quad B_5 = (7, 11, 15). \quad (4.17)$$



(a) Shows the region of positive semidefiniteness for $(i, j, k) = (1, 2, 3)$.

(b) Shows the region of positive semidefiniteness for $(i, j, k) = \{(4, 5, 6), (10, 11, 12), (13, 14, 15)\}$.



(c) Shows the region of positive semidefiniteness for $(i, j, k) = \{(7, 8, 9)\}$.

Figure 4.5: Regions of positive semidefinite operators corresponding to the five different partitions $B_\alpha, \alpha \in \{1, \dots, 5\}$ of the five POVMs of an informationally complete MUM: The yellow ball is the necessary condition for positive semidefiniteness Eq. (4.12), while the green ball is the sufficient condition Eq. (4.11). The blue volume is the positive semidefinite operators spanned by the Gell-Mann basis and its partitioning. The vertices of the red tetrahedron are the POVM elements of the maximal x -value constructed from the generalized Gell-Mann basis and this partitioning. The size of the tetrahedrons cannot be increased because they intersect with the boundary of positive semidefiniteness in Fig. 4.5b.

The positive semidefinite volumes spanned by these partitions is shown in Fig. 4.6. The first two tuples, B_1 and B_2 , represent partitions of single-particle Pauli matrices. However, the volume is computed with single-particle Pauli matrices. It is only bounded with a sphere of radius $1/\sqrt{2}$ and does not intersect with the boundary of the sufficient condition with r_{out} in Fig. 4.6a. Therefore, the single-particle Pauli matrices are insufficient for constructing optimal MUMs. The third POVM in Fig. 4.6b is defined by the three basis elements of tensor products of identical Pauli matrices. The volume of the positive semidefinite operators is equivalent to the set of the Bell diagonal quantum states. While the tetrahedron edges form an optimal single POVM, the other POVMs restrict the positive semidefiniteness to much smaller x -values. The volume of the positive semidefinite operators of the remaining operators is shown in Fig. 4.6c, which is slightly larger than the minimal sphere. To construct a (5,4)-POVM, all element of the POVMs must be positive semidefinite. The edges of the red tetrahedrons represent a possible (5,4)-POVM outside the volume of the always positive semidefinite operators. Cutting the 15-dimensional vector space into five 3-dimensional subspaces defined by this partitioning has not succeeded in constructing optimal (5,4)-POVMs. Relation (3.16) for two different elements of an optimal MUM is given by Eq. (3.16)

$$\text{tr}\{\Pi_{i(\alpha,a)}\Pi_{i(\alpha,b)}\} = 0 \quad (4.18)$$

for all $\alpha \in \{1, \dots, 5\}$ and $a, b \in \{1, \dots, 4\}$ with $a \neq b$ and can be used to construct a MUB. Furthermore, the POVM elements have rank one. Therefore, the elements of a single POVM can be simultaneously diagonalized. Thus, the basis elements of a single tuple representing a POVM must also be simultaneously diagonalizable and commuting. The partitioning of Eq. (4.17) only contains simultaneously diagonalizable basis elements in the third tuple. Another way to choose the partitions is

$$B_1 = (1, 4, 7), \quad B_2 = (2, 5, 11), \quad B_3 = (3, 6, 15), \quad B_4 = (8, 12, 13), \quad \text{and} \quad B_5 = (9, 10, 14). \quad (4.19)$$

These partitions contain only tuples of commuting basis elements. Even the tuples of simultaneously diagonalizable basis elements differ from those in Eq. (4.17). The Hermitian operators defined from this partition are

$$2\Pi_{i(l,a)} = \frac{\mathbb{1}_4}{2} + g_{i(l,a)}\mathbb{1}_2 \otimes \sigma_l + g_{j(l,a)}\sigma_l \otimes \mathbb{1}_2 + g_{k(l,a)}\sigma_l \otimes \sigma_l \quad (4.20)$$

$$2\Pi_{i(4,a)} = \frac{\mathbb{1}_4}{2} - g_{i(4,a)}\sigma_1 \otimes \sigma_2 + g_{j(4,a)}\sigma_2 \otimes \sigma_3 + g_{k(4,a)}\sigma_3 \otimes \sigma_1 \quad (4.21)$$

$$2\Pi_{i(5,a)} = \frac{\mathbb{1}_4}{2} - g_{i(5,a)}\sigma_1 \otimes \sigma_3 + g_{j(5,a)}\sigma_2 \otimes \sigma_1 + g_{k(5,a)}\sigma_3 \otimes \sigma_2 \quad (4.22)$$

for $l = 1, 2, 3$. The eigenvalues of the operators are independent of α and the eigenvalues are only denoted by a

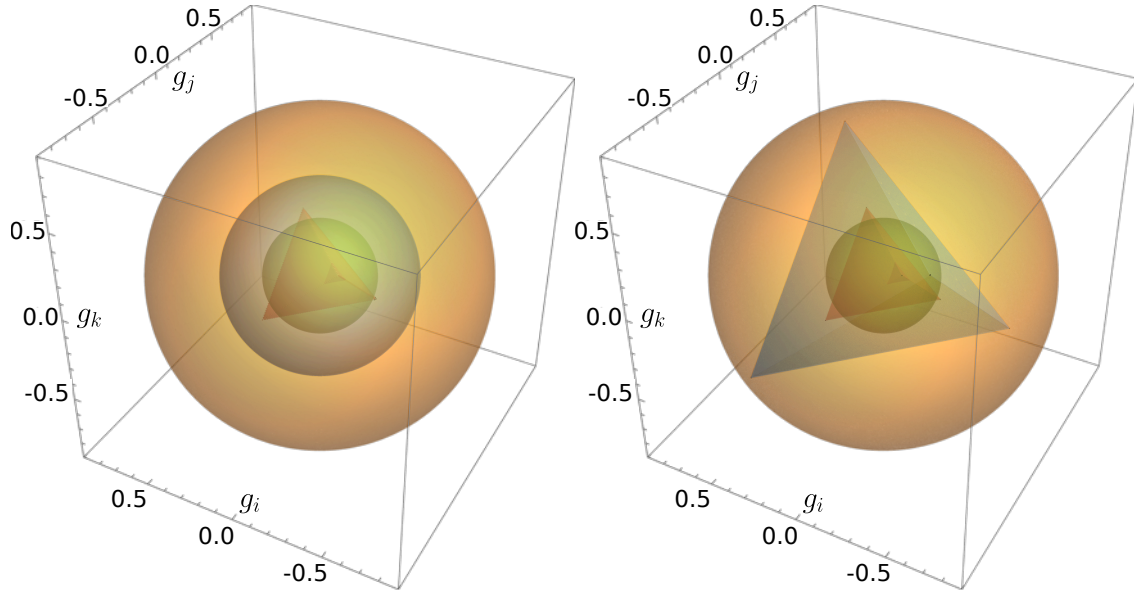
$$\begin{aligned} \lambda_1 &= \frac{1}{4}(1 + g_{(1,a)} - 2g_{(2,a)} - 2g_{(3,a)}), & \lambda_2 &= \frac{1}{4}(1 - g_{(1,a)} + 2g_{(2,a)} - 2g_{(3,a)}) \\ \lambda_3 &= \frac{1}{4}(1 - g_{(1,a)} - 2g_{(2,a)} + 2g_{(3,a)}), & \lambda_4 &= \frac{1}{4}(1 + g_{(1,a)} + 2g_{(2,a)} + 2g_{(3,a)}). \end{aligned} \quad (4.23)$$

The subset of positive semidefinite operators defined by this partition of the basis elements is geometrically equivalent to Fig. 4.6b up to a 3-dimensional rotation. The solution for optimal (5,4)-POVMs or MUBs is given by the (N, M) -vectors

$$2\mathbf{g}_a = \{(1, -1, -1), (-1, 1, -1), (-1, -1, 1), (1, 1, 1)\} \quad (4.24)$$

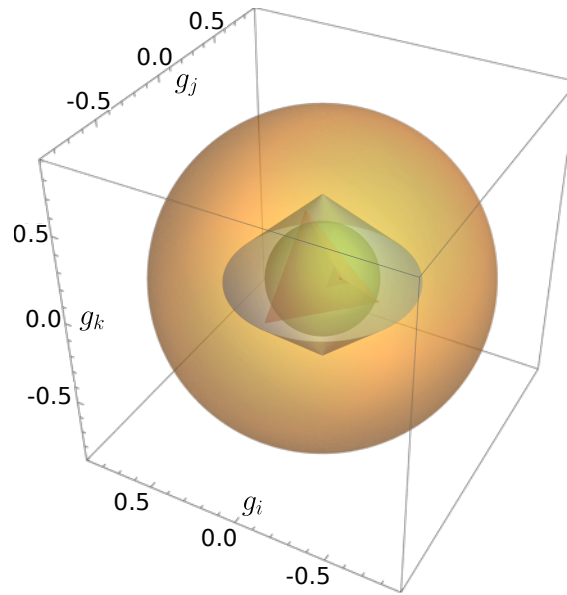
which represent the edges of the convex set of positive semidefinite operators within the subspaces. The Hermitian operators' simple eigenvalue relation allows the construction of a MUB. The POVM element of the solution $2\mathbf{g}_4 = (1, 1, 1)$ aligns with the POVM element $(a = M = d)$ constructed from Eq. (3.32). However, the other remaining constructed matrices do not belong to the positive semidefinite operator subspace. The fixed position of the tetrahedron in Eq. (3.32) prohibits the construction of an optimal MUM. This highlights the significance of permitting $O(3)$ transformations of the basis elements within a tuple B_α .

From these examples, it has been demonstrated that regardless of the chosen dimension, the shape of the POVM elements in the real vector space is a tetrahedron for $M = 4$. In the case where $d = 2$ and GSICs, a criterion for positive semidefiniteness exists, making the construction trivial. Constructing (N, M) -POVM with large x -values for $d > 2$ is more difficult when there is a significant difference between the outer and inner radius. Additionally, the shape of the positive semidefinite operators can be greatly influenced by the selected traceless Hermitian orthonormal operator basis and its partitioning. The example shows that the Clifford basis with the correct partitioning can construct an optimal MUM. The commonly used basis of the generalized Gell-Mann matrices can only construct (N, M) -POVMs that are close to the limited by x_{in} . To construct optimal (N, M) -POVMs, it is important to first select a suitable traceless Hermitian orthonormal operator basis, partition it, and then orient the tetrahedrons inside the positive semidefinite operators. The examples presented clarify the challenge of constructing optimal (N, M) -POVMs induced by the positive semidefiniteness. The subsequent section will explore necessary and sufficient conditions for the existence of optimal (N, M) -POVMs in arbitrary dimensions.



(a) Shows the region of positive semidefiniteness for $(i, j, k) = \{(1, 2, 3), (4, 5, 6)\}$

(b) Shows the region of positive semidefiniteness for $(i, j, k) = (7, 11, 15)$.



(c) Shows the region of positive semidefiniteness for $(i, j, k) = \{(8, 9, 10), (14, 13, 12)\}$.

Figure 4.6: Regions of positive semidefinite operators corresponding to the five different partitions $B_\alpha, \alpha \in \{1, \dots, 5\}$ of the five POVMs of an informationally complete MUM: The yellow ball marks the necessary condition for positive semidefiniteness Eq. (4.12), while the green ball is the sufficient condition Eq. (4.11). The blue volume comprises the positive semidefinite operators that are spanned by the Clifford basis and its partitioning. The vertices of the red tetrahedrons describe POVM elements of a MUM whose x -value surpasses the bound of the always achievable limit.

4.2 NECESSARY CONDITIONS FOR CONSTRUCTING (N, M) -POVMS

In the previous section, the construction of (N, M) -POVMS from a given basis has been discussed. It has been shown in Section 3.3 that the fulfillment of relations (3.15)–(3.17), regardless of the positive semidefiniteness of the POVM elements, is always possible. However, the construction of (N, M) -POVMS from a traceless Hermitian orthonormal operator basis and its partitioning is limited by positive semidefiniteness, which restricts the eligible x -values. Already in the figures of the previous section, the condition for the (N, M) -POVMS, which can be constructed from arbitrary traceless Hermitian orthonormal operators and their partitioning has been visualized. A sufficient condition is derived that all constructed operators are (N, M) -POVMS independent of the chosen traceless Hermitian orthonormal operator basis. The derivation of the condition under which all POVM elements are positive semidefinite relies on the general properties of positive semidefinite matrices [74, 75]. This relation is established by considering a single POVM element. For this purpose, a single POVM in a d -dimensional Hilbert space is considered and its spectral representation

$$\Pi_{i(\alpha, a)} = \frac{\mathbb{1}_d}{d} + \mathbf{g}_{\alpha, a} \cdot \tilde{\mathbf{G}} = \sum_{\sigma=1}^d \lambda_{\sigma} P_{\sigma}. \quad (4.25)$$

with $\tilde{\mathbf{G}}$ the vector of traceless Hermitian orthonormal basis elements and the (N, M) -vector $\mathbf{g}_{\alpha, a}$ defining the POVM elements. The spectral decomposition is given by the non-negative eigenvalues and the one-dimensional orthogonal projection P_{σ} with $P_{\sigma}P_{\sigma'} = P_{\sigma}\delta_{\sigma\sigma'}$, which sum up to the identity $\sum_{\sigma=1}^d P_{\sigma} = \mathbb{1}_d$. The vectors $\mathbf{g}_{\alpha, a}$, describing positive semidefinite operators, form a convex set. The constraint (3.15) yields

$$\text{tr}\{\Pi_{i(\alpha, a)}\} = \frac{d}{M} = \sum_{\sigma=1}^d \lambda_{\sigma}. \quad (4.26)$$

Therefore, for a given set of projection operators P_{σ} , the positive semidefinite operators with a trace equal to d/M form a $(d-1)$ -dimensional simplex Δ_{d-1} . The boundary of the simplex is given by the positive semidefinite operators. These operators have at least one eigenvalue equal to zero. The surface areas of the simplex Δ_{d-1} are given by $(d-2)$ -dimensional simplexes $\Delta_{d-2} := \partial\Delta_{d-1}$. The centroid of the simplex is given by

$$C_{d-1} = \frac{\text{tr}\{\Pi_{i(\alpha, a)}\}}{d} \sum_{\sigma=1}^d P_{\sigma} = \frac{1}{M} \mathbb{1}_d. \quad (4.27)$$

The simplex Δ_{d-1} is visualized in Fig. 4.7. The closest distance from the centroid of the simplex Δ_{d-1} to the boundary is the distance between the centroids of Δ_{d-1} and $\Delta_{d-2} = \partial\Delta_{d-1}$ and is calculated by

$$\begin{aligned} r_{\text{in}}^2 &= \text{tr}\{(C_{d-1} - C_{d-2})^2\} = (\text{tr}\{\Pi_{i(\alpha, a)}\})^2 \left[(d-1) \left(\frac{1}{d} - \frac{1}{d-1} \right)^2 + \frac{1}{d^2} \right] \\ &= \frac{(\text{tr}\{\Pi_{i(\alpha, a)}\})^2}{d(d-1)} = \frac{d}{M^2(d-1)}. \end{aligned} \quad (4.28)$$

This distance r_{in} defines the radius of the largest possible circle with center C_{d-1} , which lies within Δ_{d-1} and touches Δ_{d-1} in one of its d centroids C_{d-1} . A sufficient condition for positive semidefiniteness of a single operator follows from using Eqs. (3.15) and (3.16)

$$0 < |\mathbf{g}_{\alpha, a}|^2 = x - \frac{d}{M^2} = \text{tr}\{(\Pi_{i(\alpha, a)} - \mathbb{1}_d/M)^2\} \leq r_{\text{in}}^2 = \frac{d}{M^2(d-1)}. \quad (4.29)$$

The centroid of the simplex C_{d-1} Eq. (4.27) and the radius r_{in} are independent of the chosen spectral projections P_σ . Therefore, the condition for positive semidefiniteness can be applied to all POVM elements and guarantees the existence of (N, M) -POVMS with $x \leq r_{\text{in}}^2 + d/M^2$. The radius r_{in} has already been visualized in the figures of Section 4.2 and is a basis and partition-independent value. A necessary condition for the positive semidefiniteness is derived from Eq. (3.16)

$$|\mathbf{g}_{\alpha,a}|^2 = x - \frac{d}{M^2} \leq \min\left(\frac{dM-d}{M^2}, \frac{d^2-d}{M^2}\right) = r_{\text{out}}^2. \quad (4.30)$$

The term $(dM-d)/M^2$ arises from the non-negativity of Eq. (3.16) for two different POVM elements. This expression is the upper bound for (N, M) -POVMS with $M < d$. Therefore, the possible elements of (N, M) -POVMS are a subset the k -simplex, see Fig. 4.7b. This figure shows that for $d=3$ and $M=2$, the optimal (N, M) -POVMS cannot have rank one.

To be an optimal (N, M) -POVM, all the (N, M) -vectors have to take the upper bound

$$|\mathbf{g}_{\alpha,a}| = r_{\text{out}}. \quad (4.31)$$

These necessary and sufficient conditions are independent of the chosen basis of traceless Hermitian orthonormal operators \tilde{G} . For density matrices, this is a common result and can be seen in [74, 75]. An arbitrary (N, M) -POVM can be constructed for all x -values bounded by

$$x \leq \frac{1}{d-1} \frac{d^2}{M^2} = x_{\text{in}}, \quad (4.32)$$

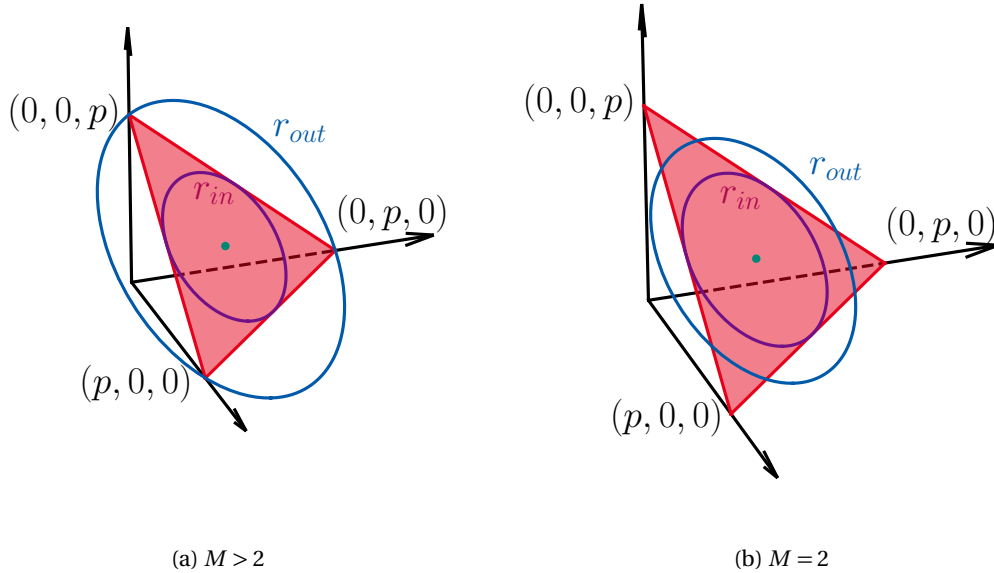


Figure 4.7: The 2-simplex of the eigenvalues of $d=3$: The red area depicts the positive semidefinite operators, while the blue circle illustrates the boundary of the necessary condition for positive semidefinite operators, Eq. (4.30). The violet circle represents the sufficient condition Eq. (4.29). The green dot represents the centroid of the simplex. The intersection of the simplex with the coordinate axis is at $p = d/M$.

independent of the chosen orthonormal basis of traceless Hermitian operators. The ratio of the interval length of the always achievable x -values to their maximum interval length is given by

$$R(d) = \frac{x_{\text{in}} - \frac{d}{M^2}}{x_{\text{max}} - \frac{d}{M^2}} = \frac{\frac{1}{d-1} \frac{d^2}{M^2} - \frac{d}{M^2}}{x_{\text{max}} - \frac{d}{M^2}} = \begin{cases} \frac{1}{(d-1)^2} & , \quad M \geq d \\ \frac{1}{(d-1)(M-1)} \leq \frac{1}{d-1} & , \quad 2 \leq M < d \end{cases} \quad (4.33)$$

The interval length ratio is plotted against the dimension in Fig. 4.8. It is apparent that as the dimension of the quantum system increases, the interval length ratio steadily approaches zero. Consequently, the length of the x -intervals rapidly converges towards zero. The case where $2 < M < d$ lies between the two curves and also approaches zero. In the qubit scenario where $d = 2$, the inner and outer radii are identical $r_{\text{in}} = r_{\text{out}}$. This implies that the set of positive semidefinite operators with a trace $\text{tr}\{\Pi_{i(\alpha, a)}\} = d/M$ is described by a 3-dimensional ball of radius $r = 2/M^2$. For $M = 2$, the set of positive semidefinite operators is known as the Bloch ball. A density matrix is represented by a single point, while (N, M) -POVMS are represented by a set of NM points with a fixed distance to the centroid. Optimal (N, M) -POVMS, such as SIC-POVMS, have been found in dimensions up to $d = 151$ and beyond [65]. This means that the discussed construction methods in Sections 3.2.1 and 3.2.2 depend significantly on the selected traceless Hermitian orthonormal basis. The existence of optimal (N, M) -POVMS induces restrictions on the traceless Hermitian operator bases that can be used to construct optimal (N, M) -POVMS with the ansatz of Sections 3.2.1 and 3.2.2. Furthermore, necessary and sufficient conditions for the existence of optimal (N, M) -POVMS are derived by establishing a connection between optimal (N, M) -POVMS and traceless Hermitian orthonormal operator bases in the subsequent subsections.

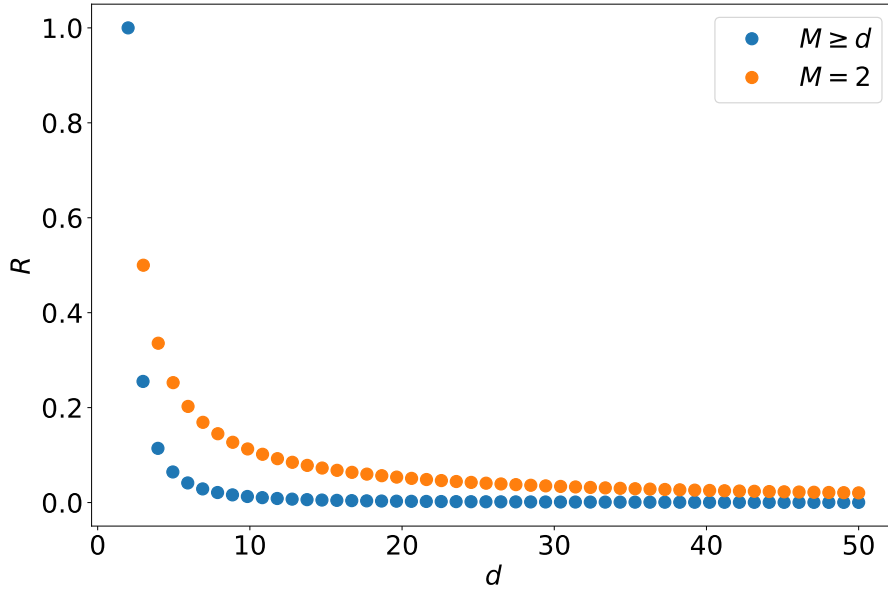


Figure 4.8: Interval ratio of the constructible (N, M) -POVMS in arbitrary bases to the maximum allowed interval: The ratio of the interval lengths decays to zero for increasing dimensions d . The $2 < M < d$ case is between the two cases.

4.2.1 Optimal (N, M) -POVMS for $M \geq d$

The construction methods outlined in Sections 3.2.1 and 3.2.2 demonstrate how to construct informationally complete (N, M) -POVMS using a given basis of traceless Hermitian operators $\{\tilde{G}_{i(\alpha,a)}\}$. Conversely, it is also possible to construct a set of orthonormal traceless Hermitian operators from a given (N, M) -POVM by

$$\tilde{G}_{i(\alpha,a)} = \frac{\sqrt{M-1}}{\sqrt{x-d/M^2 M(\sqrt{M+1})}} [\mathbb{1}_d + \sqrt{M}\Pi_{i(\alpha,M)} - \sqrt{M}(\sqrt{M+1})\Pi_{i(\alpha,a)}]. \quad (4.34)$$

It can easily be shown that the operators are orthonormal, i.e. $\text{tr}\{\tilde{G}_{i(\alpha,a)}\tilde{G}_{i(\beta,b)}\} = \delta_{\alpha\beta}\delta_{ab}$ for all $\alpha, \beta \in \{1, \dots, N\}$ and $a, b \in \{1, \dots, M-1\}$ [59]. The influence of optimal informationally complete (N, M) -POVMS on the constructed traceless Hermitian operator elements is examined in this section. The derivations are restricted to informationally complete (N, M) -POVMS where $N(M-1) = d^2 - 1$. Cases of $N(M-1) < d^2 - 1$ can be derived analogously. Optimal (N, M) -POVMS reach their upper bound of $x = d^2/M^2$ for $M \geq d$. The eigenvalues λ_i of an optimal (N, M) -POVM element $\Pi_{i(\alpha,a)}$ fulfill the defining relations (3.15-3.17) and must be positive semidefinite. Therefore, the spectrum of informationally complete optimal (N, M) -POVMS has to fulfill:

- (1) $\text{tr}\{\Pi_{i(\alpha,a)}\} = \sum_{i=1}^d \lambda_i = \frac{d}{M}$
- (2) $\text{tr}\{\Pi_{i(\alpha,a)}^2\} = \sum_{i=1}^d \lambda_i^2 = \frac{d^2}{M^2}$
- (3) $\lambda_i \geq 0$ for $i \in \{1, \dots, d\}$.

Combining conditions 1) and 2) leads to

$$\sum_{i=1}^d \lambda_i^2 = \left(\sum_{i=1}^d \lambda_i \right)^2 = \sum_{i=1}^d \lambda_i^2 + \sum_{i=1, i < j}^d \lambda_i \lambda_j \quad (4.35)$$

$$\Rightarrow \sum_{i=1, i < j}^d \lambda_i \lambda_j = 0. \quad (4.36)$$

Due to the positive semidefiniteness, it follows that one eigenvalue has to be d/M and the remaining eigenvalues have to be zero. This leads to the conclusion that the (N, M) -POVM elements are rank one operators and there are unit vectors $|\alpha, a\rangle$ so that the (N, M) -POVM elements can be written as

$$\Pi_{i(\alpha,a)} = \frac{d}{M} |\alpha, a\rangle \langle \alpha, a|. \quad (4.37)$$

The overlap of the vectors is given by

$$|\langle \alpha, a | \alpha, a' \rangle| = \sqrt{\frac{\frac{M}{d} - 1}{M-1}}, \quad (4.38)$$

$$|\langle \alpha, a | \beta, b \rangle| = \frac{1}{\sqrt{d}} \quad (4.39)$$

for $\alpha, \beta \in \{1, \dots, N\}$ and $a, a', b \in \{1, \dots, M\}$ with $\alpha \neq \beta$ and $a \neq a'$. The traceless Hermitian orthonormal basis of an optimal POVM for $M \geq d$ is given by Eq. (4.34)

$$\tilde{G}_{i(\alpha,a)} = \frac{\sqrt{M-1}}{(\sqrt{M+1})\sqrt{d^2-d}} [\mathbb{1}_d + \sqrt{M}\Pi_{i(\alpha,M)} - \sqrt{M}(\sqrt{M+1})\Pi_{i(\alpha,a)}]. \quad (4.40)$$

The spectrum of $\tilde{G}_{i(\alpha,a)}$ is examined by calculating the eigenvalues of the matrix

$$A_{i(\alpha,a)} = \sqrt{M}\Pi_{i(\alpha,M)} - \sqrt{M}(\sqrt{M}+1)\Pi_{i(\alpha,a)} \quad (4.41)$$

$$= \frac{d}{\sqrt{M}}|\alpha, M\rangle\langle\alpha, M| - \frac{d(\sqrt{M}+1)}{\sqrt{M}}|\alpha, a\rangle\langle\alpha, a|. \quad (4.42)$$

By definition, this matrix has maximal rank two, indicating that the eigenvalue zero has a multiplicity of at least $d-2$. The characteristic polynomial for the rank two matrix $A_{i(\alpha,a)}$ is given by

$$0 = \Lambda^d + c_{d-1}\Lambda^{d-1} + c_{d-2}\Lambda^{d-2}. \quad (4.43)$$

For the calculation of the coefficients c_{d-2} and c_{d-1} , the following properties are needed

$$\text{tr}\{A_{i(\alpha,a)}\} = \frac{d}{\sqrt{M}} - \frac{d(\sqrt{M}+1)}{\sqrt{M}} = -d \quad (4.44)$$

$$\begin{aligned} \text{tr}\{A_{i(\alpha,a)}^2\} &= \text{tr}\{M\Pi_{i(\alpha,M)}^2 - 2M(\sqrt{M}+1)\Pi_{i(\alpha,M)}\Pi_{i(\alpha,a)} + M(\sqrt{M}+1)^2\Pi_{i(\alpha,a)}^2\} \\ &= \frac{d^2}{M} - 2(\sqrt{M}+1)\frac{d-d^2/M}{M-1} + (\sqrt{M}+1)^2\frac{d^2}{M} \\ &= \frac{d(d\sqrt{M}+d-2)}{\sqrt{M}-1}. \end{aligned} \quad (4.45)$$

The Cayley-Hamilton theorem can be used to calculate the coefficients of the characteristic polynomial [88]

$$c_{d-1} = -\text{tr}\{A_{i(\alpha,a)}\} = d \quad (4.46)$$

$$\begin{aligned} c_{d-2} &= \frac{1}{2}[\text{tr}\{A_{i(\alpha,a)}\}^2 - \text{tr}\{A_{i(\alpha,a)}^2\}] = \frac{1}{2}\left[d^2 - \frac{d(d\sqrt{M}+d-2)}{\sqrt{M}-1}\right] \\ &= -\frac{d^2-d}{\sqrt{M}-1} \end{aligned} \quad (4.47)$$

and the polynomial is given by

$$0 = \Lambda^d + d\Lambda^{d-1} - \frac{d^2-d}{\sqrt{M}-1}\Lambda^{d-2} \quad (4.48)$$

$$= \left(\Lambda^2 + d\Lambda - \frac{d^2-d}{\sqrt{M}-1}\right)\Lambda^{d-2}. \quad (4.49)$$

The non-zero eigenvalues of the matrix $A_{i(\alpha,a)}$ are given by

$$\Lambda_{\pm} = \frac{1}{2}\left(-d \pm \sqrt{d^2 + 4\frac{d^2-d}{\sqrt{M}-1}}\right). \quad (4.50)$$

With these results, the eigenvalues Λ_i of $\tilde{G}_{i(\alpha,a)}$ can be calculated easily by Eq. (4.40)

$$\begin{aligned} \Lambda_j &= \frac{\sqrt{M-1}}{(\sqrt{M}+1)\sqrt{d^2-d}} \\ \Lambda_{d-1} &= \frac{\sqrt{M-1}}{(\sqrt{M}+1)\sqrt{d^2-d}}(1 + \Lambda_+) \\ \Lambda_d &= \frac{\sqrt{M-1}}{(\sqrt{M}+1)\sqrt{d^2-d}}(1 + \Lambda_-) \end{aligned} \quad (4.51)$$

for $\{j = 1, \dots, d-2\}$. These results are independent of the chosen basis elements, so their spectrum is given by

$$\text{Sp}(\tilde{G}_{i(\alpha, a)}) = \frac{\sqrt{M-1}}{(\sqrt{M+1})\sqrt{d^2-d}} \{1^{(d-2)}, (1+\Lambda_+)^{(1)}, (1+\Lambda_-)^{(1)}\}, \quad (4.52)$$

where the number in brackets denotes the degeneracy of the eigenvalues. Thus, the basis $\{\tilde{G}_{i(\alpha, a)}\}$ is an IHOB. This result has already been derived for the special case of informationally complete GSICs ($N=1, M=d^2$) [62]. If an optimal (N, M) -POVMs is not informationally complete, the IHOB is replaced by an isospectral traceless Hermitian orthonormal system of $N(M-1) < d^2 - 1$ operators, which are defined in Eq. (4.40). Therefore, the existence of such an orthonormal system is necessary for the existence of optimal (N, M) -POVMs which are not informationally complete.

Two examples of IHOBs have been used in Section 4.1.1. The first is the SIC basis constructed from the SIC-POVM in Eq. (A.7), which leads to basis elements with the spectrum Eq. (B.19)

$$\text{Sp}(\tilde{G}_i^{\text{SIC}}) = \left\{ \frac{1}{12}(-\sqrt{3}-3\sqrt{7}), \frac{1}{12}(-\sqrt{3}+3\sqrt{7}), \frac{1}{2\sqrt{3}} \right\}. \quad (4.53)$$

The exact numeration and structure of these basis elements are shown in Eq. (B.20). The second basis is constructed from the MUB in Eq. (A.3) and has the spectrum Eq. (B.21)

$$\text{Sp}(\tilde{G}_i^{\text{MUB}}) = \left\{ \frac{3-\sqrt{3}}{6}, \frac{-3-\sqrt{3}}{6}, \frac{1}{\sqrt{3}} \right\}. \quad (4.54)$$

The exact numeration and structure of these basis elements are shown in Eq. (B.22). The subsequent subsections derive equivalent necessary conditions for (N, M) -POVMs with $2 \leq d < M$.

4.2.2 Optimal (N, M) -POVMs for $2 < M < d$

In this subsection, a necessary and sufficient condition for the existence of optimal (N, M) -POVMs for $2 < M < d$ is proposed. The following derivations are restricted to informationally complete (N, M) -POVMs with $N(M-1) = d^2 - 1$, while the cases of $N(M-1) < d^2 - 1$ can be derived analogously. It will be demonstrated that the elements of optimal (N, M) -POVMs with $2 < M < d$ are projection operators of rank d/M . The necessary condition also holds for $M=2$. However, this case will be discussed in detail in Section 4.2.3. An optimal (N, M) -POVM has a maximum value of $x = d/M$ and its elements fulfill

$$\text{tr}\{\Pi_{i(\alpha, a)}\} = \sum_{\sigma=1}^d \lambda_{\sigma} = \frac{d}{M} > 1 \quad (4.55)$$

$$\text{tr}\{\Pi_{i(\alpha, a)}^2\} = \sum_{\sigma=1}^d \lambda_{\sigma}^2 = \frac{d}{M} > 1 \quad (4.56)$$

with non-negative eigenvalues $\lambda_{\sigma} \geq 0$ of $\Pi_{i(\alpha, a)}$. The spectrum of these operators is further restricted by relation (3.16). Any pair of elements of a single optimal (N, M) -POVM has to fulfill

$$\begin{aligned} 0 &= \text{tr}\{\Pi_{i(\alpha, a)}\Pi_{i(\alpha, b)}\} = \text{tr}\{\sqrt{\Pi_{i(\alpha, a)}\Pi_{i(\alpha, b)}}\sqrt{\Pi_{i(\alpha, b)}\Pi_{i(\alpha, a)}}\} \\ &= \left\| \sqrt{\Pi_{i(\alpha, b)}\Pi_{i(\alpha, a)}} \right\|_{\text{HS}}^2 \end{aligned} \quad (4.57)$$

for all $\alpha \in \{1, \dots, N\}$ and $a, b \in \{1, \dots, M\}$ with $a \neq b$. The Hilbert-Schmidt scalar product induced norm in Eq. 4.57 vanishes and therefore, the matrices have to be zero

$$\sqrt{\Pi_{i(\alpha,b)}\Pi_{i(\alpha,a)}} = 0, \quad \sqrt{\Pi_{i(\alpha,a)}\Pi_{i(\alpha,b)}} = 0. \quad (4.58)$$

Thus, the product of two different elements of a single POVM has to be zero $\Pi_{i(\alpha,a)}\Pi_{i(\alpha,b)} = 0$ for all $\alpha \in \{1, \dots, N\}$ and $a, b \in \{1, \dots, M\}$ with $a \neq b$. From the completeness relation (3.1) follows

$$\Pi_{i(\alpha,a)} = \Pi_{i(\alpha,a)} \sum_{b=1}^M \Pi_{i(\alpha,b)} = \Pi_{i(\alpha,a)}^2. \quad (4.59)$$

Thus, all (N, M) -POVM elements have to be of rank d/M orthogonal projections and can only exist if d is an integer multiple of M . Furthermore, for optimal (N, M) -POVMs with $2 < M < d$ the defining relation (3.16) is equivalent to

$$\text{tr}\{\Pi_{i(\alpha,a)}\Pi_{i(\alpha,b)}\} = \frac{d}{M}\delta_{ab} \Leftrightarrow \Pi_{i(\alpha,a)}\Pi_{i(\alpha,b)} = \delta_{ab}\Pi_{i(\alpha,a)} \quad (4.60)$$

while the conditions (3.15) and (3.17) remain unchanged. The spectrum of optimal (N, M) -POVM elements is given by

$$\text{Sp}(\Pi_{i(\alpha,a)}) = (\mathbf{1}^{(d/M)}, \mathbf{0}^{(d-d/M)}). \quad (4.61)$$

The number in the brackets indicates the degeneracy of the eigenvalues. Following the necessary condition, the $(21, 4)$ -POVM in dimension $d = 8$ with $x = 2$ is the smallest dimension in which such an informationally complete optimal (N, M) -POVM can exist. The POVM elements are rank two projections.

Analog to the case of $M \geq d$, a traceless Hermitian orthonormal operator basis can be constructed from an optimal (N, M) -POVM with $2 < M < d$ by Eq. (4.40)

$$\tilde{G}_{i(\alpha,a)} = \frac{1}{(\sqrt{M}+1)\sqrt{d}} [\mathbb{1}_d + \sqrt{M}\Pi_{i(\alpha,M)} - \sqrt{M}(\sqrt{M}+1)\Pi_{i(\alpha,a)}]. \quad (4.62)$$

The POVM elements $\Pi_{i(\alpha,a)}$ and $\Pi_{i(\alpha,b)}$ commute for all $\alpha \in \{1, \dots, N\}$ and $a, b \in \{1, \dots, M\}$, indicating that they share a common eigenbasis. Therefore, the POVM elements of a single POVM can be represented by

$$\Pi_{i(\alpha,a)} = \sum_{k=(a-1)d/M+1}^{ad/M} |\alpha, k\rangle \langle \alpha, k|, \quad (4.63)$$

where $\{|\alpha, k\rangle | k \in \{1, \dots, d\}\}$ is a common eigenbasis of all elements of a single POVM, denoted by α . By using this representation, the spectrum of Eq. (4.62) reads

$$\begin{aligned} \text{Sp}(\tilde{G}_{i(\alpha,a)}) &= \left\{ \left(\frac{1}{(\sqrt{M}+1)\sqrt{d}} \right)^{(d-2d/M)}, \left(\frac{1}{\sqrt{d}} \right)^{(d/M)}, \left(\frac{1-\sqrt{M}(\sqrt{M}+1)}{(\sqrt{M}+1)\sqrt{d}} \right)^{(d/M)} \right\} \\ &= \{(\Lambda_1)^{(d-2d/M)}, (\Lambda_2)^{(d/M)}, (\Lambda_3)^{(d/M)}\}. \end{aligned} \quad (4.64)$$

The number in the brackets indicates the degeneracy of the eigenvalues. The eigenvalue Λ_1 , which belongs to the eigenvectors $|\alpha, k\rangle$ orthogonal to both POVM elements is degenerated by a factor $d - 2d/M$. The second eigenvalue Λ_2 has a multiplicity of d/M and has the eigenvectors $|\alpha, k\rangle$ for $k \in \{(M-1)d/M + 1, \dots, d\}$. The third eigenvalue, Λ_3 , has the eigenvectors $|\alpha, k\rangle$

for $k \in \{(a-1)d/M + 1, \dots, ad/M\}$ and has multiplicity of d/M . Such a basis exists for each POVM, which means all the basis elements have an identical spectrum. The basis elements constructed from a single optimal POVM for a given α must commute. This means that the basis elements fulfill the additional relations

$$\begin{aligned}\tilde{G}_{i(\alpha,a)}|\alpha, l\rangle &= \frac{1 - \sqrt{M}(\sqrt{M} + 1)}{(\sqrt{M} + 1)\sqrt{d}}|\alpha, l\rangle, \\ \tilde{G}_{i(\alpha,a)}|\alpha, k\rangle &= \frac{1}{\sqrt{d}}|\alpha, k\rangle, \\ [\tilde{G}_{i(\alpha,a)}, \tilde{G}_{i(\alpha,b)}] &= 0\end{aligned}\quad (4.65)$$

for all $a, b \in \{1, \dots, M-1\}$, $\alpha \in \{1, \dots, M-1\}$, $k \in \{(M-1)d/M + 1, \dots, d/M\}$ and $l \in \{(a-1)d/M + 1, \dots, ad/M\}$. This result shows that the isospectrality of the traceless Hermitian orthonormal operator basis and its partitioning is important for constructing optimal informationally complete (N, M) -POVMs with $2 < M < d$. Furthermore, if the IHOB exists according to Eq. (4.64) and fulfills additionally the relations (4.65) for a partitioning then the construction method, Eq. (3.32), leads to an informationally complete (N, M) -POVM

$$\begin{aligned}\Pi_{i(\alpha,a)} &= \frac{\mathbb{1}_d}{M} + \frac{\sqrt{d}}{M(1 + \sqrt{M})} \left(\sum_{b=1}^{M-1} \tilde{G}_{i(\alpha,b)} - \sqrt{M}(\sqrt{M} + 1)\tilde{G}_{i(\alpha,a)} \right) \\ \Pi_{i(\alpha,M)} &= \frac{\mathbb{1}_d}{M} + \frac{\sqrt{d}}{M} \sum_{b=1}^{M-1} \tilde{G}_{i(\alpha,b)}.\end{aligned}\quad (4.66)$$

More than one POVM can only be simultaneously diagonalizable if relation (3.17)

$$\text{tr}\{\Pi_{i(\alpha,a)}\Pi_{i(\beta,b)}\} = \sum_{k=(a-1)d/M+1}^{ad/M} \sum_{l=(b-1)d/M+1}^{bd/M} |\langle \alpha, k | \beta, l \rangle|^2 = \frac{d}{M^2} \in \mathbb{N} \quad (4.67)$$

is a natural number for all $a, b \in \{1, \dots, M\}$ and $\alpha, \beta \in \{1, \dots, N\}$ with $\alpha \neq \beta$. It is summarized that the elements of an optimal (N, M) -POVM are projections of rank d/M and the elements of a single POVM share a common eigenbasis and satisfy $\Pi_{i(\alpha,a)}\Pi_{i(\alpha,b)} = \delta_{ab}\Pi_{i(\alpha,a)}$ for all α, a and b . Additionally, the existence of an IHOB $\{\tilde{G}_{i(\alpha,a)}\}$, whose common spectrum is given by Eq. (4.64) and the basis elements fulfill (4.65), is a necessary and sufficient for the existence of an optimal informationally complete (N, M) -POVM. If an optimal (N, M) -POVM is not informationally complete, the IHOB is replaced by an isospectral traceless Hermitian orthonormal system of $N(M-1) < d^2 - 1$ operators, which are defined in Eq. (4.62).

In the subsequent subsection, optimal $(N, 2)$ -POVMs are discussed in detail.

4.2.3 Optimal $(N, 2)$ -POVMs

In this subsection, the existence of optimal $(N, 2)$ -POVMs of d -dimensional quantum systems with $x = d/2$ is analyzed. The additional properties of such POVMs can be used to extend the necessary condition of the existence of an IHOB to a sufficient condition. This criterion holds for all POVMs with $N \leq d^2 - 1$, including the informationally complete ones for $N = d^2 - 1$. For $M = 2$, the construction methods described in Sections 3.2.1 and 3.2.2 are identical and the elements of the POVMs are given by

$$\Pi_{i(\alpha,1)} = \frac{\mathbb{1}_d}{2} + \pi_{i(\alpha,1)} \quad (4.68)$$

$$\Pi_{i(\alpha,2)} = \frac{\mathbb{1}_d}{2} + \pi_{i(\alpha,2)} = \frac{\mathbb{1}_d}{2} - \pi_{i(\alpha,1)}. \quad (4.69)$$

The completeness relation of POVMs (3.1) has been used for $\Pi_{i(\alpha,2)}$. The eigenvalues of the POVM elements $\lambda_\sigma = 1/2 + \eta_\sigma$ are analyzed to understand the existence of such POVMs with the eigenvalues of η_σ of traceless Hermitian operators $\pi_{i(\alpha,a)}$. According to the result of Section 4.2.2, the eigenvalues have to fulfill $|\eta_\sigma| = 1/2$ so that the eigenvalues are $\lambda_\sigma = \{0, 1\}$. In addition to fulfill

$$0 = \text{tr}\{\pi_{i(\alpha,a)}\} = \sum_{\sigma=1}^d \eta_\sigma \quad (4.70)$$

the value $d/2 \in \mathbb{N}$ has to be a natural number, which can only be achieved if the dimension of the quantum system is even. The spectrum of the POVM elements is given by

$$\text{Sp}(\pi_{i(\alpha,a)}) = \left\{ +\frac{1}{2} \begin{matrix} (d/2) \\ \end{matrix}, -\frac{1}{2} \begin{matrix} (d/2) \\ \end{matrix} \right\} \quad (4.71)$$

for each $i(\alpha, a) \in \{1, \dots, 2N\}$. From the POVM elements isospectral traceless Hermitian operators can be derived by $\tilde{G}_\alpha = \pi_{i(\alpha,1)}/\sqrt{d}$. The common spectrum is

$$\text{Sp}(\tilde{G}_{i(\alpha,a)}) = \left\{ +\frac{1}{\sqrt{d}} \begin{matrix} (d/2) \\ \end{matrix}, -\frac{1}{\sqrt{d}} \begin{matrix} (d/2) \\ \end{matrix} \right\} \quad (4.72)$$

for each $\alpha \in \{1, \dots, N\}$. Thus, the existence of an isospectral traceless Hermitian orthonormal system of N elements is both sufficient and necessary for constructing $(N, 2)$ -POVMs. In the case of informational completeness $N = d^2 - 1$, the isospectral traceless orthonormal system is a complete basis. This generalizes the recently derived result of Siudzińska [59].

The IHOB can easily be constructed from the Clifford algebra for quantum systems of dimension $d = 2^k$ for $k \in \mathbb{N}$. This basis is generated by the tensor product of the Pauli matrices Eq. (B.8) and $\sigma_0 = \mathbb{1}_2$. Furthermore, the $(M, 2)$ -POVMs in dimension $d = 2^k$ are given by

$$\Pi_{i(\alpha,1)} = \frac{\mathbb{1}_d}{2} + \frac{1}{2} \sigma_{i_1} \otimes \dots \otimes \sigma_{i_k} \quad (4.73)$$

$$\Pi_{i(\alpha,2)} = \frac{\mathbb{1}_d}{2} - \frac{1}{2} \sigma_{i_1} \otimes \dots \otimes \sigma_{i_k} \quad (4.74)$$

with $(i_1, \dots, i_k) \neq (0, \dots, 0)$. For $k = 2$, the result has been shown as an example in [59]. It is still uncertain whether optimal informationally complete $(N, 2)$ -POVMs exist in even dimensions that are not a power of two. In this section, the existence of an IHOB, whose spectrum is given by Eq. (4.72), is necessary and sufficient condition for the existence of optimal informationally complete (N, M) -POVMs. The common spectrum of the basis elements depends solely on the dimension d and the number of POVM elements M .

4.2.4 Conclusion

In the previous subsection, it has been derived that optimal (N, M) -POVMs require the existence of an IHOB, and their spectrum relies solely on d and M for all informationally complete (N, M) -POVMs Eqs. (4.52), (4.64) and (4.72). Additionally, it has been shown that informationally complete optimal (N, M) -POVM elements are rank one operators for $M \geq d$ and orthogonal projections of rank d/M for $M \leq d$. This implies that optimal (N, M) -POVMs with $M < d$ can only exist if $M/d \in \mathbb{N}$ is a natural number. However, for the special case of

MUBs the POVM elements are rank one projections and any traceless Hermitian orthonormal operator basis fulfilling the commutator relation

$$[\tilde{G}_{i(\alpha,a)}, \tilde{G}_{i(\alpha,b)}] = 0 \quad (4.75)$$

for all $\alpha \in \{1, \dots, N\}$ and $a \in \{1, \dots, M-1\}$ can be used to construct a MUB because for each α , it consists of the maximum number of orthogonal and simultaneously diagonalizable traceless Hermitian operators. Therefore, a set of $d-1$ commuting traceless Hermitian basis elements will generate an identical set of positive semidefinite matrices regardless of their spectrum. An example has been presented in Section 4.1.2 for $d=4=M$ and the Clifford basis. Examples of informationally complete optimal POVMs have been presented for cases where $M=d$, $M=d^2$ and $M=2$. However, the existence of optimal informationally complete (N, M) -POVMs for other values of M still needs to be demonstrated. The isospectrality of the basis elements indicates that there exists d^2-1 unitary matrices $U_{i(\alpha,a)}$ so that the basis elements can be written as

$$\tilde{G}_{i(\alpha,a)} = U_{i(\alpha,a)}^\dagger D U_{i(\alpha,a)} \quad (4.76)$$

with $D = \text{diag}(\Lambda_1, \dots, \Lambda_d)$ with Λ_i the eigenvalues of the IHOB elements. The orthogonality relation of such a basis reads

$$\delta_{\alpha,\beta} \delta_{a,b} = \text{tr}\{\tilde{G}_{i(\alpha,a)} \tilde{G}_{i(\beta,b)}\} = \text{tr}\{U_{i(\alpha,a)}^\dagger D U_{i(\alpha,a)} U_{i(\beta,b)}^\dagger D U_{i(\beta,b)}\} \quad (4.77)$$

for $\alpha, \beta \in \{1, \dots, N\}$ and $a, b \in \{1, \dots, M-1\}$. For $2 < M \leq d$, the basis elements constructed from a single optimal POVM are commuting, Eq. (4.65). The required unitary transformations can be reduced to U_α for $\alpha \in \{1, \dots, N-1\}$ and diagonal matrices D_a , which are permutations of the diagonal entries Λ_1 and Λ_2 [Eq. (4.64)], so that holds

$$\text{tr}\{D_a D_b\} = \delta_{a,b} \quad (4.78)$$

for $a, b \in \{1, \dots, M\}$. For the case of $2 < M < d$, it is sufficient and necessary for the existence of optimal (N, M) -POVMs if an IHOB exists with a spectrum of Eq. (4.64) and fulfills the relations in Eq. (4.65). For the case of $M=2$, the existence of an IHOB is a necessary and sufficient condition for the existence of optimal informationally complete (N, M) -POVMs. The connection between optimal (N, M) -POVMs and IHOBs has been established. The construction of optimal (N, M) -POVMs can be transformed to the construction of such basis elements or a finding the $U_{i(\alpha,a)}$ for $\alpha \in \{1, \dots, N\}$ and $a \in \{1, \dots, M-1\}$. The next two sections deal with the existence of SIC-POVMs and MUBs, which means that in all dimensions where these POVMs can be constructed, IHOBs also exist.

4.3 OVERVIEW SIC-POVMS

The special case of $(1, d^2)$ -POVMs or GSICs introduced in 2014 by Kalev and Gour [64] is a generalization of the SIC-POVMs while SIC-POVMs have been widely discussed over the last 20 years. The SIC-POVMs have been introduced to the general community of quantum information by Renes in 2004 [60]. This started the main interest of the current research of SIC-POVMs. This section briefly summarizes the existence of SIC-POVMs, the current state of the art and applications are presented.

The idea of quantum measurements represented by SIC-POVMs has been introduced independently by Zauner [111] and Caves [112]. Zauner has found the connection between

the Weyl-Heisenberg group and the existence of SIC-POVMs up to a dimension of $d = 5$. He also conjectured that for any dimension d , the d^2 vectors describing the SIC-POVM can be generated from a fiducial vector acting on unitary matrices belonging to the Weyl-Heisenberg group. The construction of SIC-POVMs in finite dimensions remains an open research subject and has been named one of the five important problems of quantum information theory [66]. In the last two decades, the dimension of numerically obtained SIC-POVMs has increased. In 2004, Renes could construct SIC-POVMs of dimension $d \leq 45$ [60]. Scott and Grassl extended the found dimension to $d \leq 67$ [113]. Scott extended his results up to $d \leq 121$ [114]. Using the supercomputer Chimera at UMass Boston and the previous formalism, SIC-POVMs have been constructed for $d \leq 151$ [65]. In dimension $d \leq 193$ and for the special dimensions $d = 204, 224, 255, 288, 528, 725, 1155, 2208$ SIC-POVMs have been determined [66]. Numerical results of the fiducial vectors are published in [115–117]. Analytical solutions have been found for dimensions up to $d \leq 53$ [60, 113, 118]. Outside this boundary, the construction of analytical SIC-POVMs is known for [116, 119–121]

$$\begin{aligned}
 d = & 57, 61 - 63, 65, 67, 73, 74, 76, 78 - 80, 84, 86, 91, 93, 95, 97 - 99, \\
 & 103, 109, 111, 120, 122, 124, 127, 129, 133, 134, 139, 143, 146, 147, \\
 & 151, 155, 157, 163, 168, 169, 172, 181 - 183, 193, 195, 199, \\
 & 201, 228, 259, 292, 323, 327, 364, 399, 403, 487, 489, 628, 787, 844, 964, \\
 & 1027, 1228, 1299, 1447, 1684, 1852, 2404, 2707, 4099, 5779, 19603, 39604. \quad (4.79)
 \end{aligned}$$

Despite continuous research, the Zauner conjecture remains unproven [66]. The SIC-POVMs also have important applications outside quantum information, quantum communication, entanglement detection and EPR steering detection. They are also relevant for signal processing in high-precision radars [122] and speech recognition [123]. In mathematics, SIC-POVMs are connected to algebraic number theory [124]. An overview of important applications and connections of SIC-POVMs can be found in [65]. Examples of SIC-POVMs in dimension $d \leq 4$ are shown in Appendix A.2.

4.4 OVERVIEW MUTUALLY UNBIASED BASIS

The existence of optimal MUBs is often discussed in current literature rather than from the point of view of optimal informationally complete MUMs. This approach drops completeness and focuses solely on counting the number of bases. The main objective is to examine the maximum number of MUBs.

Definition

A set of N orthogonal bases $\{|\alpha, a\rangle\}$ ($1 \leq \alpha \leq N$, $1 \leq a \leq d$) in d -dimensional complex Hilbert space which fulfills

$$\langle \alpha, a | \alpha, b \rangle = \delta_{a,b} \quad (4.80)$$

$$|\langle \alpha, a | \beta, b \rangle|^2 = \frac{1}{d} \quad (4.81)$$

for all $(1 \leq a, b \leq d)$, $(1 \leq \alpha, \beta, N)$ and $\alpha \neq \beta$. The maximum number of different bases is given by $N = d + 1$, which is equivalent to the existence of an optimal MUM [66]. It is currently unknown whether $d + 1$ MUBs exist for any dimension. For a representation by products of powers of primes $d = p_1^{k_1} \dots p_l^{k_l}$ with $p_1^{k_1} \leq p_2^{k_2} \leq \dots \leq p_l^{k_l}$ it has been shown that there exist at least $p_1^{k_1} + 1$ MUBs [111]. Therefore, the minimum number of MUBs is three. For the special

case where dimensions are powers of primes $d = p^k$, it has been proven that $d + 1$ MUBs exist. For other cases, the number of maximal bases remains unknown [125]. It has been shown that a collection of d MUBs can always be extended to $d + 1$, which means that the maximal number of MUBs is either $d + 1$ or less or equal to $d - 1$ [126]. The lowest dimension for which the question of complete MUB of $d + 1$ is not known is $d = 6$. The maximum number of seven bases has not been found, only three have been discovered [127, 128]. The proof of the number of the maximal set of MUBs in $d = 6$ is one of the five key questions in quantum information [66]. Examples of MUBs in dimensions $d \leq 4$ are provided in Appendix A.1.

Part III

ENTANGLEMENT DETECTION

ENTANGLEMENT DETECTION BY LOCAL MEASUREMENTS

This chapter addresses the need to verify the entanglement of bipartite quantum states using local measurements that can be carried out by observers at a great distance. For quantum information applications, such as quantum key distribution, it is necessary to detect entangled states by local measurements. Therefore, only quantum states where entanglement can be detected are suitable for these applications. In this chapter, the focus is on generalized local measurements. Sufficient conditions for entanglement detection by local informationally complete (N, M) -POVMs are discussed. The research on entanglement detection with these measurements is two-fold. In the first part, sufficient conditions based on correlation matrices and joint probability distributions are derived. The intricate dependence of such inequalities on the parameters of the used (N, M) -POVMs is analyzed analytically. The efficiency of entanglement detection can be easily determined by the scaling relation, which follows from the detailed discussions about (N, M) -POVMs in Chapter 3. The scaling relation is necessarily fulfilled for all (N, M) -POVMs. Positive semidefiniteness of the POVM elements is not necessary for the scaling relation. This part concludes with an overview of the current research on entanglement detection using local (N, M) -POVMs, as well as the well-known subclasses, including SIC-POVMs, GSICs, MUBs and MUMs.

The second part numerically evaluates the efficiency of the derived sufficient entanglement conditions over the entire state space, surpassing existing research that concentrates mainly on special single-parameter families of quantum states and isotropic quantum states. The statistical properties of the detected entangled states are examined for this purpose. With the help of the hit-and-run algorithm, discussed in Section 2.4, the Euclidean volume ratios of the detected entangled quantum states over all quantum states are discussed in low qudit dimensions. The volume ratio of the sufficient conditions based on local measurements is compared to that of the NPT states in Section 2.2.1. Additionally, the dependence of joint probability-based sufficient conditions on the (N, M) -POVM is evaluated, providing insight into which (N, M) -POVMs are the most suitable for entanglement detection.

This chapter is structured as follows. A correlation matrix-based sufficient condition is derived for arbitrary Hermitian operators as measurements in Section 5.1. The general correlation matrix is applied to LOOs as measurements in Section 5.1.1. Additionally, the sufficient condition is compared to the LOO-based sufficient condition of Section 2.2.3. The correlation matrix condition with LOOs as measurements is necessary to establish the scaling relation for (N, M) -POVMs. The general correlation matrix-based sufficient condition is specialized to local informationally complete (N, M) -POVMs in Section 5.1.2. The results of Section 3.3 are used to unify the sufficient condition of LOOs and (N, M) -POVMs by introducing the scaling relation. In Section 5.2, entanglement detection through joint probability distributions with (N, M) -POVMs is discussed. Similar to the correlation matrix condition, the results of

Section 3.3 have been used to establish a more subtle scaling relation. An overview of recent publications of sufficient entanglement conditions using (N, M) -POVMs as local measurement is given in Section 5.3. Finally, by comparing the Euclidean volume ratios of the entangled quantum states for low qubit dimensions with the sufficient Peres-Horodecki conditions, we demonstrate the efficiency of the discussed entanglement detection in Section 5.4.

5.1 CORRELATION MATRICES OF LOCAL MEASUREMENTS

In this section, an inequality for detecting entanglement through correlation matrices with arbitrary local quantum measurements is derived, similar to the case of EPR-steering [129]. Consider Alice and Bob share a composed quantum state ρ of dimension $d = d_A d_B$, where Alice's Hilbert space has the dimension d_A and Bob's d_B . Two general sets of Hermitian operators are considered for Alice $\mathcal{A} = \{A_i; i = 1, \dots, \overline{M}\}$ and Bob $\mathcal{B} = \{B_j; j = 1, \dots, \overline{N}\}$ and the correlation matrix associated with these measurements is given by

$$[C(\mathcal{A}, \mathcal{B}|\rho)]_{ij} = c_{ij} = \text{tr}\{(A_i \otimes B_j)(\rho - \rho_A \otimes \rho_B)\} \quad (5.1)$$

with the reduced local density matrices of Alice and Bob, $\rho_A = \text{tr}_B\{\rho\}$ and $\rho_B = \text{tr}_A\{\rho\}$. An arbitrary density matrix ρ is separable if and only if the quantum state can be written as a convex combination of product states Eq. (2.44)

$$\rho = \sum_k p_k \rho_{A,k} \otimes \rho_{B,k} \quad \text{with} \quad p_k \geq 0, \quad \sum_k p_k = 1. \quad (5.2)$$

The average values can be calculated by

$$\text{tr}\{A_i \otimes B_j \rho\} = \sum_k p_k \text{tr}\{A_i \rho_{A,k}\} \text{tr}\{B_j \rho_{B,k}\} \quad (5.3)$$

$$\text{tr}\{A_i \otimes B_j (\rho_A \otimes \rho_B)\} = \left(\sum_k p_k \text{tr}\{A_i \rho_{A,k}\} \right) \left(\sum_l p_l \text{tr}\{B_j \rho_{B,l}\} \right), \quad (5.4)$$

where the definitions of the local density matrices $\rho_A = \sum_k p_k \rho_{A,k}$ and $\rho_B = \sum_k p_k \rho_{B,k}$ have been used. The elements of the correlation matrix can be represented by

$$c_{ij} = \text{tr}\{(A_i \otimes B_j)(\rho - \rho_A \otimes \rho_B)\} \quad (5.5)$$

$$= \sum_k p_k \text{tr}\{A_i \rho_{A,k}\} \text{tr}\{B_j \rho_{B,k}\} - \left(\sum_k p_k \text{tr}\{A_i \rho_{A,k}\} \right) \left(\sum_l p_l \text{tr}\{B_j \rho_{B,l}\} \right) \quad (5.6)$$

$$= \frac{1}{2} \sum_{k,l} p_k p_l (\text{tr}\{A_i \rho_{A,k}\} - \text{tr}\{A_i \rho_{A,l}\}) (\text{tr}\{B_j \rho_{B,k}\} - \text{tr}\{B_j \rho_{B,l}\}). \quad (5.7)$$

The correlation vectors

$$\mathbf{V}_{k,l} = \begin{pmatrix} \text{tr}\{A_1 \rho_{A,k}\} - \text{tr}\{A_1 \rho_{A,l}\} \\ \text{tr}\{A_2 \rho_{A,k}\} - \text{tr}\{A_2 \rho_{A,l}\} \\ \vdots \\ \text{tr}\{A_{\overline{M}} \rho_{A,k}\} - \text{tr}\{A_{\overline{M}} \rho_{A,l}\} \end{pmatrix}, \quad \mathbf{W}_{k,l} = \begin{pmatrix} \text{tr}\{B_1 \rho_{B,k}\} - \text{tr}\{B_1 \rho_{B,l}\} \\ \text{tr}\{B_2 \rho_{B,k}\} - \text{tr}\{B_2 \rho_{B,l}\} \\ \vdots \\ \text{tr}\{B_{\overline{N}} \rho_{B,k}\} - \text{tr}\{B_{\overline{N}} \rho_{B,l}\} \end{pmatrix} \quad (5.8)$$

are defined to represent the correlation matrix by

$$C(\mathcal{A}, \mathcal{B}, \rho) = \frac{1}{2} \sum_{k,l} p_k p_l \mathbf{V}_{k,l} \mathbf{W}_{k,l}^T. \quad (5.9)$$

The trace norm of the correlation matrix fulfills

$$\begin{aligned}
\|C(\mathcal{A}, \mathcal{B}|\rho)\|_{\text{tr}} &= \left\| \frac{1}{2} \sum_{k,l} p_k p_l \mathbf{V}_{k,l} \mathbf{W}_{k,l}^T \right\|_{\text{tr}} \\
&\leq \frac{1}{2} \sum_{k,l} p_k p_l \|\mathbf{V}_{k,l} \mathbf{W}_{k,l}^T\|_{\text{tr}} \\
&= \frac{1}{2} \sum_{k,l} p_k p_l \|\mathbf{V}_{k,l}\| \|\mathbf{W}_{k,l}\|.
\end{aligned} \tag{5.10}$$

The first inequality follows from the triangle inequality and the last equality from the trace norm of the dyadic product of two vectors. Using the Cauchy-Schwarz inequality leads to

$$\begin{aligned}
\|C(\mathcal{A}, \mathcal{B}|\rho)\|_{\text{tr}} &\leq \frac{1}{2} \sqrt{\sum_{k,l} p_k p_l \|\mathbf{V}_{k,l}\|^2} \sqrt{\sum_{k,l} p_k p_l \|\mathbf{W}_{k,l}\|^2} \\
&= \frac{1}{2} \sqrt{\sum_{i=1}^{\bar{M}} \sum_{k,l} p_k p_l (\text{tr}\{A_i \rho_{A,k}\} - \text{tr}\{A_i \rho_{A,l}\})^2} \sqrt{\sum_{j=1}^{\bar{N}} \sum_{k,l} p_k p_l (\text{tr}\{B_j \rho_{B,k}\} - \text{tr}\{B_j \rho_{B,l}\})^2}.
\end{aligned} \tag{5.11}$$

The two terms inside the square roots will be dealt with separately for clarity. The inequality for the terms with Bob's operators reads

$$\begin{aligned}
&\sum_{j=1}^{\bar{N}} \sum_{k,l} p_k p_l (\text{tr}\{B_j \rho_{B,k}\} - \text{tr}\{B_j \rho_{B,l}\})^2 \\
&= \sum_{j=1}^{\bar{N}} \sum_{k,l} p_k p_l (\text{tr}\{B_j \rho_{B,k}\}^2 - 2 \text{tr}\{B_j \rho_{B,k}\} \text{tr}\{B_j \rho_{B,l}\} + \text{tr}\{B_j \rho_{B,l}\}^2) \\
&= \sum_{j=1}^{\bar{N}} \left(\sum_l p_l \sum_k p_k (\text{tr}\{B_j \rho_{B,k}\}^2 - 2 \left(\sum_k p_k \text{tr}\{B_j \rho_{B,k}\} \right) \left(\sum_l p_l \text{tr}\{B_j \rho_{B,l}\} \right) \right. \\
&\quad \left. + \sum_k p_k \sum_l p_l (\text{tr}\{B_j \rho_{B,l}\}^2) \right) \\
&= 2 \sum_k p_k \sum_{j=1}^{\bar{N}} \text{tr}\{B_j \rho_{B,k}\}^2 - 2 \sum_{j=1}^{\bar{N}} \text{tr}\{B_j \rho_B\}^2 \\
&\leq 2 \left(\max_{\sigma_B} \sum_{j=1}^{\bar{N}} \text{tr}\{B_j \sigma_B\}^2 - \sum_{j=1}^{\bar{N}} \text{tr}\{B_j \rho_B\}^2 \right) \\
&= 2 \Sigma_B.
\end{aligned} \tag{5.12}$$

Here, the fact that $\sum_{j=1}^{\bar{N}} \text{tr}\{B_j \rho_k\}^2 \leq \max_{\sigma_B} \sum_{j=1}^{\bar{N}} \text{tr}\{B_j \sigma_B\}^2$ holds has been used. By an analogous derivation follows

$$\Sigma_A = \max_{\sigma_A} \sum_{i=1}^{\bar{M}} \text{tr}\{A_i \sigma_A\}^2 - \sum_{i=1}^{\bar{M}} \text{tr}\{A_i \rho_A\}^2. \tag{5.13}$$

Therefore, the trace of the correlation matrix for separable states is upper-bounded by

$$\|C(\mathcal{A}, \mathcal{B}|\rho)\|_{\text{tr}} \leq \sqrt{\Sigma_{\mathcal{A}} \Sigma_{\mathcal{B}}} \quad (5.14)$$

These upper bounds involve maximizing over all local quantum states of Alice and Bob, $\sigma^{\mathcal{A}}$ and $\sigma^{\mathcal{B}}$. In particular, the upper bound of the inequality depends on the chosen local Hermitian measurement operators \mathcal{A} and \mathcal{B} . Inequality (5.14) is a general consequence of the bipartite separability of an arbitrary dimensional quantum state ρ . However, calculating the boundary of inequality (5.13) for arbitrary local Hermitian measurements \mathcal{A} and \mathcal{B} is quite challenging. Furthermore, the focus is on informationally complete measurements, which allow the complete reconstruction of a quantum state. A set of linear operators acting on elements of \mathcal{H}_d is informationally complete if and only if it contains d^2 linearly independent operators. In the context of local measurements, in theory, the set \mathcal{A} can reconstruct $\rho^{\mathcal{A}}$ and the set \mathcal{B} can reconstruct $\rho^{\mathcal{B}}$. The set of the tensor products $\mathcal{A} \otimes \mathcal{B} = \{A_i \otimes B_j; i = 1, \dots, \overline{M}, j = 1, \dots, \overline{N}\}$ is also informationally complete for the linear operators acting on the Hilbert space $\mathcal{H}_{\mathcal{A}} \otimes \mathcal{H}_{\mathcal{B}}$. The following sections discuss local informationally complete Hermitian measurement operators, which allow for analytical calculation of the upper bound. This sufficient condition is applied to LOOs discussed in Section 2.2.3 and (N, M) -POVMs discussed in detail in Chapters 3. and 4.

5.1.1 Correlation matrices of local orthonormal Hermitian operators

In this subsection, the arbitrary measurements involved in Eqs. (5.13) and (5.14) are specialized to arbitrary LOOs, say $G^{\mathcal{A}} = (G_0^{\mathcal{A}}, \dots, G_{d_{\mathcal{A}}^2-1}^{\mathcal{A}})$ and $G^{\mathcal{B}} = (G_0^{\mathcal{B}}, \dots, G_{d_{\mathcal{B}}^2-1}^{\mathcal{B}})$ as defined in Section 2.2.3. The number of the measurements on the subsystems is $d_{\mathcal{A}}^2$ and $d_{\mathcal{B}}^2$. The upper bound of inequality (5.13) is calculated with the Hilbert-Schmidt representation of the reduced density matrices Eq. (2.16)

$$\rho = \sum_{i=0}^{d^2-1} G_i \text{tr}\{G_i \rho\} = \sum_{i=0}^{d^2-1} G_i r_i = \mathbf{r} \cdot \mathbf{G} \quad (5.15)$$

and the purity of a density matrix

$$\begin{aligned} \text{tr}\{\rho^2\} &= \text{tr}\left\{ \sum_{i=0}^{d^2-1} G_i r_i \sum_{j=0}^{d^2-1} G_j r_j \right\} \\ &= \sum_{i=0}^{d^2-1} \sum_{j=0}^{d^2-1} r_i r_j \underbrace{\text{tr}\{G_i G_j\}}_{\delta_{ij}} \\ &= \sum_{i=0}^{d^2-1} r_i^2 = \sum_{i=0}^{d^2-1} \text{tr}\{G_i \rho\}^2. \end{aligned} \quad (5.16)$$

Using this relation leads to the upper bound (5.13) for LOOs

$$\Sigma_{\mathcal{A}} = \max_{\sigma_{\mathcal{A}}} \sum_{i=0}^{d_{\mathcal{A}}^2-1} \text{tr}\{G_i \sigma_{\mathcal{A}}\}^2 - \sum_{i=0}^{d_{\mathcal{A}}^2-1} \text{tr}\{G_i \rho_{\mathcal{A}}\}^2 = \max_{\sigma_{\mathcal{A}}} \text{tr}\{\sigma_{\mathcal{A}}^2\} - \text{tr}\{\rho^2\} = 1 - \text{tr}\{\rho_{\mathcal{A}}^2\}, \quad (5.17)$$

$$\Sigma_{\mathcal{B}} = \max_{\sigma_{\mathcal{B}}} \sum_{j=0}^{d_{\mathcal{B}}^2-1} \text{tr}\{G_j \sigma_{\mathcal{B}}\}^2 - \sum_{j=0}^{d_{\mathcal{B}}^2-1} \text{tr}\{G_j \rho_{\mathcal{B}}\}^2 = \max_{\sigma_{\mathcal{B}}} \text{tr}\{\sigma_{\mathcal{B}}^2\} - \text{tr}\{\rho^2\} = 1 - \text{tr}\{\rho_{\mathcal{B}}^2\}. \quad (5.18)$$

The maximum of the upper bounds is taken for an arbitrary pure quantum state of the subsystems. Therefore, inequality (5.14) reduces to

$$\|C(G^A, G^B|\rho)\|_{\text{tr}} \leq \sqrt{(1 - \text{tr}\{\rho_A^2\})(1 - \text{tr}\{\rho_B^2\})}. \quad (5.19)$$

This is already known as the special form of the covariance condition from Gittsovich *et al.* [130, 131]. Furthermore, it is identical to the enhanced realignment criterion of Zhang *et al.* [132]. The upper bound of such an inequality is independent of the chosen LOOs. Consider two LOOs (B.4)

$$O_A(G_0^A, \dots, G_{d_A^2-1}^A)^T = (\hat{G}_0^A, \dots, \hat{G}_{d_A^2-1}^A)^T \quad (5.20)$$

$$O_B(G_0^B, \dots, G_{d_B^2-1}^B)^T = (\hat{G}_0^B, \dots, \hat{G}_{d_B^2-1}^B)^T. \quad (5.21)$$

and the inequality (5.19) is independent of the chosen LOOs

$$\begin{aligned} \|C(\hat{G}^A, \hat{G}^B|\rho)\|_{\text{tr}} &= \left\| (O^A)^T C(G^A, G^B|\rho) O^B \right\|_{\text{tr}} = \|C(G^A, G^B|\rho)\|_{\text{tr}} \\ &\leq \sqrt{(1 - \text{tr}\{\rho_A^2\})(1 - \text{tr}\{\rho_B^2\})}. \end{aligned} \quad (5.22)$$

This implies that arbitrary LOOs are equally efficient for entanglement detection with correlation matrices. For an arbitrary quantum state ρ the representation of $\rho - \rho_A \otimes \rho_B$ in a LOO \tilde{G}^A and \tilde{G}^B with $\tilde{G}_0^A = \mathbb{1}/\sqrt{d_A}$ and $\tilde{G}_0^B = \mathbb{1}/\sqrt{d_B}$ is

$$\rho - \rho_A \otimes \rho_B = \sum_{i=1}^{d_A^2-1} \sum_{j=1}^{d_B^2-1} (t_{ij} - a_i b_j) \tilde{G}_i^A \otimes \tilde{G}_j^B. \quad (5.23)$$

The parameters t_{ij} , a_i and b_j are defined as in Eq. (2.90). This operator is by definition traceless and the average values of the local basis elements also vanish. Therefore, the correlation matrix fulfills the relation

$$[C(\tilde{G}^A, \tilde{G}^B|\rho)]_{0\nu} = [C(\tilde{G}^A, \tilde{G}^B|\rho)]_{\mu 0} = 0 \quad (5.24)$$

for $\mu \in \{1, \dots, d_A^2 - 1\}$ and $\nu \in \{1, \dots, d_B^2 - 1\}$. This implies that the correlation matrix for the LOOs \tilde{G}^A and \tilde{G}^B has a block diagonal structure consisting of a 1×1 block of zero and a second block of dimension $(d_A^2 - 1) \times (d_B^2 - 1)$. Only the second block contributes to the trace norm, while the zero eigenvalue that belongs to the first block is negligible. In Section 2.2.3, the CCNR condition for entanglement detection has been discussed. This inequality also includes LOOs as measurement operators, but instead of the trace norm of the correlation matrix, the joint probability distribution has been considered. The CCNR inequality (2.63) has to be related to the correlation matrix sufficient condition (5.14) by

$$\begin{aligned} \|P(G^A, G^B|\rho)\|_{\text{tr}} &= \|P(G^A, G^B|\rho - \rho^A \otimes \rho^B) + P(G^A, G^B|\rho^A \otimes \rho^B)\|_{\text{tr}} \\ &\leq \|C(G^A, G^B|\rho)\|_{\text{tr}} + \|P(G^A, G^B|\rho^A \otimes \rho^B)\|_{\text{tr}} \\ &\leq \sqrt{(1 - \text{tr}\{\rho_A^2\})(1 - \text{tr}\{\rho_B^2\})} + \sqrt{\text{tr}\{\rho_A^2\} \text{tr}\{\rho_B^2\}} \\ &\leq 1. \end{aligned} \quad (5.25)$$

In the second line, the triangle inequality has been used and the fact that the quantum state ρ fulfills inequality (5.14). The CCNR condition is fulfilled if a quantum state fulfills the correlation matrix inequality (5.14). The CCNR condition cannot detect more entanglement than the correlation matrix condition (5.14). Furthermore, both conditions are also unaffected by the LOOs selected. To check if the correlation matrix-based inequality is violated, it is necessary to know the purities of the reduced density matrices ρ_A and ρ_B , making their application more complex.

5.1.2 Correlation matrices of (N, M) -POVMs

The general sufficient condition for entanglement, as described in Eq. (5.14), is applied to local informationally complete (N, M) -POVMs as measurements. The properties and existence of the (N, M) -POVMs are discussed in Chapters 3 and 4. In the first part of this section, the sufficient condition for entanglement detection is derived, while the second part discusses the efficiency of different local informationally complete (N, M) -POVMs by relating the correlation matrix of local informationally complete (N, M) -POVMs to that of LOOs. The local informationally complete (N, M) -POVMs $\Pi^A = (\Pi_1^A, \dots, \Pi_{N_A M_A}^A)$ and $\Pi^B = (\Pi_1^B, \dots, \Pi_{N_B M_B}^B)$ are performed by Alice and Bob. These positive semidefinite operators fulfill the defining equation of the (N, M) -POVMs (3.15-3.17) and the informational completeness relations $d_A^2 - 1 = N_A(M_A - 1)$ and $d_B^2 - 1 = N_B(M_B - 1)$. For the sake of convenience, the single index of the (N, M) -POVMs is introduced by $i(\alpha, a) = (\alpha - 1)M_A + a$ and $j(\beta, b) = (\beta - 1)M_B + b$. These definitions of the single indices allow a unique identification of the POVMs by α or β and the resulting measurement results a and b . The upper bound of the entanglement inequality (5.13) is calculated by utilizing the index of coincidence and its upper bound Eqs. (3.82) and (3.83)

$$\begin{aligned} \Sigma_A &= \max_{\sigma_A} \sum_{j=1}^{N_A M_A} \left(\left(\text{tr} \{ \Pi_{i(\alpha, a)}^A \sigma_A \} \right)^2 - \left(\text{tr} \{ \Pi_{i(\alpha, a)}^A \rho_A \} \right)^2 \right) \\ &= \max_{\sigma_A} \left(\frac{d_A^3 - M_A^2 x_A + d_A(M_A^2 x_A - d_A) \text{tr} \{ \sigma_A^2 \}}{d_A M_A (M_A - 1)} - \frac{d_A^3 - M_A^2 x_A + d_A(M_A^2 x_A - d_A) \text{tr} \{ \rho_A^2 \}}{d_A M_A (M_A - 1)} \right) \\ &= \Gamma_A (1 - \text{tr} \{ \rho_A^2 \}) \end{aligned} \quad (5.26)$$

$$\begin{aligned} \Sigma_B &= \max_{\sigma_B} \sum_{i=1}^{N_B M_B} \left(\left(\text{tr} \{ \Pi_{j(\beta, b)}^B \sigma_B \} \right)^2 - \left(\text{tr} \{ \Pi_{j(\beta, b)}^B \rho_B \} \right)^2 \right) \\ &= \max_{\sigma_B} \left(\frac{d_B^3 - M_B^2 x_B + d_B(M_B^2 x_B - d_B) \text{tr} \{ \sigma_B^2 \}}{d_B M_B (M_B - 1)} - \frac{d_B^3 - M_B^2 x_B + d_B(M_B^2 x_B - d_B) \text{tr} \{ \rho_B^2 \}}{d_B M_B (M_B - 1)} \right) \\ &= \Gamma_B (1 - \text{tr} \{ \rho_B^2 \}) \end{aligned} \quad (5.27)$$

with

$$\Gamma_A = \frac{M_A^2 x_A - d_A}{M_A (M_A - 1)}, \quad \Gamma_B = \frac{M_B^2 x_B - d_B}{M_B (M_B - 1)}. \quad (5.28)$$

As a consequence, the correlation matrix-based inequality of informationally complete (N, M) -POVMs obeys

$$\|C(\Pi^A, \Pi^B | \rho)\|_{\text{tr}} \leq \sqrt{\Gamma_A \Gamma_B} \sqrt{(1 - \text{tr} \{ \rho_A^2 \})(1 - \text{tr} \{ \rho_B^2 \})} \quad (5.29)$$

for all separable bipartite quantum states. This inequality has been independently derived by Lai and Luo [133]. Special instances of GSICs and MUMs as local measurements have been discussed recently [134]. A detailed overview of different sufficient entanglement conditions with local measurements is shown in Subsection 5.3. Inequality (5.29) depends on the local (N, M) -POVMs and their parameters $x_A, x_B, N_A, N_B, M_A, M_B$, which complicates the direct comparison of the efficiency of different types of (N, M) -POVMs. The correlation matrix has a dimension of $N_A M_A \times N_B M_B$, which makes it difficult to compare (N, M) -POVMs with different values of N and M . Moreover, the comparison of the upper bounds of the inequalities for local

(N, M) -POVMs (5.29) and LOOs (5.19) shows that the boundaries are proportional to each other by the factor $\sqrt{\Gamma_A \Gamma_B}$. Therefore, the correlation matrix of (N, M) -POVM will be related to that of LOOs. This relationship avoids the apparent complexity of the correlation matrix's dependence on the (N, M) -POVMs.

For this purpose, the local informationally complete (N, M) -POVM elements are expanded in arbitrary LOOs, say G^A for Alice and G^B for Bob, i.e. $\Pi^A = (G^A)^T S^A$ and $\Pi^B = (G^B)^T S^B$. The real-valued expansion coefficient matrices S^A and S^B are defined in Section 3.3. These matrices have dimensions of $d_A^2 \times N_A M_A$ and $d_B^2 \times N_B M_B$, respectively. The local basis expansions of the (N, M) -POVMs can be used to rewrite the correlation matrix as

$$C(\Pi^A, \Pi^B | \rho) = (S^A)^T C(G^A, G^B | \rho) S^B. \quad (5.30)$$

The trace norm of the correlation matrix of local informationally complete (N, M) -POVMs is calculated by relating the correlation matrix to that of arbitrary LOOs. This leads to the scaling relation of the trace norm

$$\begin{aligned} \|C(\Pi^A, \Pi^B | \rho)\|_{\text{tr}} &= \text{tr} \left\{ \sqrt{C(\Pi^A, \Pi^B | \rho) C^T(\Pi^A, \Pi^B | \rho)} \right\} \\ &= \text{tr} \left\{ \sqrt{(S^A)^T C(G^A, G^B | \rho) S^B (S^B)^T C^T(G^A, G^B | \rho) S^A} \right\} \\ &= \text{tr} \left\{ \sqrt{(S^A)^T C(G^A, \tilde{G}^B | \rho) \Lambda^B C^T(G^A, \tilde{G}^B | \rho) S^A} \right\} \\ &= \left\| (S^A)^T C(G^A, \tilde{G}^B | \rho) \sqrt{\Lambda^B} \right\|_{\text{tr}} \\ &= \text{tr} \left\{ \sqrt{\sqrt{\Lambda^B} C^T(\tilde{G}^A, \tilde{G}^B | \rho) S^A (S^A)^T C^T(\tilde{G}^A, \tilde{G}^B | \rho) \sqrt{\Lambda^B}} \right\} \\ &= \text{tr} \left\{ \sqrt{\sqrt{\Lambda^B} C^T(\tilde{G}^A, \tilde{G}^B | \rho) \Lambda^A C(\tilde{G}^A, \tilde{G}^B | \rho) \sqrt{\Lambda^B}} \right\} \\ &= \left\| \sqrt{\Lambda^A} C(\tilde{G}^A, \tilde{G}^B | \rho) \sqrt{\Lambda^B} \right\|_{\text{tr}} \\ &= \sqrt{\Gamma_A \Gamma_B} \|C(\tilde{G}^A, \tilde{G}^B | \rho)\|_{\text{tr}} \\ &= \sqrt{\Gamma_A \Gamma_B} \|C(G^A, G^B | \rho)\|_{\text{tr}}. \end{aligned} \quad (5.31)$$

Here, Λ^A is the diagonal matrix of non-zero eigenvalues of $(S^A)^T S^A$ with $\Lambda_1^A = N_A M_A / d_A$ and $\Lambda_i^A = \Gamma_A$ for $i = 2, \dots, d_A^2$ and analogous for Bob's diagonal matrix Λ^B of the non-zero eigenvalues of $(S^B)^T S^B$ with $\Lambda_1^B = N_B M_B / d_B$ and $\Lambda_j^B = \Gamma_B$ for $j = 2, \dots, d_B^2$, given in Eq. (3.69). In addition to the detailed results of Section 3.3, leading to Eq. (3.80), have been used to define the traceless Hermitian operators bases $\tilde{G}^A = O^A G^A$ and $\tilde{G}^B = O^B G^B$ with the orthogonal transformations O^A and O^B . Furthermore, the restriction on the LOOs \tilde{G}^A and \tilde{G}^B on the correlation matrix Eq. (6.50) has been used to extract the prefactors $\sqrt{\Gamma_A}$ and $\sqrt{\Gamma_B}$. The equality of

$$\|C(\Pi^A, \Pi^B | \rho)\|_{\text{tr}} = \sqrt{\Gamma_A \Gamma_B} \|C(G^A, G^B | \rho)\|_{\text{tr}} \quad (5.32)$$

is called the scaling relation, which has to be necessarily fulfilled by (N, M) -POVMs. As a result the sufficient entanglement condition with (N, M) -POVMs simplifies to the inequality of arbitrary LOOs

$$\|C(G^A, G^B | \rho)\|_{\text{tr}} = \frac{\|C(\Pi^A, \Pi^B | \rho)\|_{\text{tr}}}{\sqrt{\Gamma_A \Gamma_B}} \leq \sqrt{(1 - \text{tr}\{\rho_A^2\})(1 - \text{tr}\{\rho_B^2\})}. \quad (5.33)$$

The main result of this section is that the correlation matrix-based sufficient condition for arbitrary local informationally complete (N, M) -POVMs is the same as that for arbitrary LOOs.

Thus, it is apparent that the inequality (5.33) is entirely independent of the local informationally complete (N, M) -POVMs. This is a direct consequence of the symmetry of the relations that define the (N, M) -POVMs (3.15)-(3.17). The positive semidefiniteness of the local POVM elements has not been utilized in this derivation. Therefore, the scaling relation can be established using sets of informationally complete Hermitian operators that fulfill the defining conditions (3.15)-(3.18) and (3.1), regardless of their positive semidefiniteness.

5.2 JOINT PROBABILITY DISTRIBUTIONS

This subsection discusses the entanglement detection of joint probability distributions of local informationally complete (N, M) -POVMs. This inequality is the analog of the CCNR condition discussed in Section 2.2.3 for local informationally complete (N, M) -POVMs instead of LOOs as local measurements. First, the general inequality is derived, followed by an analytical discussion of the efficiency of different (N, M) -POVMs for arbitrary quantum states. Consider two local informationally complete (N_A, M_A) and (N_B, M_B) -POVMs $\mathbf{\Pi}^A$ and $\mathbf{\Pi}^B$ and the joint probability distribution is defined by

$$P(\mathbf{\Pi}^A, \mathbf{\Pi}^B | \rho) = \text{tr}\{(\mathbf{\Pi}^A)^T \otimes \mathbf{\Pi}^B \rho\} \quad (5.34)$$

for an arbitrary density matrix ρ of Alice's and Bob's combined system. We assume that the quantum state is separable

$$\rho_{\text{sep}} = \sum_n p_n \rho_{A,n} \otimes \rho_{B,n} \quad (5.35)$$

with $\sum_n p_n = 1$ and $p_n \geq 0$ and the local states of Alice's and Bob's system $\rho_{A,n}$ and $\rho_{B,n}$. For the derivation of the sufficient entanglement condition, the following vectors are needed

$$\mathbf{V}_n = \left(\text{tr}\{\rho_{A,n} \Pi_1^A\}, \dots, \text{tr}\{\rho_{A,n} \Pi_{N_A M_A}^A\} \right)^T \quad (5.36)$$

$$\mathbf{W}_n = \left(\text{tr}\{\rho_{B,n} \Pi_1^B\}, \dots, \text{tr}\{\rho_{B,n} \Pi_{N_B M_B}^B\} \right)^T. \quad (5.37)$$

For separable states the trace norm of the joint probability distribution is bounded by [59]

$$\begin{aligned} \left\| P(\mathbf{\Pi}^A, \mathbf{\Pi}^B | \rho_{\text{sep}}) \right\|_{\text{tr}} &\leq \sum_n p_n \left\| P(\mathbf{\Pi}^A, \mathbf{\Pi}^B | \rho_{A,n} \otimes \rho_{B,n}) \right\|_{\text{tr}} \\ &= \sum_n p_n \left\| \mathbf{V}_n^T \mathbf{W}_n \right\|_{\text{tr}} \\ &= \sum_n p_n \|\mathbf{V}_n\| \|\mathbf{W}_n\| \\ &= \sum_n p_n \sqrt{\sum_{i=1}^{N_A M_A} (\text{tr}\{\Pi_i^A \rho_{A,n}\})^2} \sqrt{\sum_{j=1}^{N_B M_B} (\text{tr}\{\Pi_j^B \rho_{B,n}\})^2} \\ &= \sum_n p_n \sqrt{C_A(\rho_{A,n}) C_B(\rho_{B,n})} \\ &\leq \sum_n p_n \sqrt{\frac{d_A - 1}{d_A} \frac{d_A^2 + M_A^2 x_A}{M_A(M_A - 1)}} \sqrt{\frac{d_B - 1}{d_B} \frac{d_B^2 + M_B^2 x_B}{M_B(M_B - 1)}} \\ &= \sqrt{\frac{d_A - 1}{d_A} \frac{d_A^2 + M_A^2 x_A}{M_A(M_A - 1)}} \sqrt{\frac{d_B - 1}{d_B} \frac{d_B^2 + M_B^2 x_B}{M_B(M_B - 1)}} \end{aligned} \quad (5.38)$$

with the index of coincidence \mathcal{C} Eq. (3.82)

$$\begin{aligned} \mathcal{C}_A(\rho_A) &= \sum_{i=1}^{N_A M_A} (\text{tr}\{\Pi_i^A \rho_A\})^2 = \frac{d_A^3 - M_A^2 x_A + d_A(M_A^2 x_A - d_A) \text{tr}\{\rho_A^2\}}{d_A M_A (M_A - 1)} \\ \mathcal{C}_B(\rho_B) &= \sum_{j=1}^{N_B M_B} (\text{tr}\{\Pi_j^B \rho_B\})^2 = \frac{d_B^3 - M_B^2 x_B + d_B(M_B^2 x_B - d_B) \text{tr}\{\rho_B^2\}}{d_B M_B (M_B - 1)}. \end{aligned} \quad (5.39)$$

For the derivation, the triangle inequality and the cross norm property for dyadic products have been used. Additionally, the index of coincidence \mathcal{C} in Eq. (3.82) provides the sums over the square average values of the POVM elements. Furthermore, the upper bound is taken for arbitrary pure states (3.83), such as for LOOs as local measurements. A quantum state that violates this inequality is detected as entangled. This inequality has been previously discussed in [59, 135]. Simple examples, such as one-parameter families of quantum states or isotropic states have been analyzed. Furthermore, for the special case of GSICs and SIC-POVMs ($M = d^2$), this inequality has been discussed in [134, 136]. A detailed comparison with current literature is provided in Section 5.3. The advantage of this inequality is that it does not depend on the purity of the reduced density matrices of Alice's and Bob's systems, $\text{tr}\{\rho_A^2\}$ and $\text{tr}\{\rho_B^2\}$, as does inequality (5.33). The next step is to compare the joint probability distribution- and correlation matrix-based sufficient entanglement conditions. The linear dependence of the joint probability distribution from the density matrix ρ is used to connect the trace norm of such a matrix to that of the correlation matrix based on the same measurements. Using the triangle equality leads to

$$\begin{aligned} \|P(\Pi^A, \Pi^B | \rho)\|_{\text{tr}} &\leq \|C(\Pi^A, \Pi^B | \rho)\|_{\text{tr}} + \|P(\Pi^A, \Pi^B | \rho_A \otimes \rho_B)\|_{\text{tr}} \\ &\leq \sqrt{\Sigma_A \Sigma_B} + \sqrt{\mathcal{C}_A(\rho_A) \mathcal{C}_B(\rho_B)}. \end{aligned} \quad (5.40)$$

This inequality constrains the trace norm of the joint probability distributions of the local informationally complete (N, M) -POVMs. The boundary of this inequality includes the purities of Bob's and Alice's reduced states for separable quantum states. The general inequality

$$\sqrt{\Sigma_A \Sigma_B} + \sqrt{\mathcal{C}_A(\rho_A) \mathcal{C}_B(\rho_B)} \leq \sqrt{\Sigma_A + \mathcal{C}_A(\rho_A)} \sqrt{\Sigma_B + \mathcal{C}_B(\rho_B)} \quad (5.41)$$

is used to relate inequality (5.40) with inequality (5.38)

$$\begin{aligned} \|P(\Pi^A, \Pi^B | \rho)\|_{\text{tr}} &\leq \sqrt{\Sigma_A + \mathcal{C}_A(\rho_A)} \sqrt{\Sigma_B + \mathcal{C}_B(\rho_B)} \\ &= \sqrt{\frac{d_A - 1}{d_A} \frac{d_A^2 + M_A^2 x_A}{M_A(M_A - 1)}} \sqrt{\frac{d_B - 1}{d_B} \frac{d_B^2 + M_B^2 x_B}{M_B(M_B - 1)}}. \end{aligned} \quad (5.42)$$

However, this inequality detects less entanglement as inequality (5.40) and the correlation matrix-based sufficient condition (5.33). As shown in the previous section, the correlation matrix-based sufficient condition is entirely independent of chosen local informationally complete (N, M) -POVMs. The determination of the efficiency of joint probability distributions for different types of (N, M) -POVMs is complicated by the dimensionality of the joint probability matrix $P(\Pi^A, \Pi^B | \rho)$ of $N_A M_A \times N_B M_B$. Its intricate dependence on different (N, M) -POVMs with parameters $x_A, N_A, M_A, x_B, N_B, M_B$ can be circumvented by relating the joint probability matrix

to those of LOOs with the help of the linear map S . In contrast to the correlation matrix-based inequality, Eq. (6.50) is not fulfilled for the joint probability distribution and it holds

$$\begin{aligned} [P(\tilde{G}^A, \tilde{G}^B|\rho)]_{0\nu} &= b_\nu, \\ [P(\tilde{G}^A, \tilde{G}^B|\rho)]_{\mu 0} &= a_\mu, \\ [P(\tilde{G}^A, \tilde{G}^B|\rho)]_{00} &= \frac{1}{\sqrt{d_A d_B}} \end{aligned} \quad (5.43)$$

for arbitrary quantum states and for $\mu \in \{1, \dots, d_A^2 - 1\}$ and $\nu \in \{1, \dots, d_B^2 - 1\}$. Only quantum states with $0 = \text{tr}\{\tilde{G}_\mu \rho_A\} = a_\mu$ and $0 = \text{tr}\{\tilde{G}_\nu \rho_B\} = b_\nu$ fulfill the first two equalities, i.e. Bell diagonal states. The final equality is always fulfilled, resulting in a more subtle scaling relation. The sufficient condition resulting from the inequalities (5.38) and (5.40) for the joint probability distribution of local informationally complete (N, M) -POVMs also exhibits scaling, which relates them to the corresponding joint probability matrix $P(\tilde{G}^A, \tilde{G}^B|\rho)$ of dimension $d_A^2 \times d_B^2$. However, the scaling relation differs from that of correlation matrices, derived in Section 5.1.2, because the matrix components shown in Eq. (5.43) do not vanish anymore. Thus, the parameters $\sqrt{\Gamma_A}$ and $\sqrt{\Gamma_B}$ cannot be extracted from the trace norm. To derive the scaling relation the left-hand sides of inequalities (5.38) and (5.40) are related to LOOs \tilde{G}^A and \tilde{G}^B . Using the properties derived in Sec. 3.3 the joint probability distribution can be replaced by a matrix of dimension $d_A^2 \times d_B^2$ with identical trace norm in an analogous way as in Eq. (5.31)

$$\begin{aligned} \|P(\Pi^A, \Pi^B|\rho)\|_{\text{tr}} &= \left\| (S^A)^T P(\tilde{G}^A, \tilde{G}^B|\rho) S^B \right\|_{\text{tr}} \\ &= \left\| \sqrt{\Lambda^A} P(\tilde{G}^A, \tilde{G}^B|\rho) \sqrt{\Lambda^B} \right\|_{\text{tr}}. \end{aligned} \quad (5.44)$$

Here, Λ^A is the diagonal matrix of non-zero eigenvalues of $(S^A)^T S^A$ with $\Lambda_1^A = N_A M_A / d_A$ and $\Lambda_i^A = \Gamma_A$ for $i = \{2, \dots, d_A^2\}$ and analogous for Bob's diagonal matrix Λ^B of non-zero eigenvalues of $(S^B)^T S^B$ with $\Lambda_1^B = N_B M_B / d_B$ and $\Lambda_j^B = \Gamma_B$ for $j = \{2, \dots, d_B^2\}$, given in Eq. (3.69). Due to Eq. (5.43) being unfulfilled, the factors $\sqrt{\Gamma_A}$ and $\sqrt{\Gamma_B}$ cannot be extracted from the trace norm. According to Eq. (3.69) the common factors $\gamma_A = (d_A(d_A - 1)) / (M_A(M_A - 1))$ and $\gamma_B = (d_B(d_B - 1)) / (M_B(M_B - 1))$ can be extracted from the diagonal non-zero eigenvalue matrices

$$\begin{aligned} [\Lambda^A]_{11} &= \gamma_A (d_A - 1), \\ [\Lambda^A]_{\nu\nu} &= \gamma_A \frac{(d_A \tilde{x}_A - 1)}{d_A - 1} \\ [\Lambda^B]_{11} &= \gamma_B (d_B - 1) \\ [\Lambda^B]_{\mu\mu} &= \gamma_B \frac{(d_B \tilde{x}_B - 1)}{d_B - 1} \end{aligned} \quad (5.45)$$

for $\nu \in \{2, \dots, d_A^2\}$ and $\mu \in \{2, \dots, d_B^2\}$ with rescaled parameters

$$\tilde{x}_A = \frac{x_A M_A^2}{d_A^2} \quad \text{and} \quad \tilde{x}_B = \frac{x_B M_B^2}{d_B^2}. \quad (5.46)$$

The same factors can be extracted from the upper bounds on the right-hand side of the inequalities (5.38) and (5.40). Consequently, the rescaled $d_A^2 \times d_B^2$ -dimensional joint probability matrix is introduced

$$\tilde{P}(\tilde{x}_A, \tilde{x}_B) = \sqrt{\frac{\Lambda^A}{\gamma_A}} P(\tilde{G}^A, \tilde{G}^B|\rho) \sqrt{\frac{\Lambda^B}{\gamma_B}} \quad (5.47)$$

which only depends on the rescaled parameters \tilde{x}_A and \tilde{x}_B . Therefore, inequality (5.38) can be rewritten in the rescaled form

$$\|\tilde{P}(\tilde{x}_A, \tilde{x}_B)\|_{\text{tr}} \leq \sqrt{1 + \tilde{x}_A} \sqrt{1 + \tilde{x}_B} \quad (5.48)$$

and inequality (5.40) reduces to

$$\|\tilde{P}(\tilde{x}_A, \tilde{x}_B)\|_{\text{tr}} \leq \sqrt{\frac{\Sigma_A \Sigma_B}{\gamma_A \gamma_B}} + \sqrt{\frac{C_A(\rho_A) C_B(\rho_B)}{\gamma_A \gamma_B}}. \quad (5.49)$$

The main results of this subsection is that these inequalities only depend on the rescaled parameters \tilde{x}_A and \tilde{x}_B characterizing Alice's and Bob's (N, M) -POVMs for given dimensions d_A and d_B of their quantum system. Testing for violations of the inequalities (5.38) and (5.40) for (N, M) -POVMs with parameters M_A, x_A, M_B and x_B yield identical results as arbitrary (N, M) -POVMs with parameters $M'_A, x'_A = x_A M_A^2 / M_A'^2, M'_B$ and $x'_B = x_B M_B^2 / M_B'^2$. For example two local MUMs ($N_A = d_A + 1, M_A = d_A, x_A, N_B = d_B + 1$ and $M_B = d_B, x_B$) lead to the identical inequality as two GSICs with ($N'_A = 1, M'_A = d_A^2, x'_A = x_A / d_A^2, N'_B = 1, M'_B = d_B^2, x'_B = x_B / d_B^2$). The sufficient conditions (5.38) and (5.40) have been derived solely from the spectral properties of the linear maps S^A and S^B . The constraint of positive semidefiniteness on the local informationally complete (N, M) -POVMs Π^A and Π^B is irrelevant for introducing the rescaled matrix $P(\tilde{x}_A, \tilde{x}_B)$. Therefore, an explicit construction of the (N, M) -POVMs is not required to relate different sufficient entanglement conditions. The use of the rescaled parameters \tilde{x}_A and \tilde{x}_B has allowed the unification of various types of local informationally complete (N, M) -POVMs with identical efficiencies for the entanglement detection based on joint probability distributions. However, the question of identifying the optimal pair of parameters \tilde{x}_A and \tilde{x}_B to detect the most entangled quantum states remains unanswered. Thus, the efficiency of entanglement detection using (N, M) -POVMs will be numerically analyzed to identify optimal rescaled parameters for low qudit dimensions. This issue will be addressed in Section 5.4.

5.3 COMPARISON WITH LITERATURE

Entanglement detection by local (N, M) -POVMs and especially the subclasses of GSICs, SIC-POVMs, MUMs and MUBs are commonly discussed in the current literature. Therefore, an overview of publications of sufficient entanglement conditions of such local measurements is given in this subsection and is summarized in Table 5.1. First, the most efficient inequality (5.29) is analyzed

$$\|C(\Pi^A, \Pi^B | \rho)\|_{\text{tr}} \leq \sqrt{\Gamma_A \Gamma_B} \sqrt{(1 - \text{tr}\{\rho_A^2\})(1 - \text{tr}\{\rho_B^2\})}. \quad (5.50)$$

This inequality has been derived simultaneously to us by Lai and Luo [133] and has been discussed for GSICs and MUMs [134]. However, these publications do not address the scaling relation, which means that the inequality is entirely independent of the used local informationally complete (N, M) -POVMs and is identical to that of arbitrary LOOs Eq. (5.33). It has been shown in Eqs. (5.40) and (5.42) that the inequality based on joint probability distributions Eq. (5.38) is slightly weaker than Eq. (5.50)

$$\|P(\Pi^A, \Pi^B | \rho)\|_{\text{tr}} \leq \sqrt{\frac{d_A - 1}{d_A} \frac{d_A^2 + M_A^2 x_A}{M_A(M_A - 1)}} \sqrt{\frac{d_B - 1}{d_B} \frac{d_B^2 + M_B^2 x_B}{M_B(M_B - 1)}}. \quad (5.51)$$

This inequality has been addressed for (N, M) -POVMs [59, 133, 135] and for the special case of GSICs [136] and SIC-POVMs [85]. In addition to these publications, it has been shown that the efficiency of the inequality only depends on the rescaled parameters \tilde{x}_A and \tilde{x}_B . Furthermore, the efficiency for different rescaled parameters is determined numerically in Section 5.4. Finally, some weaker inequalities can be derived for identical dimensions of Alice's and Bob's subsystem and local informationally complete (N, M) -POVMs with identical parameters. With the help of the inequality $\sum_{i=1}^{NM} |\mathcal{M}_{ii}| \leq \|\mathcal{M}\|_{\text{tr}}$, valid for arbitrary $NM \times NM$ square matrices, the following inequalities can be derived from inequality (5.50) and (5.51)

$$\sum_{i=1}^{NM} |\text{tr}\{\Pi_i^A \otimes \Pi_i^B (\rho - \rho_A \otimes \rho_B)\}| \leq \Gamma \sqrt{(1 - \text{tr}\{\rho_A^2\})(1 - \text{tr}\{\rho_B^2\})} \quad (5.52)$$

$$\sum_{i=1}^{NM} \text{tr}\{\Pi_i^A \otimes \Pi_i^B \rho\} \leq \frac{d-1}{d} \frac{d^2 + M^2 x}{M(M-1)}. \quad (5.53)$$

Furthermore, it can be shown that inequality (5.52) is more efficient than (5.53)

$$\begin{aligned} \sum_{i=1}^{NM} \text{tr}\{\Pi_i^A \otimes \Pi_i^B \rho\} &\leq \sum_{i=1}^{NM} \text{tr}\{\Pi_i^A \otimes \Pi_i^B \rho_A \otimes \rho_B\} + \sum_{i=1}^{NM} |\text{tr}\{\Pi_i^A \otimes \Pi_i^B (\rho - \rho_A \otimes \rho_B)\}| \\ &\leq \sum_{i=1}^{NM} \text{tr}\{\Pi_i^A \rho_A\} \text{tr}\{\Pi_i^B \rho_B\} + \Gamma \sqrt{1 - \text{tr}\{\rho_A^2\}} \sqrt{1 - \text{tr}\{\rho_B^2\}} \\ &\leq \sqrt{\sum_{i=1}^{NM} (\text{tr}\{\Pi_i^A \rho_A\})^2} \sqrt{\sum_{i=1}^{NM} (\text{tr}\{\Pi_i^B \rho_B\})^2} + \Gamma \sqrt{1 - \text{tr}\{\rho_A^2\}} \sqrt{1 - \text{tr}\{\rho_B^2\}} \\ &\leq \sqrt{C_A C_B} + \Gamma \sqrt{1 - \text{tr}\{\rho_A^2\}} \sqrt{1 - \text{tr}\{\rho_B^2\}} \\ &\leq \sqrt{C_A + \Gamma(1 - \text{tr}\{\rho_A^2\})} \sqrt{C_B + \Gamma(1 - \text{tr}\{\rho_B^2\})} \\ &= \frac{d-1}{d} \frac{d^2 + M^2 x}{M(M-1)}. \end{aligned} \quad (5.54)$$

In the first line, the triangle inequality has been used and in the second line, the fact that the quantum state ρ fulfills inequality (5.52). The Cauchy-Schwarz inequality is applied in the third line and the definition of the index of coincidence Eq. (3.82) is used. The final result is obtained after applying the general inequality (5.41). An overview of the inequalities (5.52) and (5.53) is also given in Table 5.1. References in the round brackets only discuss entanglement detection with optimal (N, M) -POVMs, such as SIC-POVMs and MUBs. The trace norm involving inequalities (5.50) and (5.51) are the most efficient sufficient condition for given local informationally complete (N, M) -POVMs. The optimization to find optimal parameters for the joint probability-based inequality is simplified by the scaling relation. This is because only a single class of local (N, M) -POVMs, defined by the rescaled parameters \tilde{x} , is needed to determine the efficiencies for a chosen measurement. Thus, the following section presents a numerical analysis of detection efficiencies using trace norm-based inequalities.

5.4 SIMULATION RESULTS

In this section, numerical results are presented, exploring the statistical features of the discussed sufficient entanglement conditions for (N, M) -POVMs and LOOs. Only the trace norm-based sufficient conditions are tested for the detection of entanglement, as they are the most

Equation	(N, M) -POVMs	GSICs (SIC-POVMs)	MUMs(MUBs)
(5.50)	[133]	[134]	[134]
(5.51)	[59, 133, 135]	[136] ([85])	
(5.52)	[133, 137]	[138]	[138]
(5.53)	[59, 133, 135, 139]	[140]	[141] ([142])

Table 5.1: The overview of references discussing sufficient entanglement conditions (5.50-5.53) with (N, M) -POVMs as local measurements: References in the brackets discuss only optimal (N, M) -POVMs like SIC-POVMs and MUBs.

effective inequalities. The scaling relation allows for a simple optimization of the parameters of the local informationally complete (N, M) -POVMs to increase the efficiency of the sufficient conditions.

The hit-and-run Monte Carlo algorithm discussed in Section 2.4 has been utilized to sample $N = 10^8$ random quantum states throughout the complete state space to examine the effectiveness of sufficient entanglement conditions. The algorithm enables the calculation of the lower bounds on Euclidean volumes of entangled states over all quantum states for dimensions $2 \leq d_A, d_B \leq 4$ of Alice's and Bob's subsystems. Table 5.2 presents volume ratios obtained for the entangled quantum states over all quantum states R . For each pair of dimensions (d_A, d_B) , there are five different sufficient conditions. The volume ratio of the detected entangled states R_{NPT} resulting from NPT states is a sufficient condition that relies on nonlocal operations, as discussed in Section 2.2.1. The volume ratio determined by the sufficient condition based on correlation matrices R_{Cor} Eq. (5.33) is identical for arbitrary informationally complete (N, M) -POVMs and LOOs. These volume ratios are compared to the joint probability-based sufficient condition for (N, M) -POVMs $R_{NM}(\tilde{x}_A, \tilde{x}_B)$ Eq. (5.40) and $R_{NM,2}(\tilde{x}_A, \tilde{x}_B)$ Eq. (5.49), and for arbitrary LOOs R_{CCNR} Eq. (2.63). Due to the scaling relation, selecting a single class of local informationally complete (N, M) -POVMs is sufficient to determine the efficiency of different types of (N, M) -POVMs. In Table 5.2, local GSICs have been chosen $N_A = N_B = 1, M_A = d_A^2, M_B = d_B^2$. Furthermore, the GSICs have been specialized to SIC-POVMs with $x_A = 1/d_A^2$ and $x_B = 1/d_B^2$, which belong to the class of (N, M) -POVMs of rescaled parameters $\tilde{x}_A = 1 = \tilde{x}_B$. The volume ratios are given by $R_{\text{SIC1}} = R_{NM}(1, 1)$ and $R_{\text{SIC2}} = R_{NM,2}(1, 1)$. It is apparent that for identical dimensions of Alice's and Bob's quantum systems $d_A = d_B$ the volume ratios R_{SIC1} and R_{LOO} are consistent with recently obtained results [85]. The results show that all sufficient conditions with local measurements significantly underestimate the volume ratio R_{NPT} of the sufficient NPT condition. Furthermore, increasing the dimensions of Alice's and Bob's subsystems causes the volume ratio of the NPT states to approach unity, which is a lower bound for the volume ratio of the entangled quantum states. However, the volume ratios based on local measurements do not exhibit this tendency. As the dimensions of Alice's and Bob's local subsystems increase, the volume ratios based on local measurements increasingly underestimate the volume ratio of the entangled states. Nevertheless, as expected from the analytical discussion in Sections 5.1 and 5.2, the volume ratios fulfill the inequalities $R_{\text{SIC1}} \leq R_{\text{SIC2}} \leq R_{\text{Cor}}$ and $R_{\text{CCNR}} \leq R_{\text{Cor}}$ consistent with the results from Eqs. (5.33), (5.40), (5.41), (5.48), (5.49) and (5.25). Furthermore, the numerical results indicate $R_{\text{CCNR}} \leq R_{\text{SIC1}}$, which agrees with [134] for identical subsystem dimensions. It should be noted that R_{SIC1} is closer to R_{Cor} when the local quantum systems have identical dimensions. The gap between them increases when Alice's and Bob's local quantum systems have different dimensions.

The numerical results presented so far have focused on optimal (N, M) -POVMs with $\tilde{x}_A = 1$ and $\tilde{x}_B = 1$, which is only achievable when $d_A \leq M_A$ and $d_B \leq M_B$. However, the optimal

(d_A, d_B)	R_{NPT}	R_{SIC1}	R_{SIC2}	R_{Cor}	R_{CCNR}
(2, 2)	0.75784 $\pm 1.7(4)$	0.67060 $\pm 2.2(4)$	0.67947 $\pm 2.1(4)$	0.68860 $\pm 2.1(4)$	0.65481 $\pm 2.2(4)$
(2, 3)	0.97303 $\pm 7(5)$	0.39732 $\pm 5.6(4)$	0.42998 $\pm 5.5(4)$	0.43853 $\pm 5.5(4)$	0.36787 $\pm 5.6(4)$
(2, 4)	0.998696 $\pm 1.6(5)$	0.02710 $\pm 2.7(4)$	0.04361 $\pm 3.4(4)$	0.04504 $\pm 3.5(4)$	0.0182 2.2(4)
(3, 3)	0.999895 $\pm 4(6)$	0.75680 $\pm 8.2(4)$	0.75754 $\pm 8.2(4)$	0.76364 $\pm 8.1(4)$	0.74264 $\pm 8.4(4)$
(3, 4)	1	0.3605 $\pm 1.8(3)$	0.3742 $\pm 1.8(3)$	0.3795 $\pm 1.8(3)$	0.3332 $\pm 1.8(3)$
(4, 4)	1	0.6378 $\pm 7.7(3)$	0.6380 $\pm 7.7(3)$	0.6419 $\pm 7.7(3)$	0.6255 $\pm 7.8(3)$

Table 5.2: Lower bounds on volume ratios between entangled and all bipartite quantum states for different dimensions d_A and d_B of Alice's and Bob's quantum systems: Bipartite NPT states R_{NPT} , bipartite states detectable by violations of Eq. (5.48) R_{SIC1} , of Eq. (5.48) R_{SIC2} , Eq. (2.63) R_{CCNR} , and of Eq. (5.33) R_{Cor} . The numbers in brackets after the statistical errors indicate the relevant powers of 10^{-1} . The errors have been calculated by the procedure in Appendix C. For dimensions (3, 4) and (4, 4), the algorithm generated only NPT states. Therefore, the corresponding values of R_{NPT} do not involve any statistical uncertainties.

(N, M) -POVMs for $d > M$ can only achieve the rescaled parameter $\tilde{x} = M/d < 1$. To address this, the restriction of optimal (N, M) -POVMs is relaxed to (N, M) -POVMs with arbitrary \tilde{x} for inequality (5.48). Figures 5.1 and 5.2 display the volume ratios detected by inequality (5.48) or all combinations of $2 \leq d_A, d_B \leq 4$, depending on the rescaled parameters \tilde{x}_A and \tilde{x}_B of Alice's and Bob's local quantum systems. These results are based on $N = 10^7$ quantum states generated by the hit-and-run Monte Carlo algorithm of Sec. 2.4. The figures show the volume ratio of the detected entangled states to all quantum states and the dependence of the allowed range of $\tilde{x}_A \in (1/d_A, \min(1, M_A/d_A)]$ and $\tilde{x}_B \in (1/d_B, \min(1, M_B/d_B)]$. The left-hand side of Figures 5.1 and 5.2 displays the dependence for arbitrary parameters \tilde{x}_A and \tilde{x}_B , while the right-hand side shows the value centered along the maximum values and compares it with R_{SIC1} and R_{Cor} . For $d = 2$, all the allowed (N, M) -POVMs are $(N, M) \in \{(1, 4), (3, 2)\}$ and the scaled parameter interval is always $1/2 \leq \tilde{x} \leq 1$. In the case of a qutrit $d = 3$, there are four different (N, M) -POVMs, three with $(N, M) \in \{(1, 9), (4, 3), (2, 5)\}$ and $1/3 \leq \tilde{x} \leq 1$, and one with $(N, M) = (8, 2)$ and $1/3 \leq \tilde{x} \leq 2/3$. In dimension $d = 4$, there are also four different informationally complete (N, M) -POVMs. The solutions are $(N, M) = \{(1, 15), (5, 4), (3, 6)\}$ with maximal intervals $1/4 \leq \tilde{x} \leq 1$ and $(N, M) = (15, 2)$ with restricted interval $1/4 \leq \tilde{x} \leq 1/2$. The black dashed straight lines in Figures 5.1c and 5.1e mark the upper bound of \tilde{x}_B for $M_B = 2$. Values above the dashed line can only be achieved by (N, M) -POVMs with $M_B \geq d_B$. The boundaries of the (N, M) -POVMs with $M_A = 2$ and $M_B = 2$ are indicated by vertical and horizontal dashed lines in Figures 5.2a, 5.2c and 5.2e. Parameters outside the dashed line can only be achieved by (N, M) -POVM with $M_A \geq d_A$ or $M_B \geq d_B$. The figures show that (N, M) -POVMs with pairs of $(\tilde{x}_A, \tilde{x}_B)$ for all \tilde{x}_A exist, whose volume ratio is close to the maxima (dark red area). This shows that optimal (N, M) -POVMs with $\tilde{x}_A = 1$ and $\tilde{x}_B = 1$ are not necessary to maximize the volume ratio of the detected entangled states. Entanglement detection with optimal (N, M) -POVMs represents the SIC-POVM condition of Shang *et al.* [85]. It is apparent from Figures 5.1c, 5.1e and 5.2c that the volume ratios detected by SIC-POVMs are not close to the maximal amount that can be detected by local informationally complete (N, M) -POVMs.

This is consistent with the enlarged gaps between R_{SIC1} and R_{Cor} for unequal dimensions of Alice's and Bob's quantum systems $d_A < d_B$ in contrast to identical dimensions $d_A = d_B$ in Table 5.2. Every pair $(\tilde{x}_A, \tilde{x}_B)$ in the dark red area can be used for nearly optimal entanglement detection with (N, M) -POVMs. On the right-hand side of Figures 5.1 and 5.2, the volume ratio of the entangled states along the center of the dark red area is shown and compared with R_{SIC1} and R_{Cor} . In the case of identical dimensions, R_{SIC1} is a lower bound for $R_{NM}(\tilde{x}, \tilde{x})$, which represents the maxima of the dark red area, and for decreasing \tilde{x} , the volume ratio of the entangled approaches R_{Cor} . Similar behavior is seen for unequal dimensions of the subsystems, but R_{SIC1} underestimates the volume ratios along the maxima $R_{NM}(\tilde{x}_A, \tilde{x}_B(\tilde{x}_A))$ or as other pairs of optimal (N, M) -POVMs. This demonstrates that (N, M) -POVMs with well-chosen parameters x_A and x_B are capable of detecting more entangled quantum states than SIC-POVMs. Additionally, there are parameters that are close to their lower bounds, located at the lower left corner of the left-hand side in Figures 5.1 and 5.2, which have volume ratios close to the maximum value. In Section 4.2, it has been shown that local (N, M) -POVMs with

$$x_A \leq \frac{1}{d_A - 1} \frac{d_A^2}{M_A^2} \quad \text{and} \quad x_B \leq \frac{1}{d_B - 1} \frac{d_B^2}{M_B^2} \quad (5.55)$$

can be constructed from arbitrary traceless Hermitian orthonormal operator bases [c.f. Eq. (4.32)]. Therefore, it is not necessary to use optimal (N, M) -POVMs for near-optimal entanglement detection with local (N, M) -POVMs.

In this chapter simple sufficient conditions involving local informationally complete (N, M) -POVMs without the need to optimize over the measurement setting have been discussed. It has been shown that the most efficient of such conditions are trace norm-based. These conditions fulfill the scaling relation, which necessarily groups the local informationally complete (N, M) -POVMs into classes of the same efficiency for arbitrary quantum states. The positivity of the (N, M) -POVM elements is not required for the entanglement detection. This allows for a discussion of the entanglement detection efficiencies without constructing such POVMs. The correlation matrix-based condition is completely independent of the nature of the chosen (N, M) -POVMs and is identical to that of LOOs. The joint probability distribution is weaker than the correlation matrix condition and the scaling relation is more subtle than that of the correlation matrix. The entanglement detection efficiency depends only on the pair of rescaled parameters \tilde{x}_A and \tilde{x}_B , which describe the class of the used local (N, M) -POVMs. The numerical results for low qudit dimensions $2 \leq d_A, d_B \leq 4$ allow identifying the optimal parameters \tilde{x}_A and \tilde{x}_B for the entanglement detection by joint probability distributions. Furthermore, it has been shown that always a pair of parameters close to the optimal detection exists for constructible (N, M) -POVMs. It has been shown that the Euclidean volume ratio of the NPT states is increasingly underestimated by increasing local dimension by the volume ratio of the entangled states detected by local (N, M) -POVMs. Additional research is required to increase the Euclidean volume ratios of entangled quantum states detected by local measurements. One potential approach to increase the number of detected entangled quantum states is to preprocess the quantum states through local operations and classical communication [37, 38].

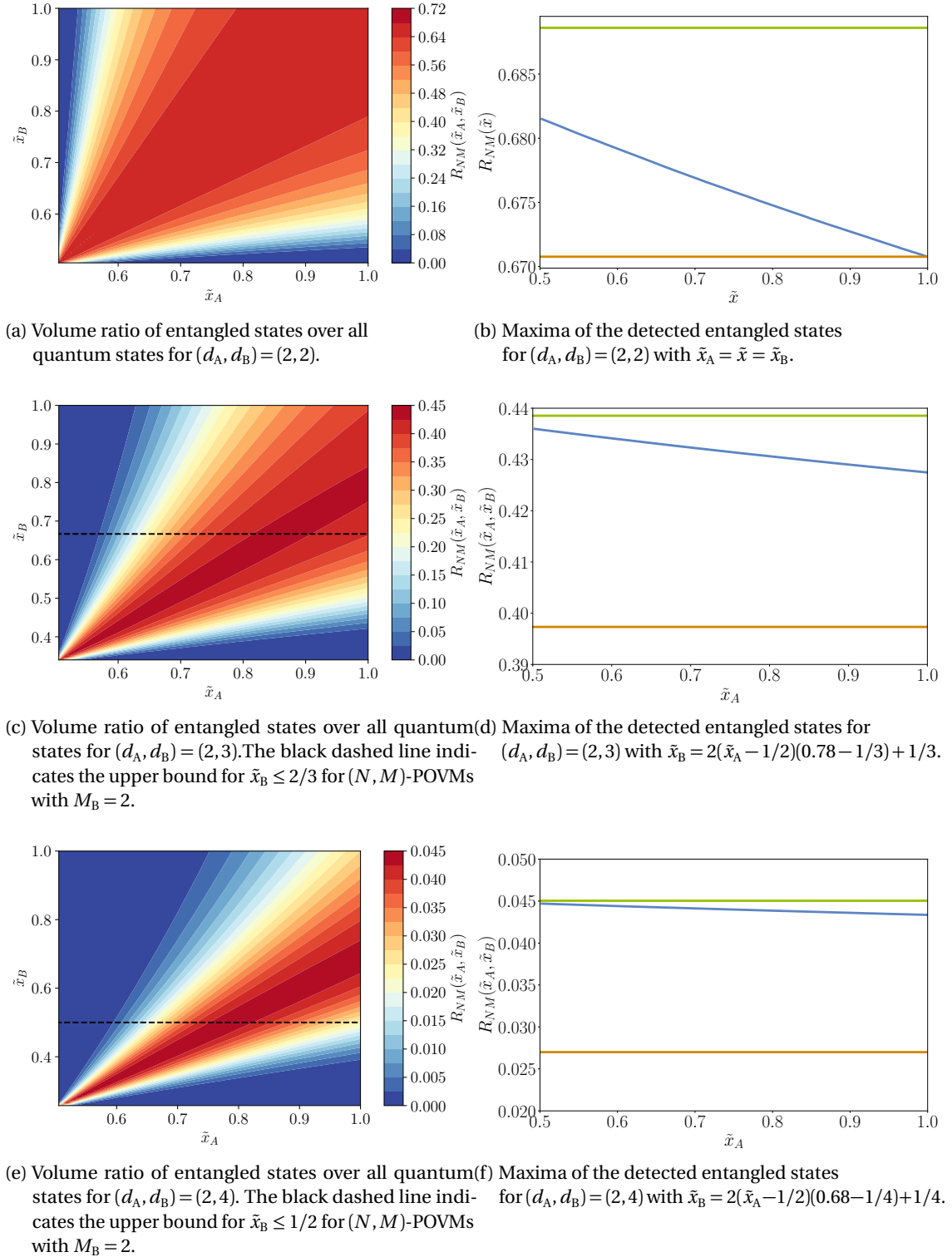


Figure 5.1: Dependence of volume ratios $R_{NM}(\tilde{x}_A, \tilde{x}_B)$ (5.48) between detected entangled and all bipartite quantum states on the scaled parameters of \tilde{x}_A and \tilde{x}_B of Alice's and Bob's informationally complete (N, M) -POVMs. This figure shows the results for qubit-qudit systems with dimension of Bob's system up to $d_A \leq 4$. Figures (b), (d) and (f) show the volume ratios of the entangled states $R_{NM}(\tilde{x}_A, \tilde{x}_B)$ along the maxima of the associated Figures (a), (c) and (e) (blue line). The green line represents the volume ratio R_{Cor} Eq. (5.33) and the orange line represents the volume ratio R_{SIC1} of local SIC-POVMs Eq. (5.48.)

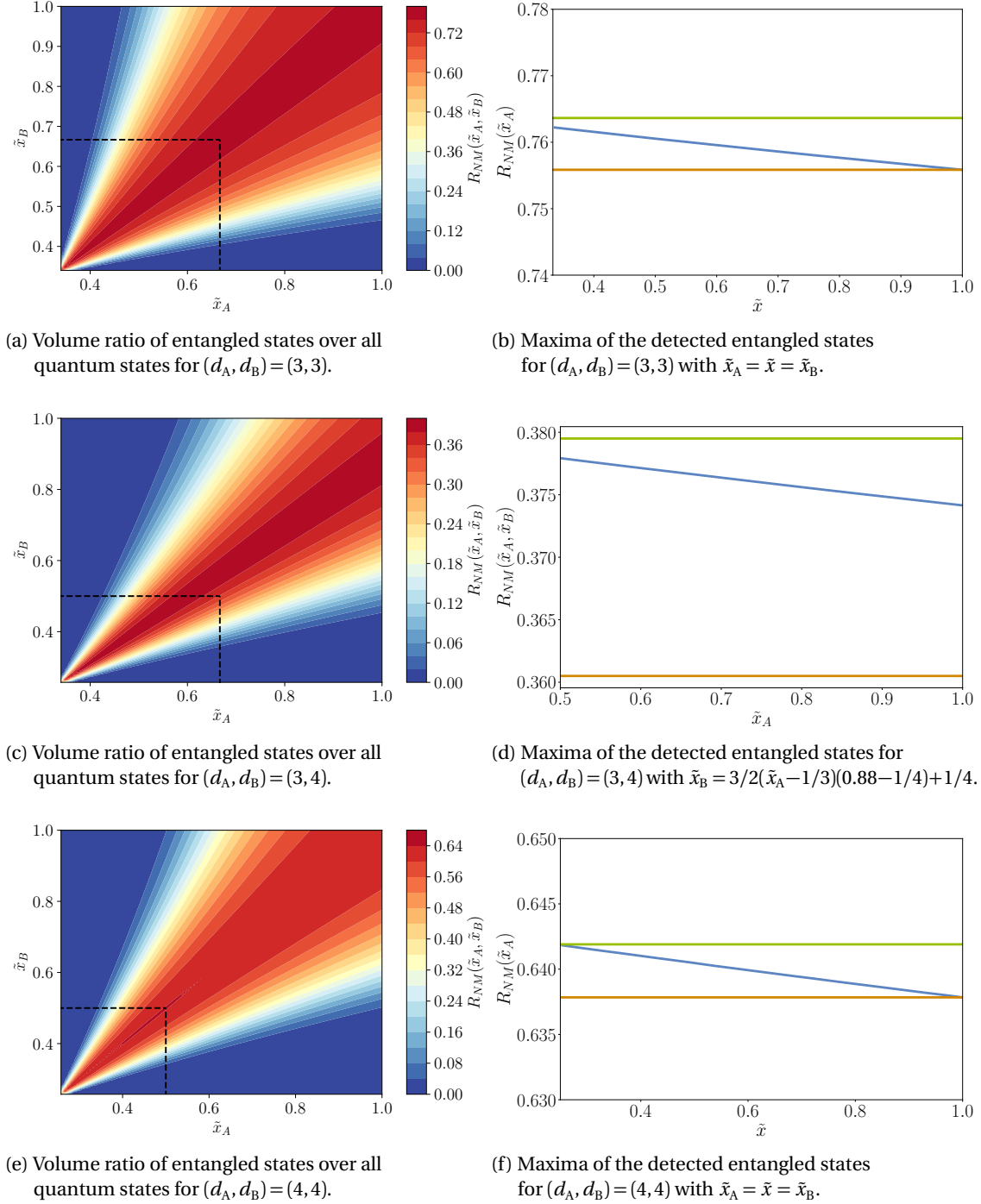


Figure 5.2: Dependence of volume ratios $R_{NM}(\tilde{x}_A, \tilde{x}_B)$ (5.48) between detected entangled and all bipartite quantum states on the scaled parameters of \tilde{x}_A and \tilde{x}_B of Alice's and Bob's informationally complete (N, M) -POVM. This figure shows the results for dimension $(d_A, d_B) = \{(3, 3), (3, 4), (4, 4)\}$. The vertical and horizontal dashed lines are the boundaries of the \tilde{x}_A and \tilde{x}_B for (N, M) -POVMs with $M_A = 2$ and $M_B = 2$. Figures (b), (d) and (f) show the volume ratios of the entangled states along the maxima of the associated Figures (a), (c) and (e) (blue line). The green line represents the volume ratio R_{Cor} Eq. (5.33) and the orange line represents the volume ratio R_{SIC1} of local SIC-POVMs Eq. (5.48).

Part IV

EINSTEIN-PODOLSKY-ROSEN STEERING

DETECTION OF EPR STEERING

Einstein-Podolsky-Rosen steering is a resource for quantum communication applications. Therefore, identifying EPR steerable quantum states is of great interest. The criteria for EPR steering [71, 143, 144] require an intricate optimization to verify EPR steerable quantum states from Alice to Bob. First, the critical radius criterion for a qubit-qubit system is discussed. Additionally, it has a closed integral form for the two-qubit T -states [71]. Furthermore, a sufficient condition for EPR unsteerability from Alice to Bob for arbitrary two-qubit states is presented, utilizing the insights gained from the unsteerable T -states. This discussion highlights the challenge of identifying the EPR steerable quantum states from Alice to Bob in a two-qubit system.

Simple sufficient conditions are needed to identify the EPR steerable quantum states of the state ensemble over the entire qudit-qudit state space. A sufficient condition for EPR steerability from Alice to Bob, based on correlation matrices of arbitrary local measurements, is discussed [129]. This sufficient condition is applied to LOOs and local informationally complete (N, M) -POVMs. The efficiency of detecting EPR steerability from Alice to Bob using such measurements is determined analytically by the scaling relation without the need to construct the local (N, M) -POVMs. The positive semidefiniteness of the local POVM elements is not required to derive the scaling relation. The second sufficient condition presented verifies EPR steering from Alice to Bob by detecting a preprocessed quantum state as entangled [145]. One disadvantage of this condition is that Alice's quantum system is restricted to a qubit. However, an advantage is that well-understood sufficient conditions for entanglement detection can be used. The volume ratios of the detected EPR steerable quantum states from Alice to Bob are calculated by these sufficient conditions.

This chapter is structured as follows: The EPR steerability of two-qubit states is discussed in detail by using the critical radius in Section 6.1. Section 6.2 discusses the correlation matrix-based sufficient condition for EPR steerability from Alice to Bob for arbitrary measurements. The following two subsections apply this condition to LOOs or local informationally complete (N, M) -POVMs as measurements. Furthermore, the efficiency of such measurements is determined by the scaling relation. Then, in Section 6.3, the detection of EPR steering from Alice to Bob through entanglement is discussed. In Section 6.4, the volume ratios of EPR steerable quantum states for low qudit dimensions are determined using these sufficient conditions.

6.1 EPR STEERABILITY FOR QUBIT-QUBIT SYSTEMS

Detecting EPR steerability from Alice to Bob can be challenging because the set of steerable quantum states depends on the local measurements of both Alice and Bob. To discuss the EPR steerability from Alice to Bob in the simplest bipartite quantum system, a two-qubit system is considered. Necessary and sufficient conditions are known [71, 143, 144]. In general, these

criteria require intricate optimization to decide whether a quantum state is EPR steerable from Alice to Bob. An exact analytical formula exists for the critical radius criterion for two-qubit T -states and projective measurements [71]. Suppose that Alice and Bob share a two-qubit quantum state. For each of Alice's measurement settings α and results a , Bob remains with a conditional unnormalized quantum state $\rho_{\alpha,a}^B$. From the completeness of the measurement results, it follows that Bob's reduced quantum state ρ_B must satisfy

$$\rho_B = \sum_{a=1}^M \rho_{\alpha,a}^B \quad (6.1)$$

for M measurement results. In the case of EPR steering from Alice to Bob, Bob tries to explain the measurements using a LHS model. The detailed definition of EPR steering from Alice to Bob is given in Section 2.5.2. Bob assumes that his quantum state was initially in a hidden state σ_λ with probability $p(\lambda)$ and the hidden parameter λ . Alice's measurement selections and results provide him with additional information about the probability distribution of the hidden states. Therefore, the conditional state has an updated probability distribution of the initial state

$$\rho_{\alpha,a}^B = \sum_{\lambda \in \Lambda} p(\lambda) p(a|\alpha, \lambda) \sigma_\lambda. \quad (6.2)$$

To decide if a quantum state is EPR steerable, one has to find a measurement setting that a LHS model cannot explain. The critical radius for a two-qubit system and projective measurements is given by [71]

$$R(\rho) = \max_{\mu} \min_C \frac{1}{\sqrt{2} \|\text{tr}_B\{\bar{\rho}(\mathbb{1}_2 \otimes C)\}\|} \int_{\sigma \in \mathcal{B}} d\mu(\sigma) |\text{tr}_B(C\sigma)|. \quad (6.3)$$

The state $\bar{\rho} = \rho - \mathbb{1}_2 \otimes \rho_B/2$ is introduced. The minimization is performed over all qubit observables C that act on Bob's systems. The integration is performed over Bob's Bloch ball \mathcal{B} , the norm is given by $\|X\| = \sqrt{\text{tr}\{X^\dagger X\}}$ and the probability measure μ of the LHS model. A quantum state is EPR steerable from Alice and Bob if and only if the critical radius fulfills $R(\rho) < 1$. The geometric interpretation of the critical radius is that $1 - R(\rho)$ is the distance of ρ to the boundary of the unsteerable states along the line to $\bar{\rho}$. An important property of the critical radius is the invariance

$$R(\tilde{\rho}) = R(\rho). \quad (6.4)$$

The transformed state $\tilde{\rho}$ is defined by

$$\tilde{\rho} = \mathcal{N}(U_A \otimes V_B \rho U_A^\dagger \otimes V_B^\dagger), \quad (6.5)$$

where U is a unitary matrix and V is an invertible matrix. The factor \mathcal{N} ensures the normalization of the density matrix. This invariance allows a simplification of the quantum state. Specifically, ρ can always be transformed into a state where Bob's reduced local quantum state is the maximal-mixed state. Additionally, the representation of a canonical state is simplified from the general representation Eq. (2.90) to

$$\tilde{\rho} = \frac{1}{4} \mathbb{1}_4 + \frac{1}{2} \left(\sum_{i=1}^3 a_i \sigma_i \otimes \mathbb{1}_2 + \sum_{i=1}^3 t_i \sigma_i \otimes \sigma_i \right) \quad (6.6)$$

with the Pauli matrices σ_i [c.f. Eq. (B.8)]. Even for the canonical quantum state, evaluating the critical radius Eq. (6.3) is difficult due to the intricate optimization required in Eq. (6.3). For an arbitrary two-qubit quantum state, the critical radius is bounded by

$$2\pi N_{\bar{T}} \geq R(\rho) \geq \frac{2\pi N_{\bar{T}} |\det(\bar{T})|}{1 + \|\bar{T}^{-1} \bar{\mathbf{a}}\|} \quad (6.7)$$

with the diagonal matrix $\bar{T} = 2\text{diag}(t_1, t_2, t_3)$ and Alice's Bloch vector $\bar{\mathbf{a}} = 2(a_1, a_2, a_3)^T$. The normalization constant $N_{\bar{T}}$ is determined by the relation

$$N_{\bar{T}}^{-1} = \int_{S_2} dS(\mathbf{n}) [\mathbf{n} \cdot \bar{T}^{-2} \mathbf{n}]^{-2} \quad (6.8)$$

with the unit vector \mathbf{n} being integrated over the surface of the unit sphere S_2 . These upper and lower bounds can determine whether a quantum state can be used for EPR steering from Alice to Bob or not

$$R(\rho) \leq 2\pi N_{\bar{T}} < 1 \quad \Rightarrow \rho \text{ is steerable}, \quad (6.9)$$

$$R(\rho) \geq \frac{2\pi N_{\bar{T}} |\det(\bar{T})|}{1 + \|\bar{T}^{-1} \bar{\mathbf{a}}\|} \geq 1 \quad \Rightarrow \rho \text{ is unsteerable}. \quad (6.10)$$

The first relation is a sufficient condition for EPR steering from Alice to Bob, while violating the second inequality is a sufficient condition to verify a quantum state as unsteerable from Alice to Bob.

The detection of steerability is best understood for T -states, which are quantum states where the reduced density matrices are maximally mixed $\rho_A = \text{tr}_B\{\rho\} = \mathbb{1}_2/2$ and $\rho_B = \text{tr}_A\{\rho\} = \mathbb{1}_2/2$. For T -states ($\mathbf{a} = 0$), the inequality (6.7) becomes an equality and the critical radius is given by [146]

$$R(\rho) = 2\pi N_{\bar{T}}. \quad (6.11)$$

The boundary of the unsteerable states is given by $R(\rho) = 1$ and can be equivalently defined by [146]

$$2\pi = \int_{S_2} dS(\mathbf{n}) \sqrt{\mathbf{n} \cdot \bar{T}^2 \mathbf{n}}. \quad (6.12)$$

This boundary can also be determined from inequality (2.125) by taking the limit of infinite measurements [99]. Furthermore, EPR steering becomes symmetric for T -states. This means that a quantum state that is steerable from Alice to Bob is also steerable from Bob to Alice and vice versa. For Bell diagonal quantum states, a subset of T -states, the EPR steerable states are shown in Figure 6.1 and compared with the correlation matrix-based EPR steering inequality with local informationally complete (N, M) -POVMs [c.f. Eq. (6.59)] or LOOs [c.f. Eq. (6.49)] as measurements. In the canonical representation Eq. (6.6), the T -states are represented by Bell diagonal quantum states. In Figure 6.1 the tetrahedron with the vertices $(-1/2, -1/2, -1/2)$, $(-1/2, 1/2, 1/2)$, $(1/2, -1/2, 1/2)$ and $(1/2, 1/2, -1/2)$ represents the Bell states. The yellow regions indicate the EPR steerable states detected by inequality (6.59). The complete set of the steerable states by projective measurements is given by the blue and yellow regions (6.3). The uncolored area inside the tetrahedron represents the unsteerable quantum states. Moreover, numerical results demonstrate that restricting measurements to projective ones does not

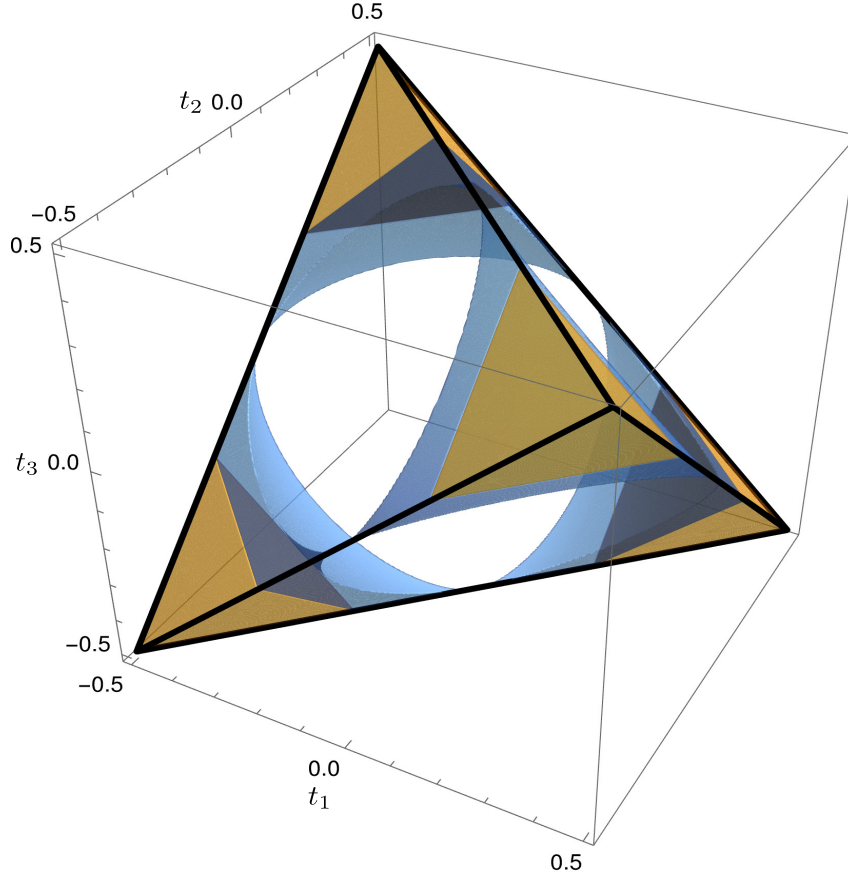


Figure 6.1: Bell diagonal two-qubit quantum states which are steerable with respect to different measurements: Steerable states with respect to local measurements involving (N,M) -POVMs due to violations of inequality (6.59) or equivalently (6.49) based on correlations matrices (yellow regions); steerable states with respect to projective measurements due to the criterion (6.3), (6.11) and (6.12) (yellow and blue regions); unsteerable states with respect to projective measurements due to the criterion (6.3), (6.11) and (6.12) (uncolored central convex region).

alter the number of EPR steerable states detected from Alice to Bob [71]. Thus, POVMs cannot detect more steerable states than projective measurements for arbitrary two-qubit states. The critical radius has been utilized to experimentally verify the EPR steerability of two-qubit quantum states [147].

The knowledge of the EPR steerability of two-qubit T -states and complete positive maps can be used to decide whether an arbitrary two-qubit state is unsteerable. To archive this, a set of complete positive maps acting on Alice's qubit transforms a T -state into a quantum state with a non-zero \mathbf{a} .

We assume that Alice and Bob share an unsteerable two-qubit quantum state from Alice to Bob. If a complete positive map Φ_A is applied to Alice's qubit then the final state $(\Phi_A \otimes \mathbb{1}_2)\rho$

will also be unsteerable from Alice to Bob [148] for all projective measurements. In the basis of Pauli matrices, a complete positive map acting on Alice's qubit can be characterized by [149]

$$\Phi(\sigma_\nu) = \sum_{\mu=0}^3 \mathcal{M}_{\mu\nu} \sigma_\mu \quad (6.13)$$

$$\mathcal{M} = \begin{pmatrix} 1 & \mathbf{0}^T \\ \mathbf{m} & \Lambda \end{pmatrix} = \begin{pmatrix} 1 & 0 & 0 & 0 \\ m_1 & \lambda_1 & 0 & 0 \\ m_2 & 0 & \lambda_2 & 0 \\ m_3 & 0 & 0 & \lambda_3 \end{pmatrix}. \quad (6.14)$$

The convexity of the complete positive maps on a single qubit makes it sufficient to consider extremal maps Φ^ϵ , which are given by

$$\mathcal{M}_{u,v}^\epsilon = \begin{pmatrix} 1 & 0 & 0 & 0 \\ 0 & \cos u & 0 & 0 \\ 0 & 0 & \cos v & 0 \\ \sin u \sin v & 0 & 0 & \cos u \cos v \end{pmatrix} \quad (6.15)$$

for $u \in [0, 2\pi)$ and $v \in [0, \pi)$. Letting this family of complete positive maps act on Bell diagonal states leads to quantum states of the form

$$\mathbf{a}' = \mathbf{m}, \quad T' = \Lambda T. \quad (6.16)$$

For a given unsteerable T -state it is known that all the states defined in Eq. (6.16) and their convex combinations are EPR unsteerable from Alice to Bob. For example, complete positive maps can be used to derive a sufficient condition for EPR unsteerability from Alice to Bob for displaced T -states with $\mathbf{a}' = a \hat{e}_z$ and T' . The displaced T -states are X -states in the canonical form. For a given quantum state, the boundary of the steerable states is given by

$$1 = \frac{1}{2\pi} \int_{S_2} dS(\mathbf{n}) \sqrt{\mathbf{n}(\Lambda_{u,v}^{-1} T'^2) \mathbf{n}} \quad (6.17)$$

with $a = \sin u \cos v$. Consider a displaced T -state of the form

$$\begin{pmatrix} t'_1 \\ t'_2 \\ t'_3 \end{pmatrix} = r \begin{pmatrix} \sin \alpha \cos \beta \\ \sin \alpha \sin \beta \\ \cos \alpha \end{pmatrix} \quad (6.18)$$

for $\alpha \in [0, \pi]$ and $\beta \in [0, 2\pi]$ and given value a . The maximum radius calculates to

$$r_{\max} = 2\pi \left[\min_{u,v} \int \int d\hat{x}^2 \sqrt{\frac{\sin^2 \alpha \cos^2 \beta}{\cos^2 u} x_1^2 + \frac{\sin^2 \alpha \sin^2 \beta}{\cos^2 v} x_2^2 + \frac{\cos^2 \alpha}{\cos^2 u \cos^2 v} x_3^2} \right]^{-1} \quad (6.19)$$

with the integral performed over the two dimensional unit sphere. The minimization is constrained by $a = \sin u \sin v$. For a given state, defined by the tuple (α, β, a) , the maximum radius r_{\max} can be calculated. Thus, two-qubit displaced T -states with $r \leq r_{\max}$ are unsteerable from Alice to Bob. Despite the use of the well-understood T -states, the necessary condition still requires an intricate optimization. Thus, a straightforward and adequate criterion is required to verify the EPR steerable quantum states from Alice to Bob. The computational workload should be capable of addressing the statistical characteristics of the state ensembles.

6.2 EPR STEERING DETECTION THROUGH CORRELATION MATRICES

In the previous section, necessary and sufficient conditions for two-qubit systems have been discussed. These criteria require intricate optimization, which can be challenging to determine even for arbitrary two-qubit states. Therefore, the focus is on sufficient conditions for detecting EPR steering from Alice to Bob without requiring an intricate optimization. The sufficient condition recently derived by Lai and Luo [129] for arbitrary local measurements can detect EPR steerable states for local qudit systems. This sufficient condition can be straightforwardly applied to GSICs, MUMs and LOOs as local measurements. In this section, this steering inequality is applied to the more general class of (N, M) -POVMs as local measurements, including GSICs and MUMs. Furthermore, this study determines the effectiveness of various (N, M) -POVMs and LOOs in detecting EPR steering from Alice to Bob. This thesis provides an overview of EPR steering inequalities that are derived from local informationally complete measurements in the current literature.

Consider Alice and Bob share a composite quantum state ρ of dimension $d = d_A d_B$, where Alice's Hilbert space has dimension d_A and Bob's has dimension d_B . Two general sets of Hermitian operators are considered for Alice $\mathcal{A} = \{A_i; i = 1, \dots, \overline{M}\}$ and Bob $\mathcal{B} = \{B_j; j = 1, \dots, \overline{N}\}$ and the correlation matrix associated with these measurements is given by

$$[C(\mathcal{A}, \mathcal{B}|\rho)]_{ij} = c_{ij} = \text{tr}\{(A_i \otimes B_j)(\rho - \rho_A \otimes \rho_B)\} \quad (6.20)$$

with the reduced local density matrices of Alice and Bob, $\rho_A = \text{tr}_B\{\rho\}$ and $\rho_B = \text{tr}_A\{\rho\}$. The possible measurement results of these operators are given by their spectra $a \in \text{Sp}(A_i)$ and $b \in \text{Sp}(B_j)$. A density matrix ρ is unsteerable if and only if the conditional joint probabilities can be expressed with a LHS model Eq. (2.121)

$$P(a, b|A_i, B_j, \rho) = \sum_{\lambda \in \Lambda} p(\lambda) P(a|A_i, \lambda) \text{tr}\{P_{j,b} \sigma_\lambda\} \quad (6.21)$$

for an ensemble of Bob's local quantum states $\{\sigma_\lambda\}$ and a hidden parameter $\{\lambda \in \Lambda\}$. The orthogonal projection onto the eigenspace of b corresponding to B_j is given by $P_{j,b}$. The spectral decomposition of Bob's operators is given by

$$B_j = \sum_{b \in \text{Sp}(B_j)} b P_{j,b}. \quad (6.22)$$

The components of the correlation matrix for an unsteerable quantum state from Alice to Bob can be calculated with the help of

$$\begin{aligned}
\text{tr}\{A_i \otimes B_j \rho\} &= \sum_{a \in \text{Sp}(A_i)} \sum_{b \in \text{Sp}(B_j)} ab P(a, b | A_i, B_j, \rho) \\
&= \sum_{a \in \text{Sp}(A_i)} \sum_{b \in \text{Sp}(B_j)} \left(\sum_{\lambda \in \Lambda} ab p(\lambda) P(A_i | a, \lambda) \text{tr}\{P_{j,b} \sigma_\lambda\} \right) \\
&= \sum_{\lambda \in \Lambda} p(\lambda) \sum_{a \in \text{Sp}(A_i)} a P(a | A_i, \lambda) \sum_{b \in \text{Sp}(B_j)} b \text{tr}\{P_{j,b} \sigma_\lambda\} \\
&= \sum_{\lambda \in \Lambda} p(\lambda) \langle A_i \rangle_\lambda \text{tr}\{B_j \sigma_\lambda\}, \tag{6.23}
\end{aligned}$$

$$\begin{aligned}
\text{tr}\{A_i \rho_A\} &= \sum_{a \in \text{Sp}(A_i)} a P(a, A_i, \rho_A) = \sum_{\lambda \in \Lambda} p(\lambda) \sum_{a \in \text{Sp}(A_i)} a P(a, A_i, \lambda) \\
&= \sum_{\lambda \in \Lambda} p(\lambda) \langle A_i \rangle_\lambda, \tag{6.24}
\end{aligned}$$

$$\begin{aligned}
\text{tr}\{B_j \rho_B\} &= \sum_{b \in \text{Sp}(B_j)} b P(b, B_j, \rho_B) = \sum_{\lambda \in \Lambda} p(\lambda) \sum_{b \in \text{Sp}(B_j)} b \text{tr}\{P_{j,b} \sigma_\lambda\} \\
&= \sum_{\lambda \in \Lambda} p(\lambda) \text{tr}\{B_j \sigma_\lambda\}. \tag{6.25}
\end{aligned}$$

The definitions of Alice's local classical average values $\langle A_i \rangle_\lambda = \sum_{a \in \text{Sp}(A_i)} a P(a, A_i, \lambda)$ and Bob's quantum mechanical average values $\text{tr}\{B_j \sigma_\lambda\} = \sum_{b \in \text{Sp}(B_j)} b \text{tr}\{P_{j,b} \sigma_\lambda\}$ are used. The elements of the correlation matrix can be represented by

$$\begin{aligned}
c_{ij} &= \text{tr}\{(A_i \otimes B_j)(\rho - \rho_A \otimes \rho_B)\} \\
&= \text{tr}\{(A_i \otimes B_j)\rho\} - \text{tr}\{A_i \rho_A\} \text{tr}\{B_j \rho_B\} \\
&= \sum_{\lambda \in \Lambda} p(\lambda) \langle A_i \rangle_\lambda \text{tr}\{B_j \sigma_\lambda\} - \sum_{\lambda \in \Lambda} p(\lambda) \langle A_i \rangle_\lambda \sum_{\lambda' \in \Lambda} p(\lambda') \text{tr}\{B_j \sigma_{\lambda'}\} \\
&= \sum_{\lambda, \lambda' \in \Lambda} (p(\lambda) p(\lambda') \langle A_i \rangle_\lambda \text{tr}\{B_j \sigma_\lambda\} - p(\lambda) \langle A_i \rangle_\lambda p(\lambda') \text{tr}\{B_j \sigma_{\lambda'}\}) \\
&= \frac{1}{2} \sum_{\lambda, \lambda' \in \Lambda} p(\lambda) p(\lambda') (\langle A_i \rangle_\lambda - \langle A_i \rangle_{\lambda'}) (\text{tr}\{B_j \sigma_\lambda\} - \text{tr}\{B_j \sigma_{\lambda'}\}). \tag{6.26}
\end{aligned}$$

The correlation vectors

$$\mathbf{V}_{\lambda, \lambda'} = \begin{pmatrix} V_1 \\ V_2 \\ \vdots \\ V_M \end{pmatrix} = \begin{pmatrix} \langle A_1 \rangle_\lambda - \langle A_1 \rangle_{\lambda'} \\ \langle A_2 \rangle_\lambda - \langle A_2 \rangle_{\lambda'} \\ \vdots \\ \langle A_M \rangle_\lambda - \langle A_M \rangle_{\lambda'} \end{pmatrix}, \quad \mathbf{W}_{\lambda, \lambda'} = \begin{pmatrix} W_1 \\ W_2 \\ \vdots \\ W_N \end{pmatrix} = \begin{pmatrix} \text{tr}\{B_1 \sigma_\lambda\} - \text{tr}\{B_1 \sigma_{\lambda'}\} \\ \text{tr}\{B_2 \sigma_\lambda\} - \text{tr}\{B_2 \sigma_{\lambda'}\} \\ \vdots \\ \text{tr}\{B_N \sigma_\lambda\} - \text{tr}\{B_N \sigma_{\lambda'}\} \end{pmatrix} \tag{6.27}$$

are defined to represent the correlation matrix by

$$C(A, B, \rho) = \frac{1}{2} \sum_{\lambda, \lambda' \in \Lambda} p(\lambda) p(\lambda') \mathbf{V}_{\lambda, \lambda'} \mathbf{W}_{\lambda, \lambda'}^T. \tag{6.28}$$

For the trace norm of the correlation matrix holds

$$\begin{aligned}
\|C(\mathcal{A}, \mathcal{B} | \rho)\|_{\text{tr}} &= \left\| \frac{1}{2} \sum_{\lambda, \lambda' \in \Lambda} p(\lambda) p(\lambda') \mathbf{V}_{\lambda, \lambda'} \mathbf{W}_{\lambda, \lambda'}^T \right\|_{\text{tr}} \\
&\leq \frac{1}{2} \sum_{\lambda, \lambda' \in \Lambda} p(\lambda) p(\lambda') \|\mathbf{V}_{\lambda, \lambda'} \mathbf{W}_{\lambda, \lambda'}^T\|_{\text{tr}} \\
&= \frac{1}{2} \sum_{\lambda, \lambda' \in \Lambda} p(\lambda) p(\lambda') \|\mathbf{V}_{\lambda, \lambda'}\| \|\mathbf{W}_{\lambda, \lambda'}\|. \tag{6.29}
\end{aligned}$$

The first inequality follows from the triangle inequality and the last equality from the trace norm of the dyadic product of two vectors. Applying the Cauchy-Schwarz inequality leads to

$$\|C(\mathcal{A}, \mathcal{B} | \rho)\|_{\text{tr}} \leq \frac{1}{2} \sqrt{\sum_{\lambda, \lambda' \in \Lambda} p(\lambda) p(\lambda') \|\mathbf{V}_{\lambda, \lambda'}\|^2} \sqrt{\sum_{\lambda, \lambda' \in \Lambda} p(\lambda) p(\lambda') \|\mathbf{W}_{\lambda, \lambda'}\|^2} \tag{6.30}$$

$$\begin{aligned}
&= \frac{1}{2} \sqrt{\sum_{i=1}^M \sum_{\lambda, \lambda' \in \Lambda} p(\lambda) p(\lambda') (\langle A_i \rangle_{\lambda} - \langle A_i \rangle_{\lambda'})^2} \\
&\quad \times \sqrt{\sum_{j=1}^{\bar{N}} \sum_{\lambda, \lambda' \in \Lambda} p(\lambda) p(\lambda') (\text{tr}\{B_j \sigma_{\lambda}\} - \text{tr}\{B_j \sigma_{\lambda'}\})^2}. \tag{6.31}
\end{aligned}$$

The two terms inside the square roots will be dealt with separately for better comprehension. The term with Bob's operators reads

$$\begin{aligned}
&\sum_{j=1}^{\bar{N}} \sum_{\lambda, \lambda' \in \Lambda} p(\lambda) p(\lambda') (\text{tr}\{B_j \sigma_{\lambda}\} - \text{tr}\{B_j \sigma_{\lambda'}\})^2 \\
&= \sum_{j=1}^{\bar{N}} \sum_{\lambda, \lambda' \in \Lambda} p(\lambda) p(\lambda') (\text{tr}\{B_j \sigma_{\lambda}\}^2 - 2 \text{tr}\{B_j \sigma_{\lambda}\} \text{tr}\{B_j \sigma_{\lambda'}\} + \text{tr}\{B_j \sigma_{\lambda'}\}^2) \\
&= \sum_{j=1}^{\bar{N}} \left(\sum_{\lambda' \in \Lambda} p(\lambda') \sum_{\lambda \in \Lambda} p(\lambda) (\text{tr}\{B_j \sigma_{\lambda}\}^2 - 2 \left(\sum_{\lambda \in \Lambda} p(\lambda) \text{tr}\{B_j \sigma_{\lambda}\} \right) \left(\sum_{\lambda' \in \Lambda} p(\lambda') \text{tr}\{B_j \sigma_{\lambda'}\} \right) \right. \\
&\quad \left. + \sum_{\lambda \in \Lambda} p(\lambda) \sum_{\lambda' \in \Lambda} p(\lambda') (\text{tr}\{B_j \sigma_{\lambda'}\}^2) \right) \\
&= 2 \sum_{\lambda \in \Lambda} p(\lambda) \sum_{j=1}^{\bar{N}} \text{tr}\{B_j \sigma_{\lambda}\}^2 - 2 \sum_{j=1}^{\bar{N}} \text{tr}\{B_j \rho_B\}^2 \\
&\leq 2 \left(\max_{\sigma_B} \sum_{j=1}^{\bar{N}} \text{tr}\{B_j \sigma_B\}^2 - \sum_{j=1}^{\bar{N}} \text{tr}\{B_j \rho_B\}^2 \right) \\
&= 2 V_B. \tag{6.32}
\end{aligned}$$

The fact that $\sum_{j=1}^{\bar{N}} \text{tr}\{B_j \sigma_B\}^2 \leq \max_{\sigma_B} \sum_{j=1}^{\bar{N}} \text{tr}\{B_j \sigma_B\}^2$ holds has been used. The term containing only Alice's observable is derived by

$$\begin{aligned}
\sum_{i=1}^{\bar{M}} \sum_{\lambda, \lambda' \in \Lambda} p(\lambda) p(\lambda') (\langle A_i \rangle_\lambda - \langle A_i \rangle_{\lambda'})^2 &= \sum_{i=1}^{\bar{M}} \sum_{\lambda, \lambda' \in \Lambda} p(\lambda) p(\lambda') (\langle A_i \rangle_\lambda^2 - 2\langle A_i \rangle_\lambda \langle A_i \rangle_{\lambda'} + \langle A_i \rangle_{\lambda'}^2) \\
&\leq \sum_{i=1}^{\bar{M}} \sum_{\lambda, \lambda' \in \Lambda} p(\lambda) p(\lambda') (\langle A_i^2 \rangle_\lambda - 2\langle A_i \rangle_\lambda \langle A_i \rangle_{\lambda'} + \langle A_i^2 \rangle_{\lambda'}) \\
&= 2 \sum_{i=1}^{\bar{M}} \left(\sum_{\lambda \in \Lambda} p(\lambda) \langle A_i^2 \rangle_\lambda - \left(\sum_{\lambda \in \Lambda} p(\lambda) \langle A_i \rangle_\lambda \right) \left(\sum_{\lambda' \in \Lambda} p(\lambda') \langle A_i \rangle_{\lambda'} \right) \right) \\
&= 2 \sum_{i=1}^{\bar{M}} \left(\text{tr}\{A_i^2 \rho_A\} - \text{tr}\{A_i \rho_A\}^2 \right) \\
&= 2 \sum_{i=1}^{\bar{M}} \mathcal{V}(A_i, \rho_A) = 2V_A. \tag{6.33}
\end{aligned}$$

The non-negativity of the variance has been used $\mathcal{V}(A) = \langle A^2 \rangle - \langle A \rangle^2 \geq 0$. The trace norm of the correlation matrix for unsteerable quantum states from Alice to Bob is upper bounded by [129]

$$\|C(\mathcal{A}, \mathcal{B} | \rho)\|_{\text{tr}} \leq \sqrt{V_A V_B}. \tag{6.34}$$

The upper bound involves a maximization over all local quantum states of Bob σ_B . A quantum state that violates this inequality is detected as EPR steerable from Alice to Bob. In particular, the upper bound depends on the chosen local Hermitian measurement operators \mathcal{A} and \mathcal{B} . Inequality (6.34) is a general consequence of the unsteerability of an arbitrary dimensional quantum state ρ . For arbitrary local Hermitian measurements \mathcal{B} , the inequality's boundary Eq. (6.32) is rather complicated to calculate. The factor V_B is defined identically to Σ_B for entanglement detection in inequality (5.13). However, the term derived from Alice's measurements differs $V_A \neq \Sigma_A$. Furthermore, the focus is on informationally complete measurements that enable a complete reconstruction of a quantum state. A set of linear operators that act on elements of \mathcal{H}_d is informationally complete if and only if it contains d^2 linearly independent operators. In the context of local measurements, this means that the set \mathcal{A} can reconstruct ρ_A and the set \mathcal{B} can reconstruct ρ_B . The set of the tensor products $\mathcal{A} \otimes \mathcal{B} = \{A_i \otimes B_j; i = 1, \dots, \bar{M}, j = 1, \dots, \bar{N}\}$ is informationally complete for the composite Hilbert space $\mathcal{H}_A \otimes \mathcal{H}_B$. In the following subsections, local informationally complete Hermitian measurement operators will be discussed, which allow the analytical calculation of the upper bound. The first type of operators are the LOOs discussed in Section 2.2.3. The second type are the (N, M) -POVMs, which have been discussed in detail in Chapters 3 and 4. The sufficient condition based on inequality (6.34) may be improved further by changing Alice's Hermitian operators to the Hermitian operators $\tilde{\mathcal{A}} = \{\tilde{A}_1, \dots, \tilde{A}_{\bar{M}}\}$ by

$$\tilde{A}_i = h_i A_i \tag{6.35}$$

for all $i \in \{1, \dots, \bar{M}\}$ and $h_i \in \mathbb{R}$. This new set of Hermitian operators also fulfills the steering inequality (6.34)

$$\|C(\tilde{\mathcal{A}}, \mathcal{B}|\rho)\|_{\text{tr}} \leq \sqrt{V_A(h_i)V_B} \quad (6.36)$$

$$V_A(h_i) = \sum_{i=1}^{\bar{M}} h_i^2 \mathcal{V}(A_i, \rho_A) = \sum_{i=1}^{\bar{M}} h_i^2 \left(\text{tr}\{A_i^2 \rho_A\} - \text{tr}\{A_i \rho_A\}^2 \right). \quad (6.37)$$

For a given quantum state ρ , it is possible to test whether there exists a parameter set $\{h_i\}$ that violates the inequality (6.36) and detects the state as steerable. If all $h_i = 1$, the steering inequality for the initial measurement is recovered. This improves the number of steerable states from Alice to Bob that can be detected by a given measurement \mathcal{A} . There may exist a set of parameters $\{h_i\}$ for which the inequality (6.36) is violated but the inequality (6.34) is not. Applying this procedure to Bob's measurements is more challenging because V_B requires an optimization over all of Bob's quantum states for all tested parameter sets $\{h_i\}$. The family of inequalities (6.36) can be used to derive further sufficient conditions. Similar to the entanglement detection, a sufficient condition involving the joint probability distribution

$$[P(\tilde{\mathcal{A}}, \mathcal{B}|\rho)]_{ij} = \text{tr}\{A_i \otimes B_j \rho\} \quad (6.38)$$

can be derived. An unsteerable quantum state ρ fulfills.

$$\begin{aligned} \|P(\tilde{\mathcal{A}}, \mathcal{B}|\rho)\|_{\text{tr}} &\leq \|C(\tilde{\mathcal{A}}, \mathcal{B}|\rho)\|_{\text{tr}} + \|P(\tilde{\mathcal{A}}, \mathcal{B}|\rho_A \otimes \rho_B)\|_{\text{tr}} \\ &\leq \sqrt{V_A(h_i)V_B} + \sqrt{\sum_{i=1}^{\bar{M}} h_i^2 \text{tr}\{A_i \rho_A\}^2} \sqrt{\sum_{j=1}^{\bar{N}} \text{tr}\{B_j \rho_B\}^2} \\ &\leq \sqrt{V_A(h_i) + \sum_{i=1}^{\bar{M}} h_i^2 \text{tr}\{A_i \rho_A\}^2} \sqrt{V_B + \sum_{j=1}^{\bar{N}} \text{tr}\{B_j \rho_B\}^2} \\ &= \sqrt{\sum_{i=1}^{\bar{M}} h_i^2 \text{tr}\{A_i^2 \rho_A\}} \sqrt{\max_{\sigma_B} \sum_{j=1}^{\bar{N}} \text{tr}\{B_j \sigma_B\}^2} \\ &= \sqrt{\Omega_A(h_i)\Omega_B} \end{aligned} \quad (6.39)$$

with

$$\Omega_A(h_i) = \sum_{i=1}^{\bar{M}} h_i^2 \text{tr}\{A_i^2 \rho_A\} \quad (6.40)$$

$$\Omega_B = \max_{\sigma_B} \sum_{j=1}^{\bar{N}} \text{tr}\{B_j \sigma_B\}^2. \quad (6.41)$$

In the first line, the triangle inequality has been used. The second line follows from inequality (6.36) that an unsteerable state fulfills. In the third line, inequality Eq. (5.41) has been used. For Ω_B the same maximization over all quantum states of Bob's systems has to be calculated. If Alice and Bob perform the same number of measurements $\bar{M} = \bar{N}$, two additional sufficient conditions can be derived. With the help of the inequality $\sum_{i=1}^{\bar{M}} |\mathcal{M}_{ii}| \leq \|\mathcal{M}\|_{\text{tr}}$, valid for arbi-

trary $\overline{M} \times \overline{M}$ square matrices, the following inequalities can be derived from inequality (6.36) and (6.39)

$$\sum_{i=1}^{\overline{M}} |\text{tr}\{h_i A_i \otimes B_i (\rho - \rho_A \otimes \rho_B)\}| \leq \sqrt{V_A(h_i) V_B} \quad (6.42)$$

$$\sum_{i=1}^{\overline{M}} |\text{tr}\{h_i A_i \otimes B_i \rho\}| \leq \sqrt{\Omega_A(h_i) \Omega_B}. \quad (6.43)$$

Furthermore, it can be shown that inequality (6.42) is more efficient than inequality (6.43)

$$\begin{aligned} \sum_{i=1}^{\overline{M}} |\text{tr}\{h_i A_i \otimes B_i \rho\}| &\leq \sum_{i=1}^{\overline{M}} |\text{tr}\{h_i A_i \otimes B_i \rho_A \otimes \rho_B\}| + \sum_{i=1}^{\overline{M}} |\text{tr}\{h_i A_i \otimes B_i (\rho - \rho_A \otimes \rho_B)\}| \\ &\leq \sum_{i=1}^{\overline{M}} |\text{tr}\{h_i A_i \rho_A\}| |\text{tr}\{B_i \rho_B\}| + \sqrt{V_A(h_i) V_B} \\ &\leq \sqrt{\sum_{i=1}^{\overline{M}} h_i^2 (\text{tr}\{A_i \rho_A\})^2} \sqrt{\sum_{i=1}^{\overline{M}} (\text{tr}\{B_i \rho_B\})^2} + \sqrt{V_A(h_i) V_B} \\ &\leq \sqrt{\sum_{i=1}^{\overline{M}} h_i^2 (\text{tr}\{A_i \rho_A\})^2 + V_A(h_i)} \sqrt{\sum_{i=1}^{\overline{M}} (\text{tr}\{B_i \rho_B\})^2 + V_B} \\ &= \sqrt{\Omega_A(h_i) \Omega_B}. \end{aligned} \quad (6.44)$$

In the first line, the triangle inequality has been used and in the second line that the quantum state ρ fulfills inequality (6.42). The Cauchy-Schwarz inequality is applied in the third line. The final result is obtained after applying the general inequality (5.41). The inequalities (6.42) have been recently derived by [150]. The efficiencies of the inequalities (6.36), (6.42) and (6.43) without inequality (6.39) have been discussed in [129]. The most efficient inequality is the correlation matrix-based sufficient condition. Therefore, this condition is further discussed and specialized for informationally complete measurements of LOOs and local (N, M) -POVMs.

6.2.1 EPR Steering detection with local Hermitian operator bases (LOOs)

In this subsection, the arbitrary Hermitian measurement operators involved in Eq. (6.34) are specialized to arbitrary LOOs, say $G^A = (G_0^A, \dots, G_{d_A^2-1}^A)$ and $G^B = (G_0^B, \dots, G_{d_B^2-1}^B)$ as defined in Section 2.2.3. The number of the measurements on the subsystems is d_A^2 and d_B^2 . The upper bound of the inequality (6.34) is calculated using the Hilbert-Schmidt representation of a density matrix Eq. (2.16)

$$\rho = \sum_{i=0}^{d^2-1} G_i \text{tr}\{G_i \rho\} = \sum_{i=0}^{d^2-1} G_i r_i = \mathbf{r} \cdot \mathbf{G} \quad (6.45)$$

and the purity of a density matrix

$$\begin{aligned}
\text{tr}\{\rho^2\} &= \text{tr}\left\{\sum_{i=0}^{d^2-1} G_i r_i \sum_{j=0}^{d^2-1} G_j r_j\right\} \\
&= \sum_{i=0}^{d^2-1} r_i r_j \sum_{j=0}^{d^2-1} \text{tr}\{G_i G_j\} \\
&= \sum_{i=0}^{d^2-1} r_i^2 = \sum_{i=0}^{d^2-1} \text{tr}\{G_i \rho\}^2.
\end{aligned} \tag{6.46}$$

These relations are used to calculate Eq. (6.32)

$$V_B = \max_{\sigma_B} \sum_{j=0}^{d_B^2-1} \text{tr}\{G_j \sigma_B\}^2 - \sum_{j=0}^{d_B^2-1} \text{tr}\{G_j \rho_B\}^2 = \max_{\sigma_B} \text{tr}\{\sigma_B^2\} - \text{tr}\{\rho^2\} = 1 - \text{tr}\{\rho_B^2\}. \tag{6.47}$$

The maximum of the upper bound is taken for arbitrary pure quantum states of Bob's subsystem. The invariant (B.18) is used to calculate Eq. (6.33)

$$V_A = \sum_{i=1}^{\bar{M}} \left(\text{tr}\{A_i^2 \rho_A\} - \text{tr}\{A_i \rho_A\}^2 \right) = d_A - \text{tr}\{\rho_A^2\}. \tag{6.48}$$

Therefore, the inequality (6.34) reduces to

$$\|C(G^A, G^B|\rho)\|_{\text{tr}} \leq \sqrt{(d_A - \text{tr}\{\rho_A^2\})(1 - \text{tr}\{\rho_B^2\})}. \tag{6.49}$$

For LOOs, this inequality has already been discussed [129]. The upper bound is independent of the chosen LOO and the trace norm of the correlation matrix is also independent of the chosen LOO [c.f. Eq. (5.22)]. This implies that arbitrary LOOs have an identical steering inequality. For an arbitrary quantum state and LOOs \tilde{G}^A and \tilde{G}^B with $\tilde{G}_0^A = \mathbb{1}/\sqrt{d_A}$ and $\tilde{G}_0^B = \mathbb{1}/\sqrt{d_B}$ the correlation matrix fulfills the relation

$$[C(\tilde{G}^A, \tilde{G}^B|\rho)]_{0\nu} = [C(\tilde{G}^A, \tilde{G}^B|\rho)]_{\mu 0} = 0 \tag{6.50}$$

for $\mu \in \{1, \dots, d_A^2 - 1\}$ and $\nu \in \{1, \dots, d_B^2 - 1\}$. This implies that the correlation matrix for such LOOs has a block diagonal structure consisting of a 1×1 block of zero and a second block of dimension $(d_A^2 - 1) \times (d_B^2 - 1)$. Only the second block contributes to the trace norm, while the eigenvalue zero belonging to the first block can be neglected. In Section 2.2.3, the CCNR condition for entanglement detection has been discussed. This inequality includes LOOs as measurement operators. However, instead of using the trace norm of the correlation matrix, it considers the joint probability distribution. Similar inequalities can be used to detect EPR steering from Alice to Bob. The joint probability inequality for LOOs is given by Eq. (6.39)

$$\|P(G^A, G^B|\rho)\|_{\text{tr}} \leq \sqrt{d_A}. \tag{6.51}$$

From the steering inequalities in Eqs. (6.49) and (6.51) by setting d_A to one the sufficient entanglement conditions for LOOs [c.f. Eqs. (5.19) and (5.25)] are recovered. Using the Schmidt decomposition of a density matrix Eq. (2.56)

$$\rho = \sum_{k=1}^d \lambda_k \tilde{G}_k^A \otimes \tilde{G}_k^B, \quad \lambda_k = \langle \tilde{G}_k^A \otimes \tilde{G}_k^B \rangle = \text{tr}\{\rho \tilde{G}_k^A \otimes \tilde{G}_k^B\} \tag{6.52}$$

for $d = \min(d_A, d_B)$ the steering inequality

$$\sum_{k=1}^d \lambda_k \leq \sqrt{d_A} \quad (6.53)$$

can be derived by inserting the Schmidt decomposition into the inequality (6.51). Similar to entanglement detection with LOOs, a family of EPR steering inequalities can be derived. The EPR steering inequalities (6.49) and (6.51) and their analogous entanglement inequalities (5.19) and (2.67) have a similar structure. The entanglement inequalities can be recovered by setting the value of d_A to 1 at the upper bound of the steering inequalities.

6.2.2 EPR steering detection with (N, M) -POVMs

The general sufficient condition Eq. (6.34) for EPR steering from Alice to Bob is applied to local informationally complete (N, M) -POVMs as local measurements. The properties and existence of the (N, M) -POVMs are discussed in Chapters 3 and 4. The section starts by deriving a correlation matrix-based sufficient condition for EPR steering from Alice to Bob using (N, M) -POVMs as local measurements based on the condition for arbitrary local measurements. The second part discusses the efficiency of various local informationally complete (N, M) -POVMs by comparing their correlation matrix to that of LOOs. Alice and Bob measure the local informationally complete (N, M) -POVMs $\Pi^A = (\Pi_1^A, \dots, \Pi_{N_A M_A}^A)$ and $\Pi^B = (\Pi_1^B, \dots, \Pi_{N_B M_B}^B)$. These positive semidefinite operators fulfill the defining relations of (N, M) -POVMs [c.f. (3.15-3.17)] and the informational completeness relations $d_A^2 - 1 = N_A(M_A - 1)$ and $d_B^2 - 1 = N_B(M_B - 1)$ [c.f. Eq. (3.18)]. For the sake of convenience, the single index of the (N, M) -POVMs is introduced by $i(\alpha, a) = (\alpha - 1)M_A + a$ and $j(\beta, b) = (\beta - 1)M_B + b$. The coefficients of the upper bound of the EPR steering inequality are given by Eqs. (6.32) and (6.33). They are calculated by using Eqs. (3.81) and (3.82)

$$\begin{aligned} V_A &= \sum_{i=1}^{N_A M_A} \left(\text{tr} \left\{ \left(\Pi_{i(\alpha, a)}^A \right)^2 \rho_A \right\} - \left(\text{tr} \left\{ \Pi_{i(\alpha, a)}^A \rho_A \right\} \right)^2 \right) \\ &= \left(\frac{(d_A^2 - 1)M_A x_A}{(M_A - 1)d_A} - \frac{d_A^3 - M_A^2 x_A + d_A(M_A^2 x_A - d_A) \text{tr} \{ \rho_A^2 \}}{d_A M_A (M_A - 1)} \right) \\ &= \Gamma_A (d_A - \text{tr} \{ \rho_A^2 \}) \end{aligned} \quad (6.54)$$

$$\begin{aligned} V_B &= \max_{\sigma_B} \sum_{j=1}^{N_B M_B} \left(\left(\text{tr} \left\{ \Pi_{j(\beta, b)}^B \sigma_B \right\} \right)^2 - \left(\text{tr} \left\{ \Pi_{j(\beta, b)}^B \rho_B \right\} \right)^2 \right) \\ &= \max_{\sigma_B} \left(\frac{d_B^3 - M_B^2 x_B + d_B(M_B^2 x_B - d_B) \text{tr} \{ \sigma_B^2 \}}{d_B M_B (M_B - 1)} - \frac{d_B^3 - M_B^2 x_B + d_B(M_B^2 x_B - d_B) \text{tr} \{ \rho_B^2 \}}{d_B M_B (M_B - 1)} \right) \\ &= \Gamma_B (1 - \text{tr} \{ \rho_B^2 \}) \end{aligned} \quad (6.55)$$

with

$$\Gamma_A = \frac{M_A^2 x_A - d_A}{M_A (M_A - 1)}, \quad \Gamma_B = \frac{M_B^2 x_B - d_B}{M_B (M_B - 1)}. \quad (6.56)$$

As a consequence, the correlation matrix-based inequality of informationally complete (N, M) -POVMs obeys

$$\|C(\Pi^A, \Pi^B | \rho)\|_{\text{tr}} \leq \sqrt{\Gamma_A \Gamma_B} \sqrt{(d_A - \text{tr} \{ \rho_A^2 \})(1 - \text{tr} \{ \rho_B^2 \})} \quad (6.57)$$

for all EPR unsteerable quantum states from Alice to Bob. A quantum state that violates this inequality is detected as EPR steerable from Alice to Bob. This general inequality has already been applied to the special instances of GSICs and MUMs as local measurements [129]. Inequality (5.29) depends on the local (N, M) -POVMs and their parameters x_A, x_B, N_A, N_B, M_A and M_B , which complicates the direct comparison of the efficiency of different types of (N, M) -POVMs for arbitrary quantum states. The correlation matrix has a dimension of $N_A M_A \times N_B M_B$, which makes it difficult to compare (N, M) -POVMs with different values of N and M . Additionally, the upper bounds of the inequalities for local (N, M) -POVMs (5.29) and LOOs (5.19) are proportional to each other by the factor $\sqrt{\Gamma_A \Gamma_B}$. Therefore, the correlation matrix of (N, M) -POVMs will be related to that of LOOs. This relation avoids the apparent complexity of the correlation matrix's dependence on (N, M) -POVMs and their parameters.

For this purpose, the local informationally complete (N, M) -POVM elements are expanded in arbitrary LOOs, say G^A for Alice and G^B for Bob, i.e. $\Pi^A = (G^A)^T S^A$ and $\Pi^B = (G^B)^T S^B$. The real-valued expansion coefficient matrices S^A and S^B are defined in Section 3.3. They are $d_A^2 \times N_A M_A$ and $d_B^2 \times N_B M_B$ dimensional matrices. The local basis expansions of the (N, M) -POVM elements can be used to rewrite the correlation matrix to

$$C(\Pi^A, \Pi^B | \rho) = (S^A)^T C(G^A, G^B | \rho) S^B. \quad (6.58)$$

Similar to the sufficient entanglement condition Eq. (5.33), the scaling relation can also be applied for the steering inequality Eq. (6.57). The sufficient EPR steering condition from Alice to Bob with (N, M) -POVMs as local measurements can be simplified to the inequality of LOOs Eq. (6.49)

$$\|C(G^A, G^B | \rho)\|_{\text{tr}} = \frac{\|C(\Pi^A, \Pi^B | \rho)\|_{\text{tr}}}{\sqrt{\Gamma_A \Gamma_B}} \leq \sqrt{(d_A - \text{tr}\{\rho_A^2\})(1 - \text{tr}\{\rho_B^2\})}. \quad (6.59)$$

The main result of this subsection is that the correlation matrix-based sufficient condition for arbitrary local informationally complete (N, M) -POVMs is identical to that of arbitrary LOOs. The scaling relation can be derived without requiring the positive semidefiniteness of the POVM elements. Therefore, the steering inequality can be calculated without constructing (N, M) -POVMs. It is apparent that the inequality (6.59) is entirely independent of the parameters x, N and M of Alice's and Bob's (N, M) -POVMs. This is a direct consequence of the symmetry of the relations defining the (N, M) -POVMs Eqs. (3.15)-(3.17). This simple steering inequality shows that all local informationally complete (N, M) -POVMs are equally well-suited for the EPR steering detection with trace norms of correlation matrices. The inequality detects the EPR steerable quantum states from Alice to Bob, which are steerable for all (N, M) -POVMs and LOOs. The typicality of EPR steerable quantum states from Alice to Bob detected by correlation matrices of local informationally (N, M) -POVMs will be examined in Section 6.4.

6.3 EPR STEERING DETECTION THROUGH ENTANGLEMENT DETECTION

For the investigation of the typicality of the EPR steerable states, sufficient conditions without intricate optimization are needed. Additionally, the similarity in structure between the correlation matrix-based sufficient condition for EPR steering Eq. (6.59) and entanglement detection Eq. (5.33) motivates an investigation into detecting EPR steerability through entanglement detection. Consider the EPR steerability from Alice to Bob for the case where Alice has a qubit

and Bob's subsystem has an arbitrary finite dimensions d_B . For this particular case, it has been shown that the detection of entanglement can be used to identify an EPR steerable state from Alice to Bob. This sufficient condition has been derived by Das *et al.* [145]. The authors show that for a bipartite mixed quantum state

$$\tau_{A \rightarrow B} := \mu \rho + \frac{1-\mu}{2} \mathbb{1}_2 \otimes \text{tr}_A\{\rho\} = \mu \rho + \frac{1-\mu}{2} \mathbb{1}_2 \otimes \rho_B \quad (6.60)$$

for $\mu \in (0, 1/\sqrt{3}]$ it is sufficient to detect the entanglement of $\tau_{A \rightarrow B}$ to verify that ρ is EPR steerable from Alice to Bob. The advantage of this sufficient condition is that it allows to detected entanglement by well-studied sufficient conditions, such as the Peres-Horodecki condition, to detect the entanglement off $\tau_{A \rightarrow B}$ [57, 58]. The Peres-Horodecki condition is even a criterion in the cases of $d_B = 2, 3$. However, the Peres-Horodecki condition is not based on local measurements. In Chapter 5, general sufficient conditions for detecting entanglement based on local measurements have been derived. To detect whether $\tau_{A \rightarrow B}$ is entangled, one can use inequality (5.31) with LOOs or local informationally complete (N, M) -POVMs as measurements. The reduced quantum states of Alice and Bob $\tau_{A \rightarrow B}$ are given by

$$\tau_A = \text{tr}_B\{\tau_{A \rightarrow B}\} = \mu \rho_A + \frac{1-\mu}{2} \mathbb{1}_2, \quad (6.61)$$

$$\tau_B = \text{tr}_A\{\tau_{A \rightarrow B}\} = \rho_B \quad (6.62)$$

with ρ_A and ρ_B Alice's and Bob's reduced quantum states of the initial state ρ . For the elements of the correlation matrix with LOOs as local measurements hold

$$\begin{aligned} c_{ij}(\tau_{A \rightarrow B}) &= \text{tr}\{G_i \otimes G_j (\tau_{A \rightarrow B} - \tau_A \otimes \tau_B)\} \\ &= \text{tr}\{G_i \otimes G_j \tau_{A \rightarrow B}\} - \text{tr}\{G_i \tau_A\} \text{tr}\{G_j \tau_B\} \\ &= \mu \text{tr}\{G_i \otimes G_j \rho\} + \frac{1-\mu}{2} \text{tr}\{G_i \mathbb{1}_2\} \text{tr}\{G_j \rho_B\} - \left(\mu \text{tr}\{G_i \rho_A\} + \frac{1-\mu}{2} \text{tr}\{G_i \mathbb{1}_2\} \right) \text{tr}\{G_j \rho_B\} \\ &= \mu (\text{tr}\{G_i \otimes G_j \rho\} - \text{tr}\{G_i \rho_A\}) \text{tr}\{G_j \rho_B\} \\ &= \mu c_{ij}(\rho). \end{aligned} \quad (6.63)$$

Furthermore, the upper bound defined by Eqs. (5.17) and (5.18) can also be connected to the reduced density matrices of ρ

$$\begin{aligned} V_A(\tau_A) &= 1 - \text{tr}\{\tau_A^2\} = 1 - \text{tr}\left\{ \mu^2 \rho_A^2 + \mu(1-\mu) \rho_A + \frac{(1-\mu)^2}{4} \mathbb{1}_2 \right\} \\ &= 1 - \mu(1-\mu) - \frac{(1-\mu)^2}{2} - \mu^2 \text{tr}\{\rho_A^2\} \\ &= \frac{1+\mu^2}{2} - \mu^2 \text{tr}\{\rho_A^2\}. \end{aligned} \quad (6.64)$$

Inserting the results into inequality (5.31)

$$\begin{aligned} \|C(G^A, G^B | \rho)\|_{\text{tr}} &= \frac{1}{\mu} \|C(G^A, G^B | \tau_{A \rightarrow B})\|_{\text{tr}} \\ &\leq \sqrt{1 - \text{tr}\{\tau_A^2\}} \sqrt{1 - \text{tr}\{\tau_B^2\}} \\ &= \sqrt{\frac{1+\mu^2}{2\mu^2} - \text{tr}\{\rho_A^2\}} \sqrt{1 - \text{tr}\{\rho_B^2\}} \end{aligned} \quad (6.65)$$

leads to a new EPR steering inequality for $\mu \in (0, 1/\sqrt{3}]$. For the maximum value of $\mu = 1/\sqrt{3}$ the steering inequality (6.59) is recovered

$$\|C(G^A, G^B|\rho)\|_{\text{tr}} \leq \sqrt{(2 - \text{tr}\{\rho_A^2\})(1 - \text{tr}\{\rho_B^2\})} \quad (6.66)$$

with $d_A = 2$. The scaling relation implies that this inequality for detecting EPR steering from Alice to Bob through entanglement detection of the state $\tau_{A \rightarrow B}$ also applies to local informationally complete (N, M) -POVMs as measurements. The verification of the EPR steerability of ρ by entanglement detection of the state $\tau_{A \rightarrow B}$ with correlation matrices based on local (N, M) -POVMs or LOOs leads to the identical inequality as the steering inequality based on correlation matrices with identical measurements Eq. (6.59). The advantage of the general inequality (6.59) is that this relation is not restricted to a qubit on Alice subsystems and holds for arbitrary dimensions d_A . The derivation of Das et al. [145] relies on qubit properties. It remains an open question whether this condition can be generalized to arbitrary dimensions of Alice's subsystem d_A . The verification that a quantum state can be used for EPR steering by detecting the entanglement of $\tau_{A \rightarrow B}$ has been shown experimentally [151].

6.4 SIMULATION RESULTS

The numerical investigation of this section is motivated by the need to identify which quantum states can be used for EPR steering from Alice to Bob. The typicality of the detected EPR steerable states for bipartite qudit systems is largely unexplored. Additionally, sufficient conditions for EPR steerability from Alice to Bob have only been applied to restricted classes of quantum states, which form a zero-measure within the convex set of all quantum sets [152]. In this section the Euclidean volume ratios from the EPR steerable states from Alice to Bob are determined for low dimensional qudit systems. For this purpose the hit-and-run Monte Carlo algorithm from Section 2.4 is used to generate N equally distributed density matrices over the complete state space. For each of these generated quantum states it is tested whether the EPR steering detection inequality is violated. If a quantum state violates such an inequality, the state is counted, otherwise, it is discarded. This formalism allows the numerical computation of lower bounds for the Euclidean volume ratios of the steerable quantum states from Alice to Bob $R_{A \rightarrow B}$. This procedure will be used to determine the efficiency of different EPR steering inequalities for various qudit dimensions of Alice's and Bob's quantum systems.

The typicality of EPR steering detection through correlation matrices with local measurements is investigated in this section. The numerical investigations are restricted to local dimensions $2 \leq d_A, d_B \leq 4$ of Alice's and Bob's quantum systems. To compute the Euclidean volume ratios $R_{A \rightarrow B}$ the hit-and-run algorithm has generated $N = 10^8$ random quantum states. The Euclidean volume ratio $R_{A \rightarrow B}$ is determined by the correlation matrix-based inequality (6.59), which is identical for LOOs or local informationally complete (N, M) -POVMs. The detected volume ratios can be further increased by optimizing the parameters $\{h_i\}$ in inequality (6.36) for LOOs or local informationally complete (N, M) -POVMs as measurements. The optimized volume ratios serve as an upper bound for $R_{A \rightarrow B}$.

The numerical results are summarized in Table 6.1 and the investigated dimensions of the local quantum systems are $2 \leq d_A, d_B \leq 4$. Cases not shown in the table are below the numerical accuracy. For non-qubit-qubit systems, the detected Euclidean volume ratios of the EPR steerable states from Alice to Bob, based on a violation of Eq. (6.36) with LOOs or local informationally complete (N, M) -POVMs, take values close to zero. The scaling relation of Section 3.3 implies that the number of quantum states violating this inequality cannot

be increased by changing the type of LOOs or (N, M) -POVMs. Furthermore, the determined volume ratios are an upper bound for the EPR steering inequalities (6.39), (6.42) and (6.43). Thus, these inequalities also underestimate the volume ratios beyond qubit-qubit systems. The underestimated volume ratios can be explained by the scaling relation, which implies that the detected steerable states from Alice to Bob are steerable for all LOOs and (N, M) -POVMs. For example, quantum states that are only EPR steerable from Alice to Bob by a single pair of local (N, M) -POVMs cannot violate this inequality.

In order to quantify the typicality of the steerable quantum states from Alice to Bob for qubit-qudit quantum systems, the sufficient EPR steering condition through entanglement detection, discussed in Section 6.3, is used. However, this condition can only be applied if Alice's local quantum system is a qubit. When combined with the Peres-Horodecki condition described in Section 2.2.1, it becomes a potent sufficient condition for EPR steerability from Alice to Bob. The Peres-Horodecki condition affirms that all quantum states whose partial transpose has a negative eigenvalue are entangled (NPT states). Recall that a quantum state ρ is EPR-steerable from Alice to Bob if the state Eq. (6.60)

$$\tau_{A \rightarrow B} = \frac{1}{\sqrt{3}}\rho + \frac{\sqrt{3}-1}{2\sqrt{3}}\mathbb{1} \otimes \rho_B \quad (6.67)$$

is entangled. Table 6.2 shows the volume ratios of the detected EPR steerable quantum states from Alice to Bob as Bob's quantum system dimension increases $2 \leq d_B \leq 7$. Comparing these results with those of the correlation matrix-based inequality of Table 6.1, it is evident that the volume ratios of the detected steerable quantum states are of the same order for the two-qubit case. However, for increasing dimensions, the volume ratio of the EPR steerable quantum states increases while the correlation matrix-based sufficient condition declines to zero. This can be explained by the fact that for higher dimensional quantum systems, the volume ratio of the NPT states converges to unity [87]. However, the Peres-Horodecki condition for entanglement detection transcends local quantum measurements. Instead, the correlation matrix-based sufficient condition for entanglement is applied to the state $\tau_{A \rightarrow B}$, leading to the correlation matrix-based steering inequality (6.66) for LOOs and (N, M) -POVMs. The local entanglement detection using these measurements is not efficient enough to detect entanglement of the quantum state $\tau_{A \rightarrow B}$. The correlation matrix-based sufficient condition is not suitable for identifying EPR steerable quantum states from Alice to Bob beyond the qubit-qubit case. The similarity between the EPR steering and entanglement sufficient conditions motivates further research into EPR steering detection through entanglement detection for arbitrary quantum systems. Such a condition would have the advantage of utilizing the powerful Peres-Horodecki condition.

Case	$d_B = 2$	$d_B = 3$
$d_A = 2$	5.011×10^{-2} $\pm 1.5 \times 10^{-4}$	1.92×10^{-5} $\pm 4.1 \times 10^{-6}$
$d_A = 3$	5.72×10^{-5} $\pm 6.4 \times 10^{-6}$	0

Table 6.1: Numerical estimates of lower bounds of the Euclidean volume ratios $R_{S:A \rightarrow B}$ between EPR steerable quantum states from Alice to Bob and all bipartite quantum states for different dimensions d_A and d_B of Alice's and Bob's quantum systems: These estimates are based on a violation of inequality (6.36) with Alice's local measurement being optimized by rescaling. The numerical errors have been estimated with the procedure described in Appendix C.

d_B	2	3	4	5	6	7
	0.05167 $\pm 1.5 \times 10^{-4}$	0.10936 $\pm 3.4 \times 10^{-4}$	0.17278 $\pm 5.6 \times 10^{-4}$	0.24009 $\pm 8.3 \times 10^{-4}$	0.3119 $\pm 1.3 \times 10^{-3}$	0.3842 $\pm 1.5 \times 10^{-3}$

Table 6.2: Numerical lower bounds on the Euclidean volume ratios $R_{A \rightarrow B}$ between EPR steerable quantum states from Alice to Bob for all bipartite quantum states for $d_A = 2$ and different dimensions $2 \leq d_B \leq 7$ of Bob's quantum system: These estimates are based on the approach of Das *et al.* [145]. The Peres-Horodecki condition has been used as a sufficient condition for bipartite entanglement of $\tau_{A \rightarrow B}$ for $d_B \geq 3$. The numerical errors have been estimated with the procedure described in Appendix C.

CONCLUSION

Entanglement is an important resource for quantum information processing, computation, communication and quantum key distribution. Especially in cases of quantum key distribution and information processing, it is crucial to reliably detect entanglement through local quantum measurements by two possible spatially separated observers. It has been shown that local informationally complete (N, M) -POVMs are appropriate measurements for detecting entanglement and EPR steering from Alice to Bob.

In the course of our research, sufficient and necessary conditions for the existence of optimal informationally complete POVMs have been derived. A sufficient condition has been derived for (N, M) -POVMs that guarantees the positive semidefiniteness of the POVM elements for small values of the continuous parameter x . This condition yields an upper bound for x and ensures that (N, M) -POVMs with a parameter x below the upper bound can always be constructed. The connection between IHOBs and the existence of optimal informationally complete (N, M) -POVMs has been established. It has been stated that the existence of such a basis is necessary for the existence of optimal (N, M) -POVMs. This necessary condition generalizes a recently derived property for GSICs [62]. In particular, the necessary condition is also sufficient for the case of $d \leq M$. This is achieved by ensuring that the basis elements constructing a single POVM are commuting and that their eigenvalues are ordered in a specific way in a common eigenbasis. Furthermore, for the cases $d \leq M$, the optimal informationally complete (N, M) -POVMs are rank d/M projections. Therefore, they can only exist if d/M is a natural number. For example, it has been shown that the Clifford basis can be used to construct optimal $(N, 2)$ -POVMs in dimensions that are powers of two. The sufficient and necessary conditions for optimal (N, M) -POVMs have been discussed, but only $(N, 2)$ -POVMs, $(d + 1, d)$ -POVMs (MUB) and $(1, d^2)$ -POVMs (SIC-POVMs) have been constructed in some dimensions. The construction of optimal (N, M) -POVMs remains an open question and further research is necessary in this direction.

Another focus of this work is the characterization of the measured correlations between local informationally complete (N, M) -POVMs. For this purpose, the linear map between (N, M) -POVM and a Hermitian orthonormal operator basis has been examined. The properties of this map give rise to the scaling relation, which allows for the calculation of the trace norm of correlation matrices without the need to construct (N, M) -POVMs. The scaling relation is solely derived from the defining relations of (N, M) -POVMs. However, the positive semidefiniteness of POVM elements is not required for the derivation. This necessarily valid relation connects equivalent measurement settings for the trace norm of correlation matrices and joint probability distributions. The correlation matrices of such local measurements can be used to detect bipartite entanglement or EPR steerability from Alice to Bob.

The focus has been on bipartite entanglement detection through correlation matrices and joint probability distributions of local informationally complete (N, M) -POVMs. The

scaling relation states that the correlation matrix-based entanglement detection is entirely independent of the chosen local informationally complete (N, M) -POVMs and identical to that of LOOs as measurements. The scaling relation implies that a single class of local (N, M) -POVMs is sufficient to compute the trace norm of joint probability distributions for a given dimension. For example GSICs can be used as local measurements, which can be constructed in local Hilbert space dimensions up to $d = 151$. These sufficient conditions have been quantitatively explored on random density matrices over the complete state space generated by the hit-and-run Monte Carlo algorithm. The numerical results indicate that the sufficient conditions become less efficient as the Hilbert space dimensions increase, compared to the Peres-Horodecki condition. Additionally, our numerical results demonstrate that local optimal informationally complete (N, M) -POVMs are not required for optimal entanglement detection. Instead, the always constructible (N, M) -POVMs can be utilized for this purpose. Well-chosen (N, M) -POVMs can detect more entanglement than optimal (N, M) -POVMs, such as SIC-POVMs, in unequal dimensions of the local Hilbert spaces. For practical applications, it is desirable to improve the detection efficiency of arbitrary quantum states. One possible method to achieve this may be by including local operations and classical communication.

The trace norm of correlation matrices can be used to verify EPR steerable quantum states from Alice to Bob, similar to entanglement detection. The correlation matrix-based sufficient conditions for EPR steerability from Alice to Bob are also simplified by the scaling relation. This relation states that all (N, M) -POVMs are equally efficient and identical to LOOs. A hit-and-run Monte Carlo algorithm has been used to quantify the Euclidean volume ratio of the steerability quantum states. Outside the qubit-qubit case, the detected steerable quantum states from Alice to Bob are significantly underestimated. Furthermore, the EPR steering detection from Alice to Bob through entanglement detection has been examined. This sufficient condition is valid when Alice's subsystem is a qubit. This condition, with correlation matrix-based entanglement detection, is identical to correlation matrix-based sufficient EPR steering condition. Combining this condition with the Peres-Horodecki condition significantly enhances the detection of EPR steerable quantum states from Alice to Bob. In this case the volumes of the steerable quantum states increase as the dimensions of Bob's subsystem increase. However, the Peres-Horodecki condition exceeds local measurements. Therefore, further research is needed to formulate efficient and straightforward sufficient conditions for the detection of EPR steerability from Alice to Bob. A possible next step is the generalization of the verification of EPR steerability from Alice to Bob through entanglement detection for arbitrary dimensions of Alice's subsystem.

Part V

APPENDIX

A

IMPORTANT (N, M) -POVMS

This appendix presents examples of optimal informationally complete (N, M) -POVMS. The optimal (N, M) -POVMS have been used to calculate the IHOBs of Eq. 4.40 (see Appendix B.1). The discussed dimensions are $d = 2, 3, 4$.

A.1 MUTUALLY UNBIASED BASES

The first class of (N, M) -POVMS discussed as example are the MUBs with $N = d + 1$ and $M = d$ in dimension d . The basis elements are defined by \mathbb{B}_d^α and the associated POVM elements are

$$\Pi_{\alpha,a} = |\alpha, a\rangle \langle \alpha, a| \quad (\text{A.1})$$

for all $\alpha \in \{1, \dots, d + 1\}$ and $|\alpha, a\rangle \in \mathbb{B}_d^\alpha$. The first index α denotes a single POVM, while the parameter $a = \{1, \dots, d\}$ denotes the measurement results of the POVM. Additionally, the vectors of each set \mathbb{B}_d^α form an orthonormal basis. Also, the orthonormal basis $\{|0\rangle, \dots, |d - 1\rangle\}$ is used to represent the POVM elements. A qubit ($d = 2$) MUB is given by [153]

$$\begin{aligned} \mathbb{B}_2^1 &= \{|0\rangle, |1\rangle\}, \\ \mathbb{B}_2^2 &= \left\{ \frac{1}{\sqrt{2}}(|0\rangle + |1\rangle), \frac{1}{\sqrt{2}}(|0\rangle - |1\rangle) \right\}, \\ \mathbb{B}_2^3 &= \left\{ \frac{1}{\sqrt{2}}(|0\rangle + i|1\rangle), \frac{1}{\sqrt{2}}(|0\rangle - i|1\rangle) \right\}. \end{aligned} \quad (\text{A.2})$$

The parameter $\omega = \exp(2\pi i/3)$ is used for the qutrit ($d = 3$) MUB [153]

$$\begin{aligned} \mathbb{B}_3^1 &= \{|0\rangle, |1\rangle, |2\rangle\}, \\ \mathbb{B}_3^2 &= \left\{ \frac{1}{\sqrt{3}}(|0\rangle + |1\rangle + |2\rangle), \frac{1}{\sqrt{3}}(|0\rangle + \omega|1\rangle + \omega^2|2\rangle), \frac{1}{\sqrt{3}}(|0\rangle + \omega^2|1\rangle + \omega|2\rangle) \right\}, \\ \mathbb{B}_3^3 &= \left\{ \frac{1}{\sqrt{3}}(|0\rangle + \omega|1\rangle + \omega^2|2\rangle), \frac{1}{\sqrt{3}}(|0\rangle + \omega^2|1\rangle + |2\rangle), \frac{1}{\sqrt{3}}(|0\rangle + |1\rangle + \omega^2|2\rangle) \right\}, \\ \mathbb{B}_3^4 &= \left\{ \frac{1}{\sqrt{3}}(|0\rangle + \omega^2|1\rangle + \omega|2\rangle), \frac{1}{\sqrt{3}}(|0\rangle + |1\rangle + \omega|2\rangle), \frac{1}{\sqrt{3}}(|0\rangle + \omega|1\rangle + |2\rangle) \right\}. \end{aligned} \quad (\text{A.3})$$

A MUB for a Hilbert space of dimension ($d = 4$) is given [153]

$$\begin{aligned}
\mathbb{B}_4^1 &= \{|0\rangle, |1\rangle, |2\rangle\}, \\
\mathbb{B}_4^2 &= \left\{ \frac{1}{2}(|0\rangle + |1\rangle + |2\rangle + |3\rangle), \frac{1}{2}(|0\rangle - |1\rangle - |2\rangle + |3\rangle), \right. \\
&\quad \left. \frac{1}{2}(|0\rangle + |1\rangle - |2\rangle - |3\rangle), \frac{1}{2}(|0\rangle - |1\rangle + |2\rangle - |3\rangle) \right\}, \\
\mathbb{B}_4^3 &= \left\{ \frac{1}{2}(|0\rangle + i|1\rangle + i|2\rangle - |3\rangle), \frac{1}{2}(|0\rangle - i|1\rangle - i|2\rangle - |3\rangle), \right. \\
&\quad \left. \frac{1}{2}(|0\rangle + i|1\rangle - i|2\rangle + |3\rangle), \frac{1}{2}(|0\rangle - i|1\rangle + i|2\rangle + |3\rangle) \right\}, \\
\mathbb{B}_4^4 &= \left\{ \frac{1}{2}(|0\rangle + |1\rangle - i|2\rangle + i|3\rangle), \frac{1}{2}(|0\rangle - |1\rangle + i|2\rangle + i|3\rangle), \right. \\
&\quad \left. \frac{1}{2}(|0\rangle + |1\rangle + i|2\rangle - i|3\rangle), \frac{1}{2}(|0\rangle - |1\rangle - i|2\rangle - i|3\rangle) \right\}, \\
\mathbb{B}_4^5 &= \left\{ \frac{1}{2}(|0\rangle - i|1\rangle + |2\rangle + i|3\rangle), \frac{1}{2}(|0\rangle + i|1\rangle - |2\rangle + i|3\rangle), \right. \\
&\quad \left. \frac{1}{2}(|0\rangle + i|1\rangle + |2\rangle - i|3\rangle), \frac{1}{2}(|0\rangle - i|1\rangle - |2\rangle - i|3\rangle) \right\}. \tag{A.4}
\end{aligned}$$

It is noted that the first two basis sets \mathbb{B}_4^1 and \mathbb{B}_4^2 only contain vectors with real-valued coefficients.

A.2 SIC-POVMS

The second important class of optimal informationally complete (N, M) -POVMS are the SIC-POVMS with $N = 1$ and $M = d^2$. The vectors $|1, a\rangle$ represent the SIC-POVMS by

$$\Pi_{1,a} = \frac{1}{d} |1, a\rangle \langle 1, a| \tag{A.5}$$

where a denotes the measurement result of the POVM. A qubit SIC POVM is given by [60]

$$\begin{aligned}
|1, 1\rangle &= |0\rangle, & |1, 2\rangle &= \frac{1}{\sqrt{3}}|0\rangle + \sqrt{\frac{2}{3}}|1\rangle, \\
|1, 3\rangle &= \frac{1}{\sqrt{3}}|0\rangle + \omega\sqrt{\frac{2}{3}}|1\rangle, & |1, 4\rangle &= \frac{1}{\sqrt{3}}|0\rangle + \omega^2\sqrt{\frac{2}{3}}|1\rangle
\end{aligned} \tag{A.6}$$

with $\omega = \exp(i2\pi/3)$. The second example is a qudit ($d = 3$) SIC-POVM [60]

$$\begin{aligned}
|1, 1\rangle &= \frac{1}{\sqrt{2}}(|1\rangle - |2\rangle), & |1, 2\rangle &= \frac{1}{\sqrt{2}}(\omega|1\rangle - \omega^2|2\rangle), & |1, 3\rangle &= \frac{1}{\sqrt{2}}(\omega^2|1\rangle - \omega|2\rangle), \\
|1, 4\rangle &= \frac{1}{\sqrt{2}}(|0\rangle - |1\rangle), & |1, 5\rangle &= \frac{1}{\sqrt{2}}(\omega|0\rangle - \omega^2|1\rangle), & |1, 6\rangle &= \frac{1}{\sqrt{2}}(\omega^2|0\rangle - \omega|1\rangle), \\
|1, 7\rangle &= \frac{1}{\sqrt{2}}(|2\rangle - |0\rangle), & |1, 8\rangle &= \frac{1}{\sqrt{2}}(\omega|2\rangle - \omega^2|0\rangle), & |1, 9\rangle &= \frac{1}{\sqrt{2}}(\omega^2|2\rangle - \omega|0\rangle).
\end{aligned} \tag{A.7}$$

A SIC-POVM for ($d = 4$) is given by [60]

$$\begin{aligned}
|1, 1\rangle &= \mathcal{N}(x|0\rangle + |1\rangle + |2\rangle + |3\rangle), & |1, 2\rangle &= \mathcal{N}(x|0\rangle + |1\rangle - |2\rangle - |3\rangle), \\
|1, 3\rangle &= \mathcal{N}(x|0\rangle - |1\rangle + |2\rangle - |3\rangle), & |1, 4\rangle &= \mathcal{N}(x|0\rangle - |1\rangle - |2\rangle + |3\rangle), \\
|1, 5\rangle &= \mathcal{N}(i|0\rangle + x|1\rangle + |2\rangle - i|3\rangle), & |1, 6\rangle &= \mathcal{N}(i|0\rangle + x|1\rangle - |2\rangle + i|3\rangle), \\
|1, 7\rangle &= \mathcal{N}(-i|0\rangle + x|1\rangle + |2\rangle + i|3\rangle), & |1, 8\rangle &= \mathcal{N}(-i|0\rangle + x|1\rangle - |2\rangle - i|3\rangle), \\
|1, 9\rangle &= \mathcal{N}(i|0\rangle + i|1\rangle + x|2\rangle - |3\rangle), & |1, 10\rangle &= \mathcal{N}(i|0\rangle - i|1\rangle + x|2\rangle + |3\rangle), \\
|1, 11\rangle &= \mathcal{N}(-i|0\rangle + i|1\rangle + x|2\rangle + |3\rangle), & |1, 12\rangle &= \mathcal{N}(-i|0\rangle - i|1\rangle + x|2\rangle - |3\rangle), \\
|1, 13\rangle &= \mathcal{N}(i|0\rangle + |1\rangle - i|2\rangle + x|3\rangle), & |1, 14\rangle &= \mathcal{N}(i|0\rangle - |1\rangle + i|2\rangle + x|3\rangle), \\
|1, 15\rangle &= \mathcal{N}(-i|0\rangle + |1\rangle + i|2\rangle + x|3\rangle), & |1, 16\rangle &= \mathcal{N}(-i|0\rangle - |1\rangle - i|2\rangle + x|3\rangle),
\end{aligned} \tag{A.8}$$

where the normalization constant $\mathcal{N} = 1/\sqrt{5 + \sqrt{5}}$ and the parameter $x = \sqrt{2 + \sqrt{5}}$ are used.

B

HERMITIAN OPERATORS BASES

In this appendix, properties of Hermitian operator bases are shown. These properties are important for the derivation of the sufficient condition for entanglement and EPR steering detection and their invariances. Furthermore, the generalized Gell-Mann matrices are introduced as a Hermitian orthonormal operator basis that can be constructed in arbitrary dimensions d . Section 2.1.1 discusses the representation of an arbitrary Hermitian operator A in a Hermitian operator basis $\mathbf{G} = (G_0, \dots, G_{d^2-1})^\top$

$$A = \sum_{i=0}^{d^2-1} G_i \operatorname{tr}\{G_i A\} = \sum_{i=0}^{d^2-1} r_i G_i = \mathbf{r} \cdot \mathbf{G} \quad (\text{B.1})$$

with the real vector $r \in \mathbb{R}^{d^2}$. To examine the mathematical structure of a basis change, a second Hermitian operator basis \tilde{G} is considered. The basis expansion of \tilde{G}_j is given by

$$\tilde{G}_j = \sum_{i=0}^{d^2-1} G_i \operatorname{tr}\{G_i \tilde{G}_j\} = \sum_{i=0}^{d^2-1} G_i O_{ij}. \quad (\text{B.2})$$

with $O_{ij} = \operatorname{tr}\{G_i \tilde{G}_j\}$. From the orthogonality of the basis elements follows

$$\begin{aligned} \delta_{ij} &= \operatorname{tr}\{\tilde{G}_i \tilde{G}_j\} = \operatorname{tr}\left\{ \sum_{k=0}^{d^2-1} G_k \operatorname{tr}\{G_k \tilde{G}_i\} \sum_{l=0}^{d^2-1} G_l \operatorname{tr}\{G_l \tilde{G}_j\} \right\} \\ &= \sum_{k=0}^{d^2-1} \sum_{l=0}^{d^2-1} \operatorname{tr}\{G_k \tilde{G}_i\} \operatorname{tr}\{G_l \tilde{G}_j\} \operatorname{tr}\{G_k G_l\} \\ &= \sum_{k=0}^{d^2-1} \sum_{l=0}^{d^2-1} O_{ki} O_{lj} \underbrace{\operatorname{tr}\{G_k G_l\}}_{\delta_{kl}} \\ &= \sum_{k=0}^{d^2-1} O_{ki} O_{li}. \end{aligned} \quad (\text{B.3})$$

This implies that the matrix O relating two Hermitian operator bases by

$$\tilde{\mathbf{G}} = \mathbf{O} \mathbf{G} \quad (\text{B.4})$$

is an orthogonal matrix $O^\top O = \mathbb{1}_d = O O^\top$. A Hermitian operator basis \tilde{G} can always be chosen, with the first basis element proportional to the identity matrix $\tilde{G}_0 = \mathbb{1}_d / \sqrt{d}$. From the orthogonality of the basis elements follows that the remaining $d^2 - 1$ basis elements are traceless

$$\operatorname{tr}\{\tilde{G}_i\} = \sqrt{d} \operatorname{tr}\{\tilde{G}_0 \tilde{G}_i\} = 0 \quad (\text{B.5})$$

for $i = \{1, \dots, d^2 - 1\}$. This basis is useful for representing Hermitian operators with a fixed trace value, such as density matrices or (N, M) -POVMs. An arbitrary Hermitian operator basis can be used to define an invariant

$$\begin{aligned}
\sum_{i=0}^{d^2-1} G_i^2 &= \sum_{i=0}^{d^2-1} \sum_{j=0}^{d^2-1} \sum_{k=0}^{d^2-1} \bar{G}_j \operatorname{tr}\{\bar{G}_j G_i\} \bar{G}_k \operatorname{tr}\{\bar{G}_k G_i\} \\
&= \sum_{j=0}^{d^2-1} \sum_{k=0}^{d^2-1} \bar{G}_j \bar{G}_k \operatorname{tr}\left\{ \bar{G}_j \sum_{i=0}^{d^2-1} G_i \operatorname{tr}\{\bar{G}_k G_i\} \right\} \\
&= \sum_{j=0}^{d^2-1} \sum_{k=0}^{d^2-1} \bar{G}_j \bar{G}_k \operatorname{tr}\{\bar{G}_j \bar{G}_k\} \\
&= \sum_{j=0}^{d^2-1} \bar{G}_j^2.
\end{aligned} \tag{B.6}$$

This invariant is important for the sufficient conditions for entanglement detection in Chapter 5 and EPR steering detection in Chapter 6. Thus, calculating the invariant for a single Hermitian operator basis is sufficient. In the case of a qubit, a basis is given by

$$\sigma = \left\{ \frac{\mathbb{1}_2}{\sqrt{2}}, \frac{\sigma_x}{\sqrt{2}}, \frac{\sigma_y}{\sqrt{2}}, \frac{\sigma_z}{\sqrt{2}} \right\} \tag{B.7}$$

and the Pauli matrices are given by

$$\sigma_x = \sigma_1 = \begin{pmatrix} 0 & 1 \\ 1 & 0 \end{pmatrix}, \quad \sigma_y = \sigma_2 = \begin{pmatrix} 0 & -i \\ i & 0 \end{pmatrix}, \quad \sigma_z = \sigma_3 = \begin{pmatrix} 1 & 0 \\ 0 & -1 \end{pmatrix}. \tag{B.8}$$

The invariant (B.6) in $d = 2$ has the value

$$\sum_{i=0}^3 G_i^2 = \frac{1}{2} \sum_{i=0}^3 \sigma_i^2 = 2\mathbb{1}_2. \tag{B.9}$$

It has been used that $\sigma_i^2 = \mathbb{1}_2$ holds for the Pauli matrices. Generalizations of the Pauli matrices for higher dimensions are the generalized Gell-Mann matrices, which can be constructed in any finite dimension. The Gell-Mann matrices for $d = 3$ are given by

$$\begin{aligned}
\tilde{G}_1^{\text{GM}} &= \begin{pmatrix} 0 & \frac{1}{\sqrt{2}} & 0 \\ \frac{1}{\sqrt{2}} & 0 & 0 \\ 0 & 0 & 0 \end{pmatrix}, & \tilde{G}_2^{\text{GM}} &= \begin{pmatrix} 0 & -\frac{i}{\sqrt{2}} & 0 \\ \frac{i}{\sqrt{2}} & 0 & 0 \\ 0 & 0 & 0 \end{pmatrix}, & \tilde{G}_3^{\text{GM}} &= \begin{pmatrix} \frac{1}{\sqrt{2}} & 0 & 0 \\ 0 & -\frac{1}{\sqrt{2}} & 0 \\ 0 & 0 & 0 \end{pmatrix}, \\
\tilde{G}_4^{\text{GM}} &= \begin{pmatrix} 0 & 0 & \frac{1}{\sqrt{2}} \\ 0 & 0 & 0 \\ \frac{1}{\sqrt{2}} & 0 & 0 \end{pmatrix}, & \tilde{G}_5^{\text{GM}} &= \begin{pmatrix} 0 & 0 & -\frac{i}{\sqrt{2}} \\ 0 & 0 & 0 \\ \frac{i}{\sqrt{2}} & 0 & 0 \end{pmatrix}, & \tilde{G}_6^{\text{GM}} &= \begin{pmatrix} 0 & 0 & 0 \\ 0 & 0 & \frac{1}{\sqrt{2}} \\ 0 & \frac{1}{\sqrt{2}} & 0 \end{pmatrix}, \\
\tilde{G}_7^{\text{GM}} &= \begin{pmatrix} 0 & 0 & 0 \\ 0 & 0 & -\frac{i}{\sqrt{2}} \\ 0 & \frac{i}{\sqrt{2}} & 0 \end{pmatrix}, & \tilde{G}_8^{\text{GM}} &= \begin{pmatrix} \frac{1}{\sqrt{6}} & 0 & 0 \\ 0 & \frac{1}{\sqrt{6}} & 0 \\ 0 & 0 & -\sqrt{\frac{2}{3}} \end{pmatrix}.
\end{aligned} \tag{B.10}$$

The canonical orthonormal basis $\{|i\rangle, i = 1, \dots, d\}$ of the Hilbert space \mathcal{H}_d is used to represent the generalized Gell-Mann matrices in dimensions $d > 3$ by [154]

$$\begin{aligned}\tilde{G}_i^{\text{GM}} &= \frac{1}{\sqrt{i(i+1)}} \left(\sum_{k=1}^i |k\rangle \langle k-i|i+1\rangle \langle i+1| \right), & \text{for } i = 1, \dots, d-1, \\ \tilde{G}_{i_1(m,n)}^{\text{GM}} &= \frac{1}{\sqrt{2}} (|m\rangle \langle n| + |n\rangle \langle m|), & \text{for } 1 \leq m < n \leq d, \\ \tilde{G}_{i_2(m,n)}^{\text{GM}} &= \frac{i}{\sqrt{2}} (|m\rangle \langle n| - |n\rangle \langle m|), & \text{for } 1 \leq m < n \leq d\end{aligned}\quad (\text{B.11})$$

and is enumerated by

$$\begin{aligned}i_1(m, n) &= (d-2)m + n - \frac{(m-1)(m-2)}{2} \\ i_2(m, n) &= \frac{d^2-d}{2} + (d-2)m + n - \frac{(m-1)(m-2)}{2}..\end{aligned}\quad (\text{B.12})$$

A complete basis of the Hermitian operators is given by $\tilde{G} = \{\tilde{G}_0, \tilde{G}_1^{\text{GM}}, \dots, \tilde{G}_{d^2-1}^{\text{GM}}\}$. The invariant Eq. (B.6) can be calculated by

$$\begin{aligned}\sum_{i=0}^{d^2-1} G_i^2 &= \sum_{i=0}^{d^2-1} \tilde{G}_i^2 \\ &= \frac{1}{d} + \sum_{i=1}^{d-1} (\tilde{G}_i^{\text{GM}})^2 + \sum_{m=1}^{d-1} \sum_{n=m+1}^d \left((\tilde{G}_{i_1(m,n)}^{\text{GM}})^2 + (\tilde{G}_{i_2(m,n)}^{\text{GM}})^2 \right) \\ &= \frac{1}{d} + c_1 + c_2.\end{aligned}\quad (\text{B.13})$$

The matrix coefficients c_1 and c_2 are calculated independently. The first coefficient

$$c_1 = \sum_{i=1}^{d-1} \frac{1}{i(i+1)} \left(\sum_{k=1}^i |k\rangle \langle k+i^2|i+1\rangle \langle i+1| \right) \quad (\text{B.14})$$

is a diagonal matrix and its entries are given by

$$\begin{aligned}\langle d|c_1|d\rangle &= \frac{d-1}{d}, \\ \langle 1|c_1|1\rangle &= \sum_{i=1}^{d-1} \frac{1}{i(i+1)} = 1 - \frac{1}{d} = \frac{d-1}{d}, \\ \langle j|c_1|j\rangle &= \sum_{i=j}^{d-1} \frac{1}{i(i+1)} + \frac{j-1}{j} \\ &= \sum_{i=1}^{d-1} \frac{1}{i(i+1)} - \sum_{i=1}^{j-1} \frac{1}{i(i+1)} + \frac{j-1}{j} \\ &= 1 - \frac{1}{d} - 1 + \frac{1}{j} + \frac{j-1}{j} = \frac{d-1}{d}\end{aligned}\quad (\text{B.15})$$

for $j = \{2, \dots, d-1\}$. This implies that the first coefficient is proportional to identity matrix $c_1 = (d-1)/d \mathbb{1}_d$. The second coefficient, derived from the non-diagonal Gell-Mann matrices, is also a diagonal matrix

$$\begin{aligned} c_2 &= \sum_{m=1}^{d-1} \sum_{n=m+1}^d \left((\tilde{G}_{i_1(m,n)}^{\text{GM}})^2 + (\tilde{G}_{i_2(m,n)}^{\text{GM}})^2 \right) \\ &= \sum_{m=1}^{d-1} \sum_{n=m+1}^d (|n\rangle\langle n| + |m\rangle\langle m|). \end{aligned} \quad (\text{B.16})$$

The matrix elements are given by

$$\begin{aligned} \langle d | c_2 | d \rangle &= \sum_{m=1}^{d-1} 1 = d-1 \\ \langle 1 | c_2 | 1 \rangle &= \sum_{n=2}^d 1 = d-1 \\ \langle j | c_2 | j \rangle &= \sum_{n=j+1}^d 1 + \sum_{m=1}^{j-1} 1 = d-j + j-1 = d-1 \end{aligned} \quad (\text{B.17})$$

for $j = 2, \dots, d-1$. The second coefficient is again proportional to the identity matrix $c_2 = (d-1) \mathbb{1}_d$. The invariant (B.6) is given by

$$\begin{aligned} \sum_{i=0}^{d^2-1} G_i^2 &= \frac{\mathbb{1}_d}{d} + c_1 + c_2 \\ &= \left(\frac{1}{d} + \frac{d-1}{d} + (d-1) \right) \mathbb{1}_d \\ &= d \mathbb{1}_d. \end{aligned} \quad (\text{B.18})$$

B.1 ISOSPECTRAL OPERATORS BASIS

Section 4.2.1 demonstrates that an IHOB can be constructed from an optimal informationally complete (N, M)-POVM with $M \geq d$. Such bases have been used as examples to visualize the positive semidefiniteness of Hermitian operators with a fixed trace in Chapter 4. For $d = 3$, the bases constructed from a SIC-POVM and MUB have been used to visualize positive semidefinite matrices in Section 4.1.2. The SIC-POVM in Eq. (A.7) is used to construct the IHOB $\tilde{G}^{\text{SIC}} = \{\tilde{G}_1^{\text{SIC}}, \dots, \tilde{G}_{d^2-1}^{\text{SIC}}\}$. The spectrum of each basis element is given by

$$\text{Sp}(\tilde{G}_i^{\text{SIC}}) = \left\{ \frac{1}{12}(-\sqrt{3} - 3\sqrt{7}), \frac{1}{12}(-\sqrt{3} + 3\sqrt{7}), \frac{1}{2\sqrt{3}} \right\} \quad (\text{B.19})$$

for $i = \{1, \dots, 8\}$. The spectrum of the basis elements is independent of the chosen SIC-POVM. The orthonormal basis constructed of the SIC-POVM is

$$\begin{aligned}
\tilde{G}_1^{\text{SIC}} &= \begin{pmatrix} -\frac{1}{4\sqrt{3}} & -\frac{\sqrt{3}}{4} - \frac{i}{2} & 0 \\ -\frac{\sqrt{3}}{4} + \frac{i}{2} & -\frac{1}{4\sqrt{3}} & 0 \\ 0 & 0 & \frac{1}{2\sqrt{3}} \end{pmatrix}, & \tilde{G}_2^{\text{SIC}} &= \begin{pmatrix} -\frac{1}{4\sqrt{3}} & -\frac{\sqrt{3}}{4} + \frac{i}{2} & 0 \\ -\frac{\sqrt{3}}{4} - \frac{i}{2} & -\frac{1}{4\sqrt{3}} & 0 \\ 0 & 0 & \frac{1}{2\sqrt{3}} \end{pmatrix}, \\
\tilde{G}_3^{\text{SIC}} &= \begin{pmatrix} \frac{\sqrt{3}}{4} & -\frac{1}{4\sqrt{3}} & 0 \\ -\frac{1}{4\sqrt{3}} & -\frac{1}{4\sqrt{3}} & \frac{1}{\sqrt{3}} \\ 0 & \frac{1}{\sqrt{3}} & -\frac{1}{2\sqrt{3}} \end{pmatrix}, & \tilde{G}_4^{\text{SIC}} &= \begin{pmatrix} \frac{\sqrt{3}}{4} & -\frac{1}{4\sqrt{3}} & 0 \\ -\frac{1}{4\sqrt{3}} & -\frac{1}{4\sqrt{3}} & -\frac{1}{2\sqrt{3}} - \frac{i}{2} \\ 0 & -\frac{1}{2\sqrt{3}} + \frac{i}{2} & -\frac{1}{2\sqrt{3}} \end{pmatrix}, \\
\tilde{G}_5^{\text{SIC}} &= \begin{pmatrix} \frac{\sqrt{3}}{4} & -\frac{1}{4\sqrt{3}} & 0 \\ -\frac{1}{4\sqrt{3}} & -\frac{1}{4\sqrt{3}} & -\frac{1}{2\sqrt{3}} + \frac{i}{2} \\ 0 & -\frac{1}{2\sqrt{3}} - \frac{i}{2} & -\frac{1}{2\sqrt{3}} \end{pmatrix}, & \tilde{G}_6^{\text{SIC}} &= \begin{pmatrix} -\frac{1}{4\sqrt{3}} & -\frac{1}{4\sqrt{3}} & \frac{1}{\sqrt{3}} \\ -\frac{1}{4\sqrt{3}} & \frac{\sqrt{3}}{4} & 0 \\ \frac{1}{\sqrt{3}} & 0 & -\frac{1}{2\sqrt{3}} \end{pmatrix}, \\
\tilde{G}_7^{\text{SIC}} &= \begin{pmatrix} -\frac{1}{4\sqrt{3}} & -\frac{1}{4\sqrt{3}} & -\frac{1}{2\sqrt{3}} - \frac{i}{2} \\ -\frac{1}{4\sqrt{3}} & \frac{\sqrt{3}}{4} & 0 \\ -\frac{1}{2\sqrt{3}} + \frac{i}{2} & 0 & -\frac{1}{2\sqrt{3}} \end{pmatrix}, & \tilde{G}_8^{\text{SIC}} &= \begin{pmatrix} -\frac{1}{4\sqrt{3}} & -\frac{1}{4\sqrt{3}} & -\frac{1}{2\sqrt{3}} + \frac{i}{2} \\ -\frac{1}{4\sqrt{3}} & \frac{\sqrt{3}}{4} & 0 \\ -\frac{1}{2\sqrt{3}} - \frac{i}{2} & 0 & -\frac{1}{2\sqrt{3}} \end{pmatrix}. \quad (\text{B.20})
\end{aligned}$$

The second basis \tilde{G}^{MUB} , used for the visualization of the positive semidefiniteness of Hermitian operators, is constructed from the MUB in Eq. (A.3). The spectrum of the basis elements is given by

$$\text{Sp}(\tilde{G}_i^{\text{MUB}}) = \left\{ \frac{3-\sqrt{3}}{6}, \frac{-3-\sqrt{3}}{6}, \frac{1}{\sqrt{3}} \right\} \quad (\text{B.21})$$

for $i \in \{1, \dots, 8\}$ and the basis elements are given by

$$\begin{aligned}
\tilde{G}_1^{\text{MUB}} &= \begin{pmatrix} \frac{1}{6}(3-\sqrt{3}) & 0 & 0 \\ 0 & \frac{1}{6}(-\sqrt{3}-3) & 0 \\ 0 & 0 & \frac{1}{\sqrt{3}} \end{pmatrix}, \\
\tilde{G}_2^{\text{MUB}} &= \begin{pmatrix} \frac{1}{6}(-\sqrt{3}-3) & 0 & 0 \\ 0 & \frac{1}{6}(3-\sqrt{3}) & 0 \\ 0 & 0 & \frac{1}{\sqrt{3}} \end{pmatrix}, \\
\tilde{G}_3^{\text{MUB}} &= \begin{pmatrix} 0 & \frac{(\frac{1}{6}-\frac{i}{6})(\sqrt{3}+3)}{\sqrt{3}+1} & \frac{(\frac{1}{6}+\frac{i}{6})(\sqrt{3}+3)}{\sqrt{3}+1} \\ \frac{(\frac{1}{6}+\frac{i}{6})(\sqrt{3}+3)}{\sqrt{3}+1} & 0 & \frac{(\frac{1}{6}-\frac{i}{6})(\sqrt{3}+3)}{\sqrt{3}+1} \\ \frac{(\frac{1}{6}-\frac{i}{6})(\sqrt{3}+3)}{\sqrt{3}+1} & \frac{(\frac{1}{6}+\frac{i}{6})(\sqrt{3}+3)}{\sqrt{3}+1} & 0 \end{pmatrix}, \\
\tilde{G}_4^{\text{MUB}} &= \begin{pmatrix} 0 & \frac{(\frac{1}{6}+\frac{i}{6})(\sqrt{3}+3)}{\sqrt{3}+1} & \frac{(\frac{1}{6}-\frac{i}{6})(\sqrt{3}+3)}{\sqrt{3}+1} \\ \frac{(\frac{1}{6}-\frac{i}{6})(\sqrt{3}+3)}{\sqrt{3}+1} & 0 & \frac{(\frac{1}{6}+\frac{i}{6})(\sqrt{3}+3)}{\sqrt{3}+1} \\ \frac{(\frac{1}{6}+\frac{i}{6})(\sqrt{3}+3)}{\sqrt{3}+1} & \frac{(\frac{1}{6}-\frac{i}{6})(\sqrt{3}+3)}{\sqrt{3}+1} & 0 \end{pmatrix}, \\
\tilde{G}_5^{\text{MUB}} &= \begin{pmatrix} 0 & \frac{(\frac{1}{6}-\frac{i}{6})(\sqrt{3}+3)}{\sqrt{3}+1} & \frac{1}{3} \left(\frac{(-1)^{2/3}}{\sqrt{3}+1} - 1 \right) \\ \frac{(\frac{1}{6}+\frac{i}{6})(\sqrt{3}+3)}{\sqrt{3}+1} & 0 & \frac{3i+(1+2i)\sqrt{3}}{6\sqrt{3}+6} \\ -\frac{3+(2+i)\sqrt{3}}{6\sqrt{3}+6} & -\frac{i(3+(2+i)\sqrt{3})}{6(\sqrt{3}+1)} & 0 \end{pmatrix},
\end{aligned}$$

$$\begin{aligned}
\tilde{G}_6^{\text{MUB}} &= \begin{pmatrix} 0 & \frac{(\frac{1}{6}+\frac{i}{6})(\sqrt{3}+3)}{\sqrt{3}+1} & \frac{3i+(1+2i)\sqrt{3}}{6\sqrt{3}+6} \\ \frac{(\frac{1}{6}-\frac{i}{6})(\sqrt{3}+3)}{\sqrt{3}+1} & 0 & \frac{1}{3}\left(\frac{(-1)^{2/3}}{\sqrt{3}+1}-1\right) \\ -\frac{i(3+(2+i)\sqrt{3})}{6(\sqrt{3}+1)} & -\frac{3+(2+i)\sqrt{3}}{6\sqrt{3}+6} & 0 \end{pmatrix}, \\
\tilde{G}_7^{\text{MUB}} &= \begin{pmatrix} 0 & \frac{(\frac{1}{6}+\frac{i}{6})(\sqrt{3}+3)}{\sqrt{3}+1} & -\frac{3+(2+i)\sqrt{3}}{6\sqrt{3}+6} \\ \frac{(\frac{1}{6}-\frac{i}{6})(\sqrt{3}+3)}{\sqrt{3}+1} & 0 & -\frac{i(3+(2+i)\sqrt{3})}{6(\sqrt{3}+1)} \\ \frac{1}{3}\left(\frac{(-1)^{2/3}}{\sqrt{3}+1}-1\right) & \frac{3i+(1+2i)\sqrt{3}}{6\sqrt{3}+6} & 0 \end{pmatrix}, \\
\tilde{G}_8^{\text{MUB}} &= \begin{pmatrix} 0 & \frac{(\frac{1}{6}-\frac{i}{6})(\sqrt{3}+3)}{\sqrt{3}+1} & -\frac{i(3+(2+i)\sqrt{3})}{6(\sqrt{3}+1)} \\ \frac{(\frac{1}{6}+\frac{i}{6})(\sqrt{3}+3)}{\sqrt{3}+1} & 0 & -\frac{3+(2+i)\sqrt{3}}{6\sqrt{3}+6} \\ \frac{3i+(1+2i)\sqrt{3}}{6\sqrt{3}+6} & \frac{1}{3}\left(\frac{(-1)^{2/3}}{\sqrt{3}+1}-1\right) & 0 \end{pmatrix}. \tag{B.22}
\end{aligned}$$

The pairs of basis elements (1, 2), (3, 4), (5, 6) and (7, 8) are defining the 2-dimensional real subspace of the traceless elements of a single POVMs. The basis element forming a single POVM commuting for MUBs, which means these basis elements are simultaneously diagonalizable.



STANDARD DEVIATIONS OF THE MONTE CARLO ALGORITHM

The estimation of the statistical errors of the Euclidean volume ratio of the entangled or EPR steerable quantum states is presented in this appendix. The procedure to obtain the standard deviation is performed identically to that of Sauer *et al.* [86]. The total number of $N = 10^8$ generated quantum states is divided into $N_I = 100$ blocks of size $N_B = 10^6$. Within a block, violations of the entanglement or steering inequality can be viewed as a Bernoulli trial with a success rate R , assuming all points are sampled equally distributed over the set of all quantum states. The quantum states that violate the inequality of a single block N_{B_i} can be approximated by a Gaussian distribution with a mean $R N_B$ and a standard deviation σ_B for large block sizes. The standard deviation for the mean \bar{R} is given by

$$\sigma_{\bar{R}}^2 = \frac{\sigma_B^2}{N_I}. \quad (\text{C.1})$$

This procedure is used to estimate the variance of the volume ratios and the standard deviation is given by $\sigma_{\bar{R}}$. The statistical uncertainty of the values in the Tables 5.2, 6.1 and 6.2 have been calculated using this method.

BIBLIOGRAPHY

- [1] M. A. Nielsen and I. L. Chuang, *Quantum computation and quantum information: 10th anniversary edition* (Cambridge University Press, 2010) (cit. on pp. [iii](#), [1](#), [7](#), [11](#), [13–14](#), [20](#)).
- [2] *Faksimile aus den Verhandlungen der Deutschen Physikalischen Gesellschaft 2 (1900) S. 237: Zur Theorie des Gesetzes der Energieverteilung im Normalspectrum; von M. Planck, Physikalische Blätter* **4**, 146–151 (1948) (cit. on p. [1](#)).
- [3] M. Planck, *Über das Gesetz der Energieverteilung im Normalspectrum*, *Annalen der Physik* **309**, 553–563 (1901) (cit. on p. [1](#)).
- [4] A. Einstein, *Über einen die Erzeugung und Verwandlung des Lichtes betreffenden heuristischen Gesichtspunkt*, *Annalen der Physik* **322**, 132–148 (1905) (cit. on p. [1](#)).
- [5] W. Pauli, *Über das Wasserstoffspektrum vom Standpunkt der neuen Quantenmechanik*, *Zeitschrift für Physik* **36**, 336–363 (1926) (cit. on p. [1](#)).
- [6] G. Gamow, *Zur Quantentheorie des Atomkernes*, *Zeitschrift für Physik* **51**, 204–212 (1928) (cit. on p. [1](#)).
- [7] M. v. Laue, *Notiz zur Quantentheorie des Atomkernes*, *Zeitschrift für Physik* **52**, 726–734 (1928) (cit. on p. [1](#)).
- [8] L. Mensing, *Die Rotations-Schwingungsbanden nach der Quantenmechanik*, *Zeitschrift für Physik* **36**, 814–823 (1926) (cit. on p. [1](#)).
- [9] E. Schrödinger, *An undulatory theory of the mechanics of atoms and molecules*, *Phys. Rev.* **28**, 1049 (1926) (cit. on p. [1](#)).
- [10] L. de Broglie, *Research on the theory of quanta*, in *Annales de physique*, Vol. 10, 3 (1925), pp. 22–128 (cit. on p. [1](#)).
- [11] W. Heisenberg, *Über quantentheoretische Umdeutung kinematischer und mechanischer Beziehungen*, *Zeitschrift für Physik* **33**, 879–893 (1925) (cit. on p. [1](#)).
- [12] J. Von Neumann, *Mathematische Grundlagen der Quantenmechanik*, Vol. 38 (Springer-Verlag, 2013) (cit. on p. [1](#)).
- [13] P. A. M. Dirac, *The principles of quantum mechanics*, Oxford, 1996 (cit. on p. [1](#)).
- [14] A. Einstein, B. Podolsky, and N. Rosen, *Can quantum-mechanical description of physical reality be considered complete?*, *Phys. Rev.* **47**, 777 (1935) (cit. on pp. [1](#), [27](#), [30](#)).
- [15] N. Bohr, *Can quantum-mechanical description of physical reality be considered complete?*, *Phys. Rev.* **48**, 696–702 (1935) (cit. on p. [1](#)).
- [16] E. Schrödinger, *Discussion of probability relations between separated systems*, *Mathematical Proceedings of the Cambridge Philosophical Society* **31**, 555–563 (1935) (cit. on pp. [1](#), [30](#)).
- [17] E. Schrödinger, *Probability relations between separated systems*, *Mathematical Proceedings of the Cambridge Philosophical Society* **32**, 446–452 (1936) (cit. on pp. [1](#), [30](#)).

- [18] T. Maiman, *Stimulated optical radiation in ruby*, *Nature* **187**, 493–494 (1960) (cit. on p. 1).
- [19] S. Chu, L. Hollberg, J. E. Bjorkholm, et al., *Three-dimensional viscous confinement and cooling of atoms by resonance radiation pressure*, *Phys. Rev. Lett.* **55**, 48–51 (1985) (cit. on p. 1).
- [20] W. Paul, *Electromagnetic traps for charged and neutral particles*, *Rev. Mod. Phys.* **62**, 531–540 (1990) (cit. on p. 1).
- [21] D. J. Wineland, R. E. Drullinger, and F. L. Walls, *Radiation-pressure cooling of bound resonant absorbers*, *Phys. Rev. Lett.* **40**, 1639–1642 (1978) (cit. on p. 1).
- [22] J. S. Bell, *On the Einstein Podolsky Rosen paradox*, *Physics Physique Fizika* **1**, 195 (1964) (cit. on pp. 1, 29).
- [23] M. Redhead, *Incompleteness, nonlocality, and realism: a prolegomenon to the philosophy of quantum mechanics*, Oxford, 1987 (cit. on p. 1).
- [24] S. J. Freedman and J. F. Clauser, *Experimental test of local hidden-variable theories*, *Phys. Rev. Lett.* **28**, 938 (1972) (cit. on pp. 1, 30).
- [25] A. Zeilinger, *Experiment and the foundations of quantum physics*, *Rev. Mod. Phys.* **71**, S288 (1999) (cit. on pp. 1, 30).
- [26] A. Aspect, P. Grangier, and G. Roger, *Experimental tests of realistic local theories via Bell's theorem*, *Phys. Rev. Lett.* **47**, 460 (1981) (cit. on pp. 1, 30).
- [27] S. Storz, J. Schär, A. Kulikov, et al., *Loophole-free Bell inequality violation with superconducting circuits*, *Nature* **617**, 265–270 (2023) (cit. on p. 1).
- [28] B. Hensen, H. Bernien, A. E. Dréau, et al., *Loophole-free Bell inequality violation using electron spins separated by 1.3 kilometres*, *Nature* **526**, 682–686 (2015) (cit. on pp. 1–2).
- [29] M. Giustina, M. A. M. Versteegh, S. Wengerowsky, et al., *Significant-loophole-free test of Bell's theorem with entangled photons*, *Phys. Rev. Lett.* **115**, 250401 (2015) (cit. on p. 1).
- [30] L. K. Shalm, E. Meyer-Scott, B. G. Christensen, et al., *Strong loophole-free test of local realism*, *Phys. Rev. Lett.* **115**, 250402 (2015) (cit. on p. 1).
- [31] M.-H. Li, C. Wu, Y. Zhang, et al., *Test of local realism into the past without detection and locality loopholes*, *Phys. Rev. Lett.* **121**, 080404 (2018) (cit. on p. 1).
- [32] W. Rosenfeld, D. Burchardt, R. Garthoff, et al., *Event-ready Bell test using entangled atoms simultaneously closing detection and locality loopholes*, *Phys. Rev. Lett.* **119**, 010402 (2017) (cit. on p. 1).
- [33] H. M. Wiseman, S. J. Jones, and A. C. Doherty, *Steering, entanglement, nonlocality, and the Einstein-Podolsky-Rosen paradox*, *Phys. Rev. Lett.* **98**, 140402 (2007) (cit. on pp. 1, 31).
- [34] S. P. Neumann, A. Buchner, L. Bulla, et al., *Continuous entanglement distribution over a transnational 248 km fiber link*, *Nature Communications* **13**, 6134 (2022) (cit. on pp. 1–2).
- [35] A. Acín, I. Bloch, H. Buhrman, et al., *The quantum technologies roadmap: a European community view*, *New J. Phys.* **20**, 080201 (2018) (cit. on p. 2).
- [36] A. E. Piceno-Martínez, L. E. C. Rosales-Zárata, and P. Ornelas-Cruces, *Certification and applications of quantum nonlocal correlations*, *J. Phys. Photonics* **5**, 042001 (2023) (cit. on p. 2).

- [37] M. A. Nielsen, *Conditions for a class of entanglement transformations*, *Phys. Rev. Lett.* **83**, 436–439 (1999) (cit. on pp. 2, 91).
- [38] W. Dür, G. Vidal, and J. I. Cirac, *Three qubits can be entangled in two inequivalent ways*, *Phys. Rev. A* **62**, 062314 (2000) (cit. on pp. 2, 91).
- [39] A. K. Ekert, *Quantum cryptography based on Bell's theorem*, *Phys. Rev. Lett.* **67**, 661–663 (1991) (cit. on p. 2).
- [40] C. H. Bennett and G. Brassard, *Quantum cryptography: public key distribution and coin tossing*, *Theoretical Computer Science* **560**, 7–11 (2014) (cit. on p. 2).
- [41] C. H. Bennett and S. J. Wiesner, *Communication via one- and two-particle operators on Einstein-Podolsky-Rosen states*, *Phys. Rev. Lett.* **69**, 2881–2884 (1992) (cit. on p. 2).
- [42] C. H. Bennett, G. Brassard, C. Crépeau, et al., *Teleporting an unknown quantum state via dual classical and Einstein-Podolsky-Rosen channels*, *Phys. Rev. Lett.* **70**, 1895–1899 (1993) (cit. on p. 2).
- [43] H. Buhrman, R. Cleve, S. Massar, et al., *Nonlocality and communication complexity*, *Rev. Mod. Phys.* **82**, 665–698 (2010) (cit. on p. 2).
- [44] D. Deutsch and R. Penrose, *Quantum theory, the church-turing principle and the universal quantum computer*, *Proceedings of the Royal Society of London. A. Mathematical and Physical Sciences* **400**, 97–117 (1985) (cit. on p. 2).
- [45] P. W. Shor, *Polynomial-time algorithms for prime factorization and discrete logarithms on a quantum computer*, *SIAM Journal on Computing* **26**, 1484–1509 (1997) (cit. on p. 2).
- [46] R. Raussendorf and H. J. Briegel, *A one-way quantum computer*, *Phys. Rev. Lett.* **86**, 5188–5191 (2001) (cit. on p. 2).
- [47] S. Lloyd, *Universal quantum simulators*, *Science* **273**, 1073–1078 (1996) (cit. on p. 2).
- [48] B. Yurke, *Input states for enhancement of fermion interferometer sensitivity*, *Phys. Rev. Lett.* **56**, 1515–1517 (1986) (cit. on p. 2).
- [49] V. Giovannetti, S. Lloyd, and L. Maccone, *Quantum-enhanced measurements: beating the standard quantum limit*, *Science* **306**, 1330–1336 (2004) (cit. on p. 2).
- [50] V. Giovannetti, S. Lloyd, and L. Maccone, *Quantum metrology*, *Phys. Rev. Lett.* **96**, 010401 (2006) (cit. on p. 2).
- [51] Y. Xia, A. R. Agrawal, C. M. Pluchar, et al., *Entanglement-enhanced optomechanical sensing*, *Nature Photonics* **17**, 470–477 (2023) (cit. on p. 2).
- [52] D. Boschi, S. Branca, F. De Martini, et al., *Experimental realization of teleporting an unknown pure quantum state via dual classical and Einstein-Podolsky-Rosen channels*, *Phys. Rev. Lett.* **80**, 1121–1125 (1998) (cit. on p. 2).
- [53] D. Bouwmeester, J.-W. Pan, K. Mattle, et al., *Experimental quantum teleportation*, *Nature* **390**, 575–579 (1997) (cit. on p. 2).
- [54] C.-Y. Lu, Y. Cao, C.-Z. Peng, et al., *Micius quantum experiments in space*, *Rev. Mod. Phys.* **94**, 035001 (2022) (cit. on p. 2).
- [55] R. Ursin, F. Tiefenbacher, T. Schmitt-Manderbach, et al., *Entanglement-based quantum communication over 144 km*, *Nature physics* **3**, 481–486 (2007) (cit. on p. 2).
- [56] R. Horodecki, P. Horodecki, M. Horodecki, et al., *Quantum entanglement*, *Rev. Mod. Phys.* **81**, 865 (2009) (cit. on pp. 2, 15–17).

- [57] A. Peres, *Separability criterion for density matrices*, *Phys. Rev. Lett.* **77**, 1413–1415 (1996) (cit. on pp. 2, 15–16, 111).
- [58] M. Horodecki, P. Horodecki, and R. Horodecki, *Separability of mixed states: necessary and sufficient conditions*, *Physics Letters A* **223**, 1–8 (1996) (cit. on pp. 2, 15–16, 111).
- [59] K. Siudzińska, *All classes of informationally complete symmetric measurements in finite dimensions*, *Phys. Rev. A* **105**, 042209 (2022) (cit. on pp. 2, 35, 38–39, 48, 65, 70, 84–85, 88–89).
- [60] J. M. Renes, R. Blume-Kohout, A. J. Scott, et al., *Symmetric informationally complete quantum measurements*, *J. Math. Phys.* **45**, 2171–2180 (2004) (cit. on pp. 2, 71–72, 120–121).
- [61] A. E. Rastegin, *Notes on general SIC-POVMs*, *Phys. Scr.* **89**, 085101 (2014) (cit. on p. 2).
- [62] G. Gour and A. Kalev, *Construction of all general symmetric informationally complete measurements*, *J. Phys. A: Math. Theor.* **47**, 335302 (2014) (cit. on pp. 2, 38–39, 67, 115).
- [63] W. K. Wootters and B. D. Fields, *Optimal state-determination by mutually unbiased measurements*, *Annals of Physics* **191**, 363–381 (1989) (cit. on p. 2).
- [64] A. Kalev and G. Gour, *Mutually unbiased measurements in finite dimensions*, *New Journal of Physics* **16**, 053038 (2014) (cit. on pp. 2, 39, 71).
- [65] C. A. Fuchs, M. C. Hoang, and B. C. Stacey, *The SIC question: History and state of play*, *Axioms* **6**, 21 (2017) (cit. on pp. 2, 64, 72).
- [66] P. Horodecki, Ł. Rudnicki, and K. Życzkowski, *Five open problems in quantum information theory*, *PRX Quantum* **3**, 010101 (2022) (cit. on pp. 2, 72–73).
- [67] C. Branciard, E. G. Cavalcanti, S. P. Walborn, et al., *One-sided device-independent quantum key distribution: security, feasibility, and the connection with steering*, *Phys. Rev. A* **85**, 010301(R) (2012) (cit. on p. 2).
- [68] Y. Wang, W.-s. Bao, H.-w. Li, et al., *Finite-key analysis for one-sided device-independent quantum key distribution*, *Phys. Rev. A* **88**, 052322 (2013) (cit. on p. 2).
- [69] J. Xin, X.-M. Lu, X. Li, et al., *One-sided device-independent quantum key distribution for two independent parties*, *Optics Express* **28**, 11439 (2020) (cit. on p. 2).
- [70] T. Heinosaari and M. M. Wolf, *Nondisturbing quantum measurements*, *J. Math. Phys.* **51**, 092201 (2010) (cit. on pp. 2, 32).
- [71] H. C. Nguyen, H.-V. Nguyen, and O. Gühne, *Geometry of Einstein-Podolsky-Rosen correlations*, *Phys. Rev. Lett.* **122**, 240401 (2019) (cit. on pp. 2, 97–98, 100).
- [72] J. A. Bergou, M. Hillery, and M. Saffman, *Quantum information processing* (Springer, 2021) (cit. on pp. 7, 20, 22–23).
- [73] A. M. Mathai and H. J. Haubold, *Linear algebra: a course for physicists and engineers* (De Gruyter, Berlin, Boston, 2017) (cit. on pp. 8, 12, 19, 25, 44).
- [74] I. Bengtsson and K. Życzkowski, *Geometry of quantum states: an introduction to quantum entanglement* (Cambridge university press, 2017) (cit. on pp. 8, 10, 15, 62–63).
- [75] G. Kimura and A. Kossakowski, *The bloch-vector space for n-level systems: the spherical-coordinate point of view*, *Open Systems & Information Dynamics* **12**, 207–229 (2005) (cit. on pp. 10, 62–63).

- [76] R. Wüst, *Mathematik für Physiker und Mathematiker: Band 1: Reelle Analysis und Lineare Algebra*, Vol. 1 (John Wiley & Sons, 2003) (cit. on p. 11).
- [77] B. M. Terhal, *Bell inequalities and the separability criterion*, *Physics Letters A* **271**, 319–326 (2000) (cit. on p. 16).
- [78] R. T. Rockafellar, *Convex analysis*, Vol. 11 (Princeton university press, 1997) (cit. on p. 16).
- [79] M. Lewenstein, B. Kraus, J. I. Cirac, et al., *Optimization of entanglement witnesses*, *Phys. Rev. A* **62**, 052310 (2000) (cit. on p. 16).
- [80] R. F. Werner, *Quantum states with Einstein-Podolsky-Rosen correlations admitting a hidden-variable model*, *Phys. Rev. A* **40**, 4277 (1989) (cit. on p. 16).
- [81] O. Gühne and G. Tóth, *Entanglement detection*, *Physics Reports* **474**, 1–75 (2009) (cit. on p. 18).
- [82] O. Rudolph, *Further results on the cross norm criterion for separability*, *Quantum Information Processing* **4**, 219–239 (2005) (cit. on p. 18).
- [83] K. Chen and L.-A. Wu, *A matrix realignment method for recognizing entanglement*, *Quantum Inf. Comput.* **3**, 193–202 (2002) (cit. on p. 18).
- [84] K. Chen and L.-A. Wu, *Test for entanglement using physically observable witness operators and positive maps*, *Phys. Rev. A* **69**, 022312 (2004) (cit. on p. 18).
- [85] J. Shang, A. Asadian, H. Zhu, et al., *Enhanced entanglement criterion via symmetric informationally complete measurements*, *Phys. Rev. A* **98**, 022309 (2018) (cit. on pp. 19, 88–90).
- [86] A Sauer, J. Bernád, H. Moreno, et al., *Entanglement in bipartite quantum systems: euclidean volume ratios and detectability by Bell inequalities*, *J. Phys. A: Math. Theor.* **54**, 495302 (2021) (cit. on pp. 24–26, 29, 129).
- [87] A Sauer and J. Bernád, *Quantitative characterization of several entanglement detection criteria*, *Phys. Rev. A* **106**, 032423 (2022) (cit. on pp. 24, 26, 113).
- [88] G. Frobenius, *Über lineare Substitutionen und bilineare Formen*. *Journal für die reine und angewandte Mathematik* **84**, 1–63 (1877) (cit. on pp. 25, 66).
- [89] R. A. Horn and C. R. Johnson, *Matrix analysis* (Cambridge University Press, 1985) (cit. on p. 26).
- [90] R. L. Smith, *Efficient Monte Carlo procedures for generating points uniformly distributed over bounded regions*, *Operations Research* **32**, 1296–1308 (1984) (cit. on p. 26).
- [91] L. Lovász, *Hit-and-run mixes fast*, *Mathematical programming* **86**, 443–461 (1999) (cit. on p. 26).
- [92] L. Lovász and S. Vempala, *Hit-and-run from a corner*, *SIAM Journal on Computing* **35**, 985–1005 (2006) (cit. on p. 26).
- [93] R. Kannan and L. Rademacher, *Optimization of a convex program with a polynomial perturbation*, *Operations research letters* **37**, 384–386 (2009) (cit. on p. 26).
- [94] J. S. Bell, *Speakable and unspeakable in quantum mechanics: collected papers on quantum philosophy* (Cambridge university press, 2004) (cit. on p. 27).
- [95] N. Brunner, D. Cavalcanti, S. Pironio, et al., *Bell nonlocality*, *Rev. Mod. Phys.* **86**, 419 (2014) (cit. on p. 29).

- [96] J. F. Clauser, M. A. Horne, A. Shimony, et al., *Proposed experiment to test local hidden-variable theories*, *Phys. Rev. Lett.* **23**, 880 (1969) (cit. on p. 29).
- [97] S. J. Jones, H. M. Wiseman, and A. C. Doherty, *Entanglement, Einstein-Podolsky-Rosen correlations, Bell nonlocality, and steering*, *Phys. Rev. A* **76**, 052116 (2007) (cit. on p. 31).
- [98] D. J. Saunders, S. J. Jones, H. M. Wiseman, et al., *Experimental EPR-steering using Bell-local states*, *Nature Physics* **6**, 845–849 (2010) (cit. on p. 32).
- [99] X.-G. Fan, F. Zhao, H. Yang, et al., *Detecting the steerability through an optimized steering criterion in two-photon systems*, *Optics Express* **31**, 16719–16728 (2023) (cit. on pp. 32, 99).
- [100] J. Li, C.-Y. Wang, T.-J. Liu, et al., *Experimental verification of steerability via geometric Bell-like inequalities*, *Phys. Rev. A* **97**, 032107 (2018) (cit. on p. 32).
- [101] V. Händchen, T. Eberle, S. Steinlechner, et al., *Observation of one-way Einstein-Podolsky-Rosen steering*, *Nature Photonics* **6**, 596–599 (2012) (cit. on p. 32).
- [102] K. Sun, X.-J. Ye, J.-S. Xu, et al., *Experimental quantification of asymmetric Einstein-Podolsky-Rosen steering*, *Phys. Rev. Lett.* **116**, 160404 (2016) (cit. on p. 32).
- [103] Y. Xiao, X.-J. Ye, K. Sun, et al., *Demonstration of multisetting one-way Einstein-Podolsky-Rosen steering in two-qubit systems*, *Phys. Rev. Lett.* **118**, 140404 (2017) (cit. on p. 32).
- [104] N. Tischler, F. Ghafari, T. J. Baker, et al., *Conclusive experimental demonstration of one-way Einstein-Podolsky-Rosen steering*, *Phys. Rev. Lett.* **121**, 100401 (2018) (cit. on p. 32).
- [105] A. J. Bennet, D. A. Evans, D. J. Saunders, et al., *Arbitrarily loss-tolerant Einstein-Podolsky-Rosen steering allowing a demonstration over 1 km of optical fiber with no detection loophole*, *Phys. Rev. X* **2**, 031003 (2012) (cit. on p. 32).
- [106] M. Sedlák, D. Reitzner, G. Chiribella, et al., *Incompatible measurements on quantum causal networks*, *Phys. Rev. A* **93**, 052323 (2016) (cit. on p. 32).
- [107] R. Uola, T. Moroder, and O. Gühne, *Joint measurability of generalized measurements implies classicality*, *Phys. Rev. Lett.* **113**, 160403 (2014) (cit. on p. 32).
- [108] M. T. Quintino, T. Vértesi, and N. Brunner, *Joint measurability, Einstein-Podolsky-Rosen steering, and Bell nonlocality*, *Phys. Rev. Lett.* **113**, 160402 (2014) (cit. on p. 32).
- [109] R. Uola, C. Budroni, O. Gühne, et al., *One-to-one mapping between steering and joint measurability problems*, *Phys. Rev. Lett.* **115**, 230402 (2015) (cit. on p. 32).
- [110] G. Kimura, *The Bloch vector for n -level systems*, *Physics Letters A* **314**, 339–349 (2003) (cit. on p. 52).
- [111] G. Zauner, *Grundzüge einer nichtkommutativen Designtheorie*, PhD thesis (1999) (cit. on pp. 71–72).
- [112] C. M. Caves, *Symmetric informationally complete POVMs*, <http://info.phys.unm.edu/~caves/reports/infopovm.pdf> (visited on 08/20/2023) (cit. on p. 71).
- [113] A. J. Scott and M. Grassl, *Symmetric informationally complete positive-operator-valued measures: A new computer study*, *J. Math. Phys.* **51**, 042203 (2010) (cit. on p. 72).
- [114] A. J. Scott, *Sics: extending the list of solutions*, arXiv preprint arXiv:1703.03993 (2017) (cit. on p. 72).
- [115] J. DeBrotta, C. Fuchs, M. C. Hoang, et al., *QBism research group*, <http://www.physics.umb.edu/Research/QBism> (visited on 08/20/2023) (cit. on p. 72).

- [116] M. Grassel, *SIC-POVMs*, <http://sicpovm.markus-grassl.de/> (visited on 08/20/2023) (cit. on p. 72).
- [117] *Exact SIC fiducial vectors*, <http://www.physics.usyd.edu.au/~sflammia/SIC/> (visited on 08/20/2023) (cit. on p. 72).
- [118] M. Appleby, T.-Y. Chien, S. Flammia, et al., *Constructing exact symmetric informationally complete measurements from numerical solutions*, *J. Phys. A: Math. Theor.* **51**, 165302 (2018) (cit. on p. 72).
- [119] M. Grassl and A. J. Scott, *Fibonacci-Lucas SIC-POVMs*, *J. Math. Phys.* **58**, 122201 (2017) (cit. on p. 72).
- [120] M. Appleby and I. Bengtsson, *Simplified exact SICs*, *J. Math. Phys.* **60**, 062203 (2019) (cit. on p. 72).
- [121] M. Appleby, I. Bengtsson, M. Grassl, et al., *SIC-POVMs from Stark units: Prime dimensions $n2 + 3$* , *J. Math. Phys.* **63**, 112205 (2022) (cit. on p. 72).
- [122] S. D. Howard, A. R. Calderbank, and W. Moran, *The finite Heisenberg-Weyl groups in radar and communications*, *EURASIP J. Adv. Signal Process.* **2006**, 085685 (2006) (cit. on p. 72).
- [123] R. Balan, B. G. Bodmann, P. G. Casazza, et al., *Painless reconstruction from magnitudes of frame coefficients*, *Journal of Fourier Analysis and Applications* **15**, 488–501 (2009) (cit. on p. 72).
- [124] M. Appleby, S. Flammia, G. McConnell, et al., *SICs and algebraic number theory*, *Foundations of Physics* **47**, 1042–1059 (2017) (cit. on p. 72).
- [125] G. Alber and C. Charnes, *Mutually unbiased bases: a group and graph theoretical approach*, *Phys. Scr.* **94**, 014007 (2018) (cit. on p. 73).
- [126] M. Weiner, *A gap for the maximum number of mutually unbiased bases*, *Proceedings of the American Mathematical Society* **141**, 1963–1969 (2013) (cit. on p. 73).
- [127] J. Batle, A. Farouk, M. Naseri, et al., *New approach to finding the maximum number of mutually unbiased bases in C_6* , *Appl. Math* **10**, 2077–2082 (2016) (cit. on p. 73).
- [128] L. Chen and L. Yu, *Mutually unbiased bases in dimension six containing a product-vector basis*, *Quantum Information Processing* **17**, 198 (2018) (cit. on p. 73).
- [129] L. Lai and S. Luo, *Detecting Einstein-Podolsky-Rosen steering via correlation matrices*, *Phys. Rev. A* **106**, 042402 (2022) (cit. on pp. 78, 97, 102, 105, 107–108, 110).
- [130] O. Gittsovich, O. Gühne, P. Hyllus, et al., *Unifying several separability conditions using the covariance matrix criterion*, *Phys. Rev. A* **78**, 052319 (2008) (cit. on p. 81).
- [131] O. Gittsovich and O. Gühne, *Quantifying entanglement with covariance matrices*, *Phys. Rev. A* **81**, 032333 (2010) (cit. on p. 81).
- [132] C.-J. Zhang, Y.-S. Zhang, S. Zhang, et al., *Entanglement detection beyond the computable cross-norm or realignment criterion*, *Phys. Rev. A* **77**, 060301(R) (2008) (cit. on p. 81).
- [133] L. Lai and S. Luo, *Separability criteria based on a class of symmetric measurements*, *Commun. Theor. Phys.* **75**, 065101 (2023) (cit. on pp. 82, 87–89).
- [134] S.-Q. Shen, M. Li, X. Li-Jost, et al., *Improved separability criteria via some classes of measurements*, *Quantum Information Processing* **17**, 1–9 (2018) (cit. on pp. 82, 85, 87, 89).

- [135] L. Tang and F. Wu, *Enhancing some separability criteria in many-body quantum systems*, *Phys. Scr.* **98**, 065114 (2023) (cit. on pp. 85, 88–89).
- [136] L.-M. Lai, T. Li, S.-M. Fei, et al., *Entanglement criterion via general symmetric informationally complete measurements*, *Quantum Information Processing* **17**, 1–11 (2018) (cit. on pp. 85, 88–89).
- [137] L. Tang and F. Wu, *Improved bounds on some entanglement criteria in bipartite quantum systems*, *Results in Physics*, 106663 (2023) (cit. on p. 89).
- [138] S.-Q. Shen, M. Li, and X.-F. Duan, *Entanglement detection via some classes of measurements*, *Phys. Rev. A* **91**, 012326 (2015) (cit. on p. 89).
- [139] L. Tang, *The entanglement criteria via a broad class of symmetric informationally complete measurements*, *Quantum Information Processing* **22**, 57 (2023) (cit. on p. 89).
- [140] B. Chen, T. Li, and S.-M. Fei, *General SIC measurement-based entanglement detection*, *Quantum Information Processing* **14**, 2281–2290 (2015) (cit. on p. 89).
- [141] B. Chen, T. Ma, and S.-M. Fei, *Entanglement detection using mutually unbiased measurements*, *Phys. Rev. A* **89**, 064302 (2014) (cit. on p. 89).
- [142] C. Spengler, M. Huber, S. Brierley, et al., *Entanglement detection via mutually unbiased bases*, *Phys. Rev. A* **86**, 022311 (2012) (cit. on p. 89).
- [143] B.-C. Yu, Z.-A. Jia, Y.-C. Wu, et al., *Geometric steering criterion for two-qubit states*, *Phys. Rev. A* **97**, 012130 (2018) (cit. on p. 97).
- [144] B.-C. Yu, Z.-A. Jia, Y.-C. Wu, et al., *Geometric local-hidden-state model for some two-qubit states*, *Phys. Rev. A* **98**, 052345 (2018) (cit. on p. 97).
- [145] D. Das, S. Sasmal, and S. Roy, *Detecting Einstein-Podolsky-Rosen steering through entanglement detection*, *Phys. Rev. A* **99**, 052109 (2019) (cit. on pp. 97, 111–112, 114).
- [146] S. Jevtic, M. J. Hall, M. R. Anderson, et al., *Einstein-Podolsky-Rosen steering and the steering ellipsoid*, *JOSA B* **32**, A40–A49 (2015) (cit. on p. 99).
- [147] X.-G. Fan, F. Zhao, H. Yang, et al., *Experimental detection of quantum steerability based on the critical radius in an all-optical system*, *Phys. Rev. A* **107**, 012419 (2023) (cit. on p. 100).
- [148] T. J. Baker and H. M. Wiseman, *Necessary conditions for steerability of two qubits from consideration of local operations*, *Phys. Rev. A* **101**, 022326 (2020) (cit. on p. 101).
- [149] C. King and M. B. Ruskai, *Minimal entropy of states emerging from noisy quantum channels*, *IEEE Transactions on information theory* **47**, 192–209 (2001) (cit. on p. 101).
- [150] Y.-L. Zheng, Y.-Z. Zhen, Z.-B. Chen, et al., *Efficient linear criterion for witnessing Einstein-Podolsky-Rosen nonlocality under many-setting local measurements*, *Phys. Rev. A* **95**, 012142 (2017) (cit. on p. 107).
- [151] H. Yang, Z.-Y. Ding, D. Wang, et al., *Experimental observation of Einstein-Podolsky-Rosen steering via entanglement detection*, *Phys. Rev. A* **101**, 042115 (2020) (cit. on p. 112).
- [152] R. Uola, A. C. S. Costa, H. C. Nguyen, et al., *Quantum steering*, *Rev. Mod. Phys.* **92**, 015001 (2020) (cit. on p. 112).
- [153] T. Durt, B.-G. Englert, I. Bengtsson, et al., *On mutually unbiased bases*, *International journal of quantum information* **8**, 535–640 (2010) (cit. on pp. 119–120).

-
- [154] R. A. Bertlmann and P. Krammer, *Bloch vectors for qudits*, *J. Phys. A: Math. Theor.* **41**, 235303 (2008) (cit. on p. 125).

LIST OF PUBLICATIONS

- M. Schumacher, G. Alber
Typical bipartite steerability and generalized local quantum measurements
Phys. Scr. **98**, 115234 (2023)
<https://doi.org/10.1088/1402-4896/acfc7c>
- M. Schumacher, G. Alber
Detection of typical bipartite entanglement by local generalized measurements
Phys. Rev. A **108**, 042424 (2023)
<https://doi.org/10.1103/PhysRevA.108.042424>
- M. Schumacher, G. Alber
Conditions for the existence of positive operator valued measures
Canadian Journal of Physics (submitted)
<https://arxiv.org/abs/2310.12302>

LEBENS LAUF

Persönliche Daten

Nicht enthalten in der Online Version.

Promotion

2019-2023 Doktorand und wissenschaftlicher Mitarbeiter
Technische Universität Darmstadt
Institut für Angewandte Physik
Arbeitsgruppe Theoretische Quantenphysik (Prof. Gernot Alber)

Studium

2017-2019 Master of Science in Physik
Technische Universität Darmstadt

2017-2018 Erasmus Programm
Universidade de Aveiro (Portugal)

2013-2017 Bachelor of Science in Physik
Technische Universität Darmstadt

Berufsausbildung

2009-2012 Fachinformatiker für Systemintegration
Hochsauerlandkreis in Meschede

Schulbildung

2012-2013 Fachhochschulreife mit Schwerpunkt Elektrotechnik
Berufskolleg Meschede

2003-2009 Realschule
Erich Kästner-Realschule Bad Fredeburg

1999-2003 Grundschule
Grundschule Bödefeld

DANKSAGUNG

An dieser Stelle möchte ich mich bei den Personen bedanken, ohne die mir die Fertigstellung der vorliegenden Arbeit nicht möglich gewesen wäre.

An erster Stelle möchte ich mich bei Herrn Prof. Dr. Gernot Alber für die Möglichkeit bedanken, in dessen Arbeitsgruppe promovieren und mit Ihm gemeinsam die Quantenoptik und Quantenphysik erforschen zu dürfen. Für die zahlreichen Diskussionen, konstruktiven Anregungen und Ratschlägen bedanke ich mich ganz herzlich.

Weiterhin möchte ich mich bei Prof. Dr. Enno Giese bedanken, der sich bereit erklärt hat, als Korreferent zur Verfügung zu stehen. Bedanken möchte ich mich auch bei Herrn Prof. Dr. Gerhard Birkel und Herrn Prof. Dr. Bernhard Urbaszek für ihr Engagement als Gutachter der Dissertation.

Mein Dank gilt auch meinen Kolleginnen und Kollegen aus der Arbeitsgruppe Theoretische Quantenphysik. Sie haben mir mit zahlreichen Diskussionen und Anregungen geholfen. Vielen Dank Hector Moreno, Thorsten Haase, Alexander Sauer, Vladimir Stajanovic und Zsolt Bernard.

Bedanken möchte ich mich auch bei meinen Freunden Kai Hansmann, Till Böhmer, Philipp Ritzert, Philipp Napiralla., Bastian Zapf, Matthias Seubert und Janina Willmann, die ich während meines Studiums kennengelernt habe. Mit ihnen habe ich viele aktive Diskussionen und Kaffeepausen erlebt. Außerdem bedanke ich mich bei euch für die schönen Abende in Darmstädter Kneipen. Besonders möchte ich hier Philipp Ritzert, Bastian Zapf und Till Böhmer danken, die mir den Einsteig und das Bestehen des ersten Semesters sehr vereinfacht haben. Ein besonderer Dank geht auch an Kai für die gemeinsamen Abende und die Zeit, die wir zusammen am Institut verbracht haben.

Weiterhin danke ich Philipp Ritzert, Till Böhmer, Janina Willmann, Oleksandr Marchukov und Christian Holsing für die sachliche Kritik an meiner Dissertation, ohne die ich diese Arbeit nicht hätte vorlegen können.

Außerdem danke ich meiner Freundin Verena und meinen Eltern Bernadette und Ludger, die mich während meines Studiums und der späteren Promotion immer unterstützt haben.

ERKLÄRUNG LAUT PROMOTIONSORDNUNG

§8 ABS. 1 LIT. C PROM0

Ich versichere hiermit, dass die elektronische Version meiner Dissertation mit der schriftlichen Version übereinstimmt

§8 ABS. 1 LIT. D PROM0

Ich versichere hiermit, dass zu einem vorherigen Zeitpunkt noch keine Promotion versucht wurde. In diesem Fall sind nähere Angaben über Zeitpunkt, Hochschule, Dissertationsthema und Ergebnis dieses Versuchs mitzuteilen.

§9 ABS. 1 PROM0

Ich versichere hiermit, dass die vorliegende Dissertation selbstständig und nur unter Verwendung der angegebenen Quellen verfasst wurde.

§9 ABS. 2 PROM0

Die Arbeit hat bisher noch nicht zu Prüfungszwecken gedient.

Darmstadt, April 12, 2024

Maximilian Schumacher